International Journal of Bifurcation and Chaos, Vol. 15, No. 12 (2005) 3701–3849
© World Scientific Publishing Company

A NONLINEAR DYNAMICS PERSPECTIVE OF WOLFRAM'S NEW KIND OF SCIENCE. PART V: FRACTALS EVERYWHERE

LEON O. CHUA, VALERY I. SBITNEV and SOOK YOON
Department of Electrical Engineering and Computer Sciences, University of California at Berkeley, CA 94720, USA

Received April 5, 2005; Revised July 10, 2005

This fifth installment is devoted to an in-depth study of CA *Characteristic Functions*, a unified *global* representation for all 256 one-dimensional Cellular Automata *local rules*. Except for eight rather special local rules whose global dynamics are described by an *affine* (*mod 1*) function of only one binary cell state variable, all characteristic functions exhibit a *fractal* geometry where self-similar two-dimensional substructures manifest themselves, *ad infinitum*, as the number of cells $(I+1) \to \infty$.

In addition to a complete gallery of time-1 *characteristic functions* for all 256 local rules, an accompanying table of *explicit formulas* is given for generating these characteristic functions directly from *binary* bit-strings, as in a digital-to-analog converter. To illustrate the potential applications of these fundamental formulas, we prove rigorously that the "*right-copycat*" *local* rule $\boxed{170}$ is equivalent *globally* to the classic "*left-shift*" *Bernoulli map*. Similarly, we prove the "*left-copycat*" *local* rule $\boxed{240}$ is equivalent *globally* to the "*right-shift*" *inverse Bernoulli map*.

Various geometrical and analytical properties have been identified from each characteristic function and explained rigorously. In particular, two-level *stratified subpatterns* found in most characteristic functions are shown to emerge if, and only if, $b_1 \neq 0$, where b_1 is the "synaptic coefficient" associated with the cell *differential equation* developed in Part I.

Gardens of Eden are derived from the decimal *range* of the characteristic function of each local rule and tabulated. Each of these binary strings has no predecessors (pre-image) and has therefore *no past*, but only the present and the future. Even more fascinating, many local rules are endowed with binary configurations which not only have no predecessors, but are also *fixed points* of the characteristic functions. To dramatize that such points have *no past*, and *no future*, they are henceforth christened "*Isles of Eden*". They too have been identified and tabulated.

Keywords: Cellular neural networks, CNN; cellular automata; Turing machine; universal computation; Bernoulli shift; $1/f$ power spectrum; global equivalence classes attractors; invariant orbits; Garden of Eden; Isle of Eden; characteristic function; fractal geometry; fractals.

1. Characteristic Functions: Global Representation of Local Rules

The fundamental concept of the *time*-1 *characteristic function*

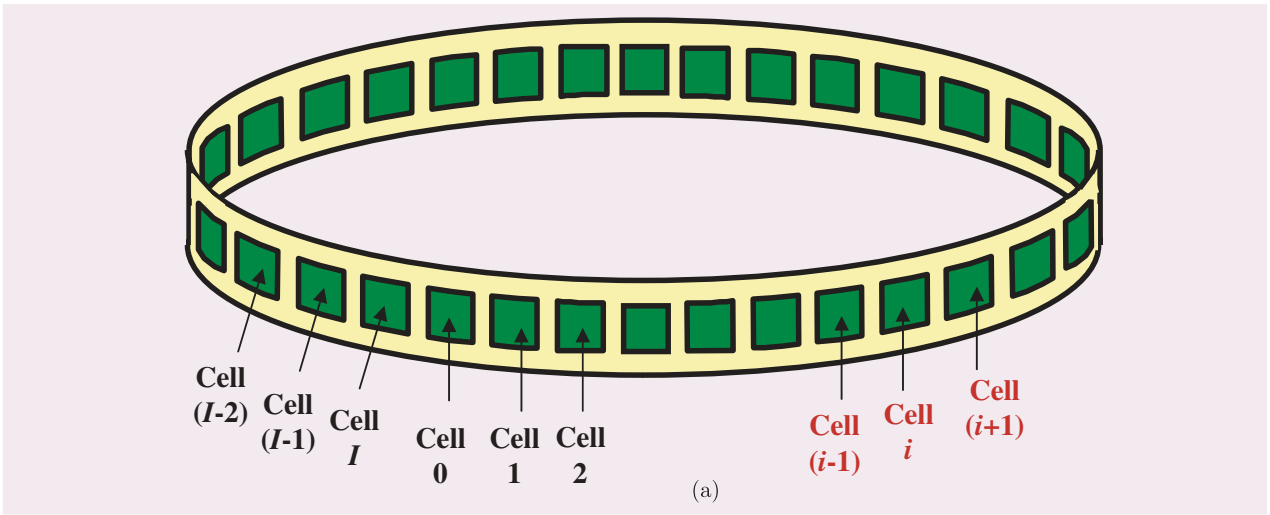
$$\chi^1_{\boxed{N}} : [0,1] \to [0,1] \tag{1}$$

of a local rule $\boxed{N}$ is defined in Part IV [Chua *et al.*, 2005] as a *function* from the *unit interval* $[0,1]$ into itself which *uniquely* maps each input *binary* string $\{x_0, x_1, x_2, \ldots, x_I\}$ represented in decimal form

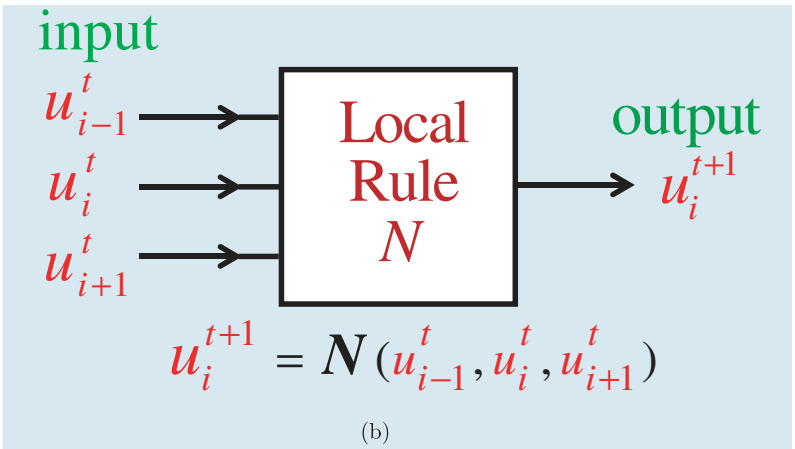
$$\phi = \sum_{i=0}^{I} 2^{-(i+1)} x_i \tag{2}$$

into an output binary string

$$\chi^1_{\boxed{N}}(\phi) = \sum_{i=0}^{I} 2^{-(i+1)} y_i \tag{3}$$



(a)



(b)

Symbolic Truth Table

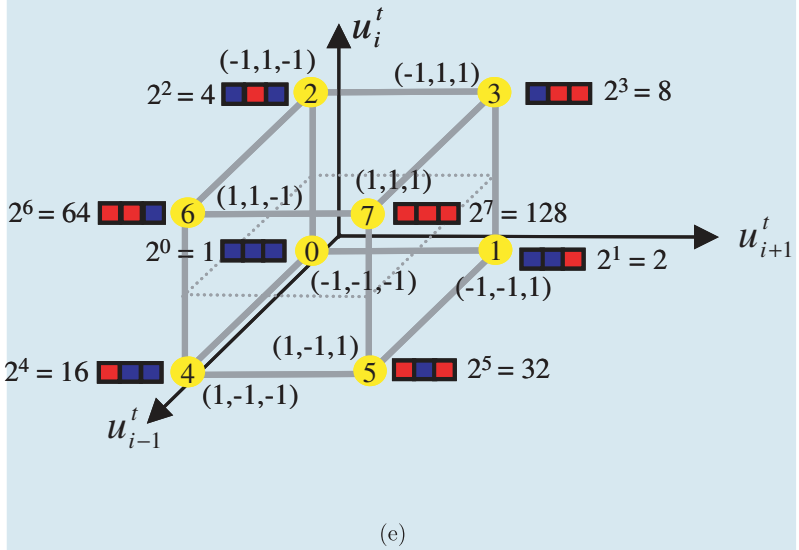
	u_{i-1}^t	u_i^t	u_{i+1}^t	u_i^{t+1}
0	0	0	0	β_0
1	0	0	1	β_1
2	0	1	0	β_2
3	0	1	1	β_3
4	1	0	0	β_4
5	1	0	1	β_5
6	1	1	0	β_6
7	1	1	1	β_7

(c)

Numeric Truth Table

	u_{i-1}^t	u_i^t	u_{i+1}^t	u_i^{t+1}
0	-1	-1	-1	γ_0
1	-1	-1	1	γ_1
2	-1	1	-1	γ_2
3	-1	1	1	γ_3
4	1	-1	-1	γ_4
5	1	-1	1	γ_5
6	1	1	-1	γ_6
7	1	1	1	γ_7

(d)



(e)

Fig. 1. (a) A one-dimensional Cellular Automata (CA) made of $(I + 1)$ identical cells with a periodic boundary condition. Each cell "i" is coupled only to its left neighbor cell $(i - 1)$ and right neighbor cell $(i + 1)$. (b) Each cell "i" is described by a local rule N, where N is a decimal number specified by a binary string $\{\beta_0, \beta_1, \ldots, \beta_7\}$, $\beta_i \in \{0, 1\}$. (c) The symbolic truth table specifying each local rule N, $N = 0, 1, 2, \ldots, 255$. (d) By recoding "0" to "−1", each row of the symbolic truth table in (c) can be recast into a numeric truth table, where $\gamma_k \in \{-1, 1\}$. (e) Each row of the numeric truth table in (d) can be represented as a *vertex* of a Boolean Cube whose color is red if $\gamma_k = 1$, and blue if $\gamma_k = -1$.

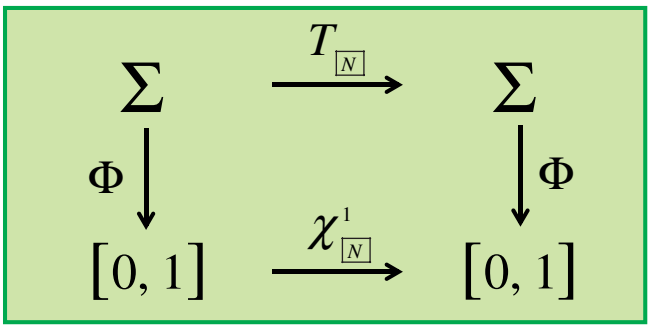


Fig. 2. A commutative diagram establishing a one-to-one correspondence between $T_{\boxed{N}}$ and $\chi^1_{\boxed{N}}$.

in decimal representation, as $I \to \infty$, where $\{y_0, y_1, y_2, \ldots, y_I\}$ is the output binary string determined from the local rule $\boxed{N}$ of the one-dimensional cellular automata under a *periodic boundary condition*, as shown in Fig. 1. Every input binary string is assumed to be finite but whose length can be chosen to be arbitrarily large. For practical calculation, the domain of the characteristic function $\chi^1_{\boxed{N}}$ consists of only a large but finite number of equally-spaced real numbers inside $[0, 1]$. In the limit $I \to \infty$, the domain of $\chi^1_{\boxed{N}}$ coincides with the entire unit interval [0, 1]. In this case, every point $\phi \in [0, 1]$ corresponds uniquely to an infinite binary string. Conversely, each infinite binary string corresponds to a unique point on [0, 1]. This one-to-one correspondence between each binary string in the set $\mathbf{\Sigma}$ of all infinite binary strings and each real number in $[0, 1]$ is depicted in Fig. 2, where ϕ is defined via Eq. (2). Observe that since the time-1 *characteristic function* $\chi^1_{\boxed{N}}$ maps each infinite binary string into another infinite binary string after *one iteration* of the local rule $\boxed{N}$, it is a *global* representation.[1]

1.1. *Deriving explicit formula for calculating* $\chi^1_{\boxed{N}}$

Recall from Eq. (8) of [Chua *et al.*, 2004] that the output of each local rule $\boxed{N}$ can be calculated from the formula

$$u_i^{t+1} = \mathrm{sgn}\{z_2 + c_2|(z_1 + c_1|(z_0 + b_1 u_{i-1}^t + b_2 u_i^t + b_3 u_{i+1}^t)|)|\} \tag{4}$$

where the eight parameters $\{z_2, c_2, z_1, c_1, z_0, b_1, b_2, b_3\}$ determining each local rule $\boxed{N}$ is given in Table 4 of [Chua *et al.*, 2003]. Since $\chi^1_{\boxed{N}}$ is defined in terms of binary variables $x_i \in \{0, 1\}$, let us apply the conversion relationship Eq. (4) from [Chua *et al.*, 2005] namely,

$$x_i = \frac{1}{2}(u_i + 1) \tag{5}$$

and define the *step* function

$$\delta(w) \triangleq \begin{cases} 1, & w > 0 \\ 0, & w \le 0 \end{cases} \tag{6}$$

to rewrite Eq. (4) into

$$x_i^{t+1} = \delta\{z_2' + c_2|(z_1' + c_1|(z_0' + b_1 x_{i-1}^t + b_2 x_i^t + b_3 x_{i+1}^t)|)|\} \tag{7}$$

where

$$\begin{aligned} z_0' &\triangleq \frac{1}{2}[z_0 - (b_1 + b_2 + b_3)] \\ z_1' &\triangleq \frac{1}{2} z_1 \\ z_2' &\triangleq \frac{1}{2} z_2 \end{aligned} \tag{8}$$

Substituting Eq. (7) for $y_i = x_i^{t+1}$ in Eq. (3), and deleting the superscripts, we obtain the following explicit formula for calculating the characteristic function $\chi^1_{\boxed{N}}$ for any local rule $\boxed{N}$, $N = 0, 1, 2, \ldots, 255$:

$$\chi^1_{\boxed{N}} = \sum_{i=0}^{I} 2^{-(i+1)} \delta\{z_2' + c_2|(z_1' + c_1|(z_0' + b_1 x_{i-1} + b_2 x_i + b_3 x_{i+1})|)|\} \tag{9}$$

where $\{z_2', c_2, z_1', c_1, z_0', b_1, b_2, b_3\}$ are defined in Eq. (8) and Table 4 of [Chua *et al.*, 2003].

Applying Eq. (9) to all 256 local rules, we obtain the explicit formulas listed in Table 1 for calculating the corresponding time-1 *characteristic functions* $\chi^1_{\boxed{N}}$, $N = 0, 1, 2, \ldots, 255$, where the binary string begins from $\phi = 0$ corresponding to

$$\begin{array}{ccccccc} \{0, & 0, & 0, & \cdots & 0\}, \\ \uparrow & \uparrow & \uparrow & & \uparrow \\ x_0 & x_1 & x_2 & & x_I \end{array}$$

[1] We can define a *time-k* characteristic function $\chi^k_{\boxed{N}} : [0, 1] \to [0, 1]$ in exactly the same way where the output string is calculated after every "k" iterations under rule $\boxed{N}$.

Table 1. Explicit formulas for calculating characteristic functions $\chi^{1}_{\boxed{N}}$ in terms of binary strings $\{x_0, x_1, x_2, \ldots, x_I\}$. Each row is partitioned into four equal parts, where each part is color coded either in *blue*, if the characteristic function has no stratification (see Tables 2 and 5), or in *pink*, otherwise.

$\chi^{1}_{\boxed{0}} = \sum_{i=0}^{I} \delta\left[0x_{i-1} + 0x_i + 0x_{i+1} - \frac{1}{2}\right] 2^{-(i+1)}$	$\chi^{1}_{\boxed{8}} = \sum_{i=0}^{I} \delta\left[-1x_{i-1} + 1x_i + 1x_{i+1} - \frac{3}{2}\right] 2^{-(i+1)}$
$\chi^{1}_{\boxed{1}} = \sum_{i=0}^{I} \delta\left[-1x_{i-1} - 1x_i - 1x_{i+1} + \frac{1}{2}\right] 2^{-(i+1)}$	$\chi^{1}_{\boxed{9}} = \sum_{i=0}^{I} \delta\left[\frac{1}{2} - \left\lvert(2x_{i-1} + 1x_i - 1x_{i+1})\right\rvert\right] 2^{-(i+1)}$
$\chi^{1}_{\boxed{2}} = \sum_{i=0}^{I} \delta\left[-1x_{i-1} - 1x_i + 1x_{i+1} - \frac{1}{2}\right] 2^{-(i+1)}$	$\chi^{1}_{\boxed{10}} = \sum_{i=0}^{I} \delta\left[-1x_{i-1} + 0x_i + 1x_{i+1} - \frac{1}{2}\right] 2^{-(i+1)}$
$\chi^{1}_{\boxed{3}} = \sum_{i=0}^{I} \delta\left[-1x_{i-1} - 1x_i + 0x_{i+1} + \frac{1}{2}\right] 2^{-(i+1)}$	$\chi^{1}_{\boxed{11}} = \sum_{i=0}^{I} \delta\left[-2x_{i-1} - 1x_i + 1x_{i+1} + \frac{1}{2}\right] 2^{-(i+1)}$
$\chi^{1}_{\boxed{4}} = \sum_{i=0}^{I} \delta\left[-1x_{i-1} + 1x_i - 1x_{i+1} - \frac{1}{2}\right] 2^{-(i+1)}$	$\chi^{1}_{\boxed{12}} = \sum_{i=0}^{I} \delta\left[-1x_{i-1} + 1x_i + 0x_{i+1} - \frac{1}{2}\right] 2^{-(i+1)}$
$\chi^{1}_{\boxed{5}} = \sum_{i=0}^{I} \delta\left[-1x_{i-1} + 0x_i - 1x_{i+1} + \frac{1}{2}\right] 2^{-(i+1)}$	$\chi^{1}_{\boxed{13}} = \sum_{i=0}^{I} \delta\left[-2x_{i-1} + 1x_i - 1x_{i+1} + \frac{1}{2}\right] 2^{-(i+1)}$
$\chi^{1}_{\boxed{6}} = \sum_{i=0}^{I} \delta\left[\frac{1}{2} - \left\lvert(2x_{i-1} - 1x_i - 1x_{i+1} + 1)\right\rvert\right] 2^{-(i+1)}$	$\chi^{1}_{\boxed{14}} = \sum_{i=0}^{I} \delta\left[-2x_{i-1} + 1x_i + 1x_{i+1} - \frac{1}{2}\right] 2^{-(i+1)}$
$\chi^{1}_{\boxed{7}} = \sum_{i=0}^{I} \delta\left[-2x_{i-1} - 1x_i - 1x_{i+1} + \frac{3}{2}\right] 2^{-(i+1)}$	$\chi^{1}_{\boxed{15}} = \sum_{i=0}^{I} \delta\left[-1x_{i-1} + 0x_i + 0x_{i+1} + \frac{1}{2}\right] 2^{-(i+1)}$

Table 1. (*Continued*)

$\chi^{1}_{\boxed{16}}=\sum_{i=0}^{I}\delta\left[1x_{i-1}-1x_{i}-1x_{i+1}-\frac{1}{2}\right]2^{-(i+1)}$	$\chi^{1}_{\boxed{24}}=\sum_{i=0}^{I}\delta\left[-1+\left\|(1x_{i-1}-1x_{i}-1x_{i+1}+\frac{1}{2})\right|\right]2^{-(i+1)}$
$\chi^{1}_{\boxed{17}}=\sum_{i=0}^{I}\delta\left[0x_{i-1}-1x_{i}-1x_{i+1}+\frac{1}{2}\right]2^{-(i+1)}$	$\chi^{1}_{\boxed{25}}=\sum_{i=0}^{I}\delta\left[\frac{3}{2}-\left\|(1x_{i-1}-2x_{i}+4x_{i+1}-1)\right|\right]2^{-(i+1)}$
$\chi^{1}_{\boxed{18}}=\sum_{i=0}^{I}\delta\left[\frac{1}{2}-\left\|(1x_{i-1}+2x_{i}+1x_{i+1}-1)\right|\right]2^{-(i+1)}$	$\chi^{1}_{\boxed{26}}=\sum_{i=0}^{I}\delta\left[\frac{3}{2}-\left\|(2x_{i-1}-1x_{i}+4x_{i+1}-3)\right|\right]2^{-(i+1)}$
$\chi^{1}_{\boxed{19}}=\sum_{i=0}^{I}\delta\left[-1x_{i-1}-2x_{i}-1x_{i+1}+\frac{3}{2}\right]2^{-(i+1)}$	$\chi^{1}_{\boxed{27}}=\sum_{i=0}^{I}\delta\left[1-\left\|(-\frac{3}{2}+\left\|(-2x_{i-1}-4x_{i}+1x_{i+1}+1)\right|)\right|\right]2^{-(i+1)}$
$\chi^{1}_{\boxed{20}}=\sum_{i=0}^{I}\delta\left[\frac{1}{2}-\left\|(-2x_{i-1}-2x_{i}+1x_{i+1}+2)\right|\right]2^{-(i+1)}$	$\chi^{1}_{\boxed{28}}=\sum_{i=0}^{I}\delta\left[\frac{3}{2}-\left\|(2x_{i-1}+4x_{i}-1x_{i+1}-3)\right|\right]2^{-(i+1)}$
$\chi^{1}_{\boxed{21}}=\sum_{i=0}^{I}\delta\left[-1x_{i-1}-1x_{i}-2x_{i+1}+\frac{3}{2}\right]2^{-(i+1)}$	$\chi^{1}_{\boxed{29}}=\sum_{i=0}^{I}\delta\left[1-\left\|(\frac{3}{2}-\left\|(-2x_{i-1}+1x_{i}-4x_{i+1}+1)\right|)\right|\right]2^{-(i+1)}$
$\chi^{1}_{\boxed{22}}=\sum_{i=0}^{I}\delta\left[\frac{1}{2}-\left\|(1x_{i-1}+1x_{i}+1x_{i+1}-1)\right|\right]2^{-(i+1)}$	$\chi^{1}_{\boxed{30}}=\sum_{i=0}^{I}\delta\left[1-\left\|(-2x_{i-1}-1x_{i}-1x_{i+1}+\frac{3}{2})\right|\right]2^{-(i+1)}$
$\chi^{1}_{\boxed{23}}=\sum_{i=0}^{I}\delta\left[-1x_{i-1}-1x_{i}-1x_{i+1}+\frac{3}{2}\right]2^{-(i+1)}$	$\chi^{1}_{\boxed{31}}=\sum_{i=0}^{I}\delta\left[-3x_{i-1}-1x_{i}-1x_{i+1}+\frac{7}{2}\right]2^{-(i+1)}$

Table 1. (*Continued*)

$$\chi^{1}_{[32]}=\sum_{i=0}^{I}\delta\left[1x_{i-1}-1x_{i}+1x_{i+1}-\frac{3}{2}\right]2^{-(i+1)}$$

$$\chi^{1}_{[33]}=\sum_{i=0}^{I}\delta\left[\frac{1}{2}-\left|(-2x_{i-1}+1x_{i}+2x_{i+1})\right|\right]2^{-(i+1)}$$

$$\chi^{1}_{[34]}=\sum_{i=0}^{I}\delta\left[0x_{i-1}-1x_{i}+1x_{i+1}-\frac{1}{2}\right]2^{-(i+1)}$$

$$\chi^{1}_{[35]}=\sum_{i=0}^{I}\delta\left[-1x_{i-1}-2x_{i}+1x_{i+1}+\frac{1}{2}\right]2^{-(i+1)}$$

$$\chi^{1}_{[36]}=\sum_{i=0}^{I}\delta\left[-1+\left|(1x_{i-1}-1x_{i}+1x_{i+1}-\frac{1}{2})\right|\right]2^{-(i+1)}$$

$$\chi^{1}_{[37]}=\sum_{i=0}^{I}\delta\left[\frac{3}{2}-\left|(2x_{i-1}-1x_{i}-4x_{i+1}+1)\right|\right]2^{-(i+1)}$$

$$\chi^{1}_{[38]}=\sum_{i=0}^{I}\delta\left[\frac{3}{2}-\left|(-1x_{i-1}+2x_{i}+4x_{i+1}-3)\right|\right]2^{-(i+1)}$$

$$\chi^{1}_{[39]}=\sum_{i=0}^{I}\delta\left[1-\left|\left(-\frac{3}{2}+\left|(-4x_{i-1}-2x_{i}+1x_{i+1}+1)\right|\right)\right|\right]2^{-(i+1)}$$

$$\chi^{1}_{[40]}=\sum_{i=0}^{I}\delta\left[\frac{1}{2}-\left|(-2x_{i-1}-2x_{i}+1x_{i+1}+1)\right|\right]2^{-(i+1)}$$

$$\chi^{1}_{[41]}=\sum_{i=0}^{I}\delta\left[\frac{1}{2}-\left|(-1x_{i-1}-1x_{i}+1x_{i+1})\right|\right]2^{-(i+1)}$$

$$\chi^{1}_{[42]}=\sum_{i=0}^{I}\delta\left[-1x_{i-1}-1x_{i}+2x_{i+1}-\frac{1}{2}\right]2^{-(i+1)}$$

$$\chi^{1}_{[43]}=\sum_{i=0}^{I}\delta\left[-1x_{i-1}-1x_{i}+1x_{i+1}+\frac{1}{2}\right]2^{-(i+1)}$$

$$\chi^{1}_{[44]}=\sum_{i=0}^{I}\delta\left[\frac{3}{2}-\left|(-4x_{i-1}-2x_{i}+1x_{i+1}+2)\right|\right]2^{-(i+1)}$$

$$\chi^{1}_{[45]}=\sum_{i=0}^{I}\delta\left[1-\left|(-2x_{i-1}-1x_{i}+1x_{i+1}+\frac{1}{2})\right|\right]2^{-(i+1)}$$

$$\chi^{1}_{[46]}=\sum_{i=0}^{I}\delta\left[1-\left|\left(\frac{3}{2}-\left|(1x_{i-1}-2x_{i}-3x_{i+1}+4)\right|\right)\right|\right]2^{-(i+1)}$$

$$\chi^{1}_{[47]}=\sum_{i=0}^{I}\delta\left[-3x_{i-1}-1x_{i}+1x_{i+1}+\frac{5}{2}\right]2^{-(i+1)}$$

Table 1. (*Continued*)

$\chi^{1}_{48}=\sum_{i=0}^{I}\delta\left[1x_{i-1}-1x_{i}+0x_{i+1}-\frac{1}{2}\right]2^{-(i+1)}$	$\chi^{1}_{56}=\sum_{i=0}^{I}\delta\left[\frac{3}{2}-\left\|(2x_{i-1}+4x_{i}-1x_{i+1}-2)\right\|\right]2^{-(i+1)}$
$\chi^{1}_{49}=\sum_{i=0}^{I}\delta\left[1x_{i-1}-2x_{i}-1x_{i+1}+\frac{1}{2}\right]2^{-(i+1)}$	$\chi^{1}_{57}=\sum_{i=0}^{I}\delta\left[1-\left\|(-1x_{i-1}-2x_{i}+1x_{i+1}+\frac{1}{2})\right\|\right]2^{-(i+1)}$
$\chi^{1}_{50}=\sum_{i=0}^{I}\delta\left[1x_{i-1}-2x_{i}+1x_{i+1}-\frac{1}{2}\right]2^{-(i+1)}$	$\chi^{1}_{58}=\sum_{i=0}^{I}\delta\left[1-\left\|(\frac{3}{2}-\left\|(-1x_{i-1}+2x_{i}-4x_{i+1}+3)\right\|)\right\|\right]2^{-(i+1)}$
$\chi^{1}_{51}=\sum_{i=0}^{I}\delta\left[0x_{i-1}-1x_{i}+0x_{i+1}+\frac{1}{2}\right]2^{-(i+1)}$	$\chi^{1}_{59}=\sum_{i=0}^{I}\delta\left[-1x_{i-1}-3x_{i}+1x_{i+1}+\frac{5}{2}\right]2^{-(i+1)}$
$\chi^{1}_{52}=\sum_{i=0}^{I}\delta\left[\frac{3}{2}-\left\|(-2x_{i-1}-4x_{i}-1x_{i+1}+3)\right\|\right]2^{-(i+1)}$	$\chi^{1}_{60}=\sum_{i=0}^{I}\delta\left[\frac{1}{2}-\left\|(1x_{i-1}+1x_{i}+0x_{i+1}-1)\right\|\right]2^{-(i+1)}$
$\chi^{1}_{53}=\sum_{i=0}^{I}\delta\left[1-\left\|(-\frac{3}{2}+\left\|(4x_{i-1}+1x_{i}-3x_{i+1}-2)\right\|)\right\|\right]2^{-(i+1)}$	$\chi^{1}_{61}=\sum_{i=0}^{I}\delta\left[\frac{3}{2}-\left\|(-2x_{i-1}-2x_{i}+1x_{i+1}+1)\right\|\right]2^{-(i+1)}$
$\chi^{1}_{54}=\sum_{i=0}^{I}\delta\left[1-\left\|(-1x_{i-1}-2x_{i}-1x_{i+1}+\frac{3}{2})\right\|\right]2^{-(i+1)}$	$\chi^{1}_{62}=\sum_{i=0}^{I}\delta\left[\frac{3}{2}-\left\|(-2x_{i-1}-2x_{i}-1x_{i+1}+2)\right\|\right]2^{-(i+1)}$
$\chi^{1}_{55}=\sum_{i=0}^{I}\delta\left[-1x_{i-1}-3x_{i}-1x_{i+1}+\frac{7}{2}\right]2^{-(i+1)}$	$\chi^{1}_{63}=\sum_{i=0}^{I}\delta\left[-1x_{i-1}-1x_{i}+0x_{i+1}+\frac{3}{2}\right]2^{-(i+1)}$

Table 1. (*Continued*)

$\chi^{1}_{64}=\sum_{i=0}^{I}\delta\left[1x_{i-1}+1x_{i}-1x_{i+1}-\frac{3}{2}\right]2^{-(i+1)}$	$\chi^{1}_{72}=\sum_{i=0}^{I}\delta\left[\frac{1}{2}-\left\|(-2x_{i-1}+1x_{i}-2x_{i+1}+1)\right\|\right]2^{-(i+1)}$
$\chi^{1}_{65}=\sum_{i=0}^{I}\delta\left[\frac{1}{2}-\left\|(2x_{i-1}-2x_{i}+1x_{i+1})\right\|\right]2^{-(i+1)}$	$\chi^{1}_{73}=\sum_{i=0}^{I}\delta\left[\frac{1}{2}-\left\|(1x_{i-1}-1x_{i}+1x_{i+1})\right\|\right]2^{-(i+1)}$
$\chi^{1}_{66}=\sum_{i=0}^{I}\delta\left[-1+\left\|(-1x_{i-1}-1x_{i}+1x_{i+1}+\frac{1}{2})\right\|\right]2^{-(i+1)}$	$\chi^{1}_{74}=\sum_{i=0}^{I}\delta\left[\frac{3}{2}-\left\|(2x_{i-1}+1x_{i}+4x_{i+1}-4)\right\|\right]2^{-(i+1)}$
$\chi^{1}_{67}=\sum_{i=0}^{I}\delta\left[\frac{3}{2}-\left\|(2x_{i-1}-4x_{i}-1x_{i+1}+1)\right\|\right]2^{-(i+1)}$	$\chi^{1}_{75}=\sum_{i=0}^{I}\delta\left[1-\left\|(2x_{i-1}-1x_{i}+1x_{i+1}-\frac{1}{2})\right\|\right]2^{-(i+1)}$
$\chi^{1}_{68}=\sum_{i=0}^{I}\delta\left[0x_{i-1}+1x_{i}-1x_{i+1}-\frac{1}{2}\right]2^{-(i+1)}$	$\chi^{1}_{76}=\sum_{i=0}^{I}\delta\left[-1x_{i-1}+2x_{i}-1x_{i+1}-\frac{1}{2}\right]2^{-(i+1)}$
$\chi^{1}_{69}=\sum_{i=0}^{I}\delta\left[-1x_{i-1}+1x_{i}-2x_{i+1}+\frac{1}{2}\right]2^{-(i+1)}$	$\chi^{1}_{77}=\sum_{i=0}^{I}\delta\left[-1x_{i-1}+1x_{i}-1x_{i+1}+\frac{1}{2}\right]2^{-(i+1)}$
$\chi^{1}_{70}=\sum_{i=0}^{I}\delta\left[\frac{3}{2}-\left\|(-1x_{i-1}+4x_{i}+2x_{i+1}-3)\right\|\right]2^{-(i+1)}$	$\chi^{1}_{78}=\sum_{i=0}^{I}\delta\left[1-\left\|\left(-\frac{3}{2}+\left\|(3x_{i-1}-1x_{i}+2x_{i+1})\right\|\right)\right\|\right]2^{-(i+1)}$
$\chi^{1}_{71}=\sum_{i=0}^{I}\delta\left[1-\left\|\left(\frac{3}{2}-\left\|(-4x_{i-1}+1x_{i}-2x_{i+1}+1)\right\|\right)\right\|\right]2^{-(i+1)}$	$\chi^{1}_{79}=\sum_{i=0}^{I}\delta\left[-3x_{i-1}+1x_{i}-1x_{i+1}+\frac{5}{2}\right]2^{-(i+1)}$

Table 1. (*Continued*)

$\chi^{1}_{80}=\sum_{i=0}^{I}\delta\left[1x_{i-1}+0x_i-1x_{i+1}-\frac{1}{2}\right]2^{-(i+1)}$	$\chi^{1}_{88}=\sum_{i=0}^{I}\delta\left[\frac{3}{2}-\left\lvert(-4x_{i-1}-1x_i-2x_{i+1}+4)\right\rvert\right]2^{-(i+1)}$
$\chi^{1}_{81}=\sum_{i=0}^{I}\delta\left[1x_{i-1}-1x_i-2x_{i+1}+\frac{1}{2}\right]2^{-(i+1)}$	$\chi^{1}_{89}=\sum_{i=0}^{I}\delta\left[1-\left\lvert(1x_{i-1}-1x_i+2x_{i+1}-\frac{1}{2})\right\rvert\right]2^{-(i+1)}$
$\chi^{1}_{82}=\sum_{i=0}^{I}\delta\left[\frac{3}{2}-\left\lvert(-2x_{i-1}-1x_i-4x_{i+1}+3)\right\rvert\right]2^{-(i+1)}$	$\chi^{1}_{90}=\sum_{i=0}^{I}\delta\left[\frac{1}{2}-\left\lvert(1x_{i-1}+0x_i+1x_{i+1}-1)\right\rvert\right]2^{-(i+1)}$
$\chi^{1}_{83}=\sum_{i=0}^{I}\delta\left[1-\left\lvert(\frac{3}{2}-\left\lvert(-3x_{i-1}+4x_i-2x_{i+1}+1)\right\rvert)\right\rvert\right]2^{-(i+1)}$	$\chi^{1}_{91}=\sum_{i=0}^{I}\delta\left[\frac{3}{2}-\left\lvert(-2x_{i-1}+1x_i-2x_{i+1}+1)\right\rvert\right]2^{-(i+1)}$
$\chi^{1}_{84}=\sum_{i=0}^{I}\delta\left[1x_{i-1}+1x_i-2x_{i+1}-\frac{1}{2}\right]2^{-(i+1)}$	$\chi^{1}_{92}=\sum_{i=0}^{I}\delta\left[1-\left\lvert(\frac{3}{2}-\left\lvert(1x_{i-1}-2x_i+4x_{i+1})\right\rvert)\right\rvert\right]2^{-(i+1)}$
$\chi^{1}_{85}=\sum_{i=0}^{I}\delta\left[0x_{i-1}+0x_i-1x_{i+1}+\frac{1}{2}\right]2^{-(i+1)}$	$\chi^{1}_{93}=\sum_{i=0}^{I}\delta\left[-1x_{i-1}+1x_i-3x_{i+1}+\frac{5}{2}\right]2^{-(i+1)}$
$\chi^{1}_{86}=\sum_{i=0}^{I}\delta\left[1-\left\lvert(-1x_{i-1}-1x_i-2x_{i+1}+\frac{3}{2})\right\rvert\right]2^{-(i+1)}$	$\chi^{1}_{94}=\sum_{i=0}^{I}\delta\left[\frac{3}{2}-\left\lvert(-2x_{i-1}-1x_i-2x_{i+1}+2)\right\rvert\right]2^{-(i+1)}$
$\chi^{1}_{87}=\sum_{i=0}^{I}\delta\left[-1x_{i-1}-1x_i-3x_{i+1}+\frac{7}{2}\right]2^{-(i+1)}$	$\chi^{1}_{95}=\sum_{i=0}^{I}\delta\left[-1x_{i-1}+0x_i-1x_{i+1}+\frac{3}{2}\right]2^{-(i+1)}$

Table 1. (*Continued*)

$\chi^{1}_{[96]}=\sum_{i=0}^{I}\delta\left[\frac{1}{2}-\left\lvert(-2x_{i-1}+1x_i+1x_{i+1}+1)\right\rvert\right]2^{-(i+1)}$	$\chi^{1}_{[104]}=\sum_{i=0}^{I}\delta\left[\frac{1}{2}-\left\lvert(-1x_{i-1}-1x_i-1x_{i+1}+2)\right\rvert\right]2^{-(i+1)}$
$\chi^{1}_{[97]}=\sum_{i=0}^{I}\delta\left[\frac{1}{2}-\left\lvert(-1x_{i-1}+1x_i+1x_{i+1})\right\rvert\right]2^{-(i+1)}$	$\chi^{1}_{[105]}=\sum_{i=0}^{I}\delta\left[\frac{1}{2}-\left\lvert\left(1-\left\lvert(-1x_{i-1}+1x_i-1x_{i+1}+1)\right\rvert\right)\right\rvert\right]2^{-(i+1)}$
$\chi^{1}_{[98]}=\sum_{i=0}^{I}\delta\left[\frac{3}{2}-\left\lvert(-1x_{i-1}-2x_i-4x_{i+1}+4)\right\rvert\right]2^{-(i+1)}$	$\chi^{1}_{[106]}=\sum_{i=0}^{I}\delta\left[1-\left\lvert(1x_{i-1}+1x_i+2x_{i+1}-\frac{5}{2})\right\rvert\right]2^{-(i+1)}$
$\chi^{1}_{[99]}=\sum_{i=0}^{I}\delta\left[1-\left\lvert(-1x_{i-1}+2x_i+1x_{i+1}-\frac{1}{2})\right\rvert\right]2^{-(i+1)}$	$\chi^{1}_{[107]}=\sum_{i=0}^{I}\delta\left[-\frac{1}{2}+\left\lvert(-1x_{i-1}-1x_i+1x_{i+1}+1)\right\rvert\right]2^{-(i+1)}$
$\chi^{1}_{[100]}=\sum_{i=0}^{I}\delta\left[\frac{3}{2}-\left\lvert(-1x_{i-1}-4x_i-2x_{i+1}+4)\right\rvert\right]2^{-(i+1)}$	$\chi^{1}_{[108]}=\sum_{i=0}^{I}\delta\left[1-\left\lvert(-1x_{i-1}-2x_i-1x_{i+1}+\frac{5}{2})\right\rvert\right]2^{-(i+1)}$
$\chi^{1}_{[101]}=\sum_{i=0}^{I}\delta\left[1-\left\lvert(1x_{i-1}-1x_i-2x_{i+1}+\frac{1}{2})\right\rvert\right]2^{-(i+1)}$	$\chi^{1}_{[109]}=\sum_{i=0}^{I}\delta\left[-\frac{1}{2}+\left\lvert(-1x_{i-1}+1x_i-1x_{i+1}+1)\right\rvert\right]2^{-(i+1)}$
$\chi^{1}_{[102]}=\sum_{i=0}^{I}\delta\left[\frac{1}{2}-\left\lvert(0x_{i-1}+1x_i+1x_{i+1}-1)\right\rvert\right]2^{-(i+1)}$	$\chi^{1}_{[110]}=\sum_{i=0}^{I}\delta\left[-1+\left\lvert(1x_{i-1}+2x_i-3x_{i+1}-\frac{1}{2})\right\rvert\right]2^{-(i+1)}$
$\chi^{1}_{[103]}=\sum_{i=0}^{I}\delta\left[\frac{3}{2}-\left\lvert(-1x_{i-1}+2x_i+2x_{i+1}-1)\right\rvert\right]2^{-(i+1)}$	$\chi^{1}_{[111]}=\sum_{i=0}^{I}\delta\left[-\frac{1}{2}+\left\lvert(1x_{i-1}-2x_i+2x_{i+1}-1)\right\rvert\right]2^{-(i+1)}$

Table 1. (*Continued*)

$\chi^{1}_{[112]}=\sum_{i=0}^{I}\delta\left[2x_{i-1}-1x_i-1x_{i+1}-\frac{1}{2}\right]2^{-(i+1)}$	$\chi^{1}_{[120]}=\sum_{i=0}^{I}\delta\left[1-\left\lvert(2x_{i-1}+1x_i+1x_{i+1}-\frac{5}{2})\right\rvert\right]2^{-(i+1)}$
$\chi^{1}_{[113]}=\sum_{i=0}^{I}\delta\left[1x_{i-1}-1x_i-1x_{i+1}+\frac{1}{2}\right]2^{-(i+1)}$	$\chi^{1}_{[121]}=\sum_{i=0}^{I}\delta\left[-\frac{1}{2}+\left\lvert(-1x_{i-1}+1x_i+1x_{i+1}-1)\right\rvert\right]2^{-(i+1)}$
$\chi^{1}_{[114]}=\sum_{i=0}^{I}\delta\left[1-\left\lvert(\frac{3}{2}-\left\lvert(-4x_{i-1}+2x_i-1x_{i+1}+3)\right\rvert)\right\rvert\right]2^{-(i+1)}$	$\chi^{1}_{[122]}=\sum_{i=0}^{I}\delta\left[\frac{3}{2}-\left\lvert(-2x_{i-1}-1x_i-2x_{i+1}+3)\right\rvert\right]2^{-(i+1)}$
$\chi^{1}_{[115]}=\sum_{i=0}^{I}\delta\left[1x_{i-1}-3x_i-1x_{i+1}+\frac{5}{2}\right]2^{-(i+1)}$	$\chi^{1}_{[123]}=\sum_{i=0}^{I}\delta\left[-\frac{1}{2}+\left\lvert(2x_{i-1}+1x_i-2x_{i+1}-1)\right\rvert\right]2^{-(i+1)}$
$\chi^{1}_{[116]}=\sum_{i=0}^{I}\delta\left[1-\left\lvert(\frac{3}{2}-\left\lvert(-4x_{i-1}-1x_i+2x_{i+1}+3)\right\rvert)\right\rvert\right]2^{-(i+1)}$	$\chi^{1}_{[124]}=\sum_{i=0}^{I}\delta\left[\frac{3}{2}-\left\lvert(2x_{i-1}+2x_i+1x_{i+1}-3)\right\rvert\right]2^{-(i+1)}$
$\chi^{1}_{[117]}=\sum_{i=0}^{I}\delta\left[1x_{i-1}-1x_i-3x_{i+1}+\frac{5}{2}\right]2^{-(i+1)}$	$\chi^{1}_{[125]}=\sum_{i=0}^{I}\delta\left[-\frac{1}{2}+\left\lvert(-1x_{i-1}+1x_i+2x_{i+1}-2)\right\rvert\right]2^{-(i+1)}$
$\chi^{1}_{[118]}=\sum_{i=0}^{I}\delta\left[\frac{3}{2}-\left\lvert(-1x_{i-1}-2x_i-2x_{i+1}+2)\right\rvert\right]2^{-(i+1)}$	$\chi^{1}_{[126]}=\sum_{i=0}^{I}\delta\left[1-\left\lvert(-1x_{i-1}-1x_i-1x_{i+1}+\frac{3}{2})\right\rvert\right]2^{-(i+1)}$
$\chi^{1}_{[119]}=\sum_{i=0}^{I}\delta\left[0x_{i-1}-1x_i-1x_{i+1}+\frac{3}{2}\right]2^{-(i+1)}$	$\chi^{1}_{[127]}=\sum_{i=0}^{I}\delta\left[-1x_{i-1}-1x_i-1x_{i+1}+\frac{5}{2}\right]2^{-(i+1)}$

Table 1. (*Continued*)

$\chi^{1}_{128}=\sum_{i=0}^{I}\delta\left[1x_{i-1}+1x_{i}+1x_{i+1}-\frac{5}{2}\right]2^{-(i+1)}$	$\chi^{1}_{136}=\sum_{i=0}^{I}\delta\left[0x_{i-1}+1x_{i}+1x_{i+1}-\frac{3}{2}\right]2^{-(i+1)}$
$\chi^{1}_{129}=\sum_{i=0}^{I}\delta\left[-1+\left\lvert(1x_{i-1}+1x_{i}+1x_{i+1}-\frac{3}{2})\right\rvert\right]2^{-(i+1)}$	$\chi^{1}_{137}=\sum_{i=0}^{I}\delta\left[\frac{3}{2}-\left\lvert(-1x_{i-1}-2x_{i}+4x_{i+1}-1)\right\rvert\right]2^{-(i+1)}$
$\chi^{1}_{130}=\sum_{i=0}^{I}\delta\left[\frac{1}{2}-\left\lvert(-1x_{i-1}+1x_{i}-2x_{i+1}+2)\right\rvert\right]2^{-(i+1)}$	$\chi^{1}_{138}=\sum_{i=0}^{I}\delta\left[-1x_{i-1}+1x_{i}+2x_{i+1}-\frac{3}{2}\right]2^{-(i+1)}$
$\chi^{1}_{131}=\sum_{i=0}^{I}\delta\left[\frac{3}{2}-\left\lvert(4x_{i-1}-2x_{i}-1x_{i+1})\right\rvert\right]2^{-(i+1)}$	$\chi^{1}_{139}=\sum_{i=0}^{I}\delta\left[1-\left\lvert(-\frac{3}{2}+\left\lvert(-1x_{i-1}-2x_{i}+3x_{i+1}-2)\right\rvert)\right\rvert\right]2^{-(i+1)}$
$\chi^{1}_{132}=\sum_{i=0}^{I}\delta\left[\frac{1}{2}-\left\lvert(2x_{i-1}-1x_{i}-2x_{i+1}+1)\right\rvert\right]2^{-(i+1)}$	$\chi^{1}_{140}=\sum_{i=0}^{I}\delta\left[-1x_{i-1}+2x_{i}+1x_{i+1}-\frac{3}{2}\right]2^{-(i+1)}$
$\chi^{1}_{133}=\sum_{i=0}^{I}\delta\left[\frac{3}{2}-\left\lvert(-2x_{i-1}-1x_{i}+4x_{i+1})\right\rvert\right]2^{-(i+1)}$	$\chi^{1}_{141}=\sum_{i=0}^{I}\delta\left[1-\left\lvert(\frac{3}{2}-\left\lvert(-2x_{i-1}-4x_{i}+3x_{i+1}+2)\right\rvert)\right\rvert\right]2^{-(i+1)}$
$\chi^{1}_{134}=\sum_{i=0}^{I}\delta\left[\frac{1}{2}-\left\lvert(1x_{i-1}-1x_{i}-1x_{i+1}+1)\right\rvert\right]2^{-(i+1)}$	$\chi^{1}_{142}=\sum_{i=0}^{I}\delta\left[-1x_{i-1}+1x_{i}+1x_{i+1}-\frac{1}{2}\right]2^{-(i+1)}$
$\chi^{1}_{135}=\sum_{i=0}^{I}\delta\left[1-\left\lvert(2x_{i-1}-1x_{i}-1x_{i+1}+\frac{1}{2})\right\rvert\right]2^{-(i+1)}$	$\chi^{1}_{143}=\sum_{i=0}^{I}\delta\left[-3x_{i-1}+1x_{i}+1x_{i+1}+\frac{3}{2}\right]2^{-(i+1)}$

Table 1. (*Continued*)

$\chi^{1}_{[144]}=\sum_{i=0}^{I}\delta\left[\frac{1}{2}-\left\lvert(-2x_{i-1}+1x_i-1x_{i+1}+2)\right\rvert\right]2^{-(i+1)}$	$\chi^{1}_{[152]}=\sum_{i=0}^{I}\delta\left[\frac{3}{2}-\left\lvert(1x_{i-1}+4x_i-2x_{i+1}-2)\right\rvert\right]2^{-(i+1)}$
$\chi^{1}_{[145]}=\sum_{i=0}^{I}\delta\left[\frac{3}{2}-\left\lvert(-1x_{i-1}-2x_i+4x_{i+1})\right\rvert\right]2^{-(i+1)}$	$\chi^{1}_{[153]}=\sum_{i=0}^{I}\delta\left[\frac{1}{2}-\left\lvert(0x_{i-1}-1x_i+1x_{i+1})\right\rvert\right]2^{-(i+1)}$
$\chi^{1}_{[146]}=\sum_{i=0}^{I}\delta\left[\frac{1}{2}-\left\lvert(1x_{i-1}-1x_i+1x_{i+1}-1)\right\rvert\right]2^{-(i+1)}$	$\chi^{1}_{[154]}=\sum_{i=0}^{I}\delta\left[1-\left\lvert(1x_{i-1}-1x_i+2x_{i+1}-\frac{3}{2})\right\rvert\right]2^{-(i+1)}$
$\chi^{1}_{[147]}=\sum_{i=0}^{I}\delta\left[1-\left\lvert(1x_{i-1}-2x_i+1x_{i+1}-\frac{1}{2})\right\rvert\right]2^{-(i+1)}$	$\chi^{1}_{[155]}=\sum_{i=0}^{I}\delta\left[\frac{3}{2}-\left\lvert(-1x_{i-1}+2x_i-2x_{i+1}+1)\right\rvert\right]2^{-(i+1)}$
$\chi^{1}_{[148]}=\sum_{i=0}^{I}\delta\left[\frac{1}{2}-\left\lvert(-1x_{i-1}-1x_i+1x_{i+1}+1)\right\rvert\right]2^{-(i+1)}$	$\chi^{1}_{[156]}=\sum_{i=0}^{I}\delta\left[1-\left\lvert(1x_{i-1}+2x_i-1x_{i+1}-\frac{3}{2})\right\rvert\right]2^{-(i+1)}$
$\chi^{1}_{[149]}=\sum_{i=0}^{I}\delta\left[1-\left\lvert(-1x_{i-1}-1x_i+2x_{i+1}+\frac{1}{2})\right\rvert\right]2^{-(i+1)}$	$\chi^{1}_{[157]}=\sum_{i=0}^{I}\delta\left[\frac{3}{2}-\left\lvert(1x_{i-1}+2x_i-2x_{i+1}-1)\right\rvert\right]2^{-(i+1)}$
$\chi^{1}_{[150]}=\sum_{i=0}^{I}\delta\left[\frac{3}{2}-\left\lvert(\frac{7}{2}-\left\lvert(-4x_{i-1}-2x_i+4x_{i+1}-\frac{1}{2})\right\rvert)\right\rvert\right]2^{-(i+1)}$	$\chi^{1}_{[158]}=\sum_{i=0}^{I}\delta\left[-\frac{1}{2}+\left\lvert(1x_{i-1}-1x_i-1x_{i+1})\right\rvert\right]2^{-(i+1)}$
$\chi^{1}_{[151]}=\sum_{i=0}^{I}\delta\left[-\frac{1}{2}+\left\lvert(1x_{i-1}+1x_i+1x_{i+1}-2)\right\rvert\right]2^{-(i+1)}$	$\chi^{1}_{[159]}=\sum_{i=0}^{I}\delta\left[-\frac{1}{2}+\left\lvert(-2x_{i-1}+1x_i+1x_{i+1}+1)\right\rvert\right]2^{-(i+1)}$

Table 1. (*Continued*)

$$\chi^{1}_{160}=\sum_{i=0}^{I}\delta\left[1x_{i-1}+0x_{i}+1x_{i+1}-\frac{3}{2}\right]2^{-(i+1)}$$

$$\chi^{1}_{161}=\sum_{i=0}^{I}\delta\left[\frac{3}{2}-\left|(2x_{i-1}+1x_{i}-4x_{i+1}+1)\right|\right]2^{-(i+1)}$$

$$\chi^{1}_{162}=\sum_{i=0}^{I}\delta\left[1x_{i-1}-1x_{i}+2x_{i+1}-\frac{3}{2}\right]2^{-(i+1)}$$

$$\chi^{1}_{163}=\sum_{i=0}^{I}\delta\left[1-\left|\left(\frac{3}{2}-\left|(3x_{i-1}-4x_{i}-2x_{i+1}+1)\right|\right)\right|\right]2^{-(i+1)}$$

$$\chi^{1}_{164}=\sum_{i=0}^{I}\delta\left[-\frac{3}{2}+\left|(-2x_{i-1}+1x_{i}-2x_{i+1}+1)\right|\right]2^{-(i+1)}$$

$$\chi^{1}_{165}=\sum_{i=0}^{I}\delta\left[\frac{1}{2}-\left|(-1x_{i-1}+0x_{i}+1x_{i+1})\right|\right]2^{-(i+1)}$$

$$\chi^{1}_{166}=\sum_{i=0}^{I}\delta\left[1-\left|(1x_{i-1}-1x_{i}-2x_{i+1}+\frac{3}{2})\right|\right]2^{-(i+1)}$$

$$\chi^{1}_{167}=\sum_{i=0}^{I}\delta\left[\frac{3}{2}-\left|(-2x_{i-1}+1x_{i}+2x_{i+1}-1)\right|\right]2^{-(i+1)}$$

$$\chi^{1}_{168}=\sum_{i=0}^{I}\delta\left[1x_{i-1}+1x_{i}+2x_{i+1}-\frac{5}{2}\right]2^{-(i+1)}$$

$$\chi^{1}_{169}=\sum_{i=0}^{I}\delta\left[1-\left|(1x_{i-1}+1x_{i}-2x_{i+1}+\frac{1}{2})\right|\right]2^{-(i+1)}$$

$$\chi^{1}_{170}=\sum_{i=0}^{I}\delta\left[0x_{i-1}+0x_{i}+1x_{i+1}-\frac{1}{2}\right]2^{-(i+1)}$$

$$\chi^{1}_{171}=\sum_{i=0}^{I}\delta\left[-1x_{i-1}-1x_{i}+2x_{i+1}+\frac{1}{2}\right]2^{-(i+1)}$$

$$\chi^{1}_{172}=\sum_{i=0}^{I}\delta\left[1-\left|\left(\frac{3}{2}-\left|(-3x_{i-1}-4x_{i}+2x_{i+1}+3)\right|\right)\right|\right]2^{-(i+1)}$$

$$\chi^{1}_{173}=\sum_{i=0}^{I}\delta\left[\frac{3}{2}-\left|(-2x_{i-1}-1x_{i}+2x_{i+1})\right|\right]2^{-(i+1)}$$

$$\chi^{1}_{174}=\sum_{i=0}^{I}\delta\left[-1x_{i-1}+1x_{i}+2x_{i+1}-\frac{1}{2}\right]2^{-(i+1)}$$

$$\chi^{1}_{175}=\sum_{i=0}^{I}\delta\left[-1x_{i-1}+0x_{i}+1x_{i+1}+\frac{1}{2}\right]2^{-(i+1)}$$

Table 1. (*Continued*)

$$\chi^{1}_{[176]}=\sum_{i=0}^{I}\delta\left[2x_{i-1}-1x_{i}+1x_{i+1}-\frac{3}{2}\right]2^{-(i+1)}$$

$$\chi^{1}_{[177]}=\sum_{i=0}^{I}\delta\left[1-\left|\left(-\frac{3}{2}+\left|(4x_{i-1}-2x_{i}-1x_{i+1}-2)\right|\right)\right|\right]2^{-(i+1)}$$

$$\chi^{1}_{[178]}=\sum_{i=0}^{I}\delta\left[1x_{i-1}-1x_{i}+1x_{i+1}-\frac{1}{2}\right]2^{-(i+1)}$$

$$\chi^{1}_{[179]}=\sum_{i=0}^{I}\delta\left[1x_{i-1}-3x_{i}+1x_{i+1}+\frac{3}{2}\right]2^{-(i+1)}$$

$$\chi^{1}_{[180]}=\sum_{i=0}^{I}\delta\left[1-\left|(-2x_{i-1}-1x_{i}+1x_{i+1}+\frac{3}{2})\right|\right]2^{-(i+1)}$$

$$\chi^{1}_{[181]}=\sum_{i=0}^{I}\delta\left[\frac{3}{2}-\left|(2x_{i-1}+1x_{i}-2x_{i+1}-1)\right|\right]2^{-(i+1)}$$

$$\chi^{1}_{[182]}=\sum_{i=0}^{I}\delta\left[-\frac{1}{2}+\left|(-1x_{i-1}+1x_{i}-1x_{i+1})\right|\right]2^{-(i+1)}$$

$$\chi^{1}_{[183]}=\sum_{i=0}^{I}\delta\left[-\frac{1}{2}+\left|(1x_{i-1}-2x_{i}+1x_{i+1}+1)\right|\right]2^{-(i+1)}$$

$$\chi^{1}_{[184]}=\sum_{i=0}^{I}\delta\left[1-\left|\left(-\frac{3}{2}+\left|(1x_{i-1}-2x_{i}+3x_{i+1}-3)\right|\right)\right|\right]2^{-(i+1)}$$

$$\chi^{1}_{[185]}=\sum_{i=0}^{I}\delta\left[\frac{3}{2}-\left|(-1x_{i-1}-2x_{i}+2x_{i+1})\right|\right]2^{-(i+1)}$$

$$\chi^{1}_{[186]}=\sum_{i=0}^{I}\delta\left[1x_{i-1}-1x_{i}+2x_{i+1}-\frac{1}{2}\right]2^{-(i+1)}$$

$$\chi^{1}_{[187]}=\sum_{i=0}^{I}\delta\left[0x_{i-1}-1x_{i}+1x_{i+1}+\frac{1}{2}\right]2^{-(i+1)}$$

$$\chi^{1}_{[188]}=\sum_{i=0}^{I}\delta\left[\frac{3}{2}-\left|(2x_{i-1}+2x_{i}-1x_{i+1}-2)\right|\right]2^{-(i+1)}$$

$$\chi^{1}_{[189]}=\sum_{i=0}^{I}\delta\left[1-\left|(1x_{i-1}+1x_{i}-1x_{i+1}-\frac{1}{2})\right|\right]2^{-(i+1)}$$

$$\chi^{1}_{[190]}=\sum_{i=0}^{I}\delta\left[-\frac{1}{2}+\left|(-2x_{i-1}+2x_{i}+1x_{i+1})\right|\right]2^{-(i+1)}$$

$$\chi^{1}_{[191]}=\sum_{i=0}^{I}\delta\left[-1x_{i-1}-1x_{i}+1x_{i+1}+\frac{3}{2}\right]2^{-(i+1)}$$

Table 1. (*Continued*)

$\chi^{1}_{192}=\sum_{i=0}^{I}\delta\left[1x_{i-1}+1x_{i}+0x_{i+1}-\frac{3}{2}\right]2^{-(i+1)}$	$\chi^{1}_{200}=\sum_{i=0}^{I}\delta\left[1x_{i-1}+2x_{i}+1x_{i+1}-\frac{5}{2}\right]2^{-(i+1)}$
$\chi^{1}_{193}=\sum_{i=0}^{I}\delta\left[\frac{3}{2}-\left\|(4x_{i-1}-2x_{i}-1x_{i+1}-1)\right\|\right]2^{-(i+1)}$	$\chi^{1}_{201}=\sum_{i=0}^{I}\delta\left[1-\left\|(1x_{i-1}-2x_{i}+1x_{i+1}+\frac{1}{2})\right\|\right]2^{-(i+1)}$
$\chi^{1}_{194}=\sum_{i=0}^{I}\delta\left[\frac{3}{2}-\left\|(-2x_{i-1}+4x_{i}+1x_{i+1}-2)\right\|\right]2^{-(i+1)}$	$\chi^{1}_{202}=\sum_{i=0}^{I}\delta\left[1-\left\|(\frac{3}{2}-\left\|(3x_{i-1}-4x_{i}+2x_{i+1})\right\|)\right\|\right]2^{-(i+1)}$
$\chi^{1}_{195}=\sum_{i=0}^{I}\delta\left[\frac{1}{2}-\left\|(-1x_{i-1}+1x_{i}+0x_{i+1})\right\|\right]2^{-(i+1)}$	$\chi^{1}_{203}=\sum_{i=0}^{I}\delta\left[\frac{3}{2}-\left\|(-2x_{i-1}+2x_{i}-1x_{i+1})\right\|\right]2^{-(i+1)}$
$\chi^{1}_{196}=\sum_{i=0}^{I}\delta\left[1x_{i-1}+2x_{i}-1x_{i+1}-\frac{3}{2}\right]2^{-(i+1)}$	$\chi^{1}_{204}=\sum_{i=0}^{I}\delta\left[0x_{i-1}+1x_{i}+0x_{i+1}-\frac{1}{2}\right]2^{-(i+1)}$
$\chi^{1}_{197}=\sum_{i=0}^{I}\delta\left[1-\left\|(\frac{3}{2}-\left\|(-3x_{i-1}+4x_{i}+2x_{i+1}-2)\right\|)\right\|\right]2^{-(i+1)}$	$\chi^{1}_{205}=\sum_{i=0}^{I}\delta\left[-1x_{i-1}+2x_{i}-1x_{i+1}+\frac{1}{2}\right]2^{-(i+1)}$
$\chi^{1}_{198}=\sum_{i=0}^{I}\delta\left[1-\left\|(1x_{i-1}-2x_{i}-1x_{i+1}+\frac{3}{2})\right\|\right]2^{-(i+1)}$	$\chi^{1}_{206}=\sum_{i=0}^{I}\delta\left[-1x_{i-1}+2x_{i}+1x_{i+1}-\frac{1}{2}\right]2^{-(i+1)}$
$\chi^{1}_{199}=\sum_{i=0}^{I}\delta\left[\frac{3}{2}-\left\|(2x_{i-1}-2x_{i}-1x_{i+1}+1)\right\|\right]2^{-(i+1)}$	$\chi^{1}_{207}=\sum_{i=0}^{I}\delta\left[-1x_{i-1}+1x_{i}+0x_{i+1}+\frac{1}{2}\right]2^{-(i+1)}$

Table 1. (*Continued*)

$$\chi^{1}_{208}=\sum_{i=0}^{I}\delta\left[2x_{i-1}+1x_{i}-1x_{i+1}-\frac{3}{2}\right]2^{-(i+1)}$$

$$\chi^{1}_{209}=\sum_{i=0}^{I}\delta\left[1-\left|\left(\frac{3}{2}-\left|(2x_{i-1}+1x_{i}-4x_{i+1}-1)\right|\right)\right|\right]2^{-(i+1)}$$

$$\chi^{1}_{210}=\sum_{i=0}^{I}\delta\left[1-\left|(-2x_{i-1}+1x_{i}-1x_{i+1}+\frac{3}{2})\right|\right]2^{-(i+1)}$$

$$\chi^{1}_{211}=\sum_{i=0}^{I}\delta\left[\frac{3}{2}-\left|(-2x_{i-1}+2x_{i}-1x_{i+1}+1)\right|\right]2^{-(i+1)}$$

$$\chi^{1}_{212}=\sum_{i=0}^{I}\delta\left[1x_{i-1}+1x_{i}-1x_{i+1}-\frac{1}{2}\right]2^{-(i+1)}$$

$$\chi^{1}_{213}=\sum_{i=0}^{I}\delta\left[1x_{i-1}+1x_{i}-3x_{i+1}+\frac{3}{2}\right]2^{-(i+1)}$$

$$\chi^{1}_{214}=\sum_{i=0}^{I}\delta\left[-\frac{1}{2}+\left|(1x_{i-1}+1x_{i}-1x_{i+1})\right|\right]2^{-(i+1)}$$

$$\chi^{1}_{215}=\sum_{i=0}^{I}\delta\left[-\frac{1}{2}+\left|(2x_{i-1}+2x_{i}+1x_{i+1}-3)\right|\right]2^{-(i+1)}$$

$$\chi^{1}_{216}=\sum_{i=0}^{I}\delta\left[1-\left|\left(-\frac{3}{2}+\left|(-3x_{i-1}+1x_{i}-4x_{i+1}+4)\right|\right)\right|\right]2^{-(i+1)}$$

$$\chi^{1}_{217}=\sum_{i=0}^{I}\delta\left[\frac{3}{2}-\left|(-1x_{i-1}+2x_{i}-2x_{i+1})\right|\right]2^{-(i+1)}$$

$$\chi^{1}_{218}=\sum_{i=0}^{I}\delta\left[\frac{3}{2}-\left|(2x_{i-1}-1x_{i}+2x_{i+1}-2)\right|\right]2^{-(i+1)}$$

$$\chi^{1}_{219}=\sum_{i=0}^{I}\delta\left[1-\left|(-1x_{i-1}+1x_{i}-1x_{i+1}+\frac{1}{2})\right|\right]2^{-(i+1)}$$

$$\chi^{1}_{220}=\sum_{i=0}^{I}\delta\left[1x_{i-1}+2x_{i}-1x_{i+1}-\frac{1}{2}\right]2^{-(i+1)}$$

$$\chi^{1}_{221}=\sum_{i=0}^{I}\delta\left[0x_{i-1}+1x_{i}-1x_{i+1}+\frac{1}{2}\right]2^{-(i+1)}$$

$$\chi^{1}_{222}=\sum_{i=0}^{I}\delta\left[-\frac{1}{2}+\left|(-1x_{i-1}-2x_{i}+1x_{i+1})\right|\right]2^{-(i+1)}$$

$$\chi^{1}_{223}=\sum_{i=0}^{I}\delta\left[-1x_{i-1}+1x_{i}-1x_{i+1}+\frac{3}{2}\right]2^{-(i+1)}$$

Table 1. (*Continued*)

$\chi^{1}_{224}=\sum_{i=0}^{I}\delta\left[2x_{i-1}+1x_{i}+1x_{i+1}-\frac{5}{2}\right]2^{-(i+1)}$	$\chi^{1}_{232}=\sum_{i=0}^{I}\delta\left[1x_{i-1}+1x_{i}+1x_{i+1}-\frac{3}{2}\right]2^{-(i+1)}$
$\chi^{1}_{225}=\sum_{i=0}^{I}\delta\left[1-\left\lvert(-2x_{i-1}+1x_{i}+1x_{i+1}+\frac{1}{2})\right\rvert\right]2^{-(i+1)}$	$\chi^{1}_{233}=\sum_{i=0}^{I}\delta\left[-\frac{1}{2}+\left\lvert(1x_{i-1}+1x_{i}+1x_{i+1}-1)\right\rvert\right]2^{-(i+1)}$
$\chi^{1}_{226}=\sum_{i=0}^{I}\delta\left[1-\left\lvert(\frac{3}{2}-\left\lvert(-2x_{i-1}-1x_{i}-4x_{i+1}+5)\right\rvert)\right\rvert\right]2^{-(i+1)}$	$\chi^{1}_{234}=\sum_{i=0}^{I}\delta\left[1x_{i-1}+1x_{i}+2x_{i+1}-\frac{3}{2}\right]2^{-(i+1)}$
$\chi^{1}_{227}=\sum_{i=0}^{I}\delta\left[\frac{3}{2}-\left\lvert(2x_{i-1}-2x_{i}-1x_{i+1})\right\rvert\right]2^{-(i+1)}$	$\chi^{1}_{235}=\sum_{i=0}^{I}\delta\left[-\frac{1}{2}+\left\lvert(2x_{i-1}+2x_{i}+1x_{i+1}-2)\right\rvert\right]2^{-(i+1)}$
$\chi^{1}_{228}=\sum_{i=0}^{I}\delta\left[1-\left\lvert(\frac{3}{2}-\left\lvert(2x_{i-1}+4x_{i}+1x_{i+1}-5)\right\rvert)\right\rvert\right]2^{-(i+1)}$	$\chi^{1}_{236}=\sum_{i=0}^{I}\delta\left[1x_{i-1}+2x_{i}+1x_{i+1}-\frac{3}{2}\right]2^{-(i+1)}$
$\chi^{1}_{229}=\sum_{i=0}^{I}\delta\left[\frac{3}{2}-\left\lvert(-2x_{i-1}+1x_{i}+2x_{i+1})\right\rvert\right]2^{-(i+1)}$	$\chi^{1}_{237}=\sum_{i=0}^{I}\delta\left[-\frac{1}{2}+\left\lvert(2x_{i-1}-1x_{i}+2x_{i+1}-2)\right\rvert\right]2^{-(i+1)}$
$\chi^{1}_{230}=\sum_{i=0}^{I}\delta\left[\frac{3}{2}-\left\lvert(-1x_{i-1}+2x_{i}+2x_{i+1}-2)\right\rvert\right]2^{-(i+1)}$	$\chi^{1}_{238}=\sum_{i=0}^{I}\delta\left[0x_{i-1}+1x_{i}+1x_{i+1}-\frac{1}{2}\right]2^{-(i+1)}$
$\chi^{1}_{231}=\sum_{i=0}^{I}\delta\left[1-\left\lvert(1x_{i-1}-1x_{i}-1x_{i+1}+\frac{1}{2})\right\rvert\right]2^{-(i+1)}$	$\chi^{1}_{239}=\sum_{i=0}^{I}\delta\left[-1x_{i-1}+1x_{i}+1x_{i+1}+\frac{1}{2}\right]2^{-(i+1)}$

Table 1. (*Continued*)

$\chi^{1}_{240} = \sum_{i=0}^{I} \delta\left[1x_{i-1} + 0x_i + 0x_{i+1} - \frac{1}{2}\right] 2^{-(i+1)}$	$\chi^{1}_{248} = \sum_{i=0}^{I} \delta\left[2x_{i-1} + 1x_i + 1x_{i+1} - \frac{3}{2}\right] 2^{-(i+1)}$
$\chi^{1}_{241} = \sum_{i=0}^{I} \delta\left[2x_{i-1} - 1x_i - 1x_{i+1} + \frac{1}{2}\right] 2^{-(i+1)}$	$\chi^{1}_{249} = \sum_{i=0}^{I} \delta\left[-\frac{1}{2} + \left\lvert(2x_{i-1} - 1x_i - 1x_{i+1} + 1)\right\rvert\right] 2^{-(i+1)}$
$\chi^{1}_{242} = \sum_{i=0}^{I} \delta\left[2x_{i-1} - 1x_i + 1x_{i+1} - \frac{1}{2}\right] 2^{-(i+1)}$	$\chi^{1}_{250} = \sum_{i=0}^{I} \delta\left[1x_{i-1} + 0x_i + 1x_{i+1} - \frac{1}{2}\right] 2^{-(i+1)}$
$\chi^{1}_{243} = \sum_{i=0}^{I} \delta\left[1x_{i-1} - 1x_i + 0x_{i+1} + \frac{1}{2}\right] 2^{-(i+1)}$	$\chi^{1}_{251} = \sum_{i=0}^{I} \delta\left[1x_{i-1} - 1x_i + 1x_{i+1} + \frac{1}{2}\right] 2^{-(i+1)}$
$\chi^{1}_{244} = \sum_{i=0}^{I} \delta\left[2x_{i-1} + 1x_i - 1x_{i+1} - \frac{1}{2}\right] 2^{-(i+1)}$	$\chi^{1}_{252} = \sum_{i=0}^{I} \delta\left[1x_{i-1} + 1x_i + 0x_{i+1} - \frac{1}{2}\right] 2^{-(i+1)}$
$\chi^{1}_{245} = \sum_{i=0}^{I} \delta\left[1x_{i-1} + 0x_i - 1x_{i+1} + \frac{1}{2}\right] 2^{-(i+1)}$	$\chi^{1}_{253} = \sum_{i=0}^{I} \delta\left[1x_{i-1} + 1x_i - 1x_{i+1} + \frac{1}{2}\right] 2^{-(i+1)}$
$\chi^{1}_{246} = \sum_{i=0}^{I} \delta\left[-\frac{1}{2} + \left\lvert(-1x_{i-1} + 2x_i - 2x_{i+1})\right\rvert\right] 2^{-(i+1)}$	$\chi^{1}_{254} = \sum_{i=0}^{I} \delta\left[1x_{i-1} + 1x_i + 1x_{i+1} - \frac{1}{2}\right] 2^{-(i+1)}$
$\chi^{1}_{247} = \sum_{i=0}^{I} \delta\left[1x_{i-1} - 1x_i - 1x_{i+1} + \frac{3}{2}\right] 2^{-(i+1)}$	$\chi^{1}_{255} = \sum_{i=0}^{I} \delta\left[0x_{i-1} + 0x_i + 0x_{i+1} + \frac{1}{2}\right] 2^{-(i+1)}$

to $\phi = 1$ corresponding to

$$\begin{array}{cccccc} \{1, & 1, & 1, & \cdots & & 1\}. \\ \uparrow & \uparrow & \uparrow & & & \uparrow \\ x_0 & x_1 & x_2 & & & x_I \end{array}$$

1.2. *Graphs of characteristic functions* $\chi^1_{\boxed{N}}$

For future reference, we have plotted the time-1 characteristic functions $\chi^1_{\boxed{N}}$ for all 256 local rules with $I = 65$, and displayed them in Table 2 showing only 201 points for each rule to avoid clutter. In other words, each graph of $\chi^1_{\boxed{N}}$ in Table 2 shows only 201 values of $\chi^1_{\boxed{N}}$, each one calculated from a 66-bit binary string. To enhance clarity, every pair of adjacent points in each graph are plotted as a small "red" square "$\square$" and a small "blue" square "$\square$" on top of alternating red and blue color bars emanating from each value of $\phi \in [0, 1]$ corresponding to the 201 uniformly distributed points with spacing $\Delta\phi = 0.005$.

A careful examination of Table 2 reveals that adjacent pairs of points of $\chi^1_{\boxed{N}}$ are either located in "close proximity" of each other, or they exhibit an "abrupt jump" from each other. We will henceforth refer to those subintervals where adjacent red and blue squares are close to each other as "*smooth*", and those exhibiting "*abrupt jumps*" as "*discontinuous*". A careful analysis of these subintervals reveal that they extend over a minimum range of $\Delta\phi = 0.25$ for *all* 256 rules. For example, only the second subinterval $\phi \in [0.25, 0.50)$ of rule $\boxed{2}$ is discontinuous. On the other hand, the first and second subintervals $[0, 0.25)$ and $[0.25, 0.50)$ of rule $\boxed{3}$ are discontinuous. For rule $\boxed{110}$, we find only the fourth subinterval $[0.75, 1.00]$ is discontinuous. For rule $\boxed{30}$, we find all four subintervals $[0, 0.25)$, $[0.25, 0.50)$, $[0.50, 0.75)$ and $[0.75, 1.00)$ are discontinuous. Since these properties are quite useful for understanding the global dynamics of local rules, we have divided the area to the right of the equality sign of each characteristic function $\chi^1_{\boxed{N}}$ in Table 1 into the above four corresponding equal parts, and painted each part with a *light blue* background color if the corresponding subinterval has *smooth* adjacent red and blue squares, or in a *light pink* background color if adjacent red and blue squares exhibit *discontinuous* jumps from each other.

1.3. *Deriving the Bernoulli map from* $\chi^1_{\boxed{170}}$

As an application of the explicit formulas listed in Table 1, let us apply the *characteristic function* $\chi^1_{\boxed{170}}$ of $\boxed{170}$ to an $(I+1)$-bit binary string $\{x_0, x_1, x_2, \ldots, x_I\}$ with *decimal* representation

$$\phi = \sum_{i=0}^{I} 2^{-(i+1)} x_i \tag{10}$$

to obtain

$$\begin{aligned} \chi^1_{\boxed{170}}(\phi) &= \sum_{i=0}^{I} 2^{-(i+1)} x_{i+1} = \sum_{j=1}^{I+1} 2^{-j} x_j + x_0 - x_0 \\ &= 2\left[\sum_{j=0}^{I+1} 2^{-(j+1)} x_j\right] - x_0 \\ &= \begin{cases} 2\phi, & \phi < 0.5 \\ 2\phi - 1, & \phi \geq 0.5 \end{cases} \end{aligned} \tag{11}$$

as $I \to \infty$.

It follows from Eq. (11) that the *characteristic function* $\chi^1_{\boxed{170}}$ of the rule $\boxed{170}$ converges to the well-known *Bernoulli map* [Billingsley, 1978]

$$\boxed{\chi^1_{\boxed{170}}(\phi) = 2\phi \bmod 1} \tag{12}$$

as $I \to \infty$.

Since the output of each pixel "i" of rule $\boxed{170}$ in Table 1 is given simply by $y_i = x_{i+1}$, the local rule $\boxed{170}$ consists of simply *copying* the "state" of the pixel "$i+1$" of the *right-neighboring* pixel. We will henceforth call rule $\boxed{170}$ the *right-copycat rule*. The graph of the *right-copycat rule* $\boxed{170}$ is shown in Fig. 3.

1.4. *Deriving inverse Bernoulli map from* $\chi^1_{\boxed{240}}$

Let us apply the *characteristic function* $\chi^1_{\boxed{240}}$ of $\boxed{240}$ from Table 1 to the $(I+1)$-bit binary string ϕ defined in Eq. (10) to obtain

$$\begin{aligned} \chi^1_{\boxed{240}}(\phi) &= \sum_{i=0}^{I} 2^{-(i+1)} x_{i-1} = \frac{1}{2} \sum_{j=-1}^{I-1} 2^{-(j+1)} x_j \\ &= \frac{1}{2}\left[\sum_{j=0}^{I-1} 2^{-(j+1)} x_j\right] + \frac{1}{2} x_I \\ &= \frac{1}{2}\phi + \frac{1}{2} x_I \end{aligned} \tag{13}$$

as $I \to \infty$.

Table 2. Gallery of characteristic functions.

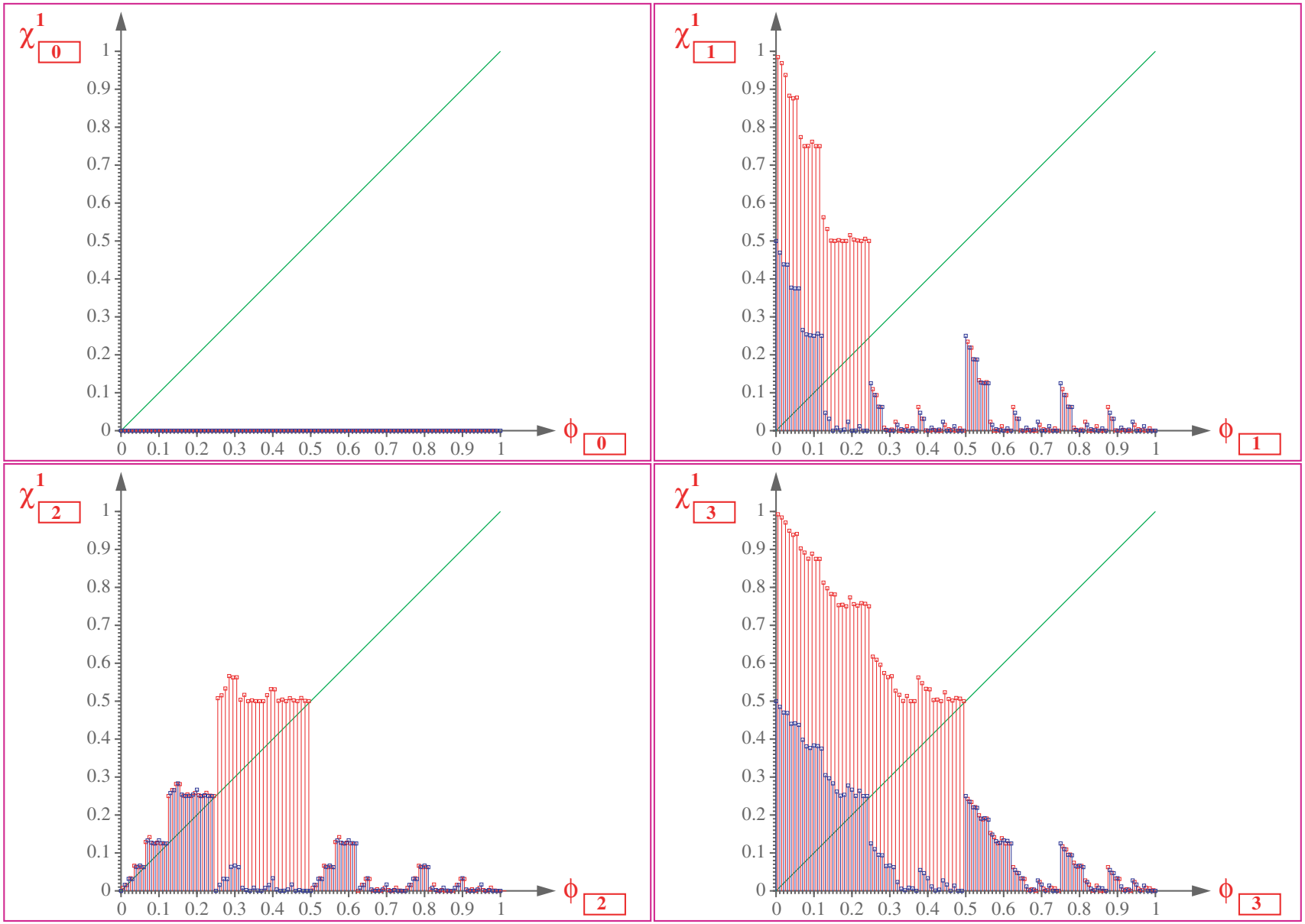


Table 2. (*Continued*)

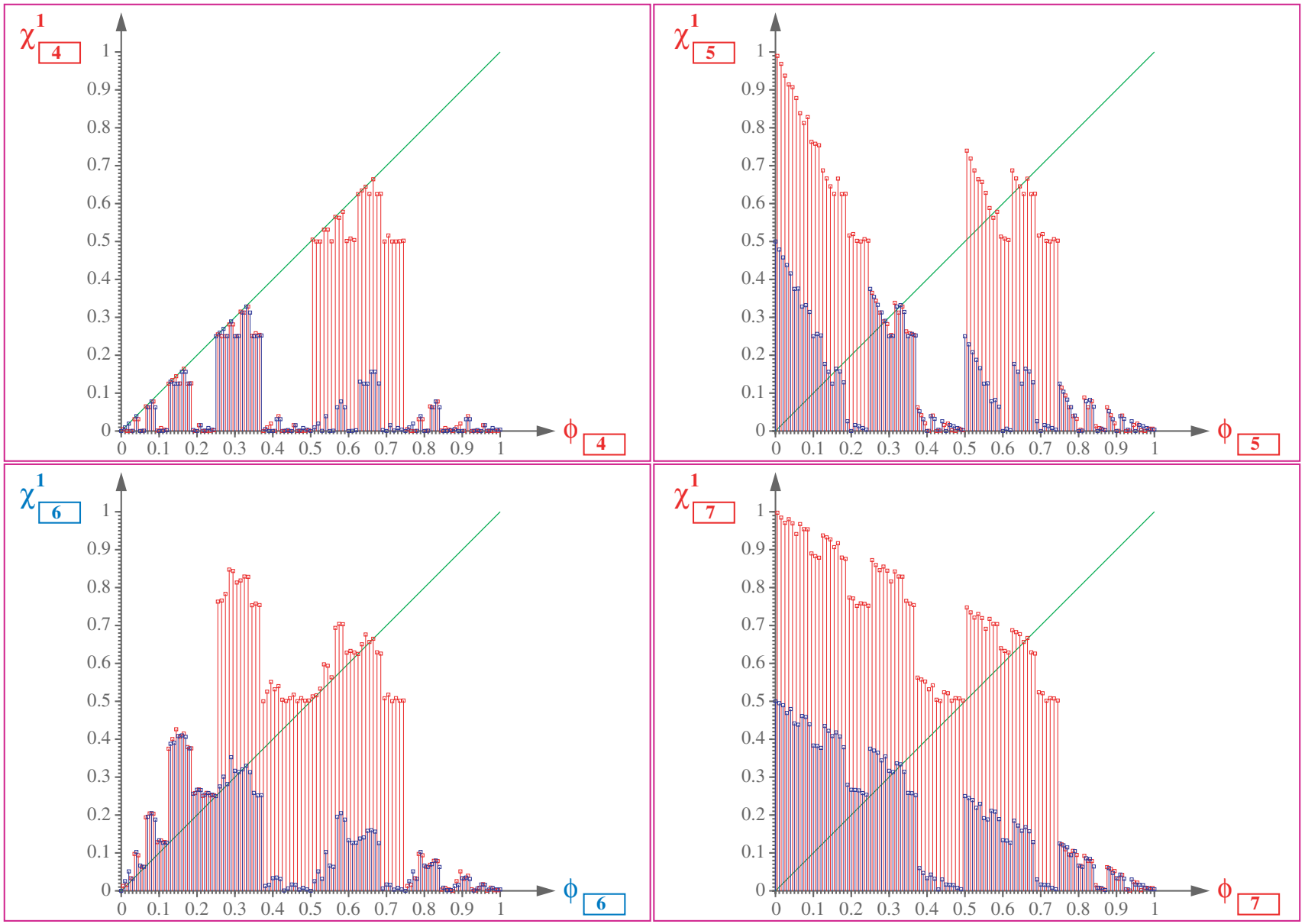


Table 2. (*Continued*)

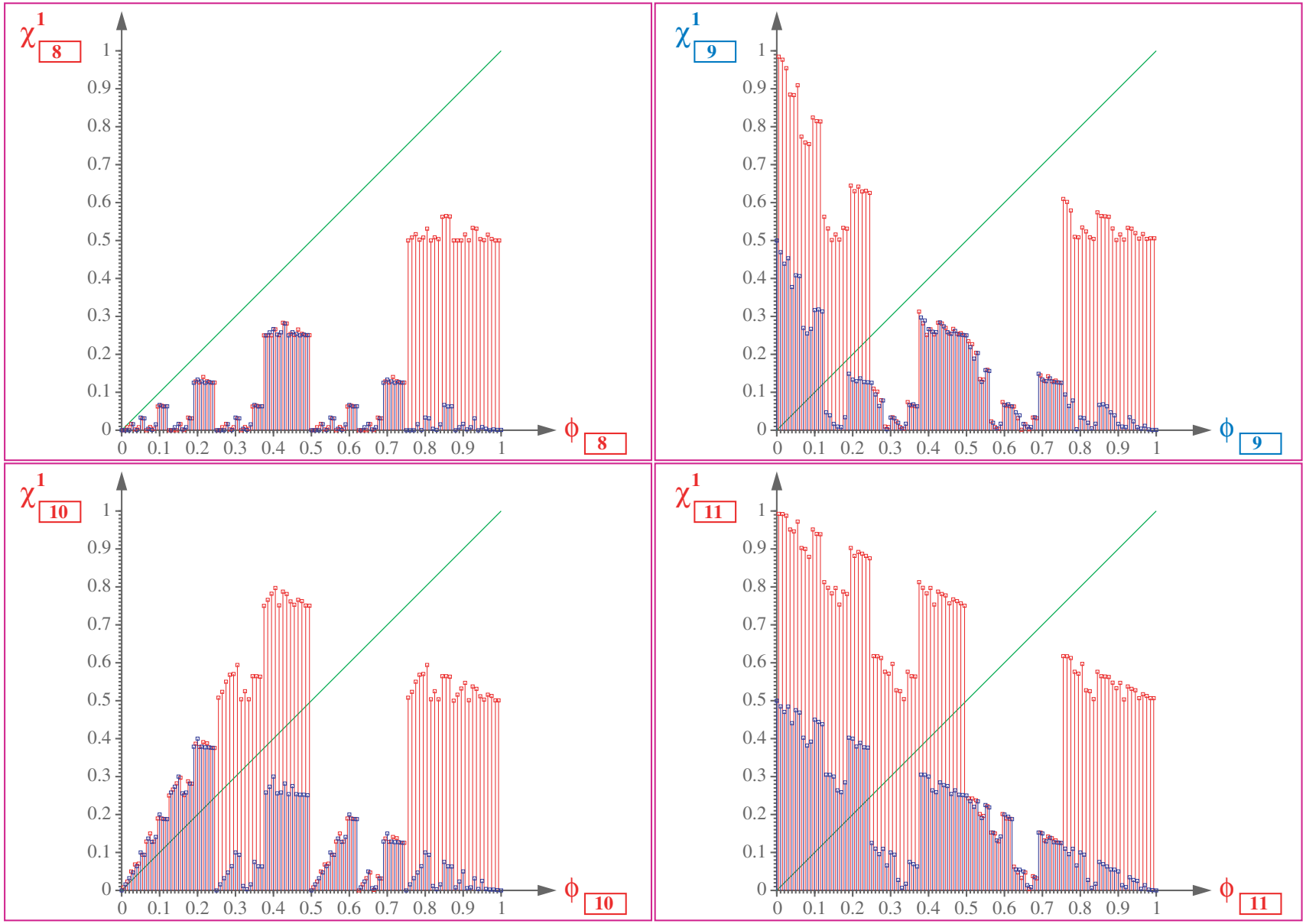


Table 2. (*Continued*)

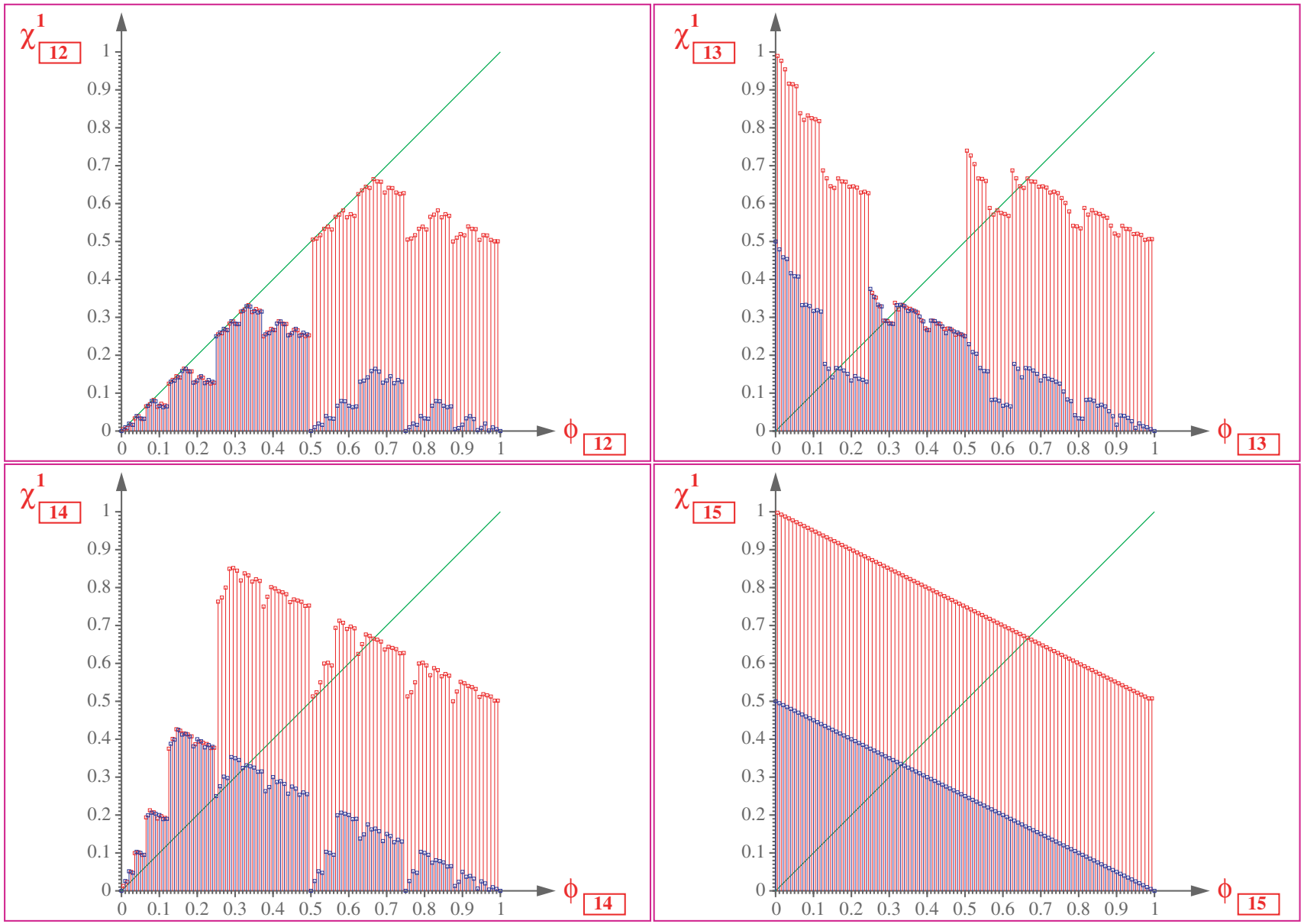


Table 2. (*Continued*)

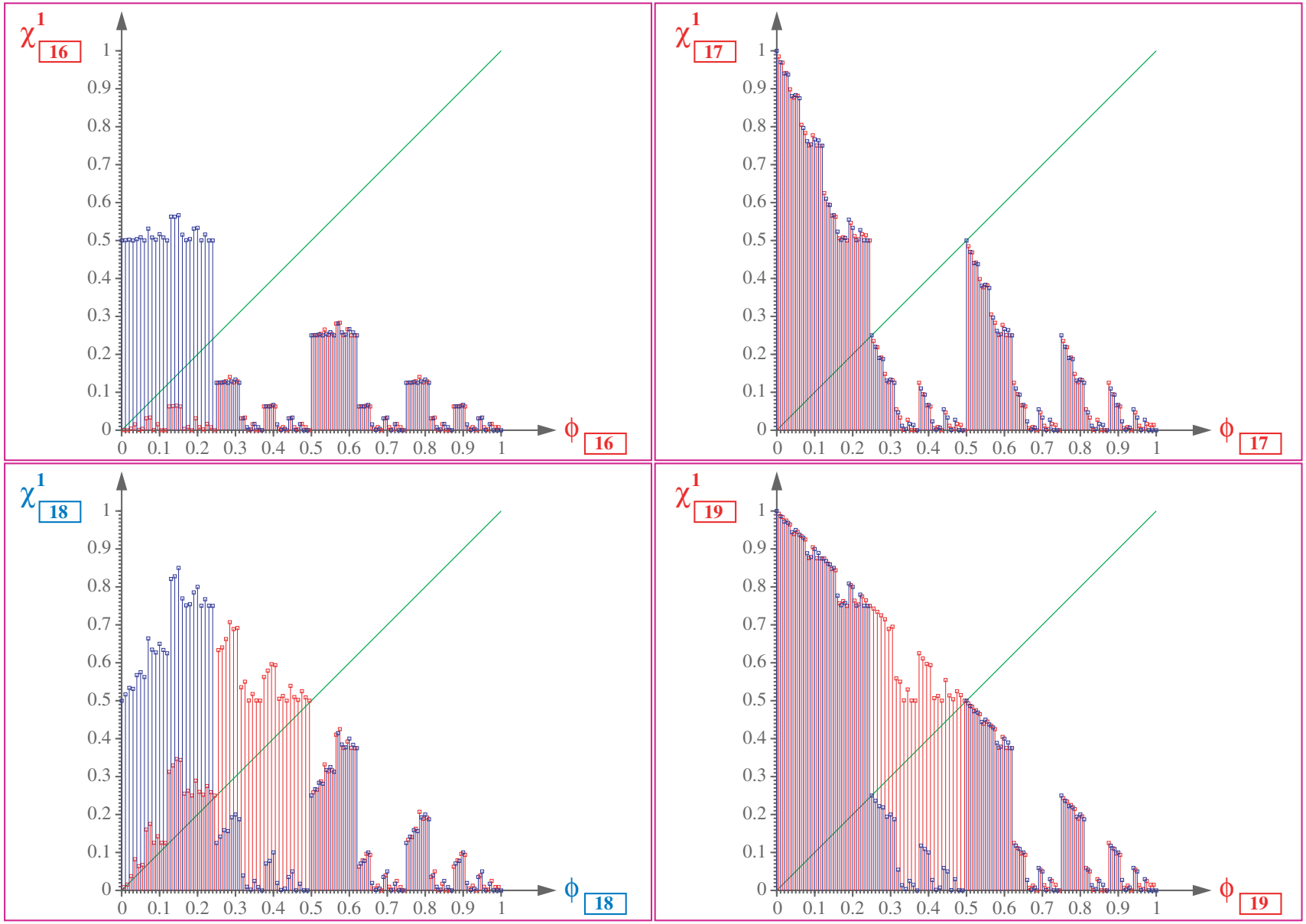


Table 2. (*Continued*)

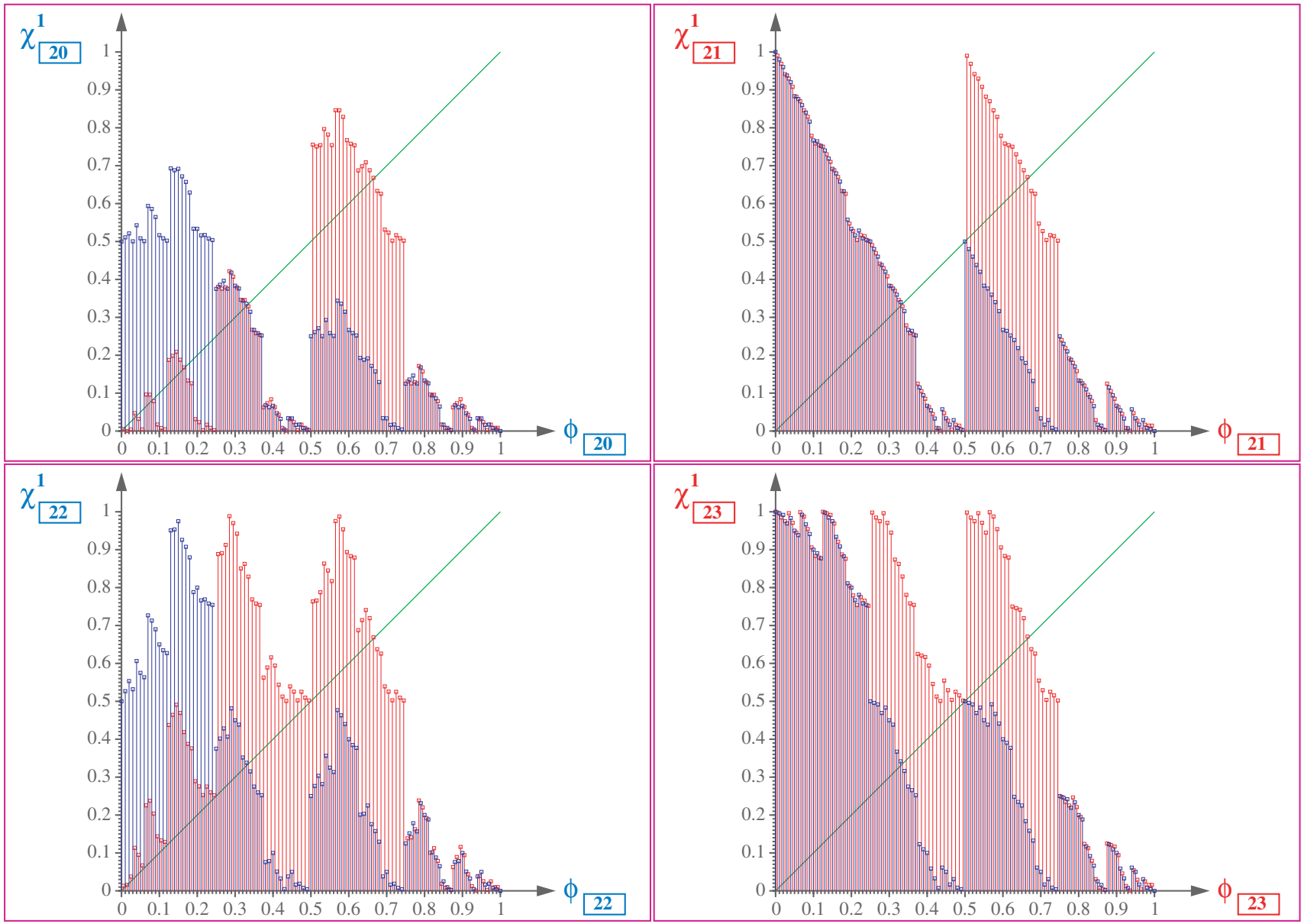


Table 2. (*Continued*)

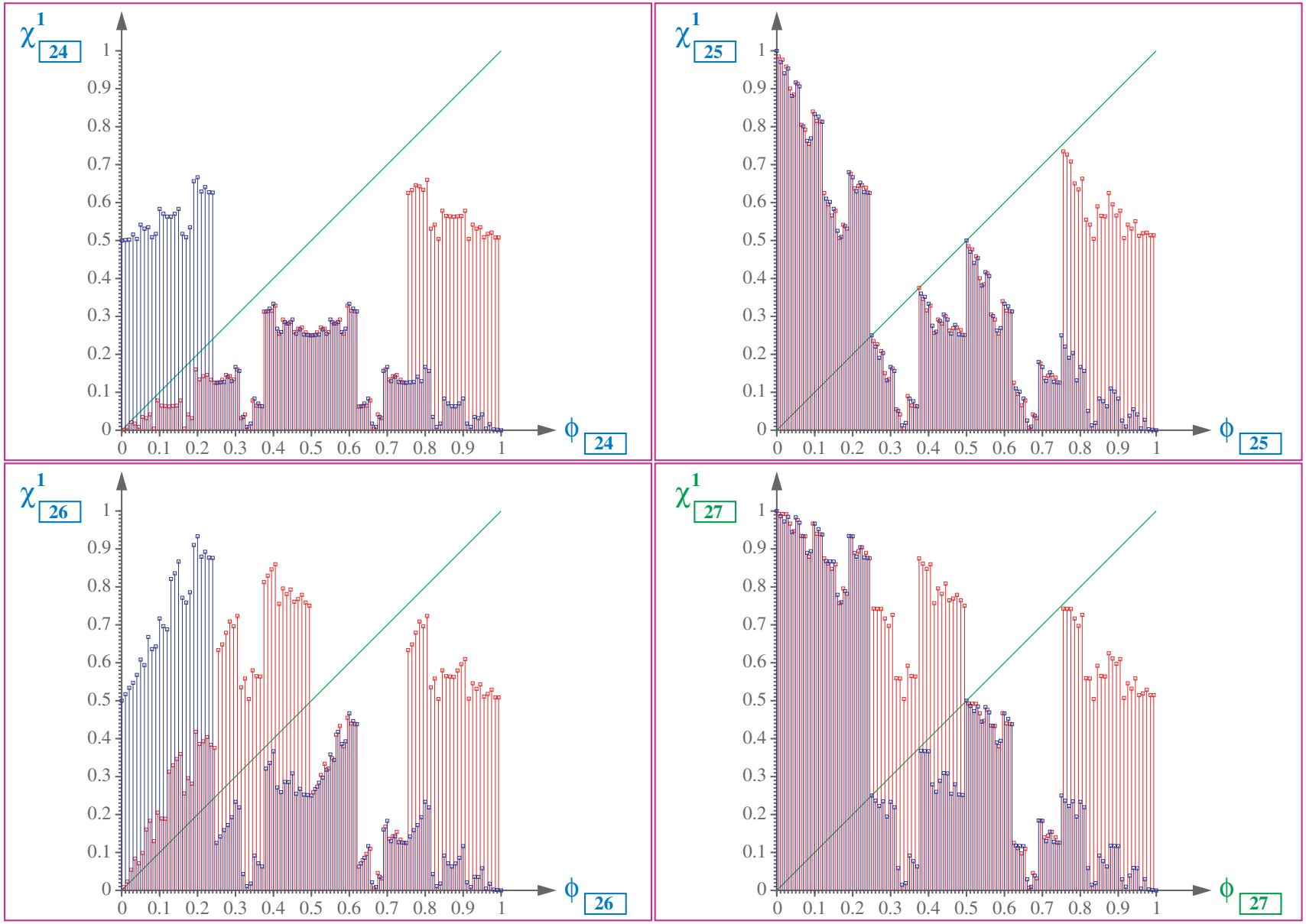


Table 2. (*Continued*)

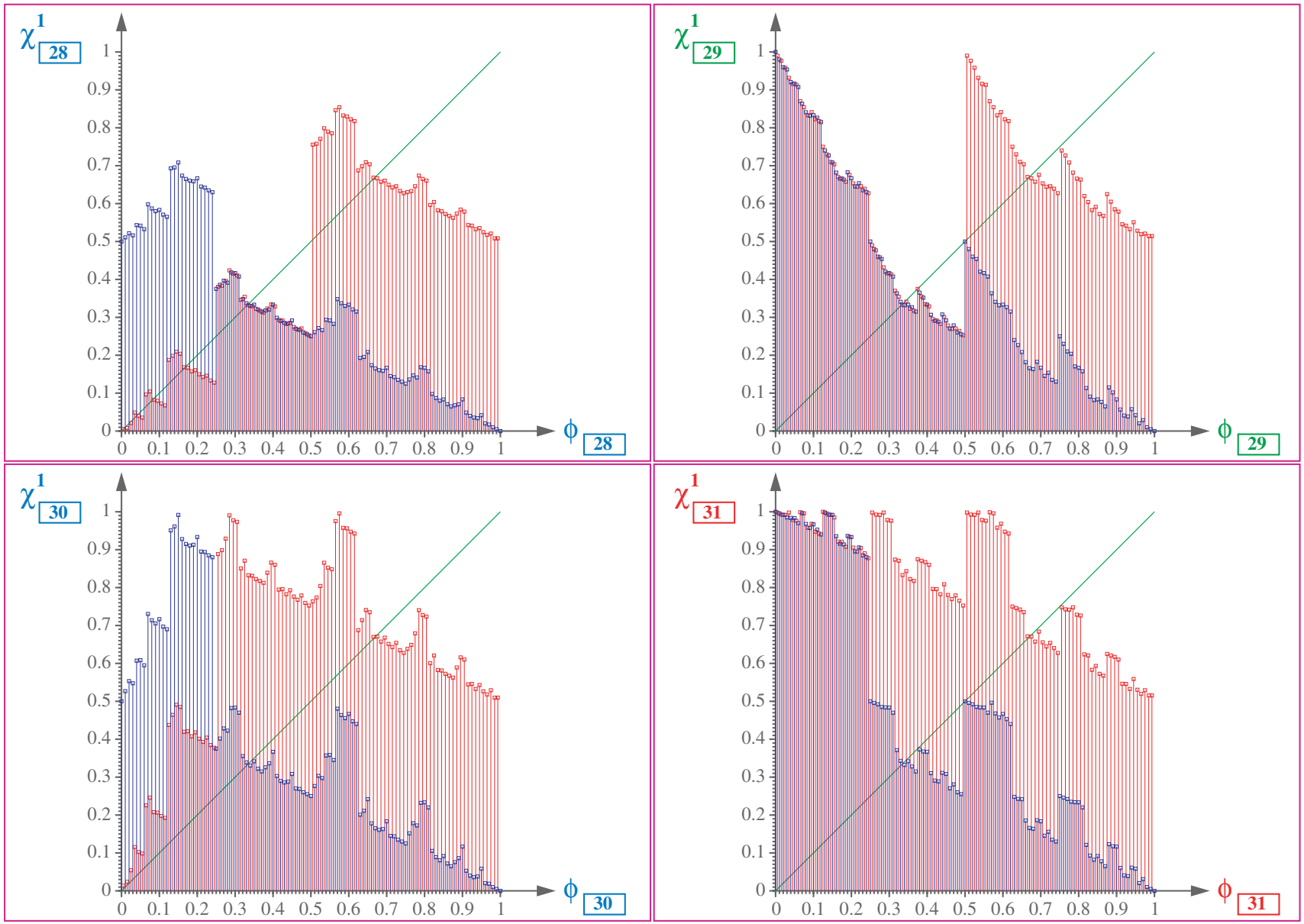


Table 2. (*Continued*)

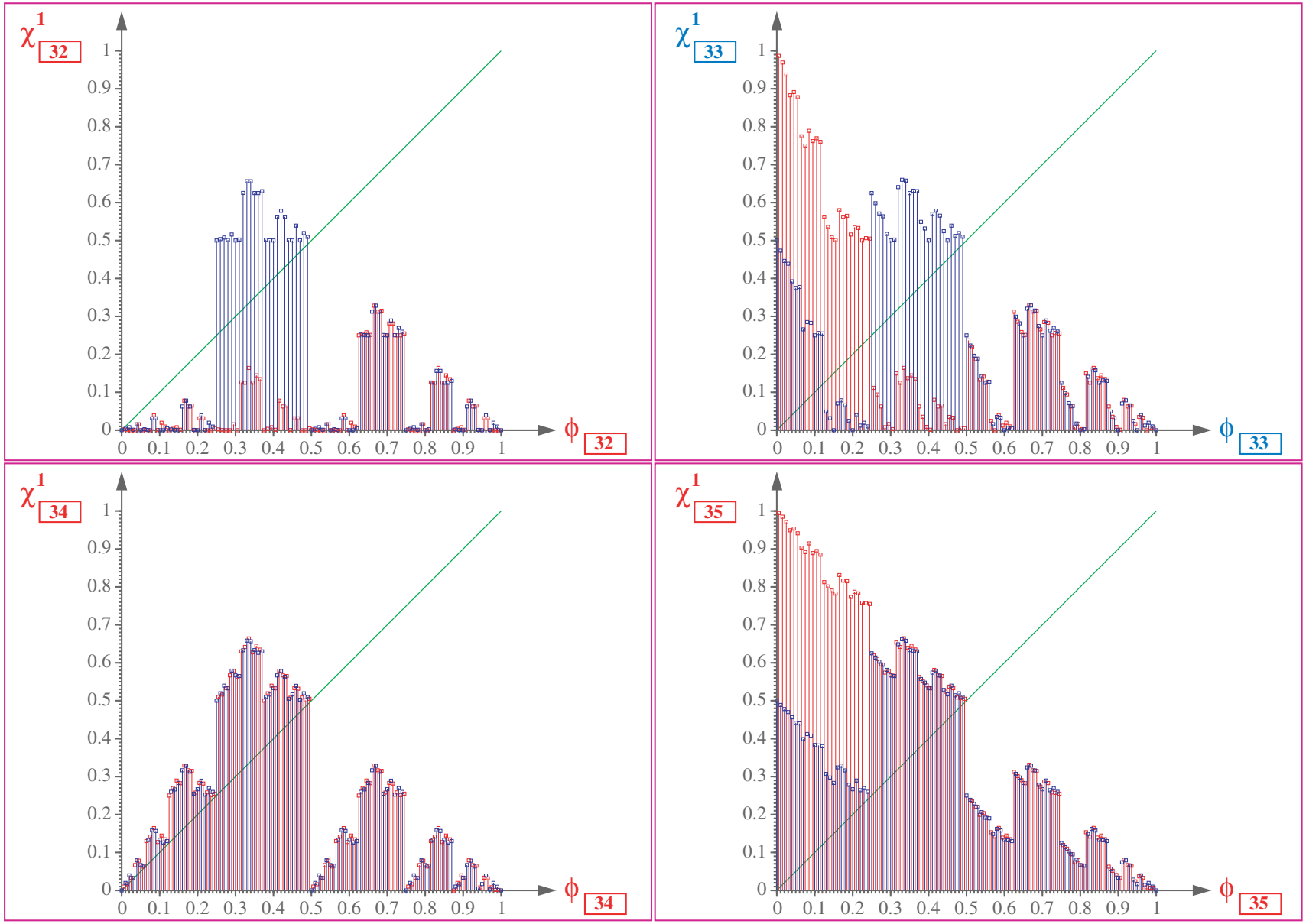


Table 2. (*Continued*)

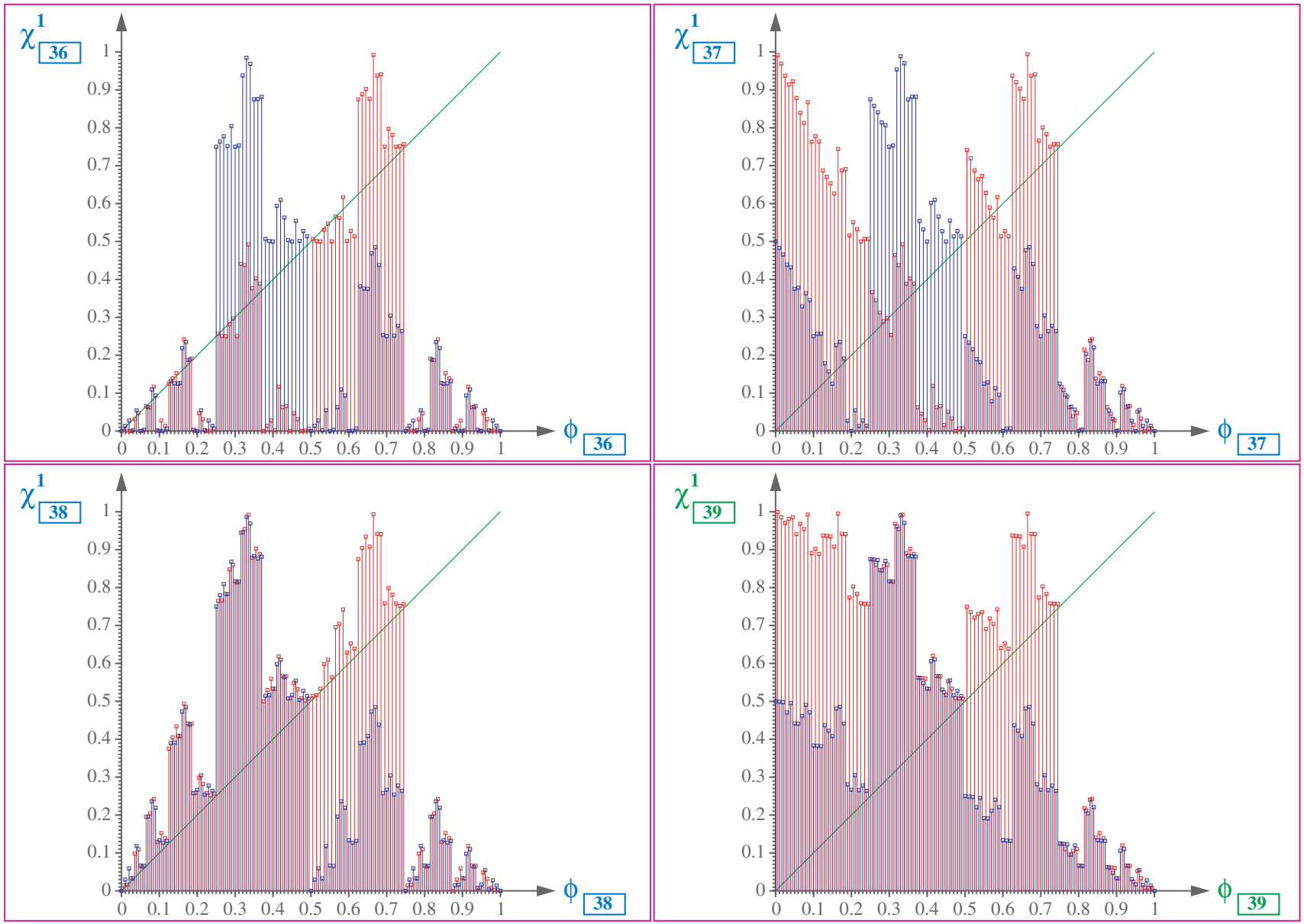


Table 2. (*Continued*)

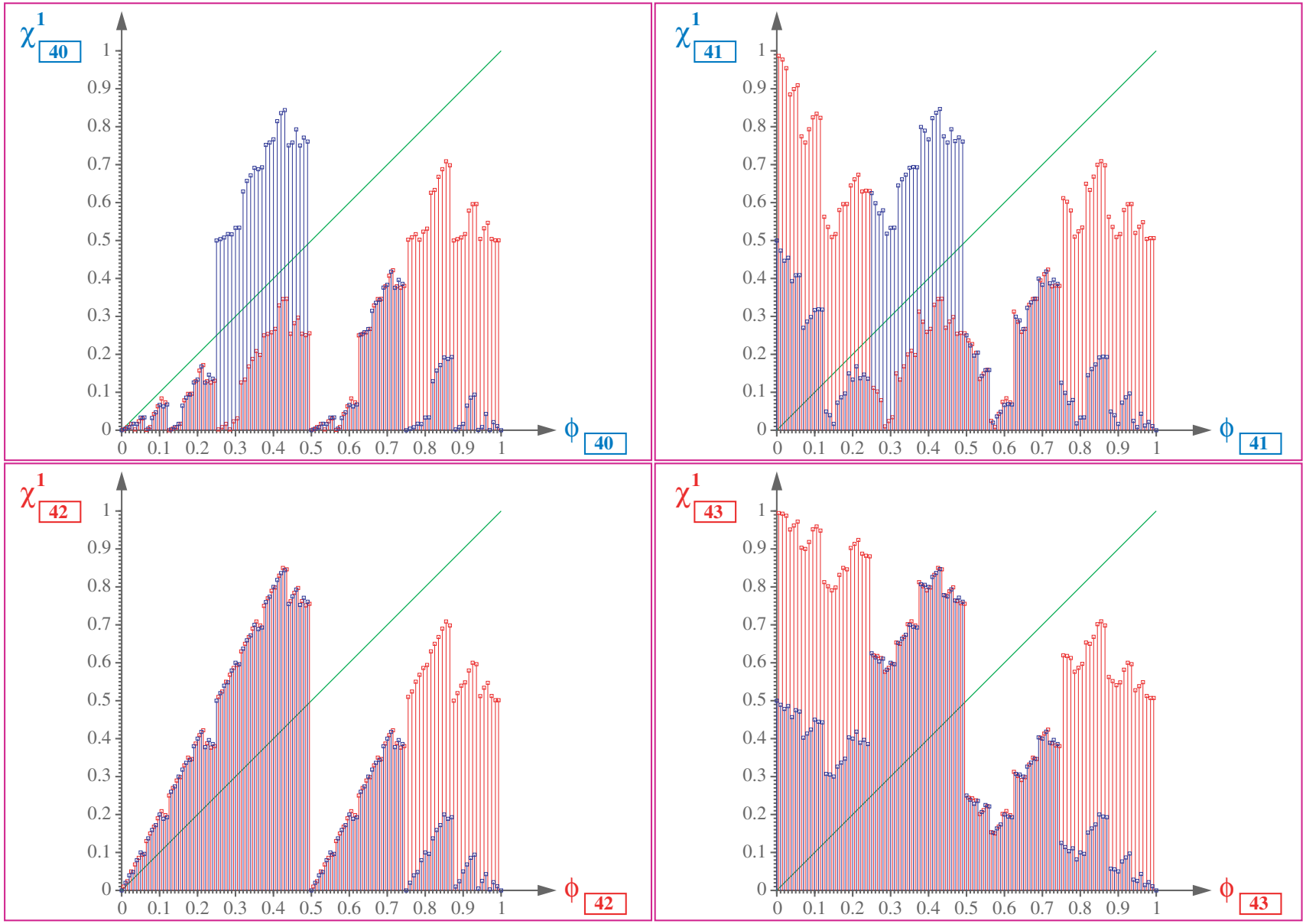


Table 2. (*Continued*)

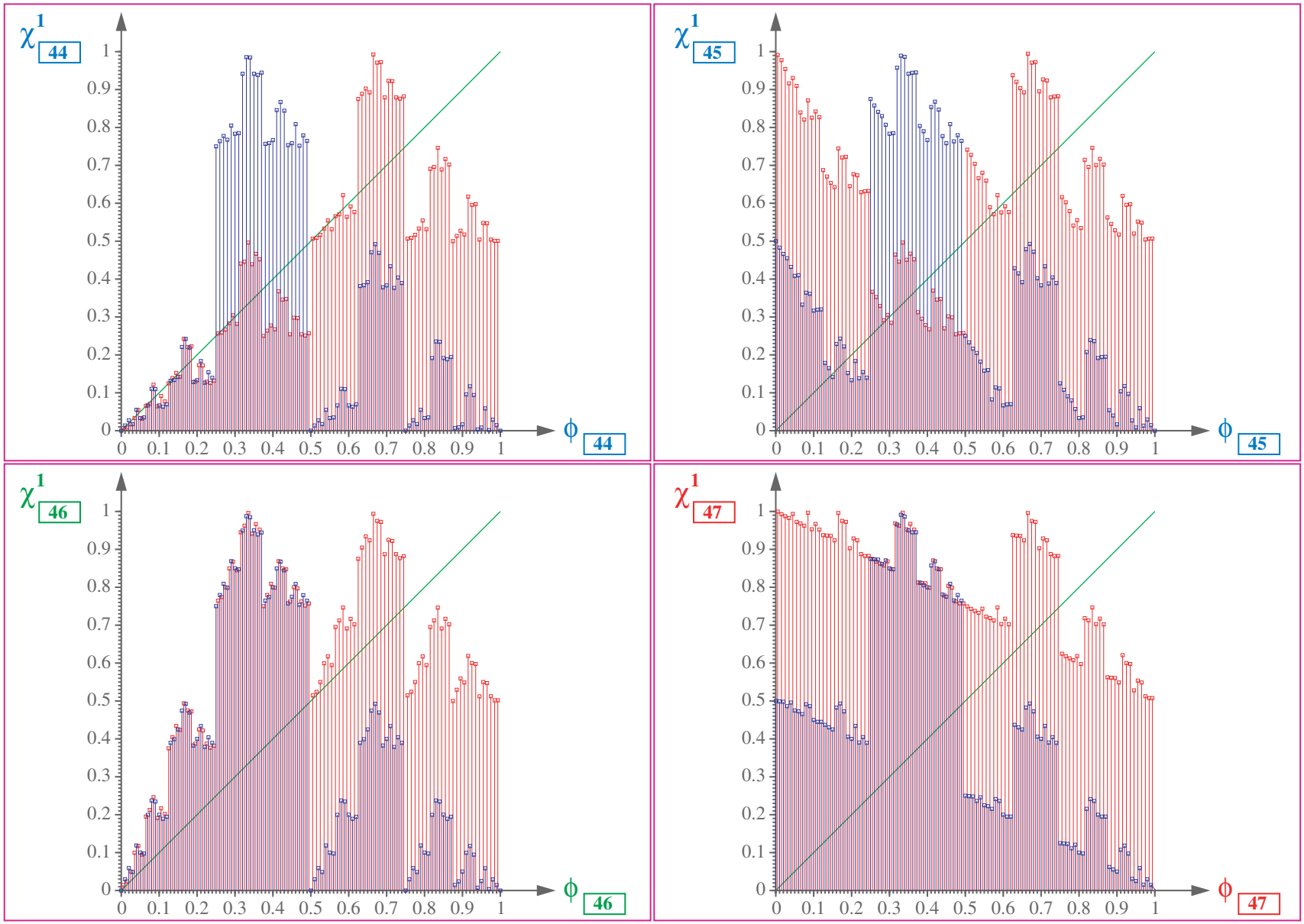


Table 2. (*Continued*)

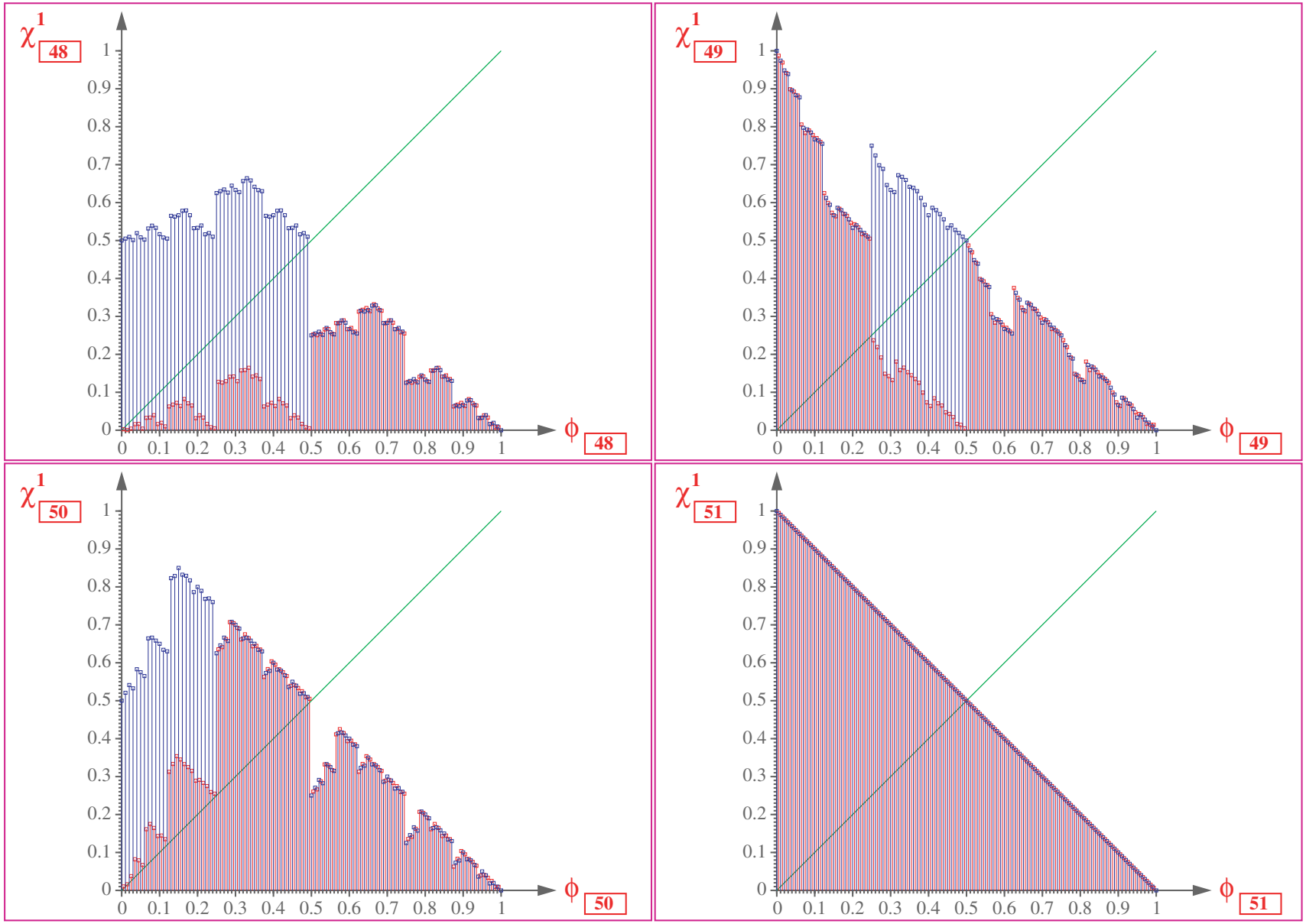


Table 2. (*Continued*)

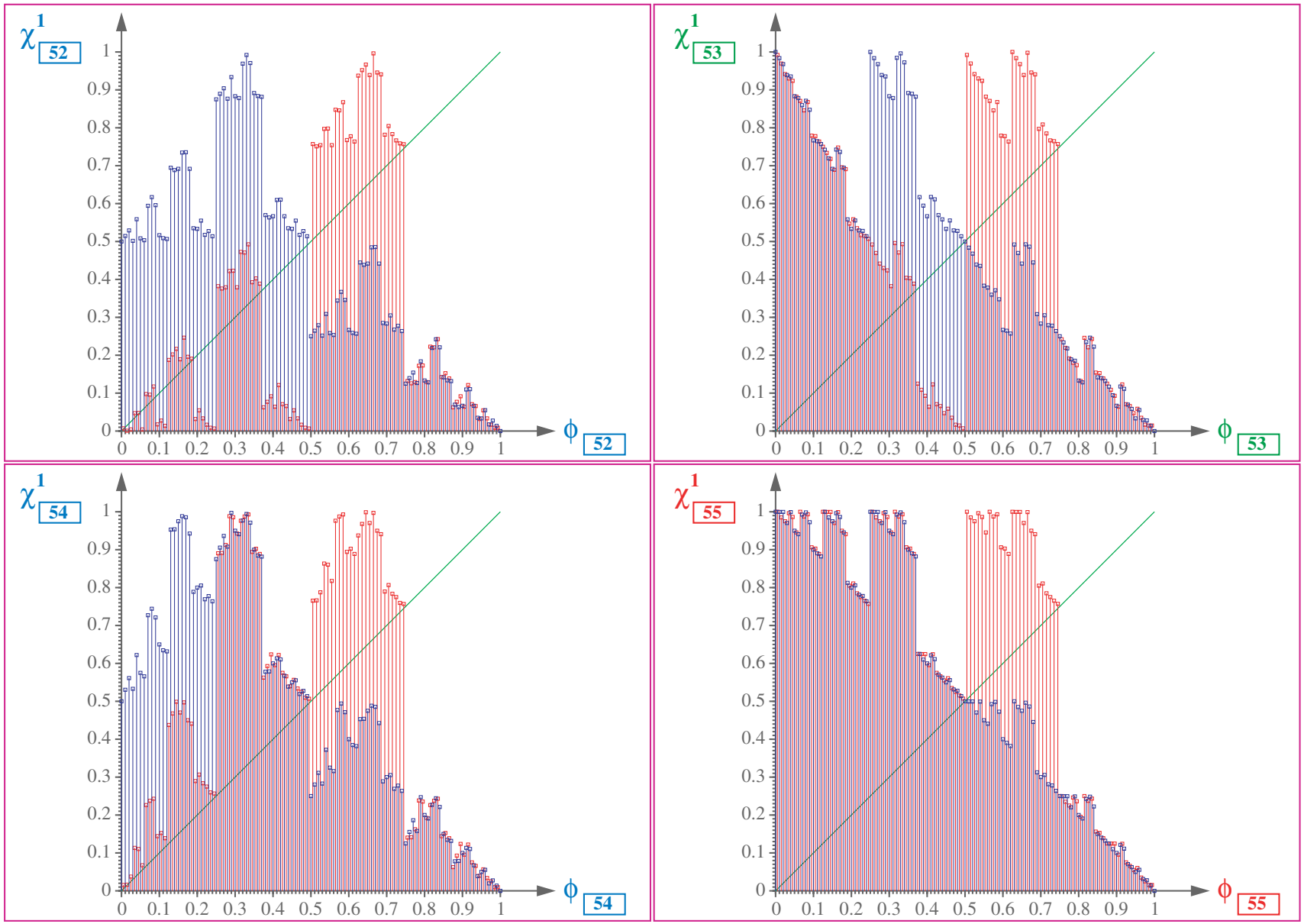


Table 2. (*Continued*)

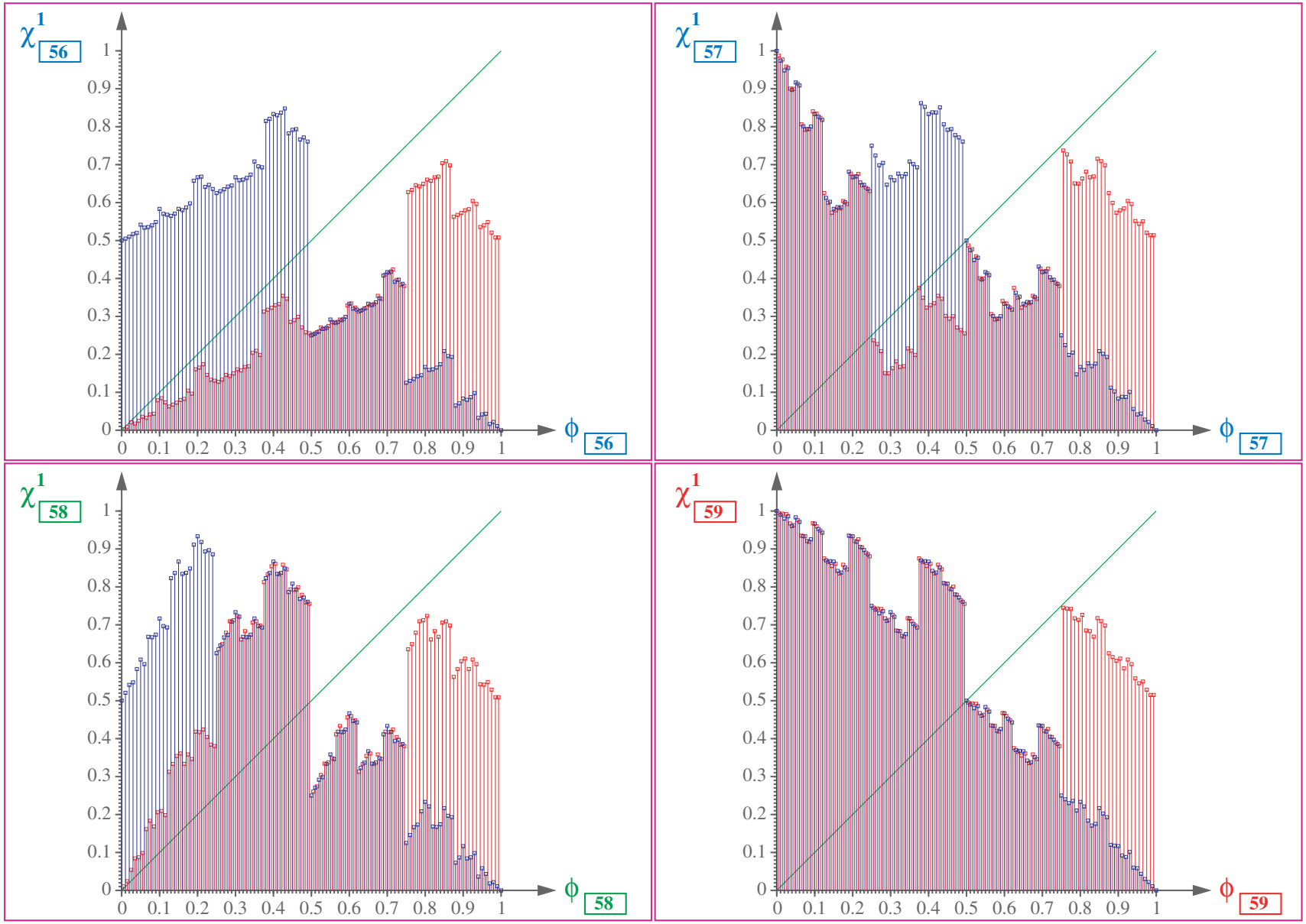


Table 2. (*Continued*)

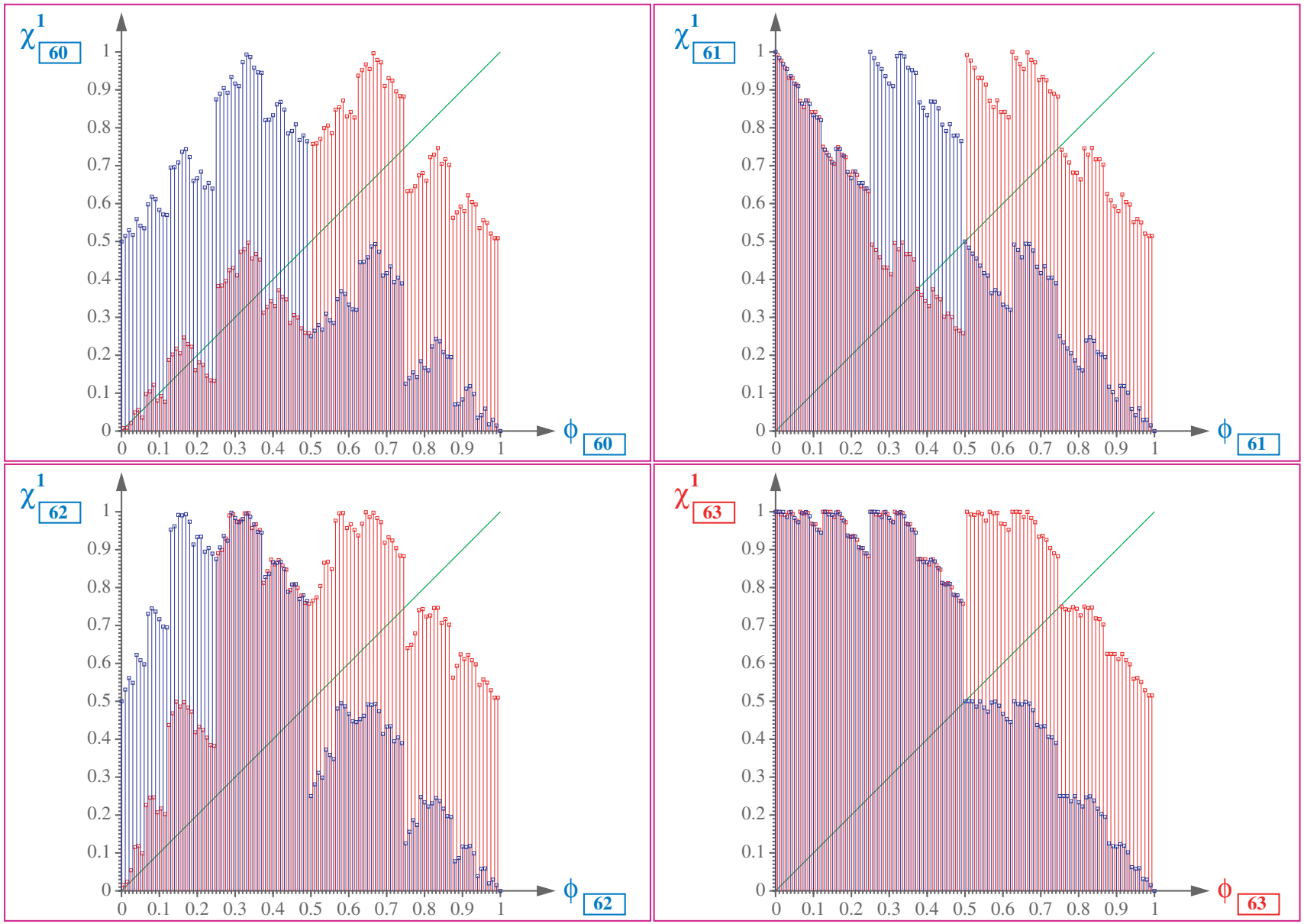


Table 2. (*Continued*)

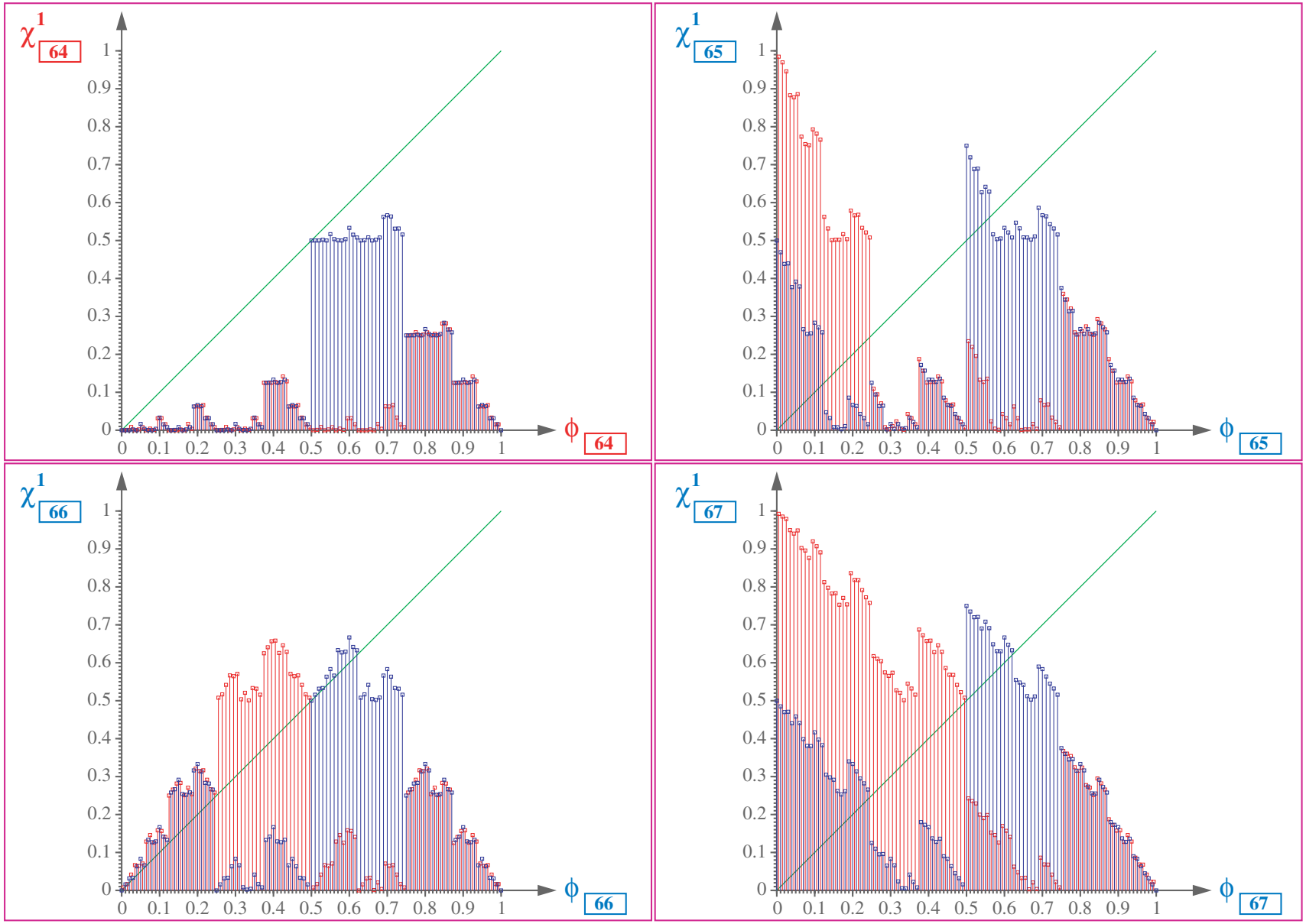


Table 2. (*Continued*)

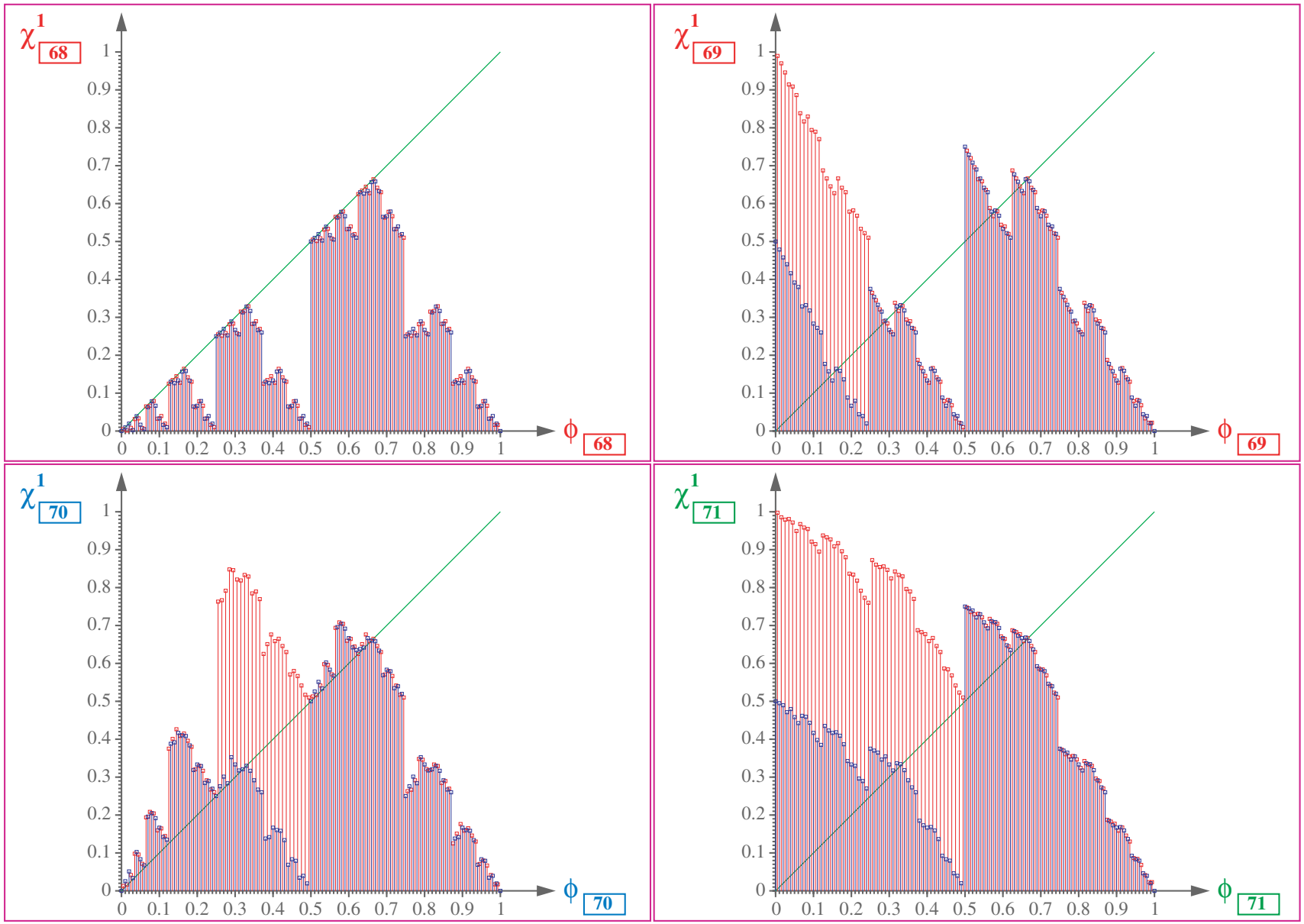


Table 2. (*Continued*)

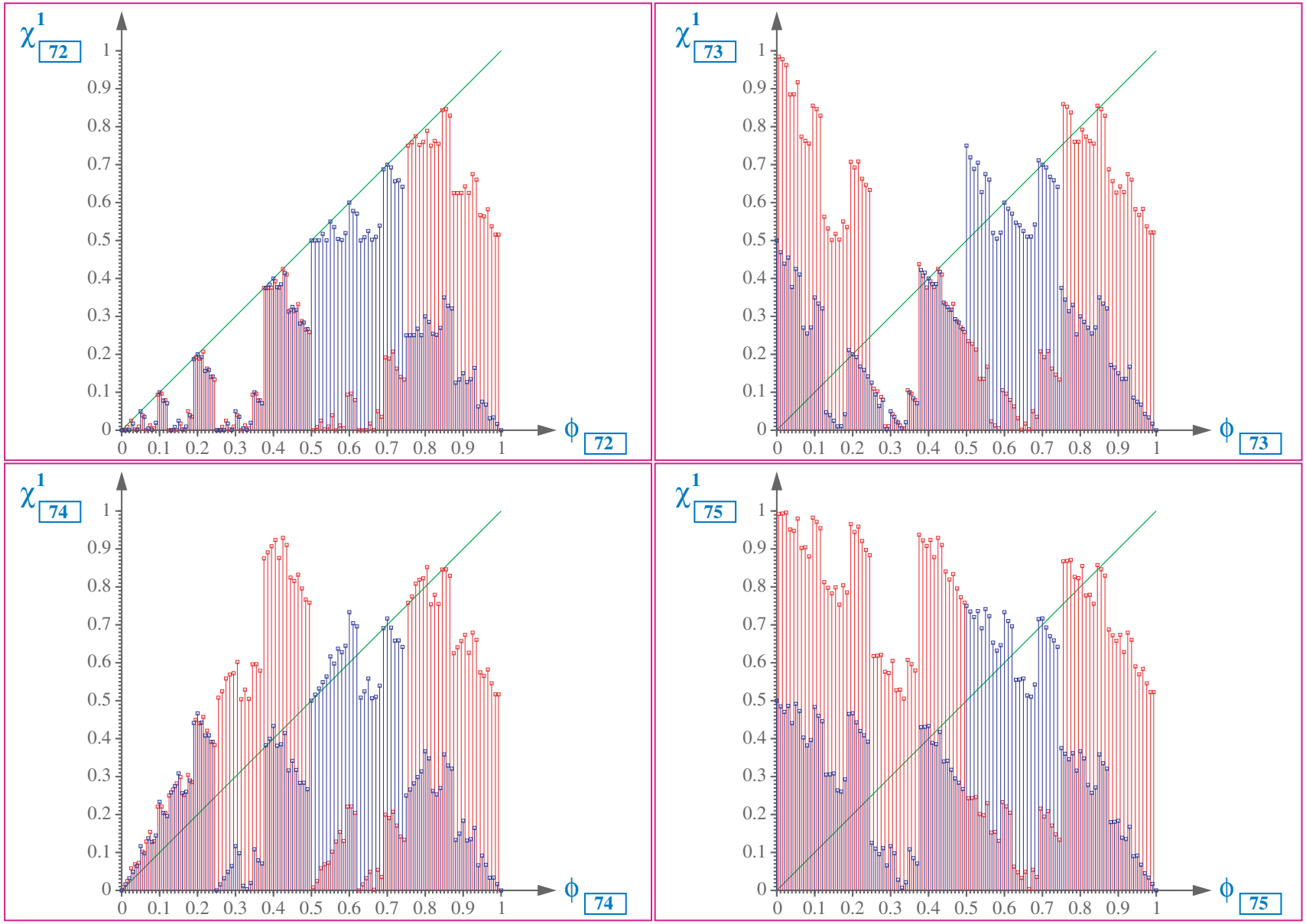


Table 2. (*Continued*)

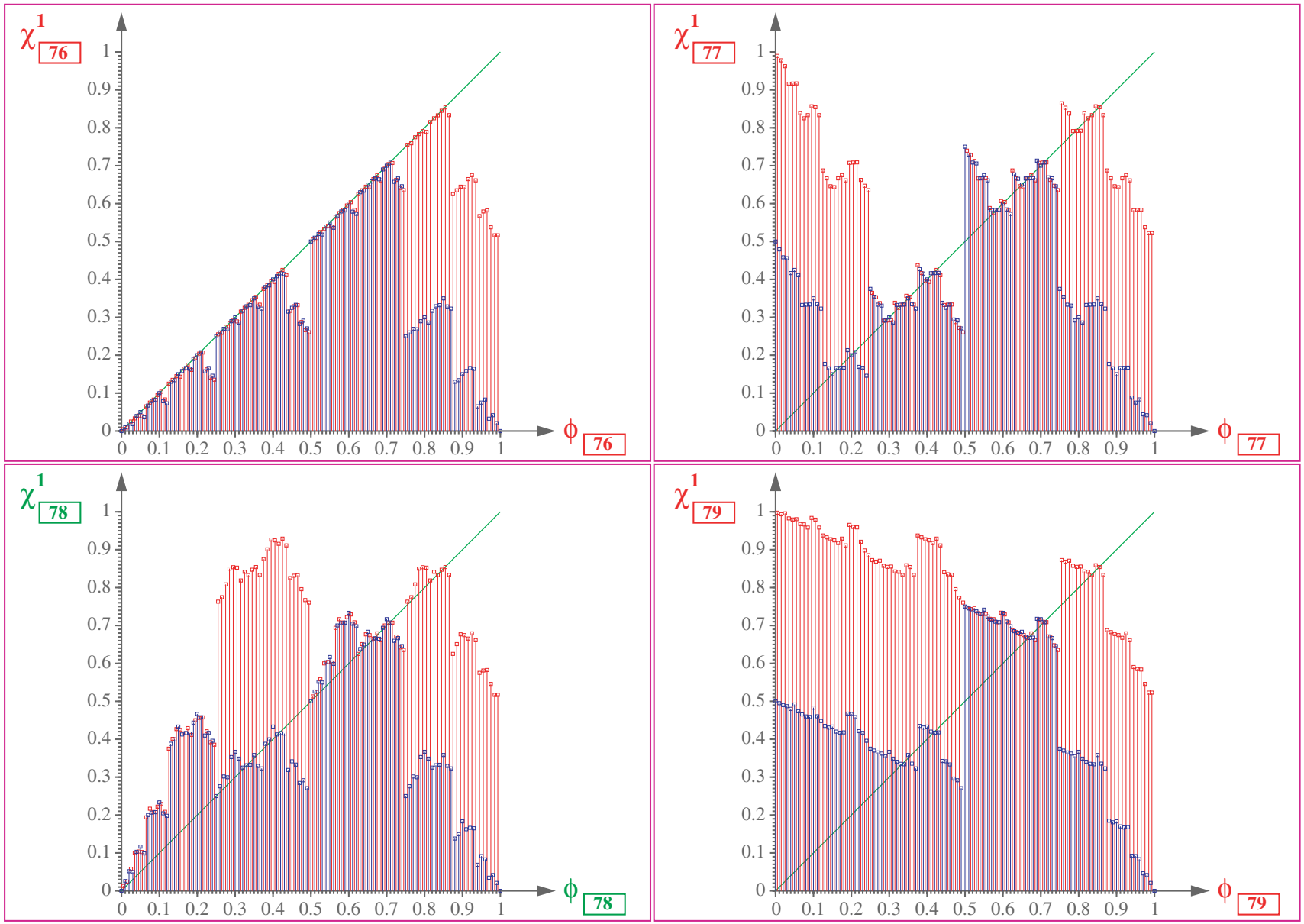


Table 2. (*Continued*)

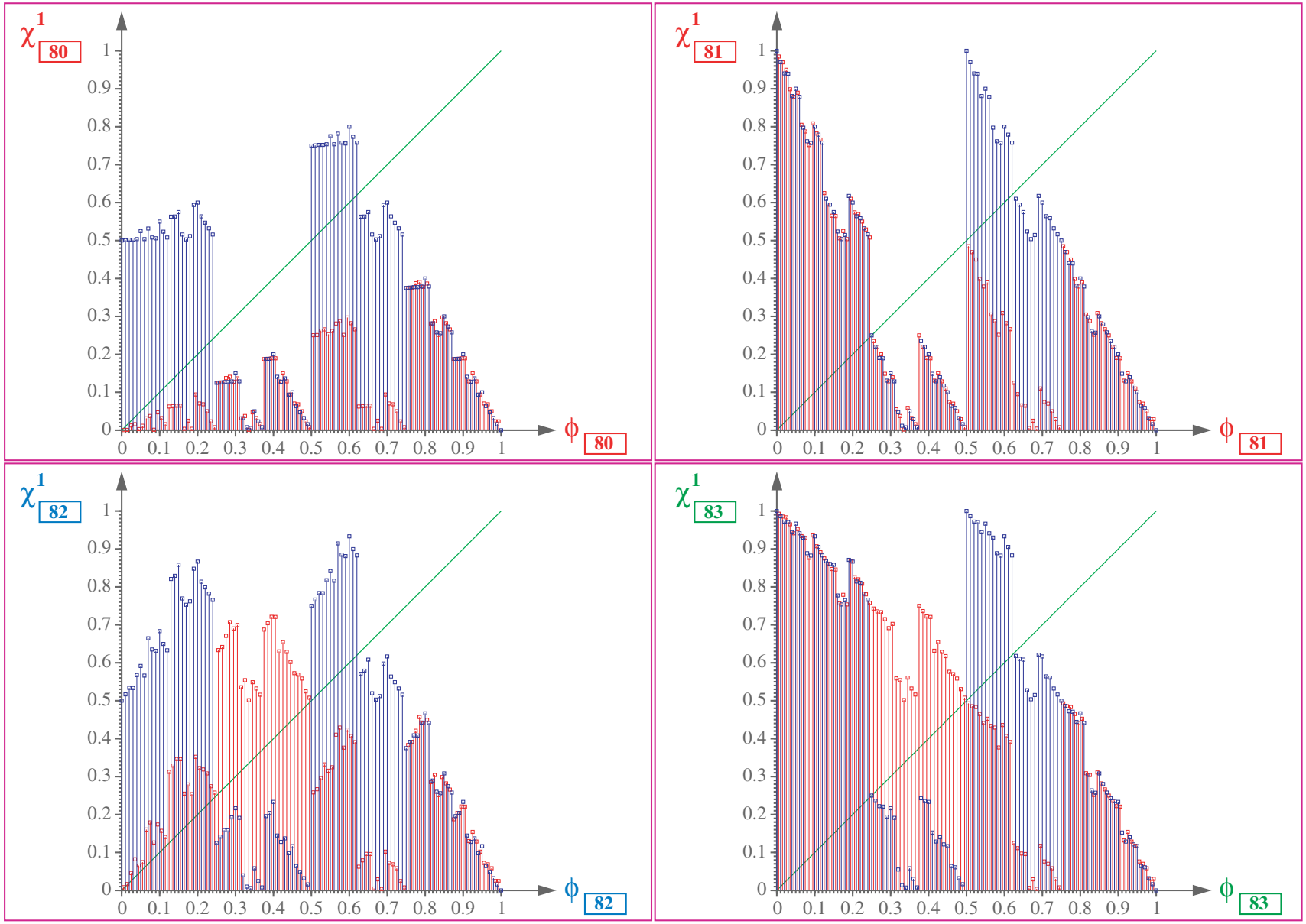


Table 2. (*Continued*)

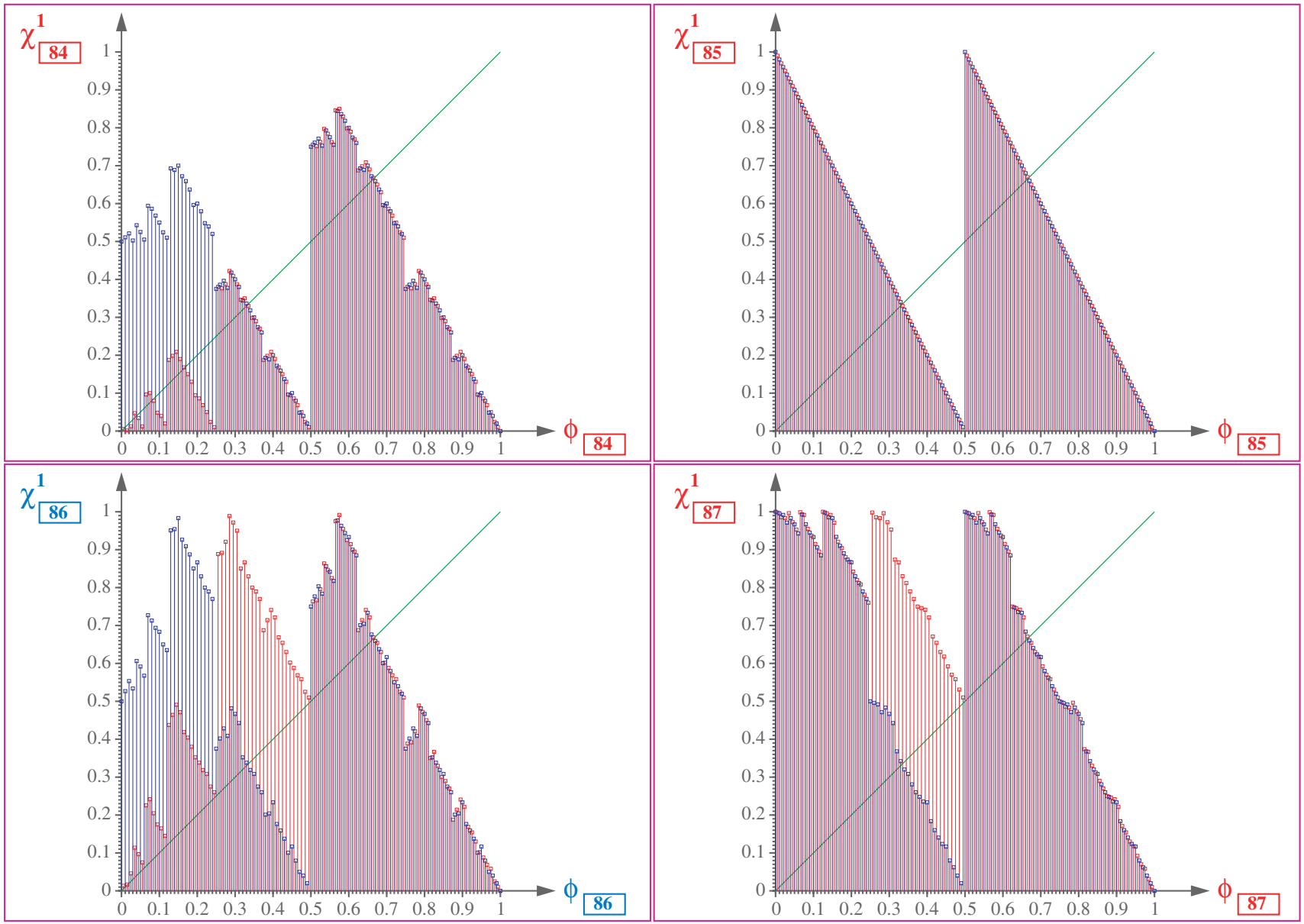


Table 2. (*Continued*)

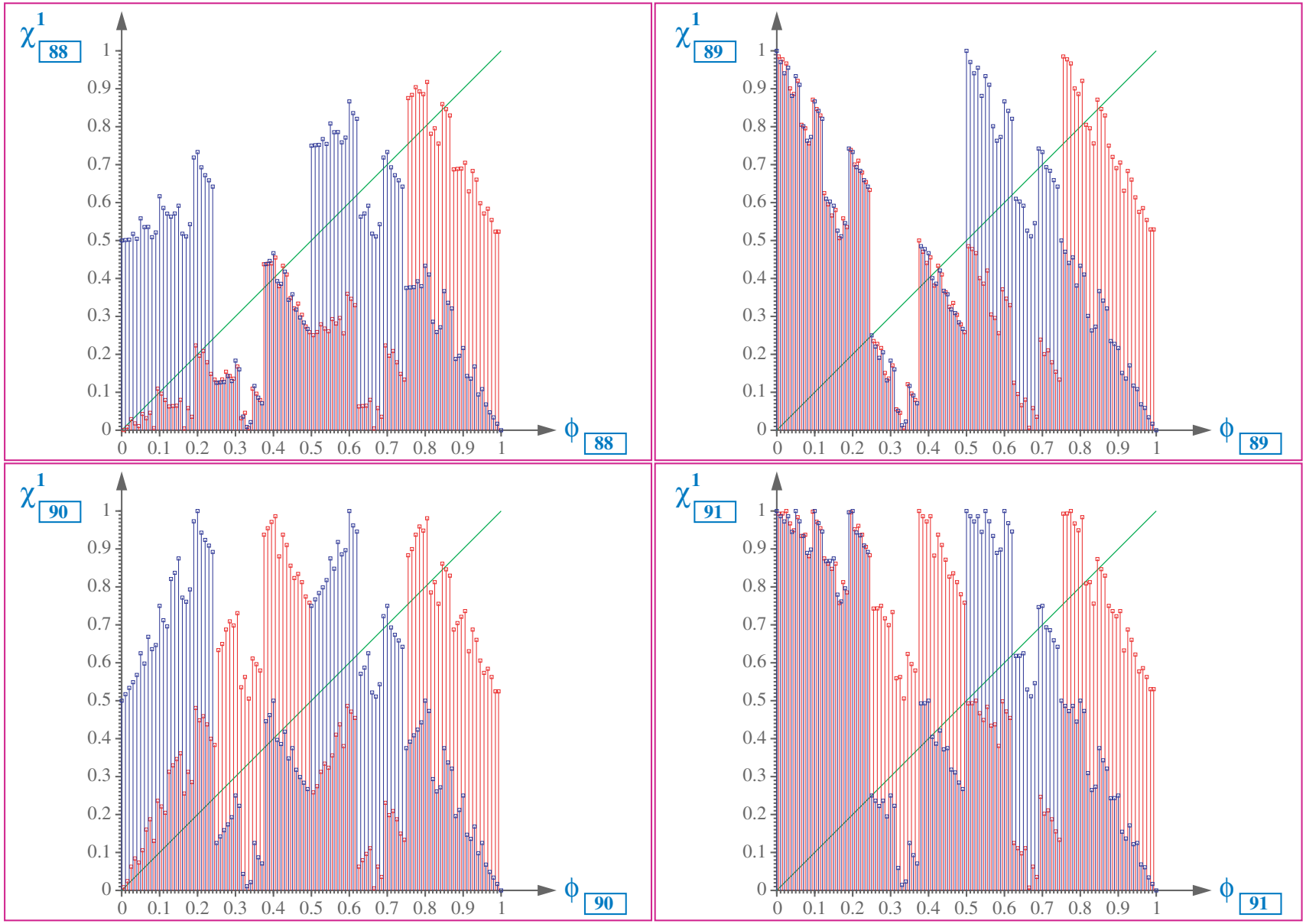


Table 2. (*Continued*)

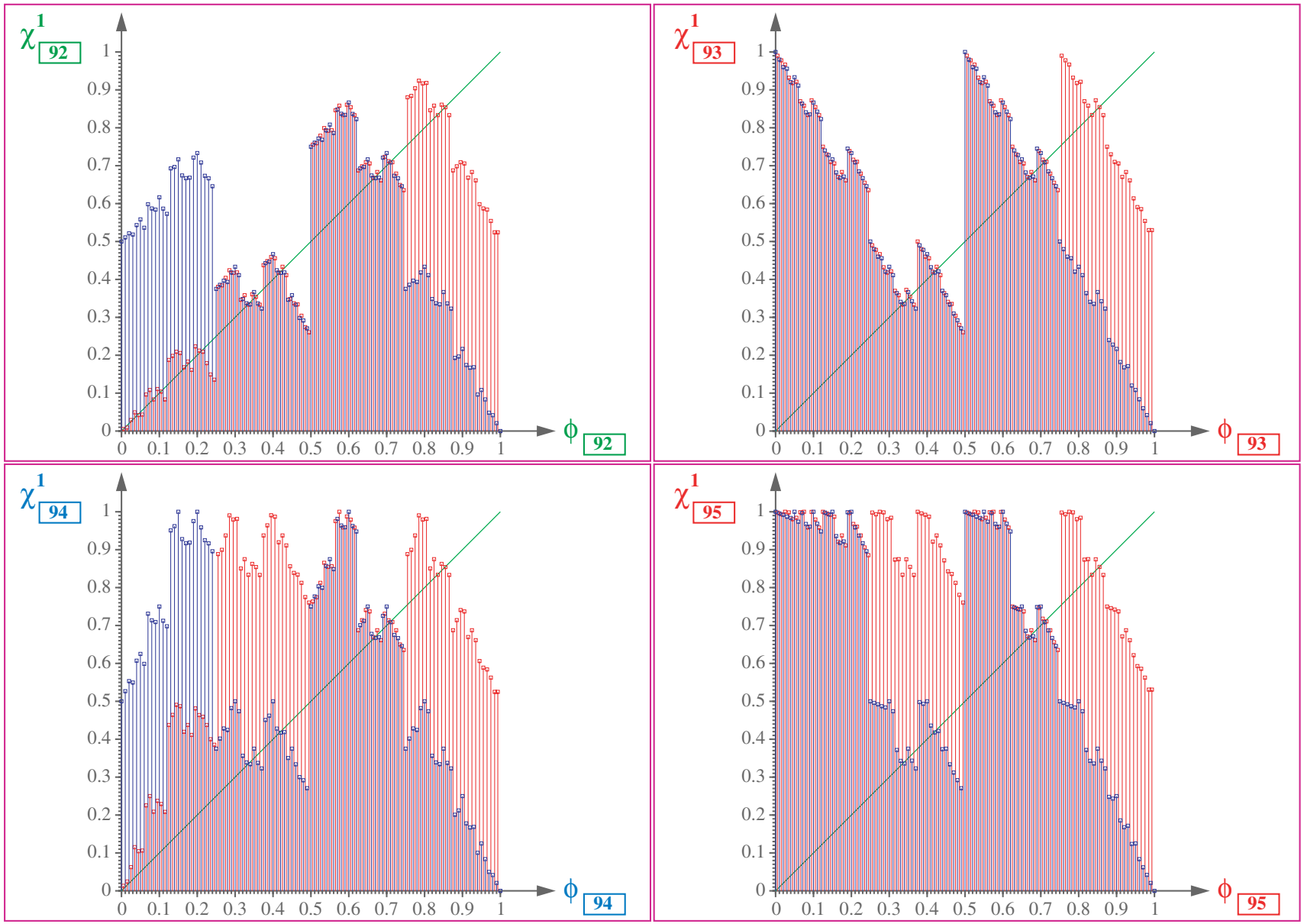


Table 2. (*Continued*)

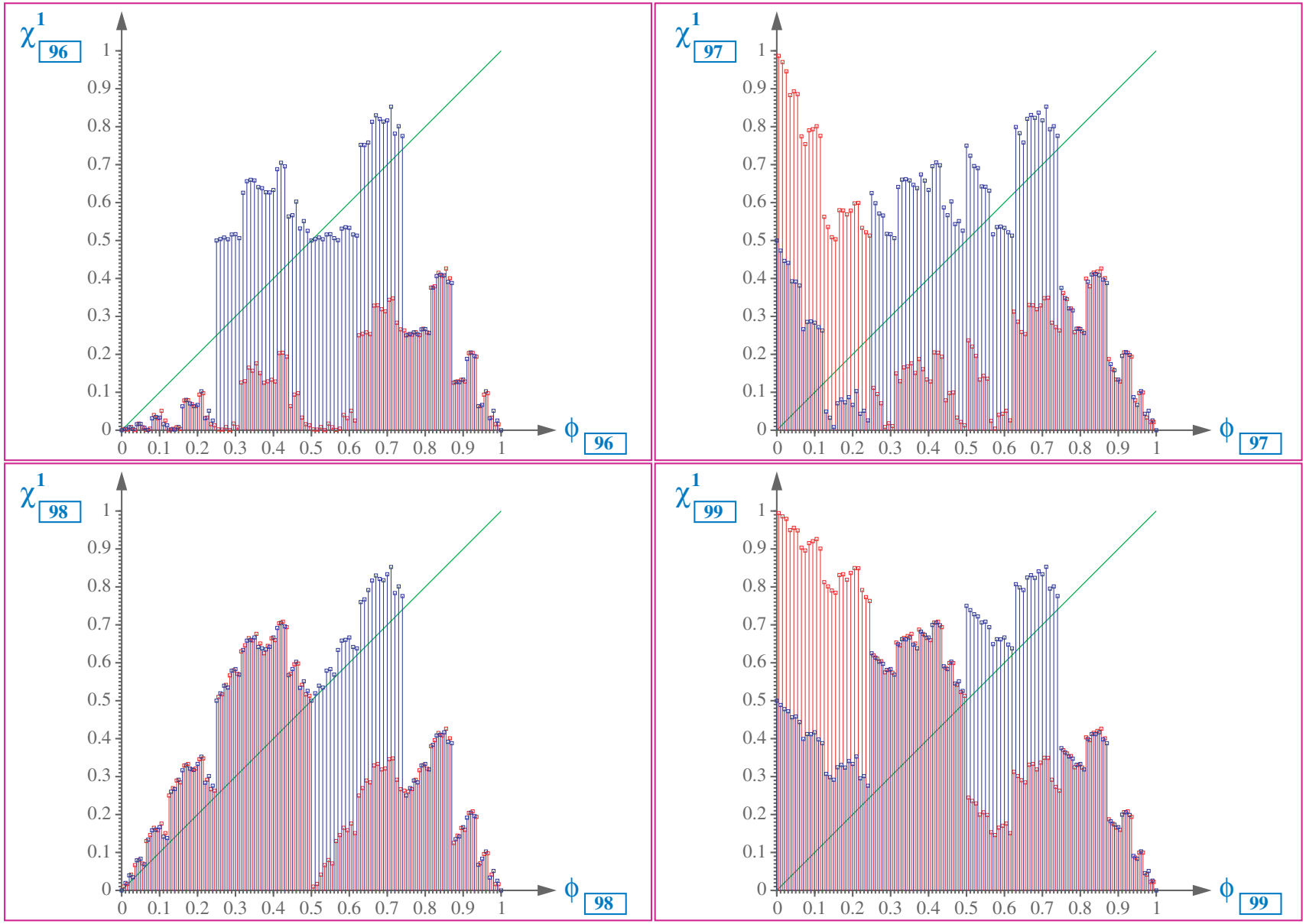


Table 2. (*Continued*)

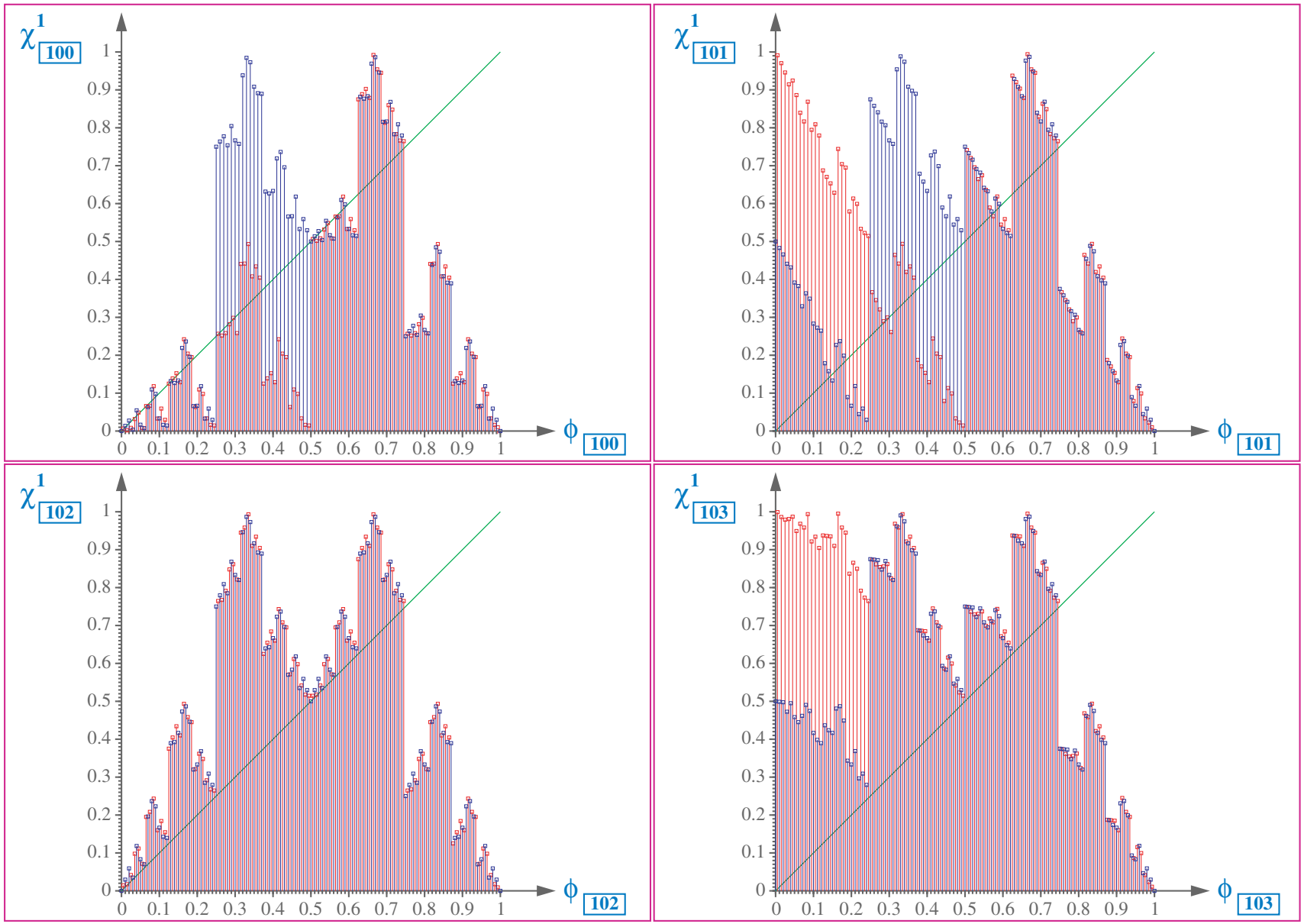


Table 2. (*Continued*)

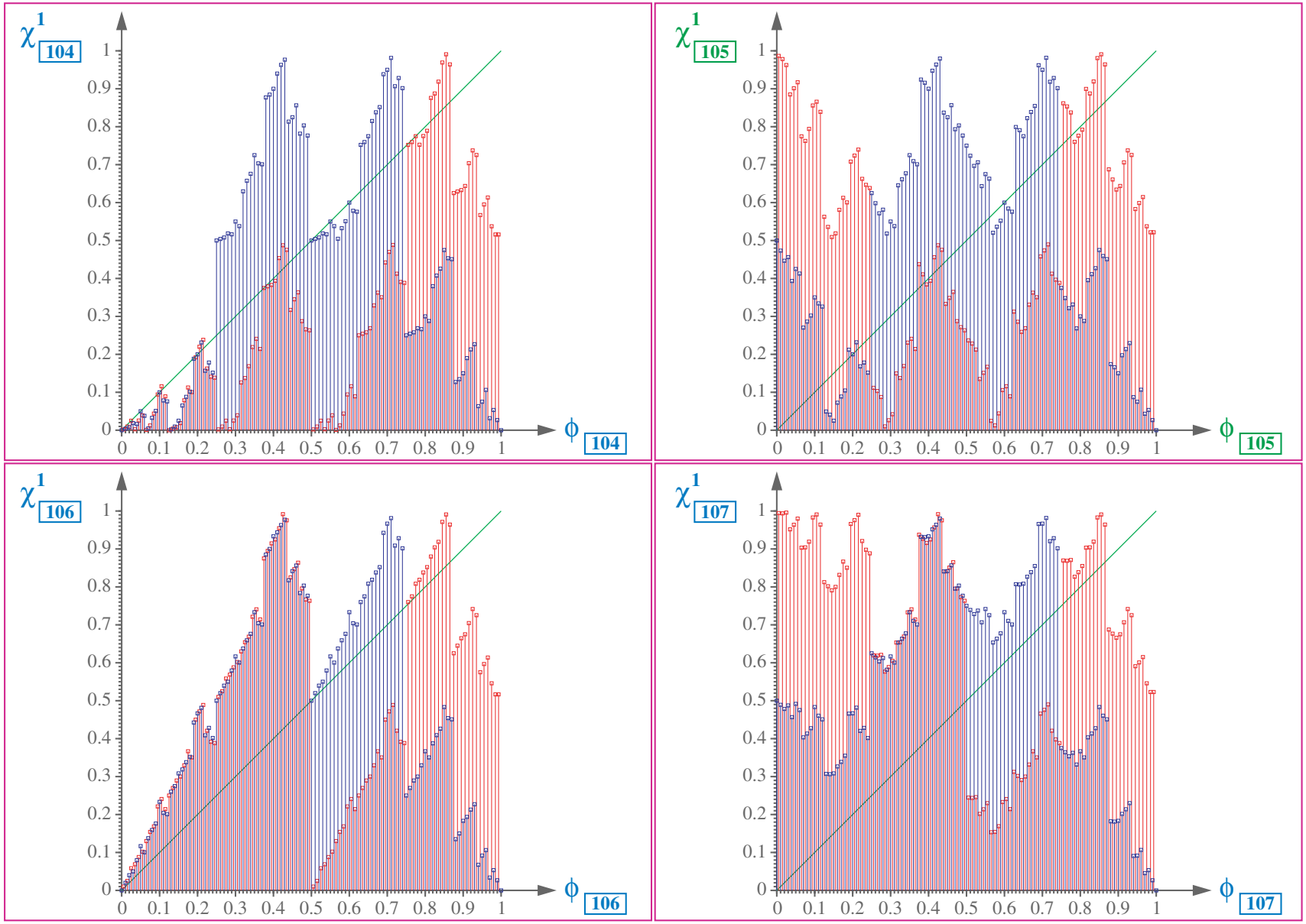


Table 2. (*Continued*)

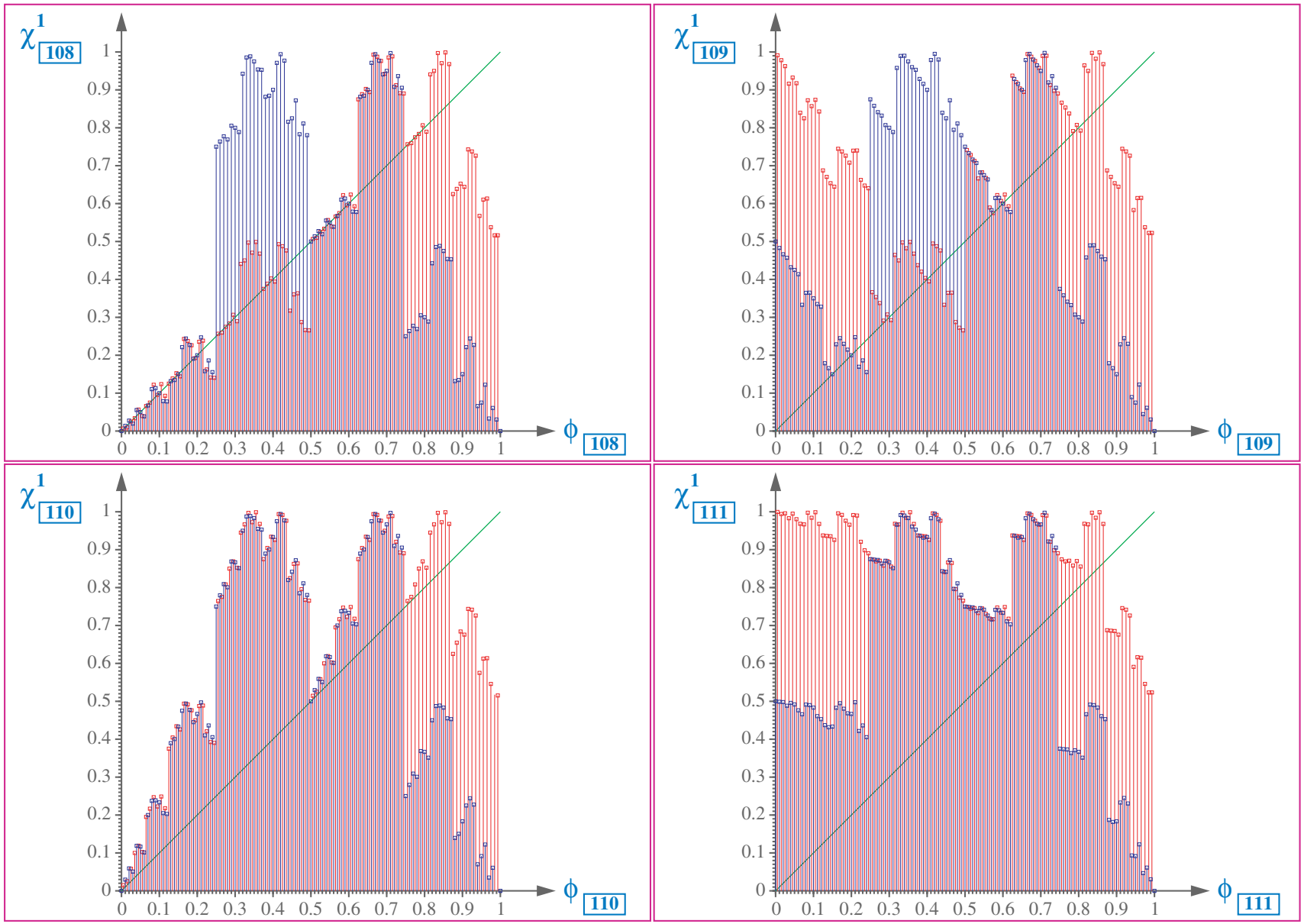


Table 2. (*Continued*)

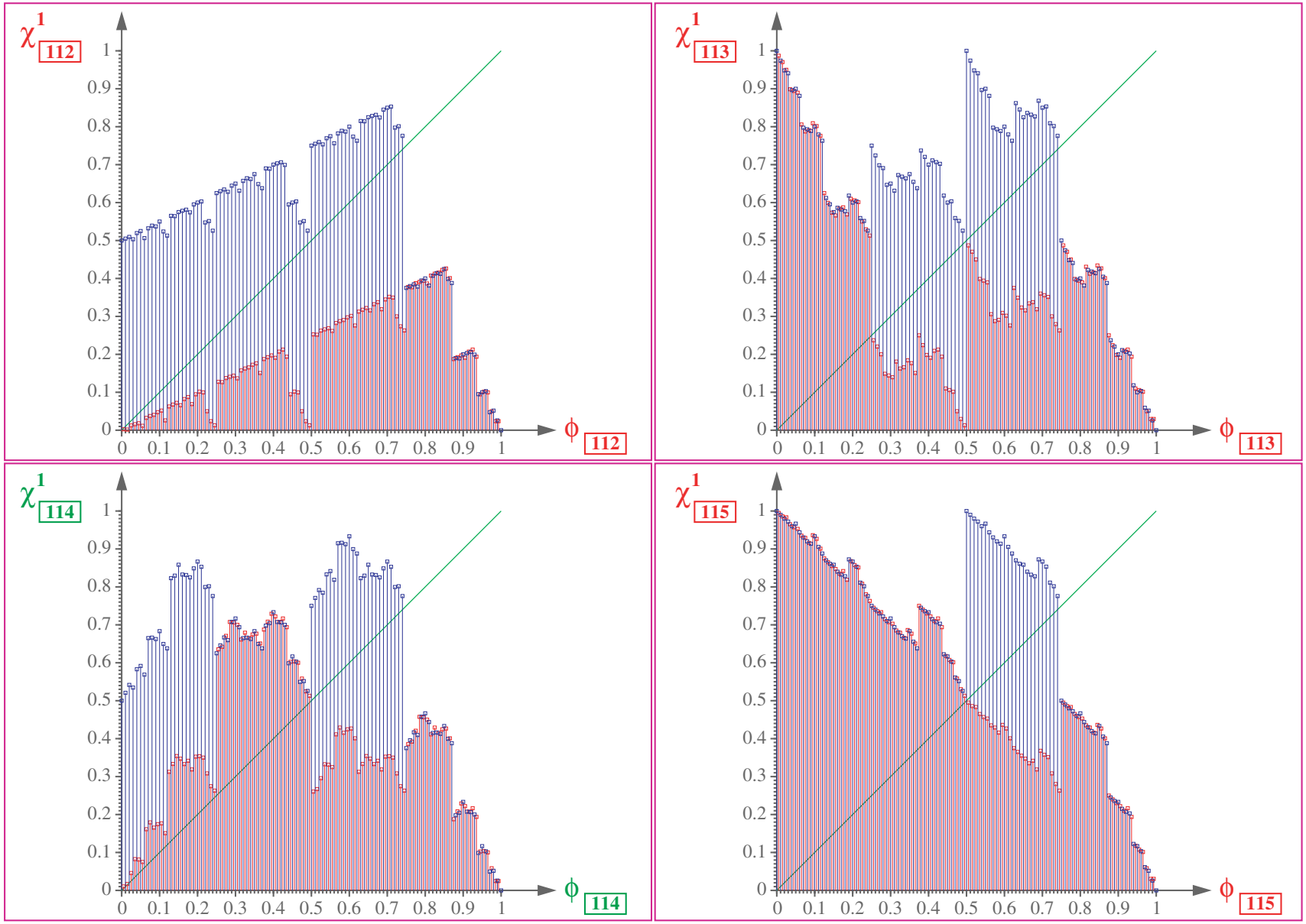


Table 2. (*Continued*)

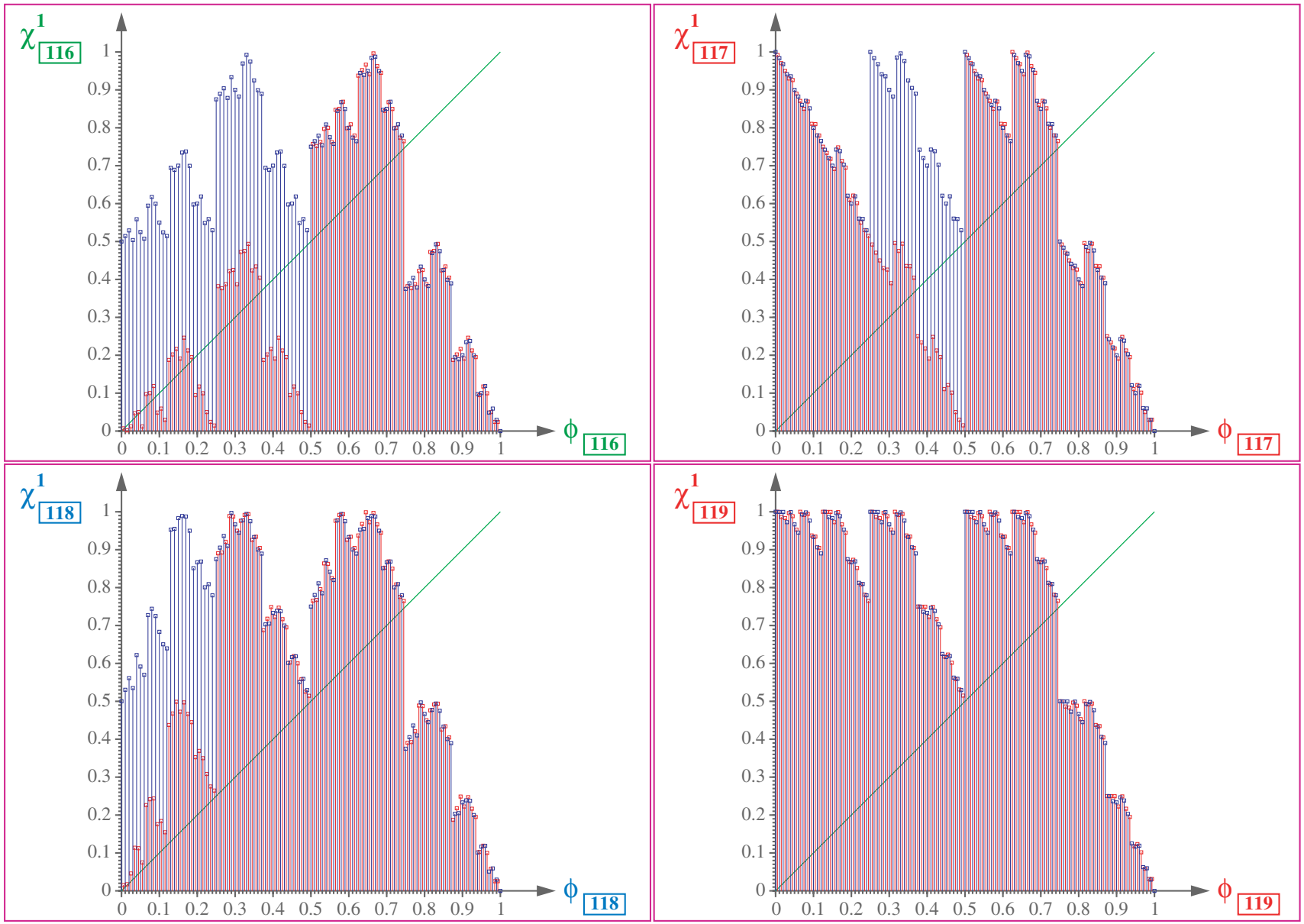


Table 2. (*Continued*)

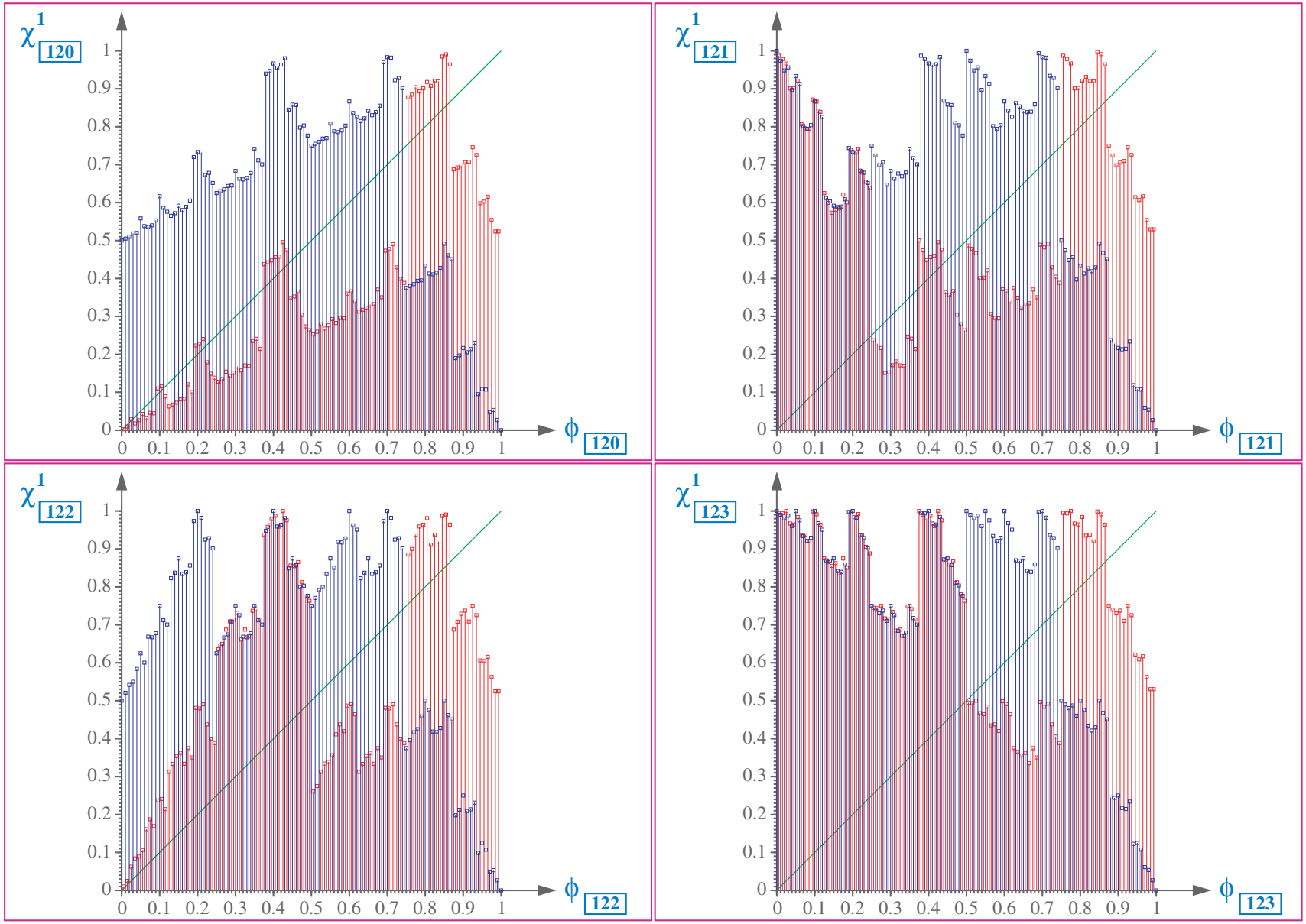


Table 2. (*Continued*)

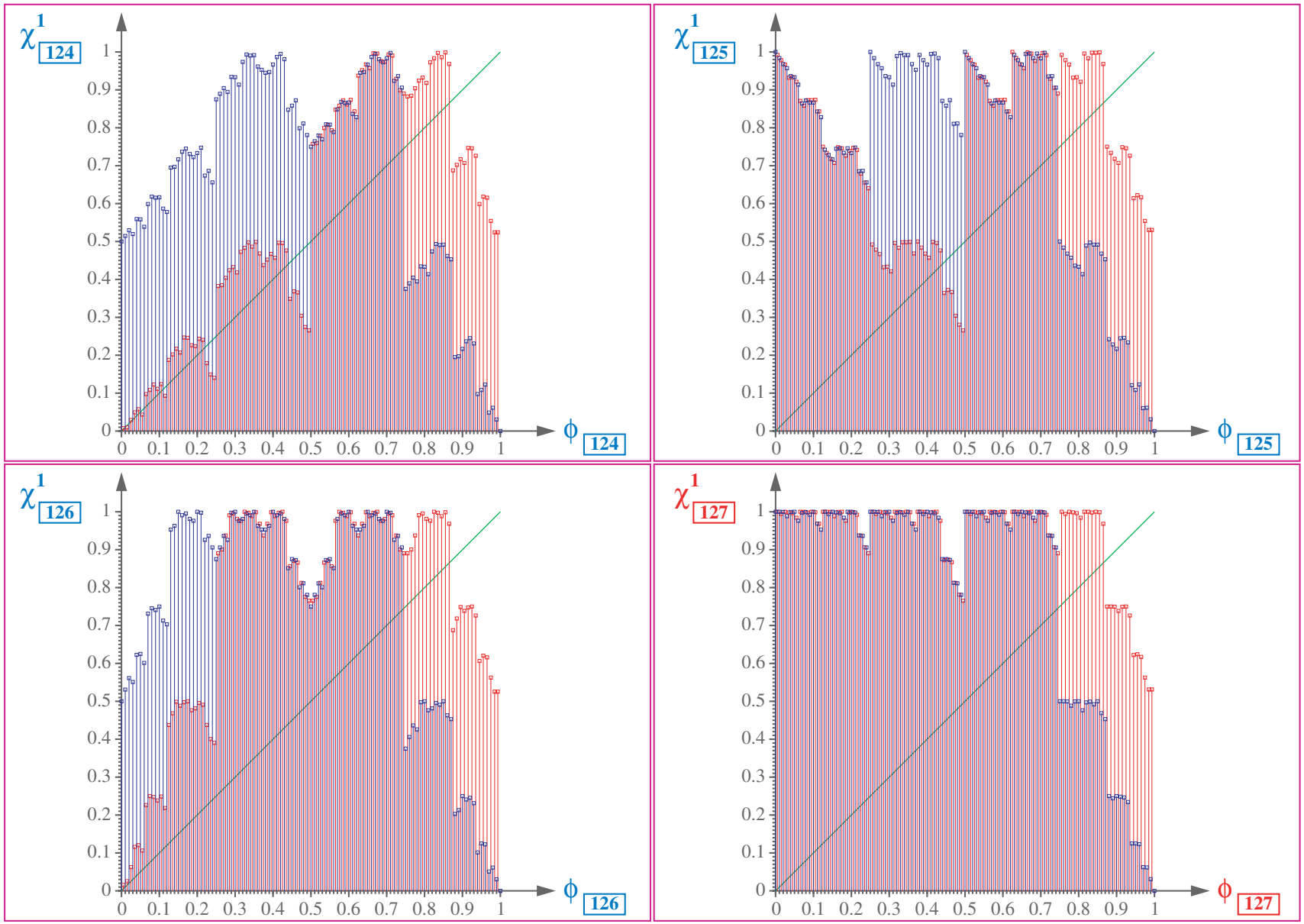


Table 2. (*Continued*)

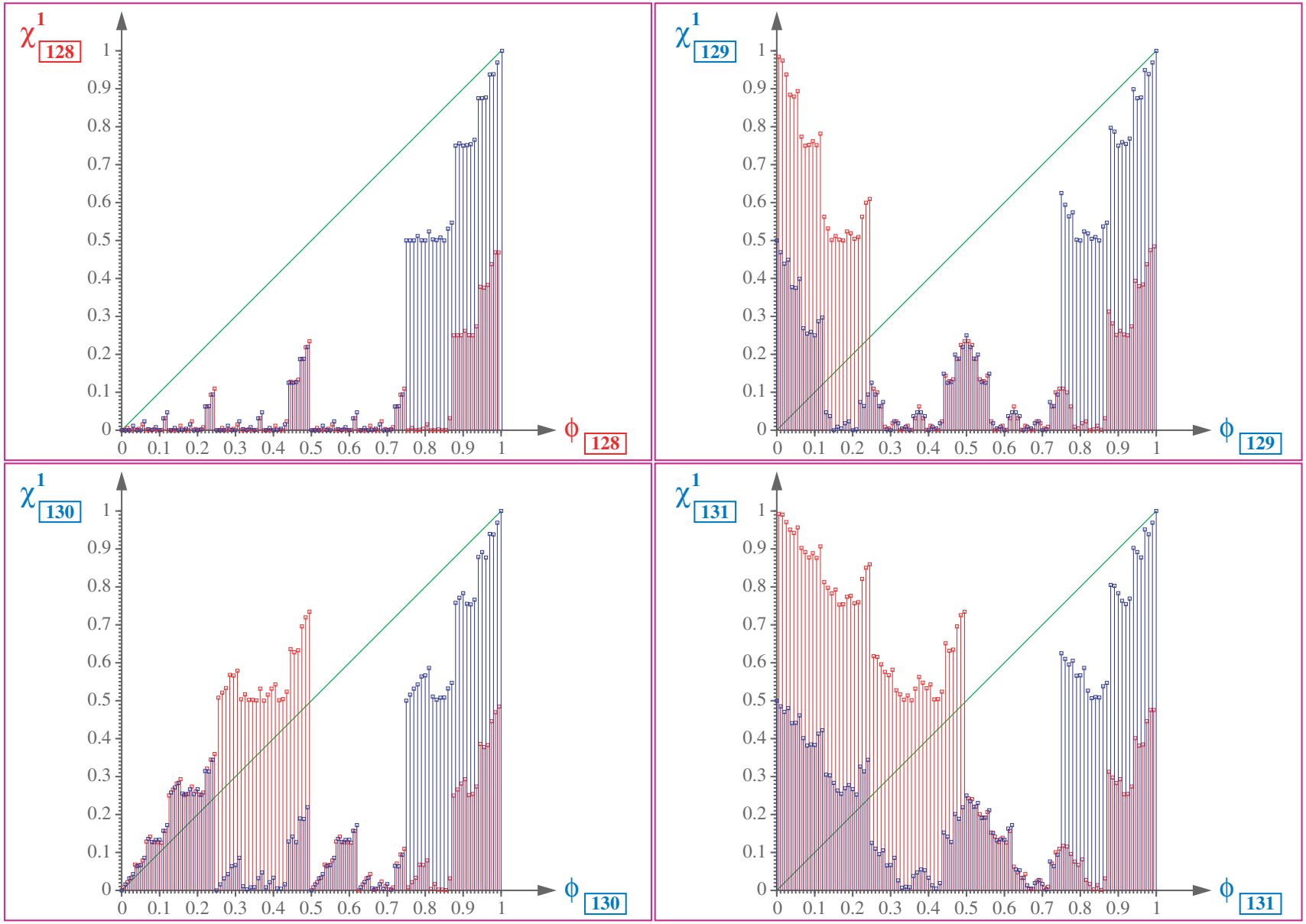


Table 2. (*Continued*)

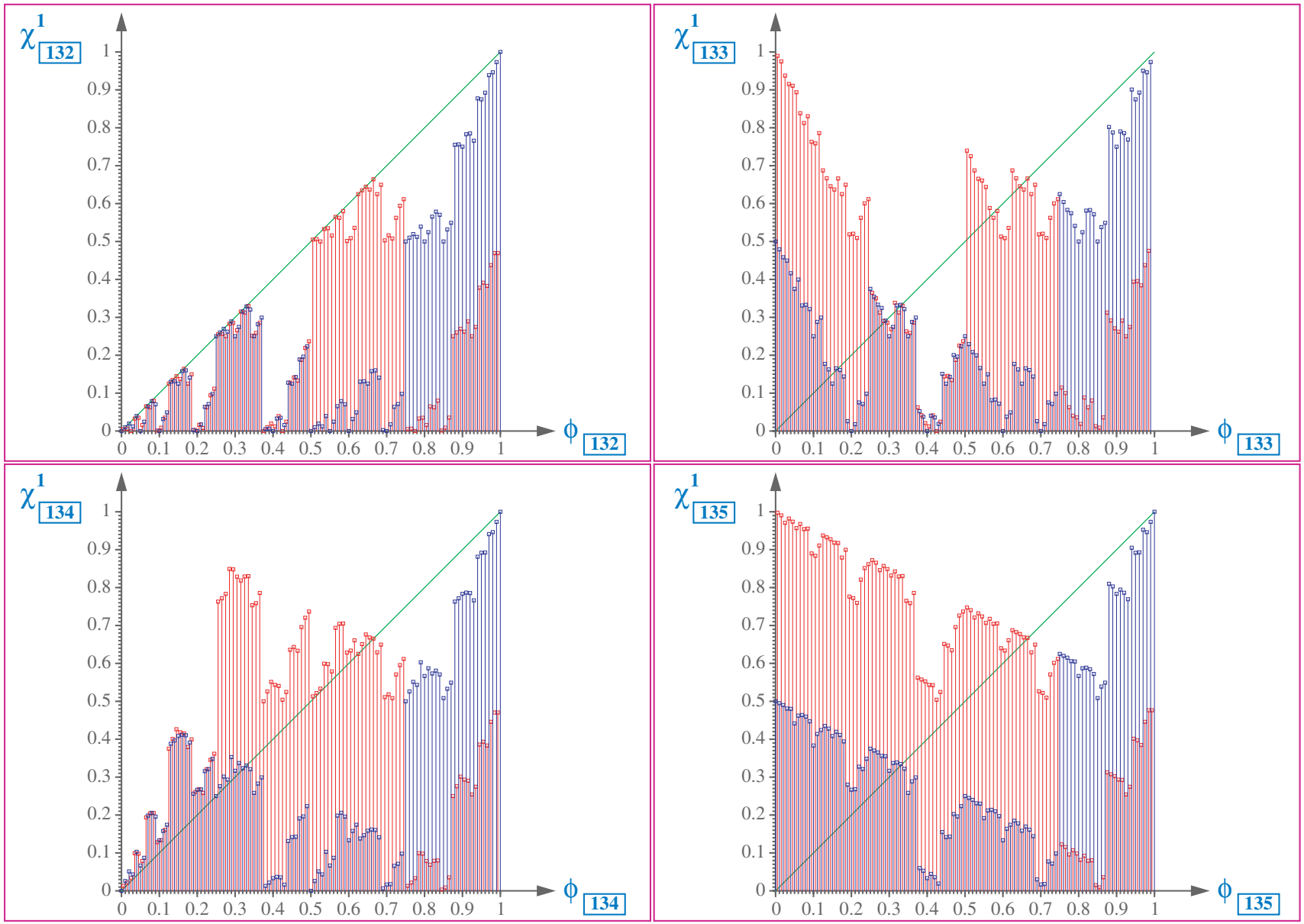


Table 2. (*Continued*)

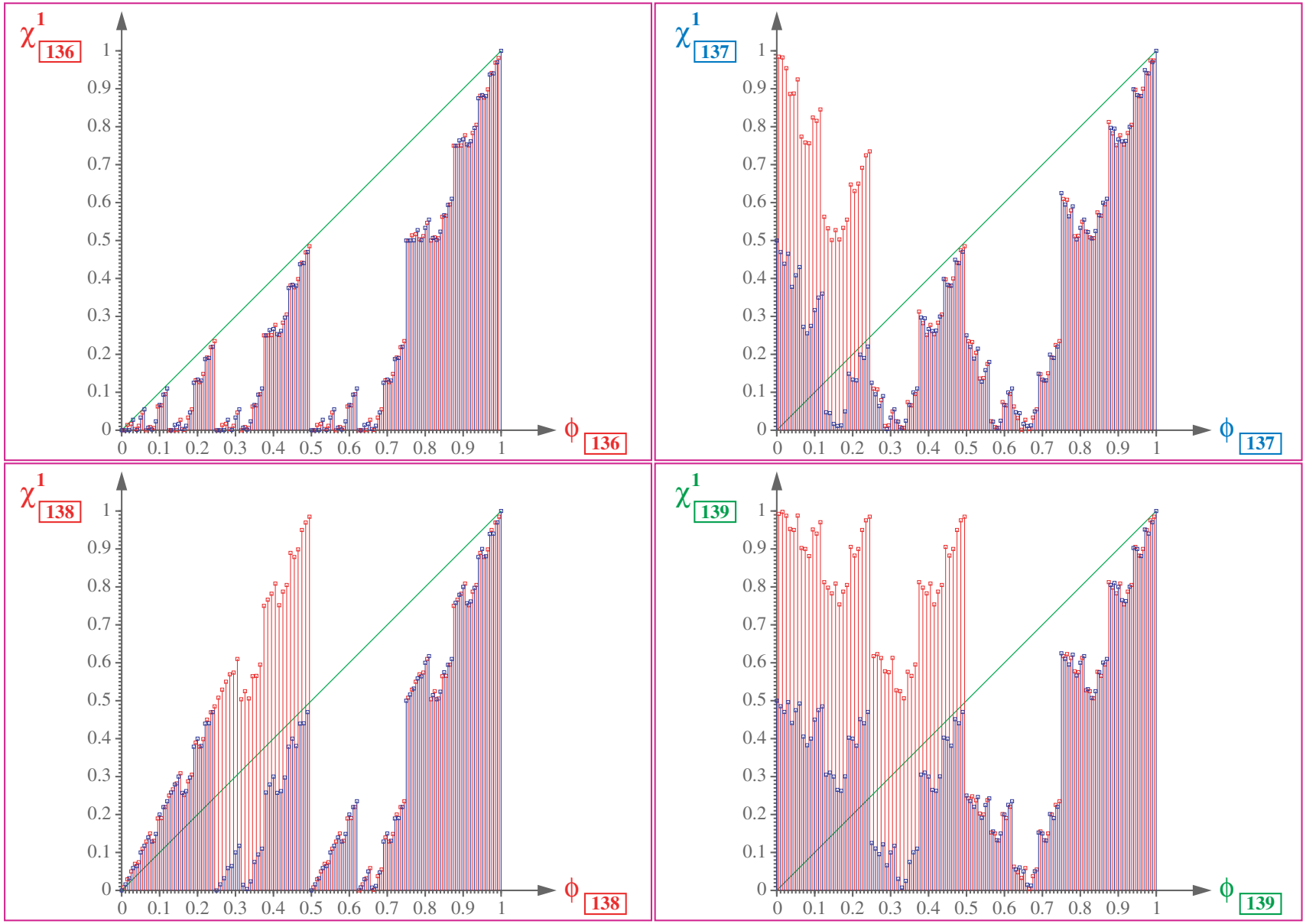


Table 2. (*Continued*)

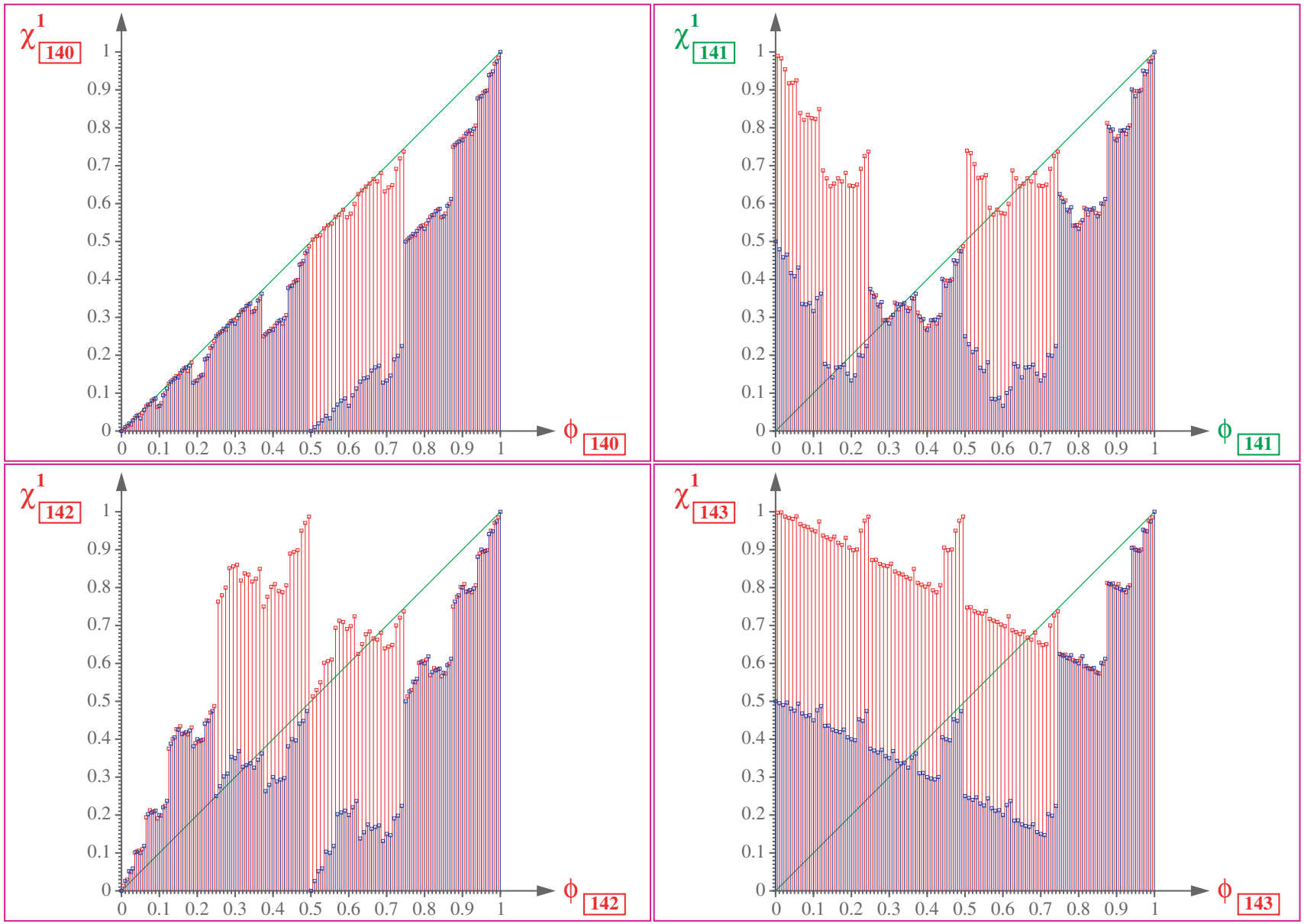


Table 2. (*Continued*)

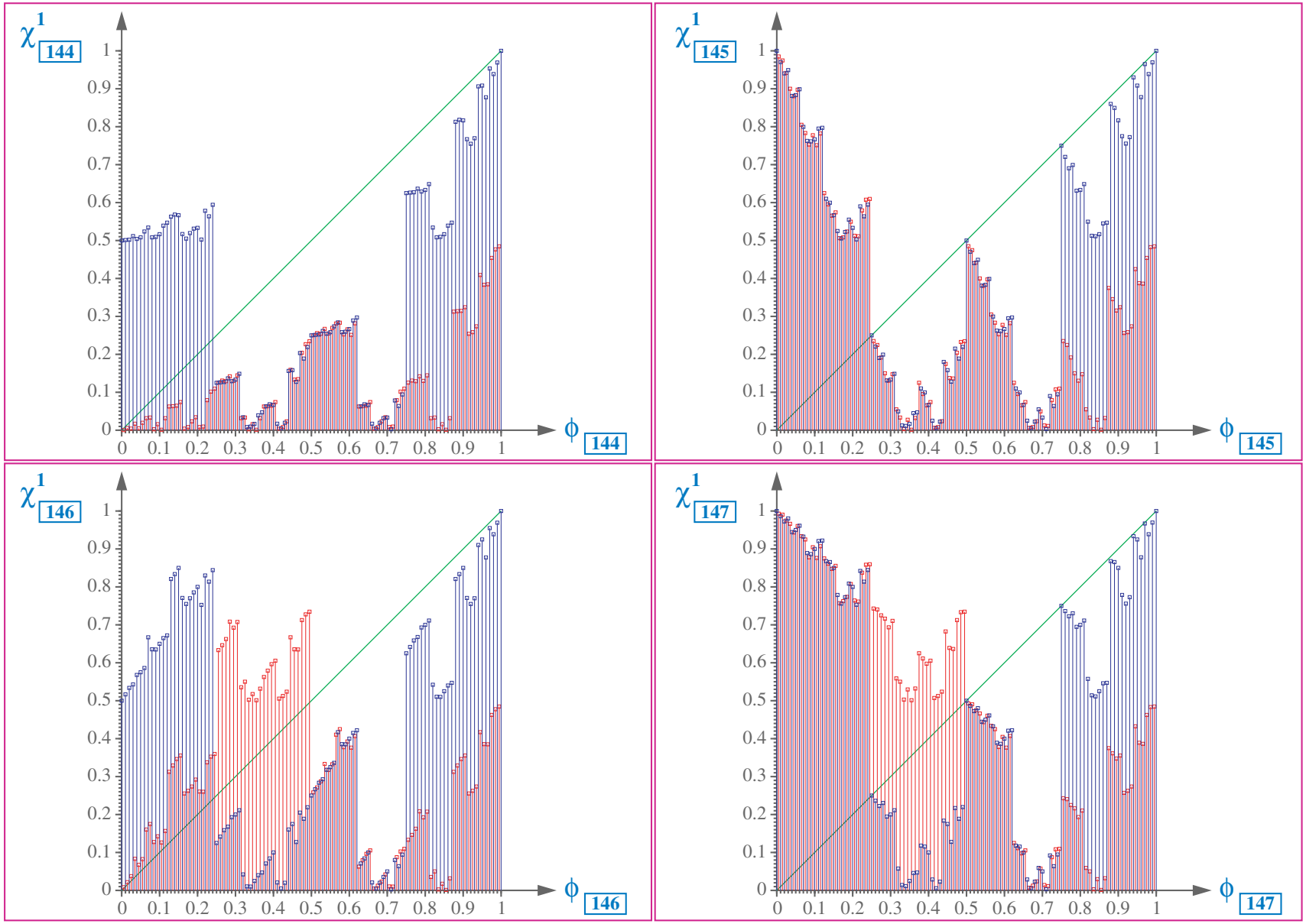


Table 2. (*Continued*)

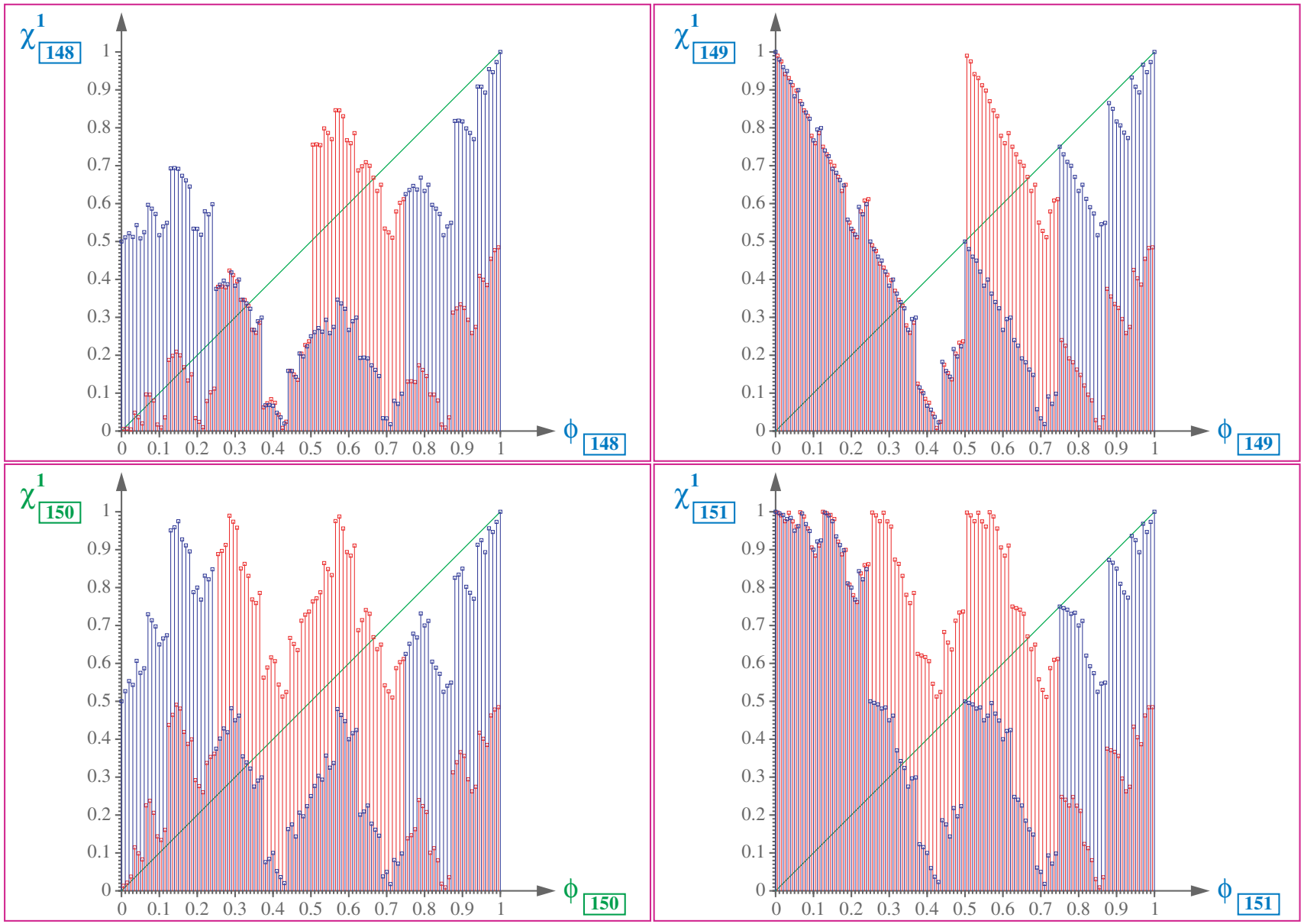


Table 2. (*Continued*)

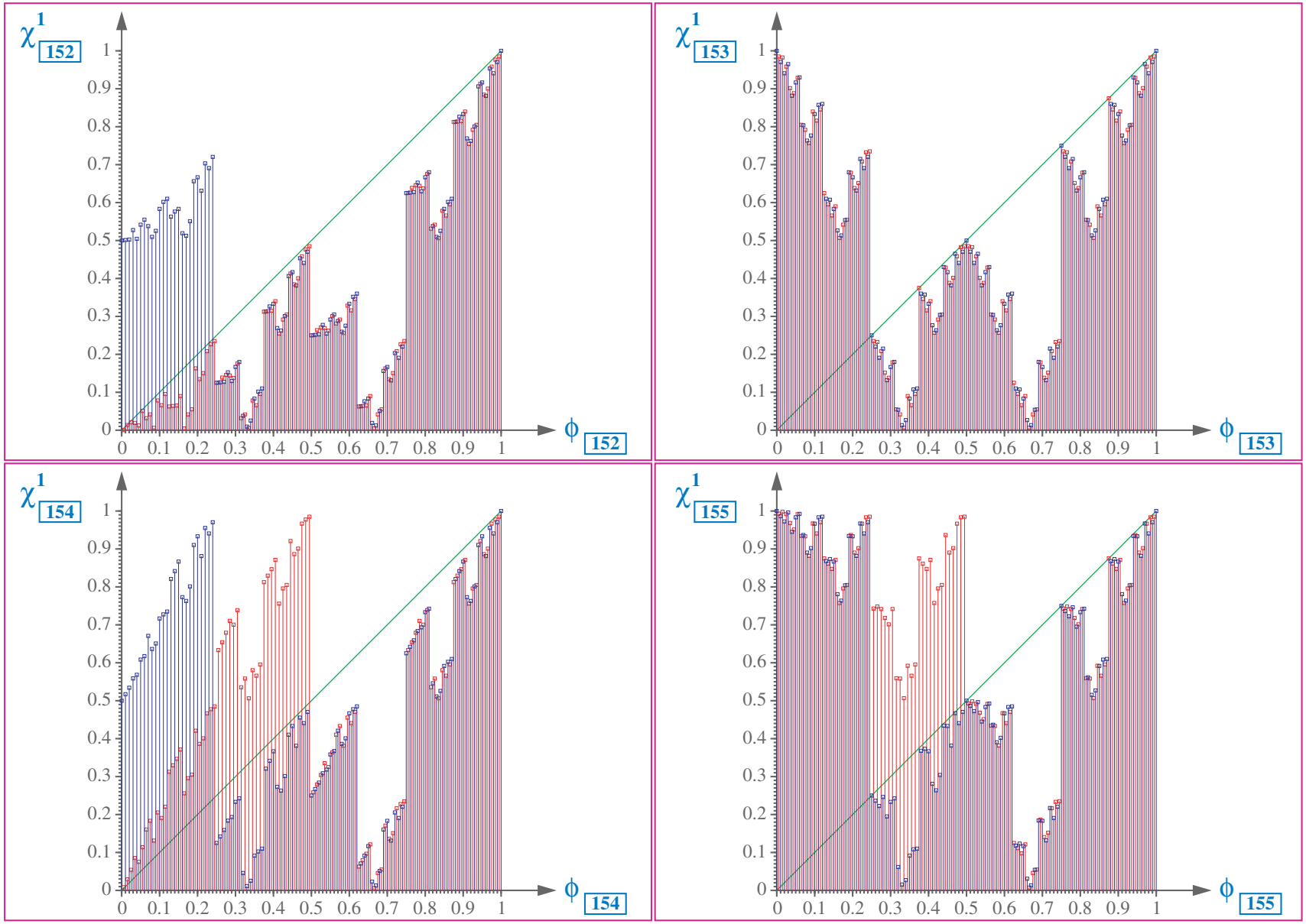


Table 2. (*Continued*)

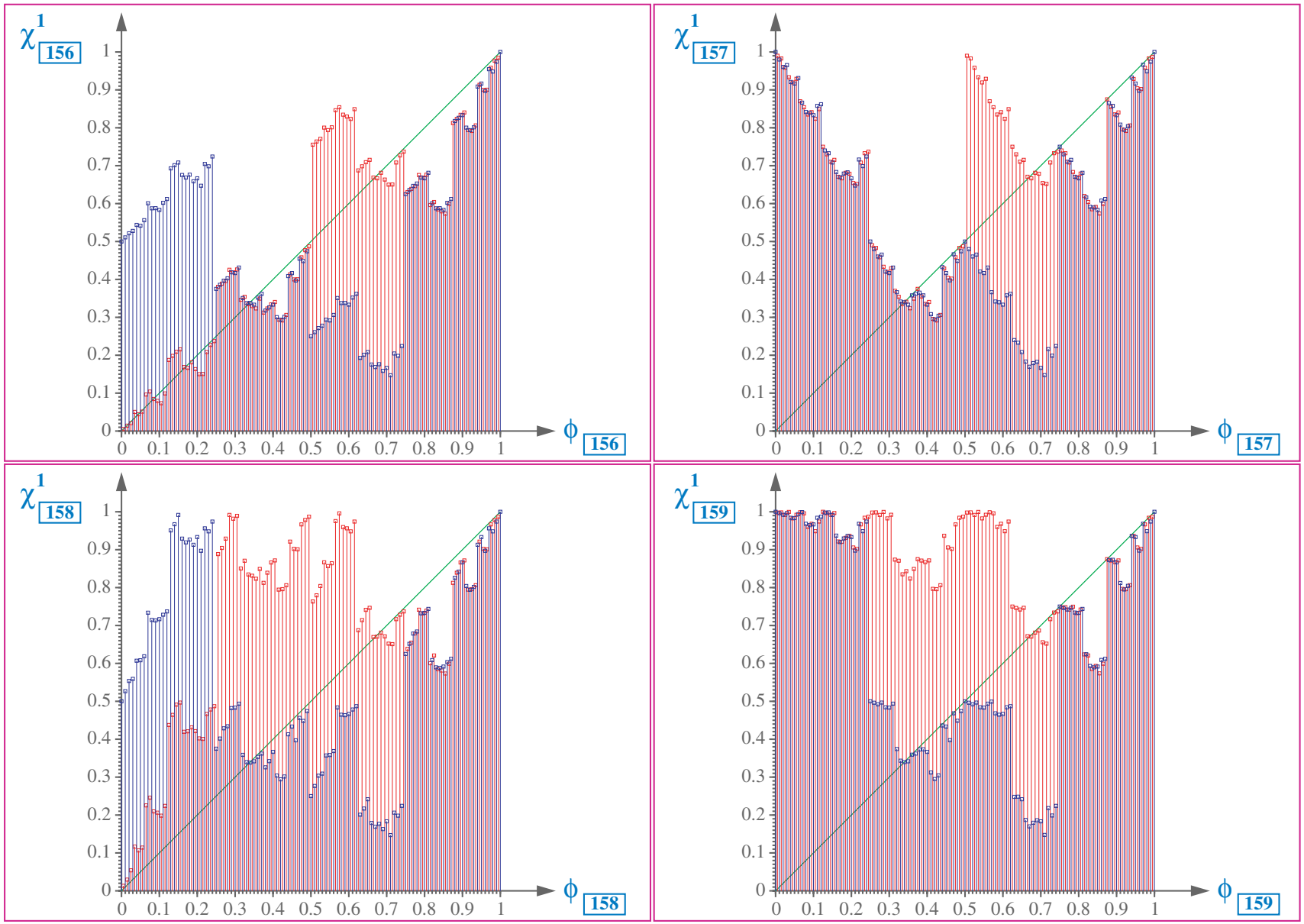


Table 2. (*Continued*)

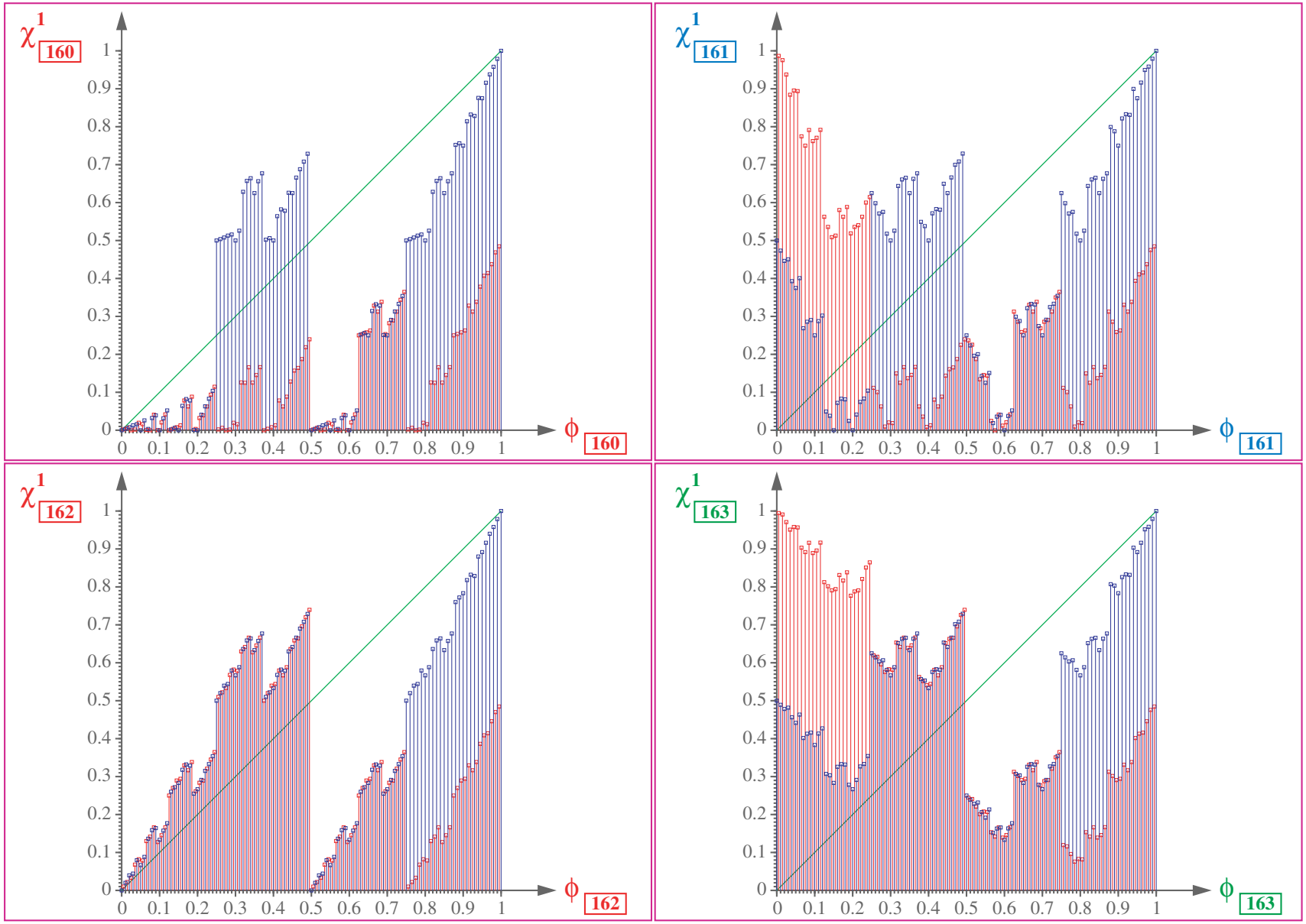


Table 2. (*Continued*)

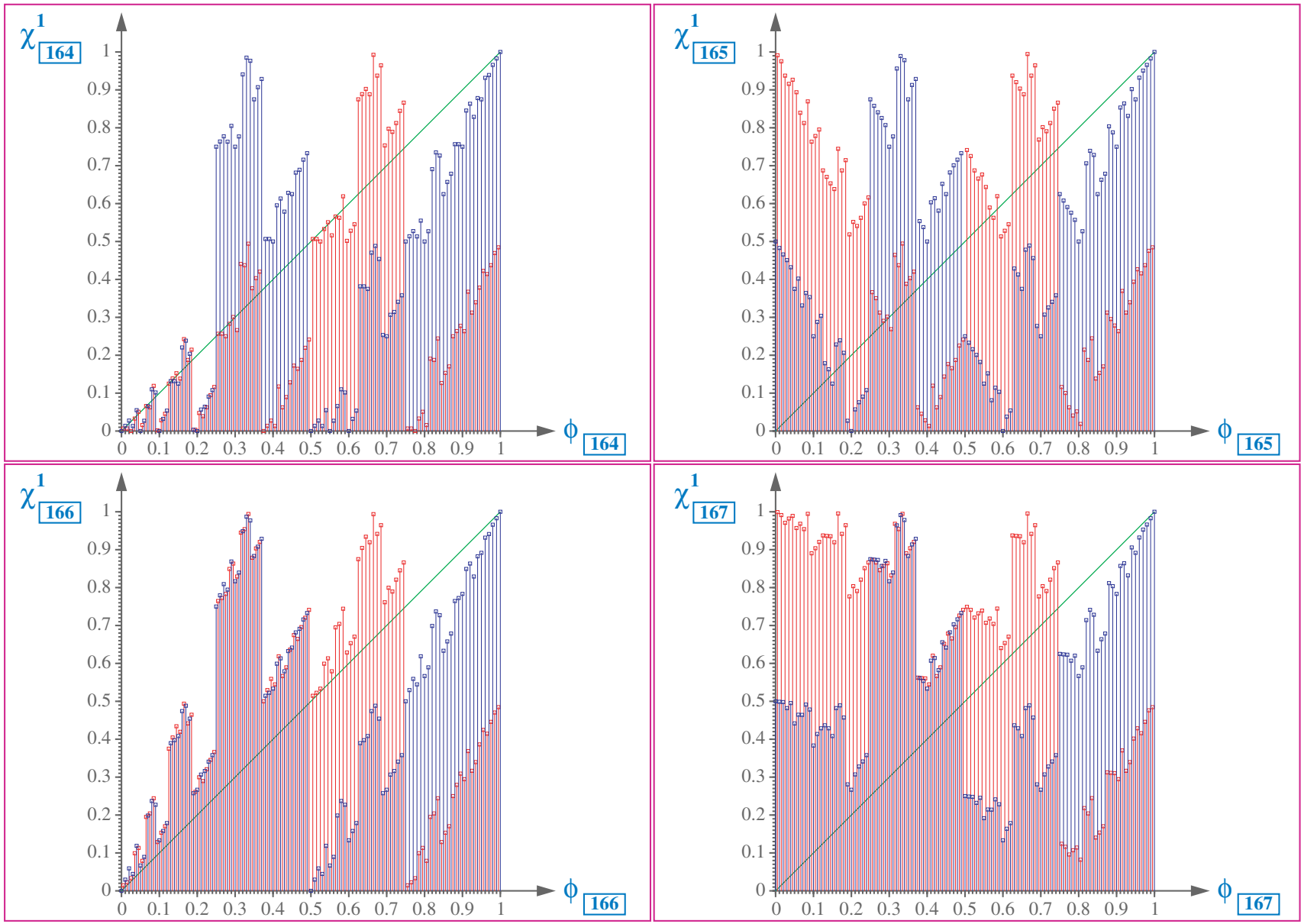


Table 2. (*Continued*)

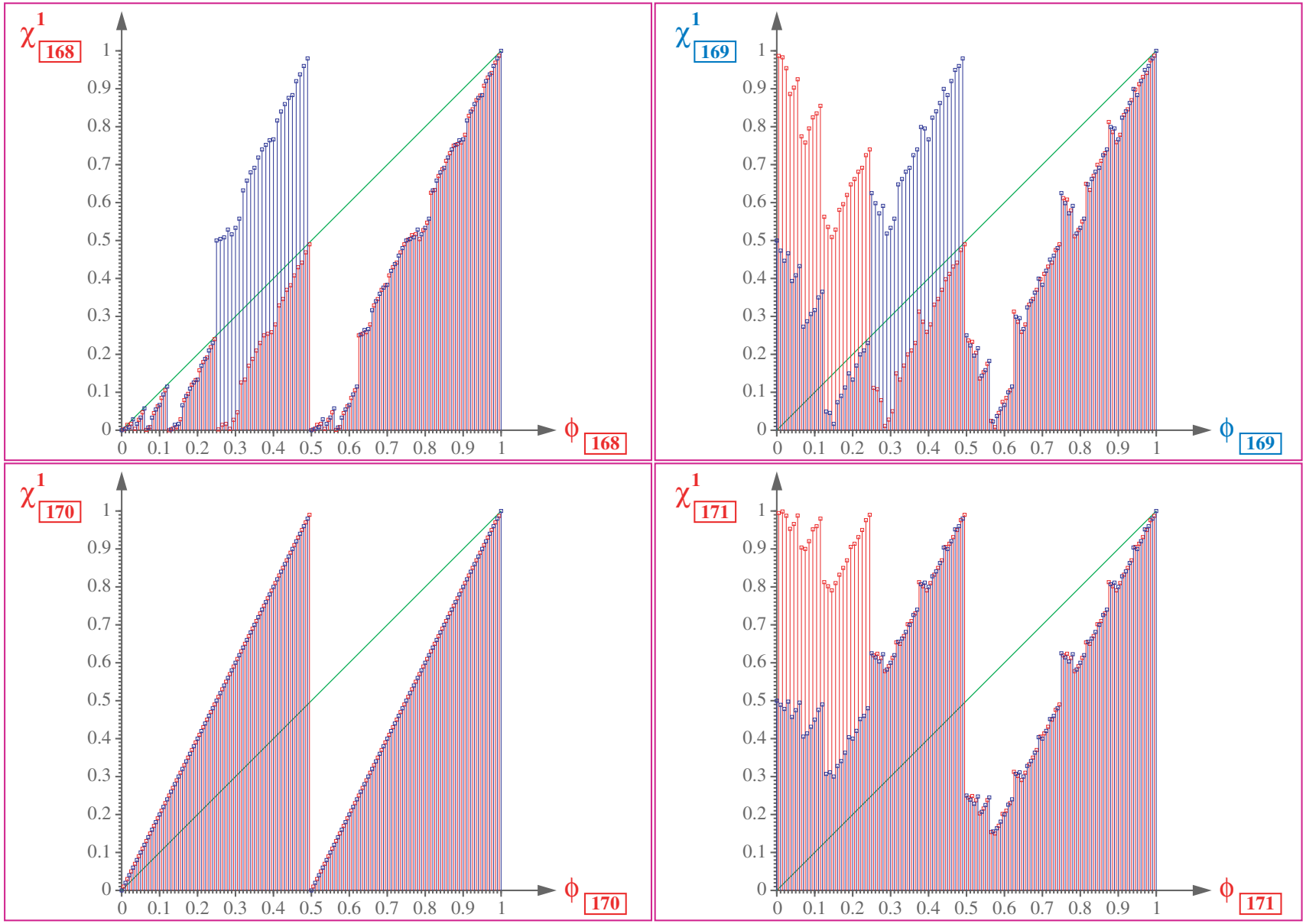


Table 2. (*Continued*)

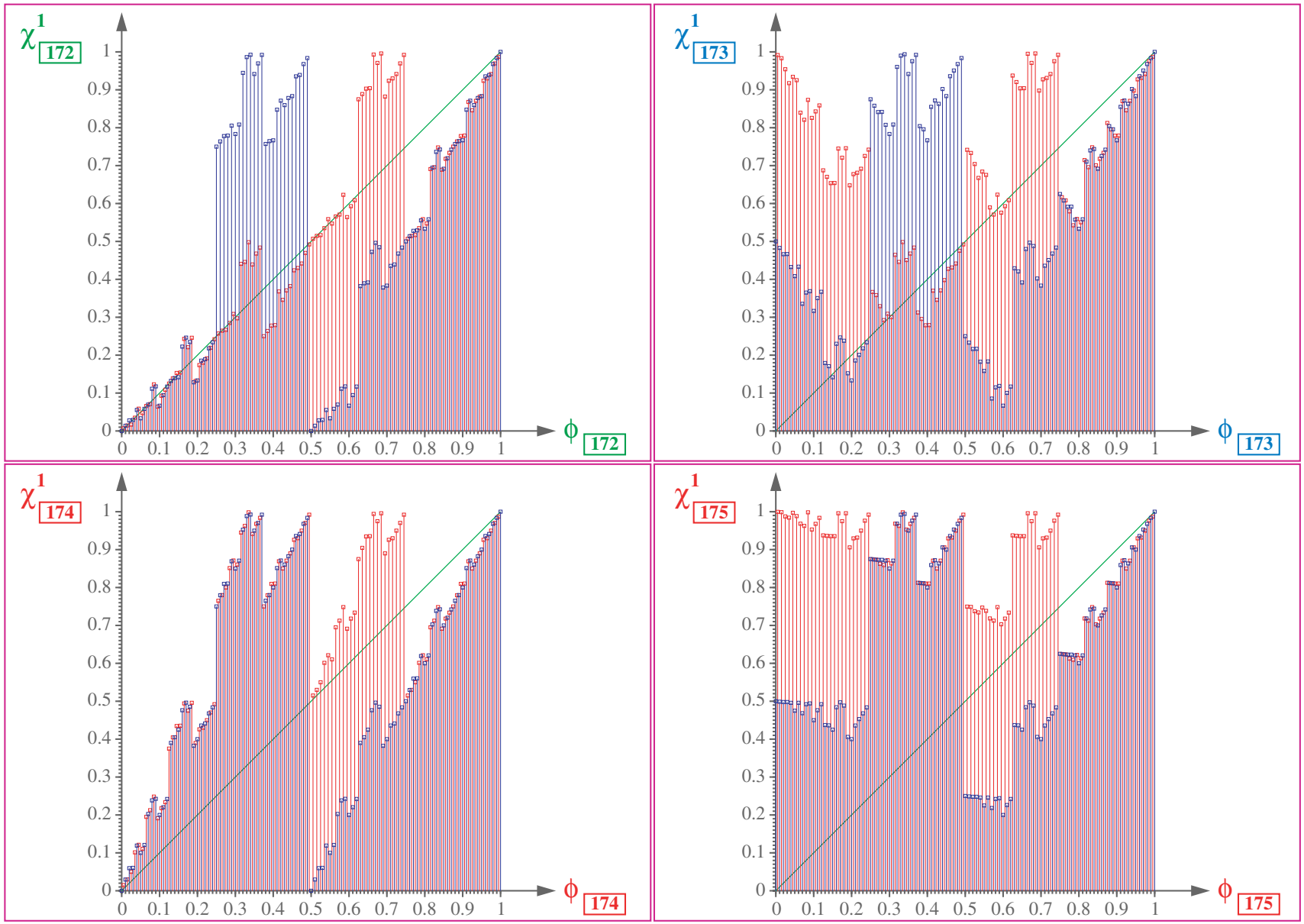


Table 2. (*Continued*)

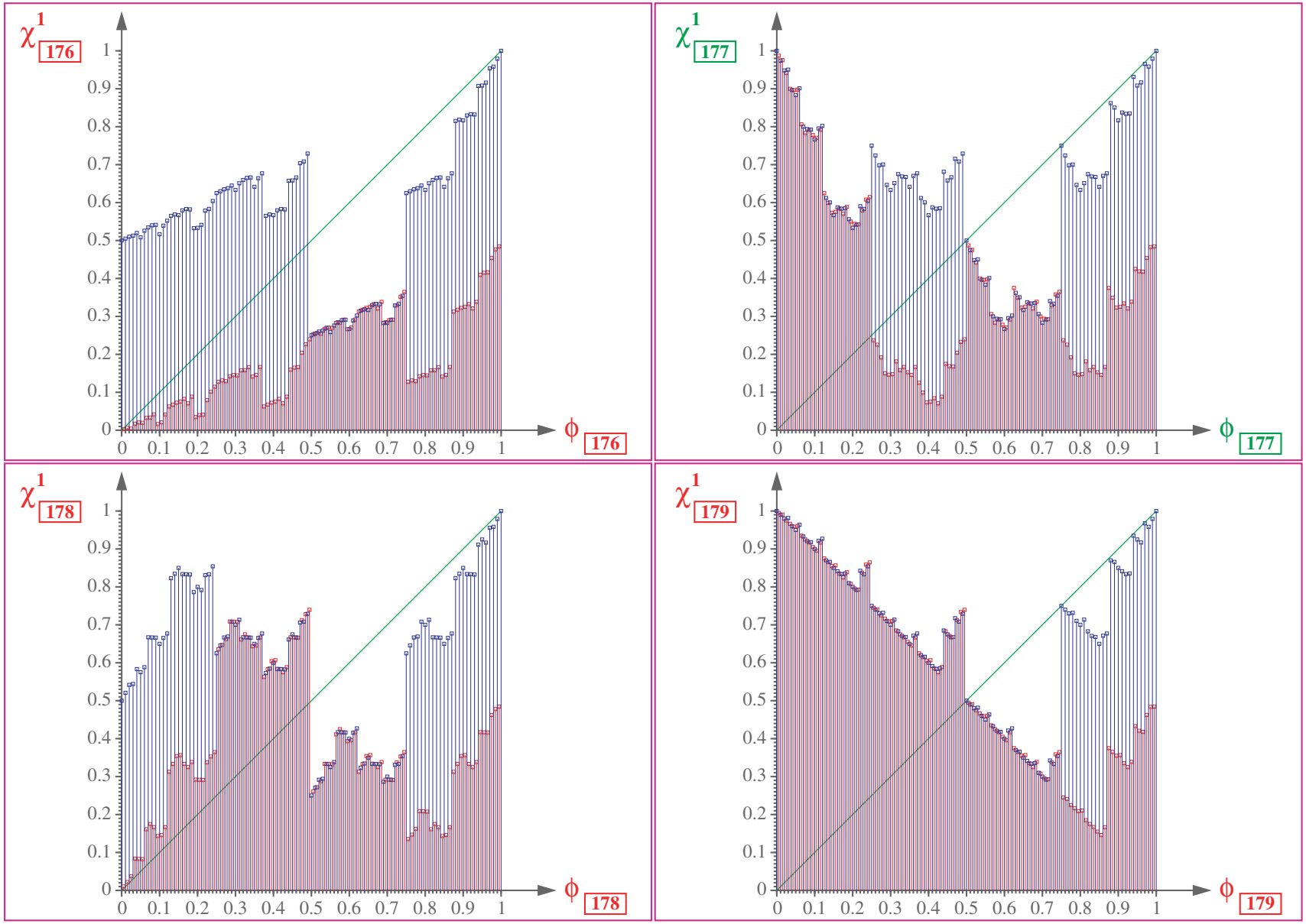


Table 2. (*Continued*)

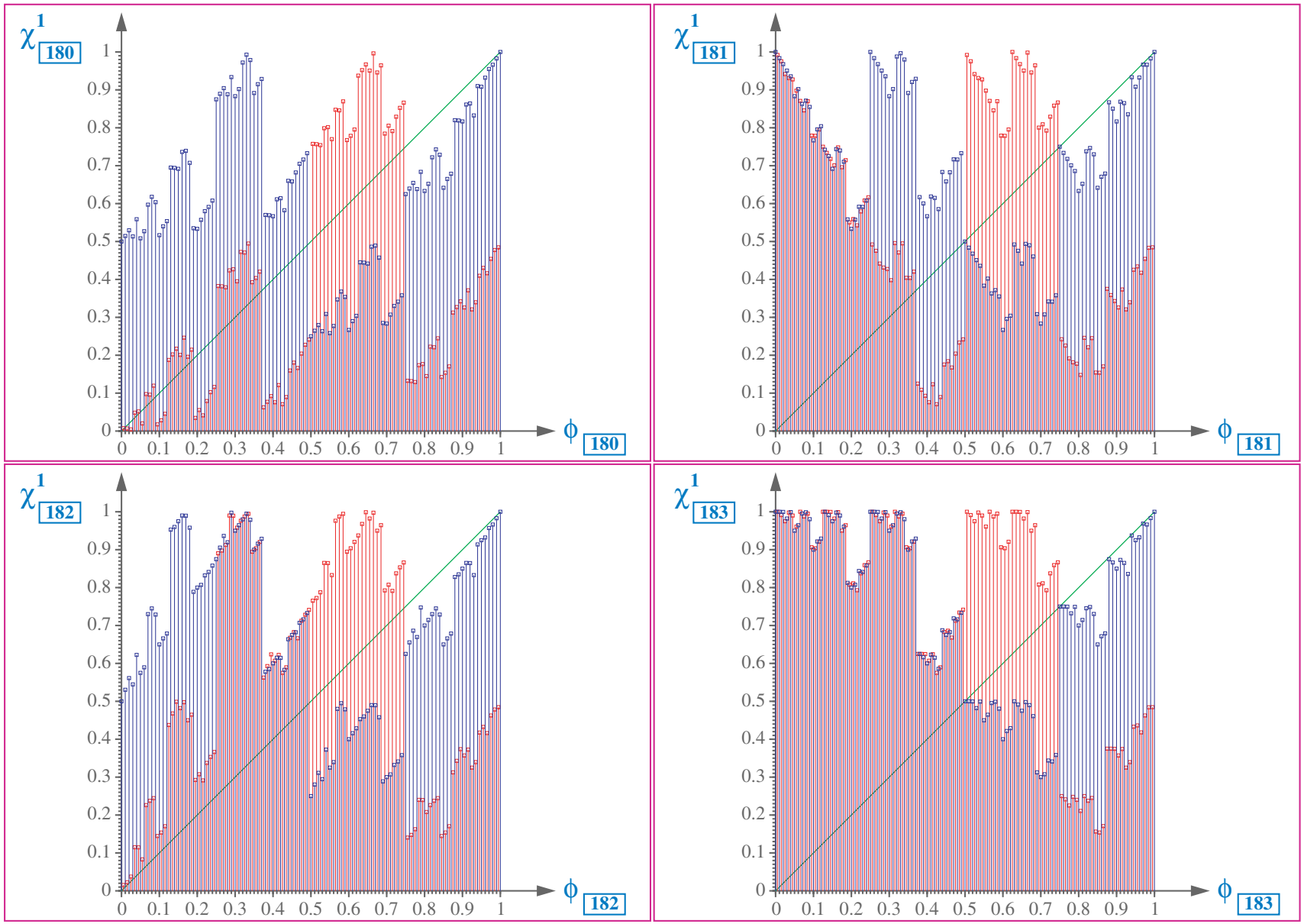


Table 2. (*Continued*)

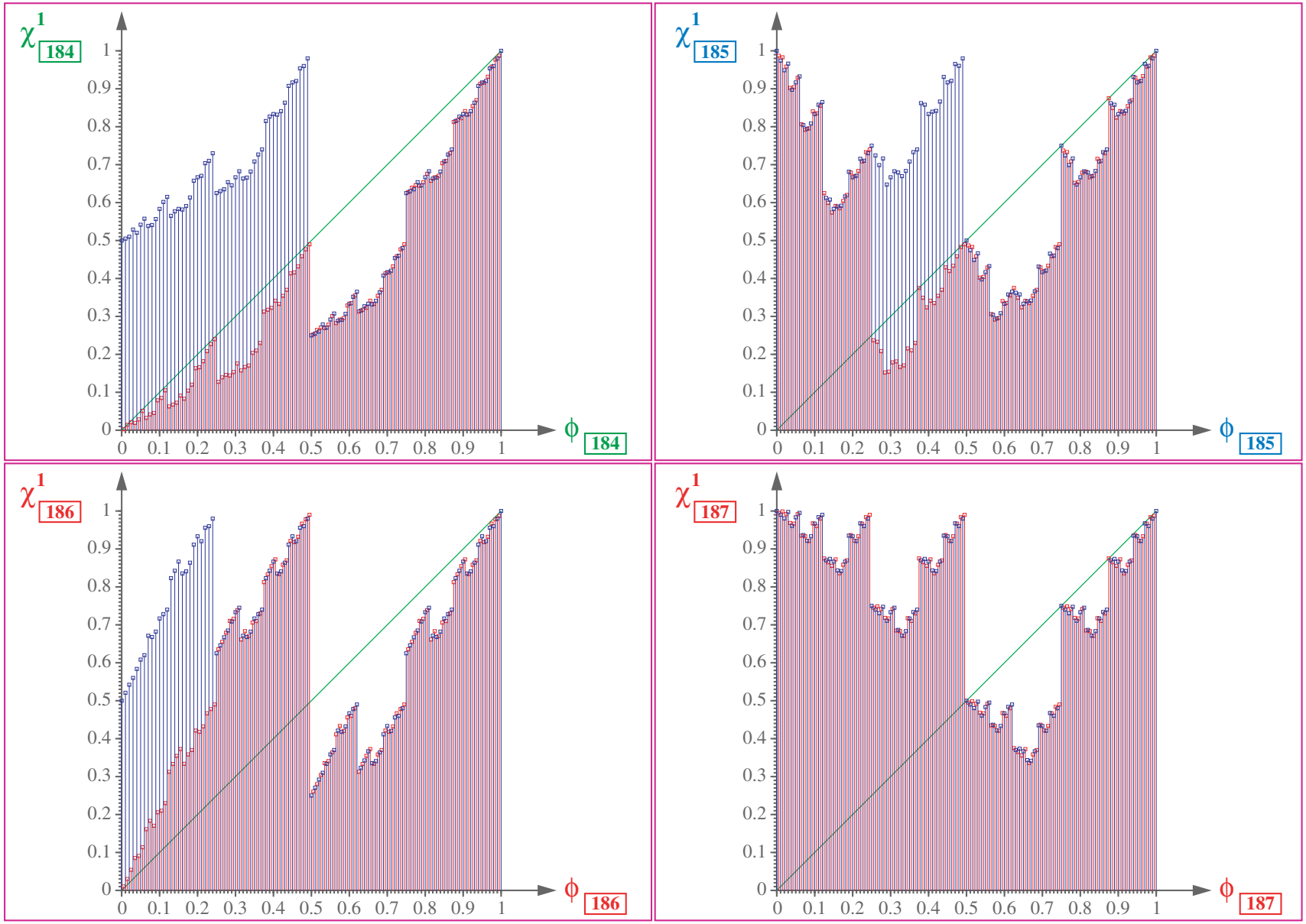


Table 2. (*Continued*)

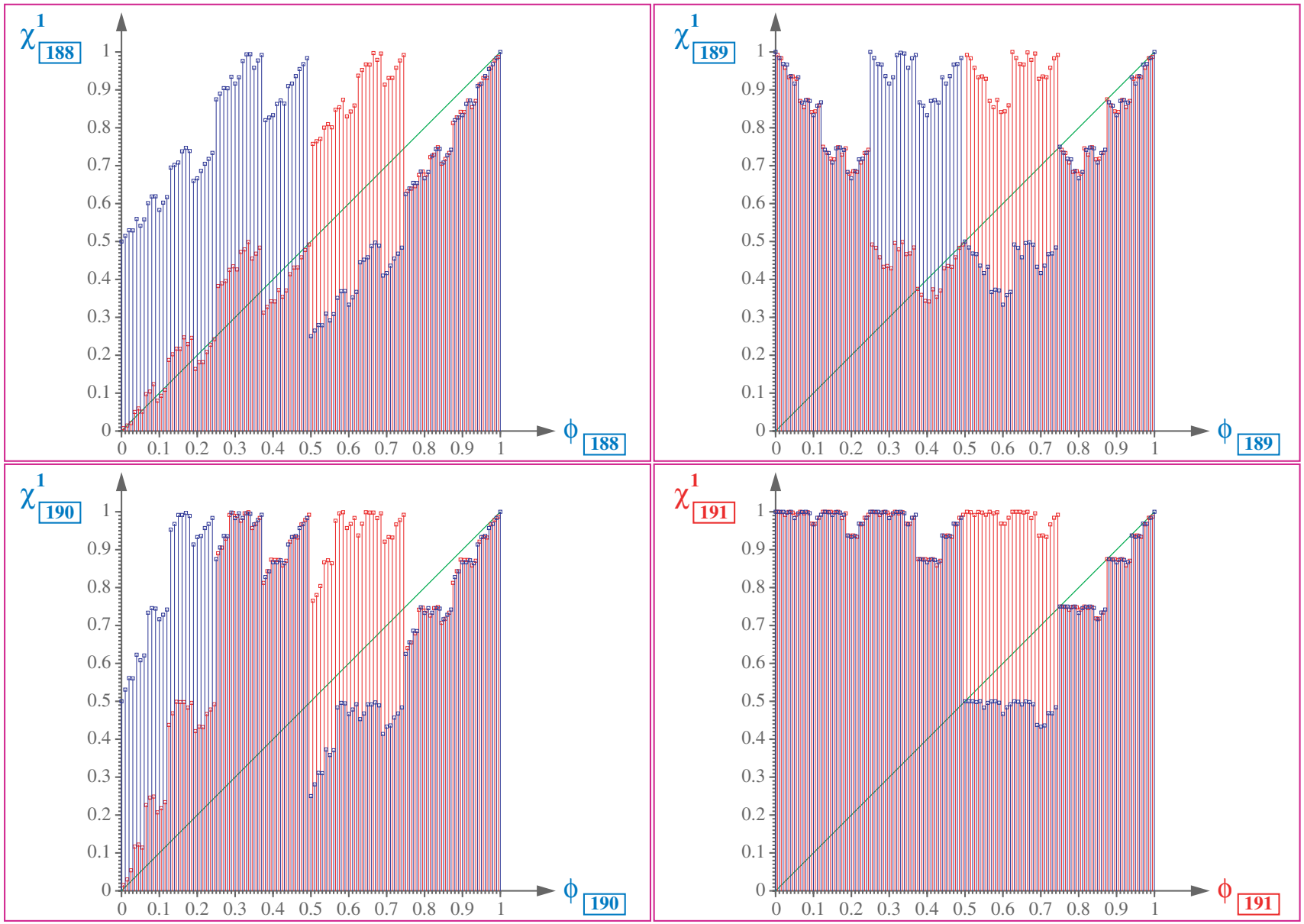


Table 2. (*Continued*)

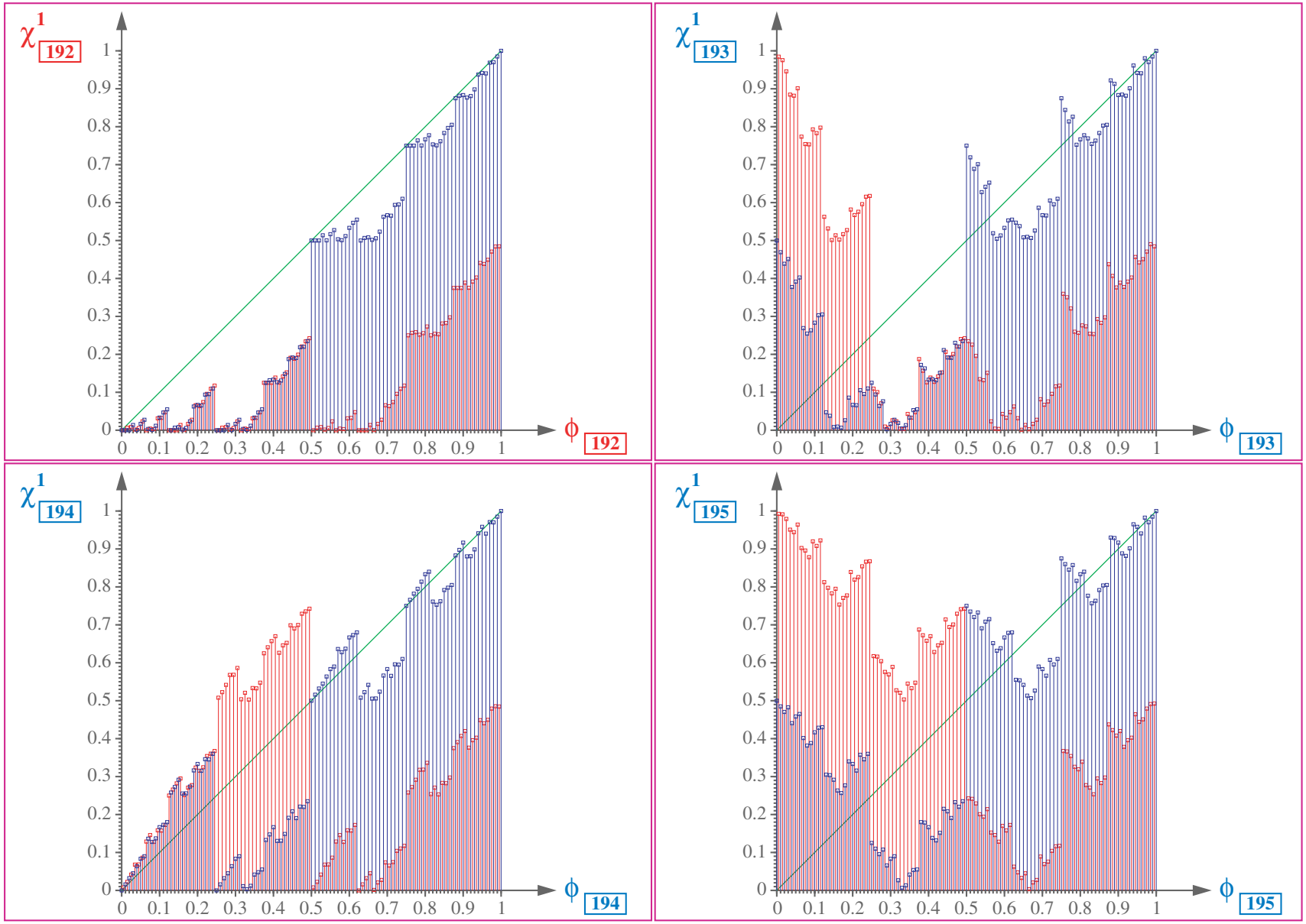


Table 2. (*Continued*)

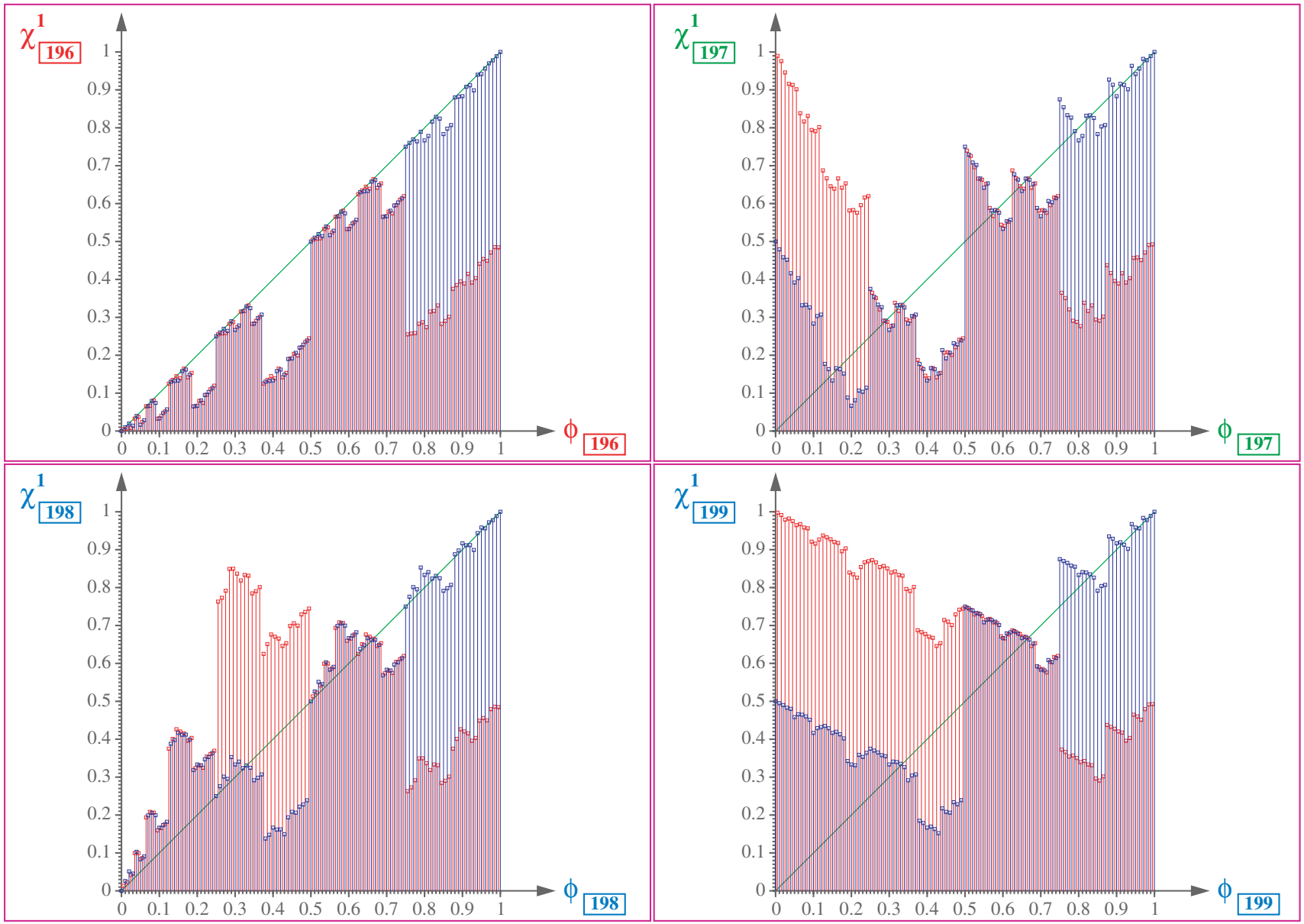


Table 2. (*Continued*)

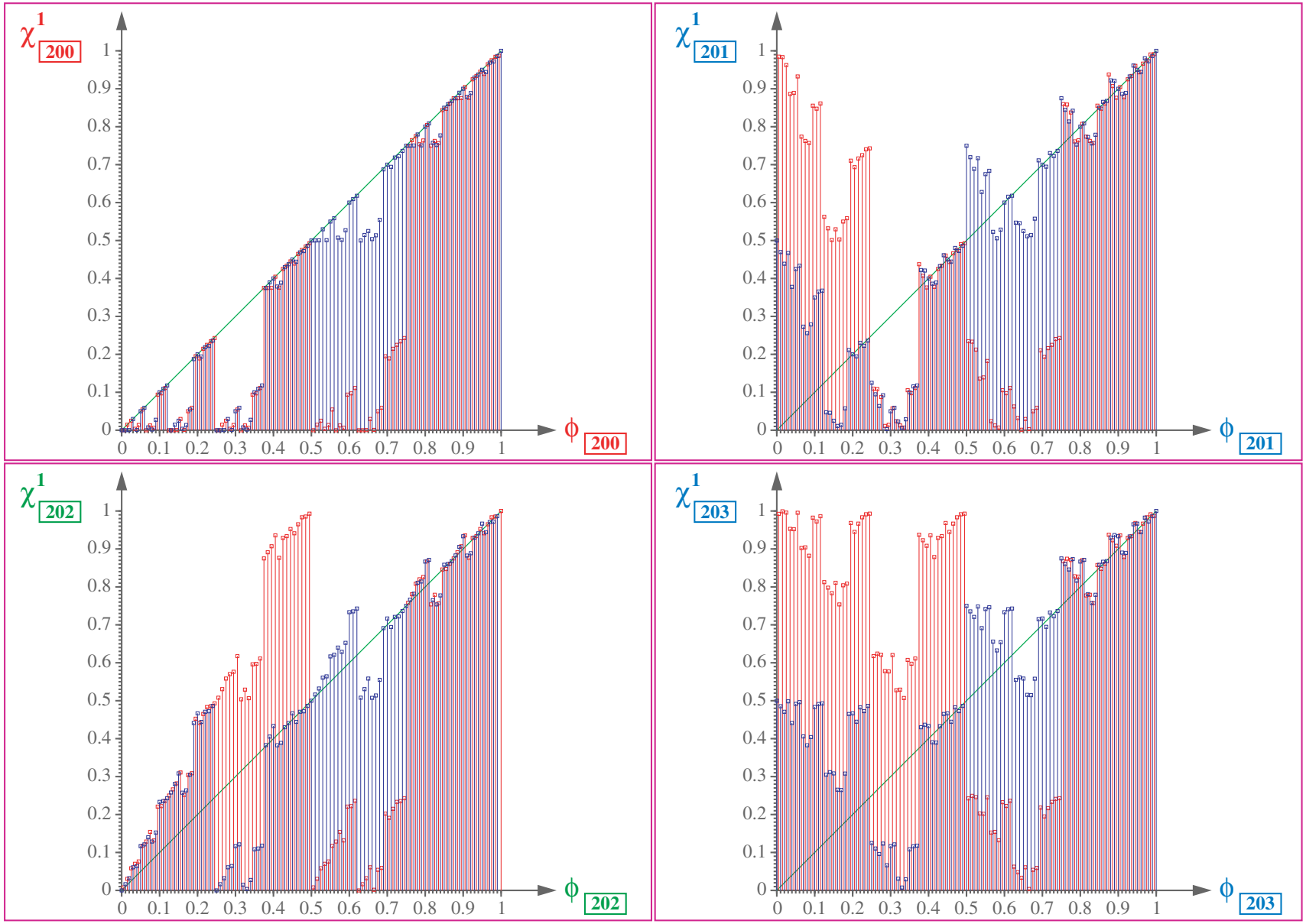


Table 2. (*Continued*)

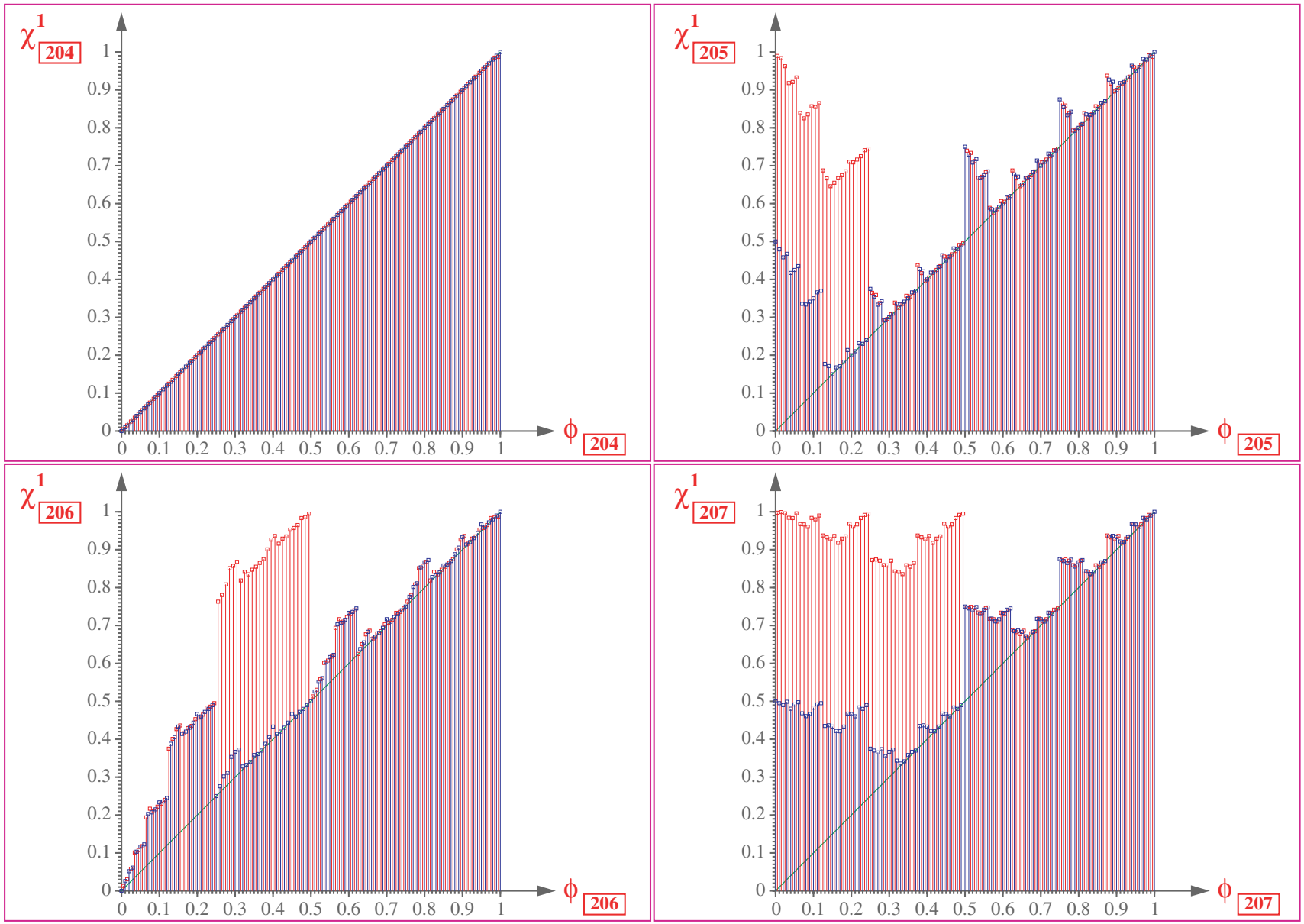


Table 2. (*Continued*)

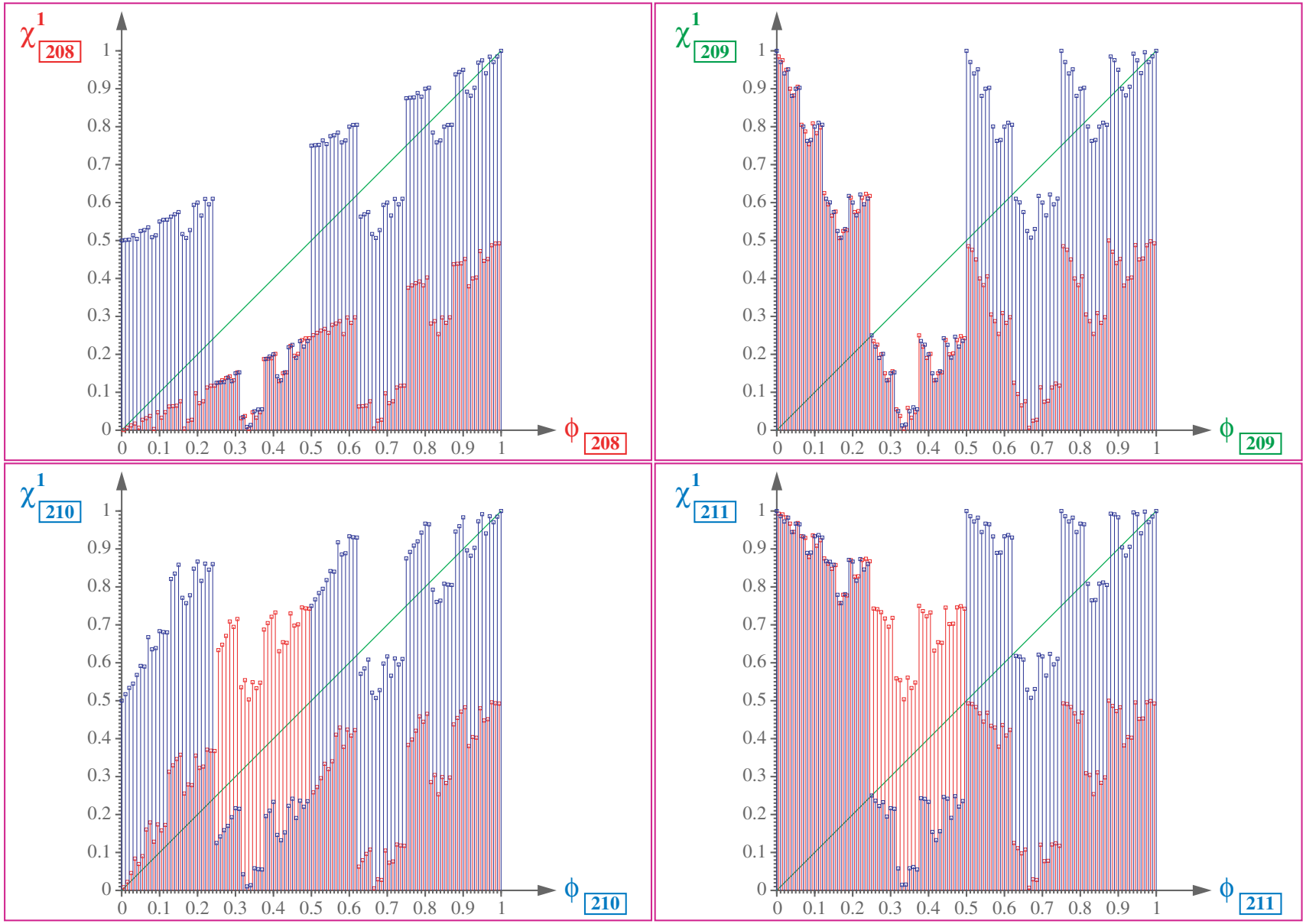


Table 2. (*Continued*)

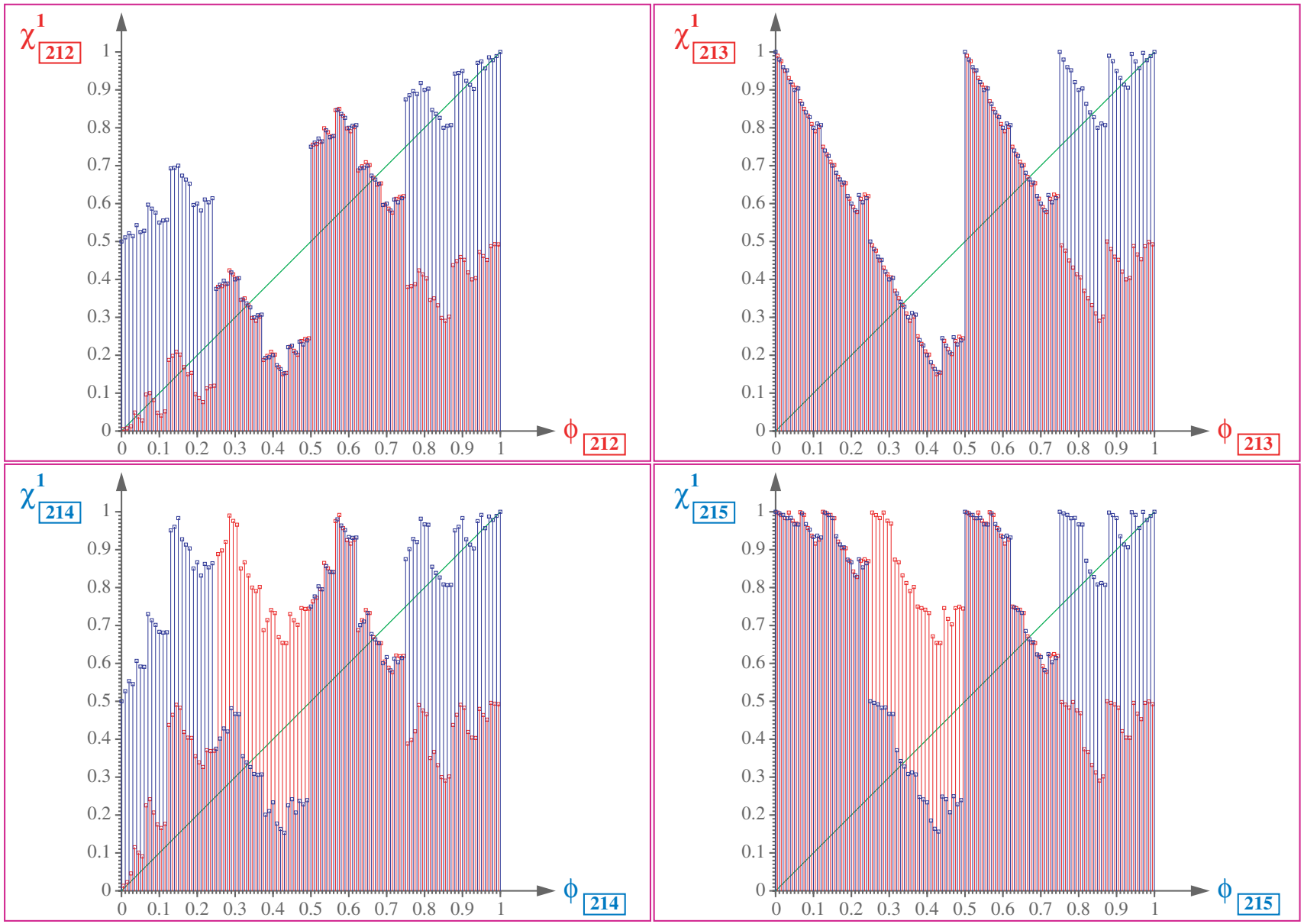


Table 2. (*Continued*)

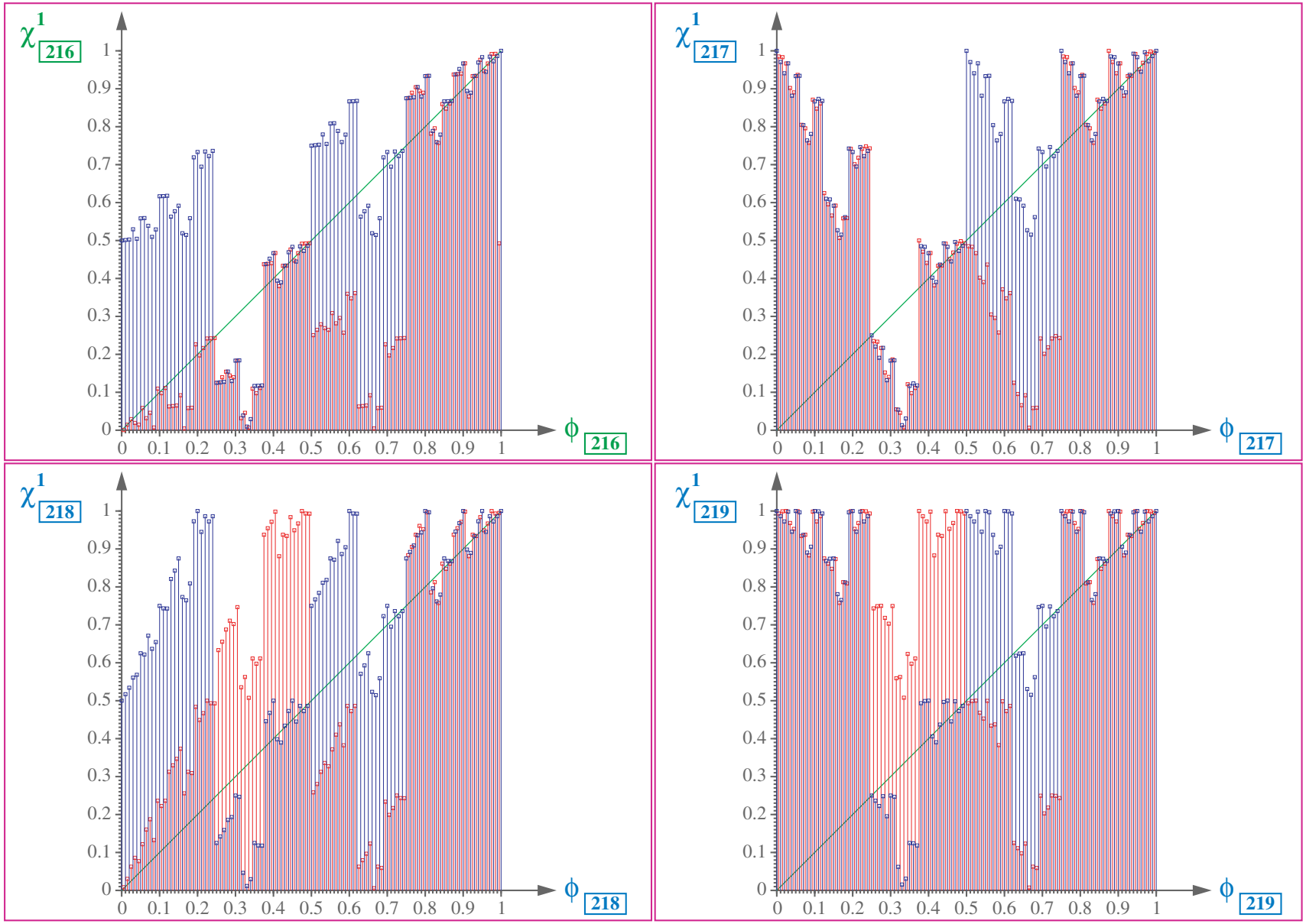


Table 2. (*Continued*)

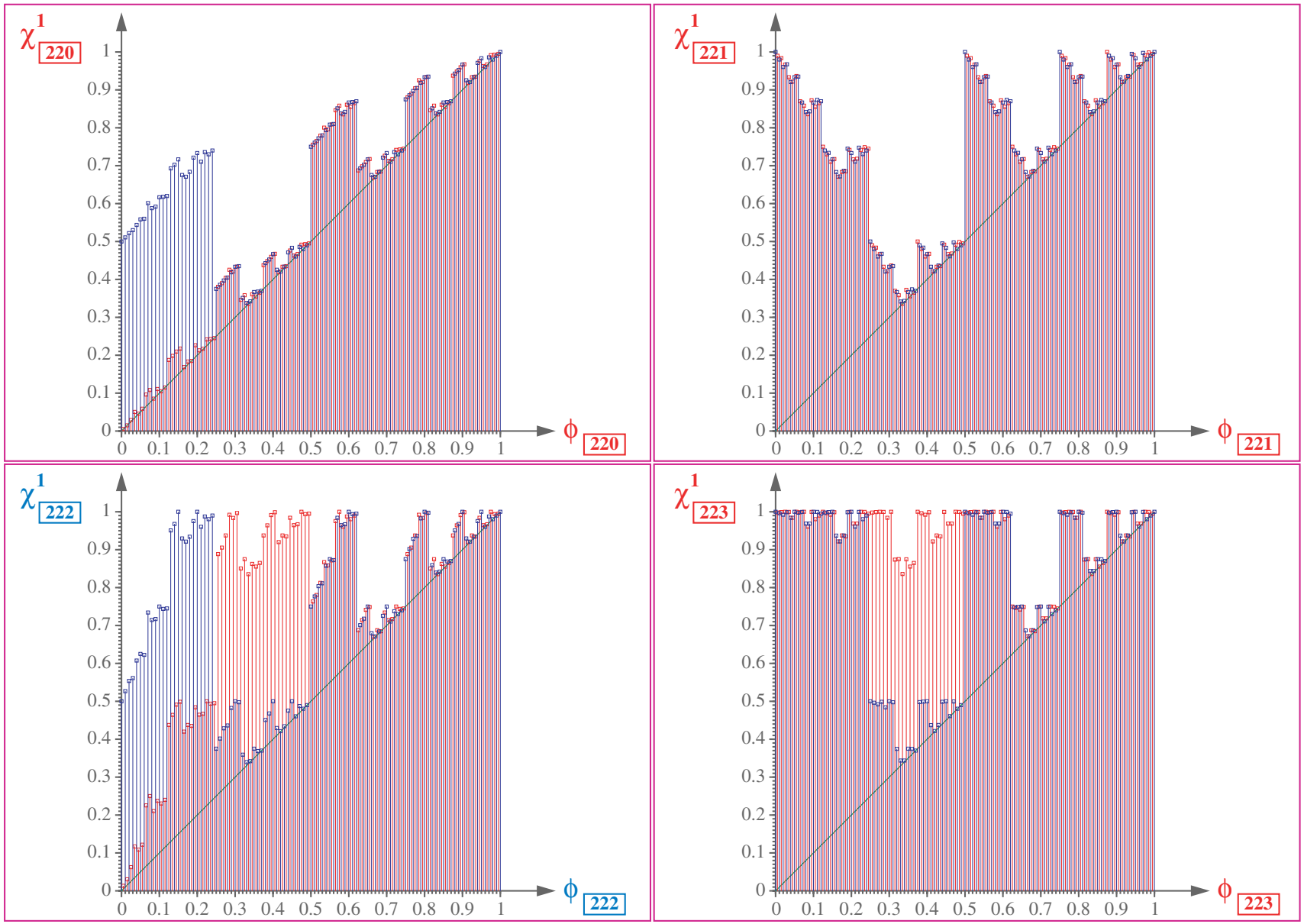


Table 2. (*Continued*)

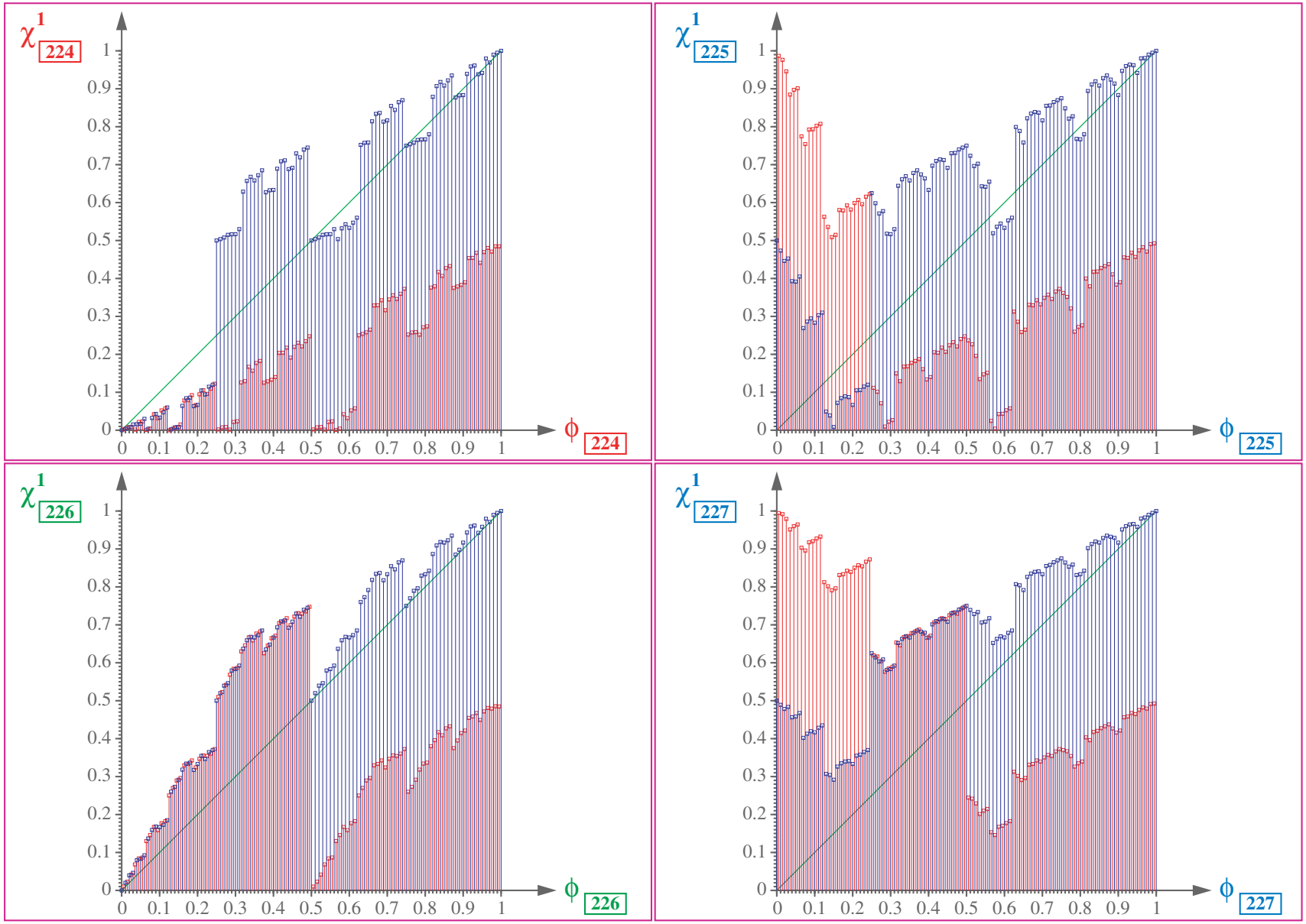


Table 2. (*Continued*)

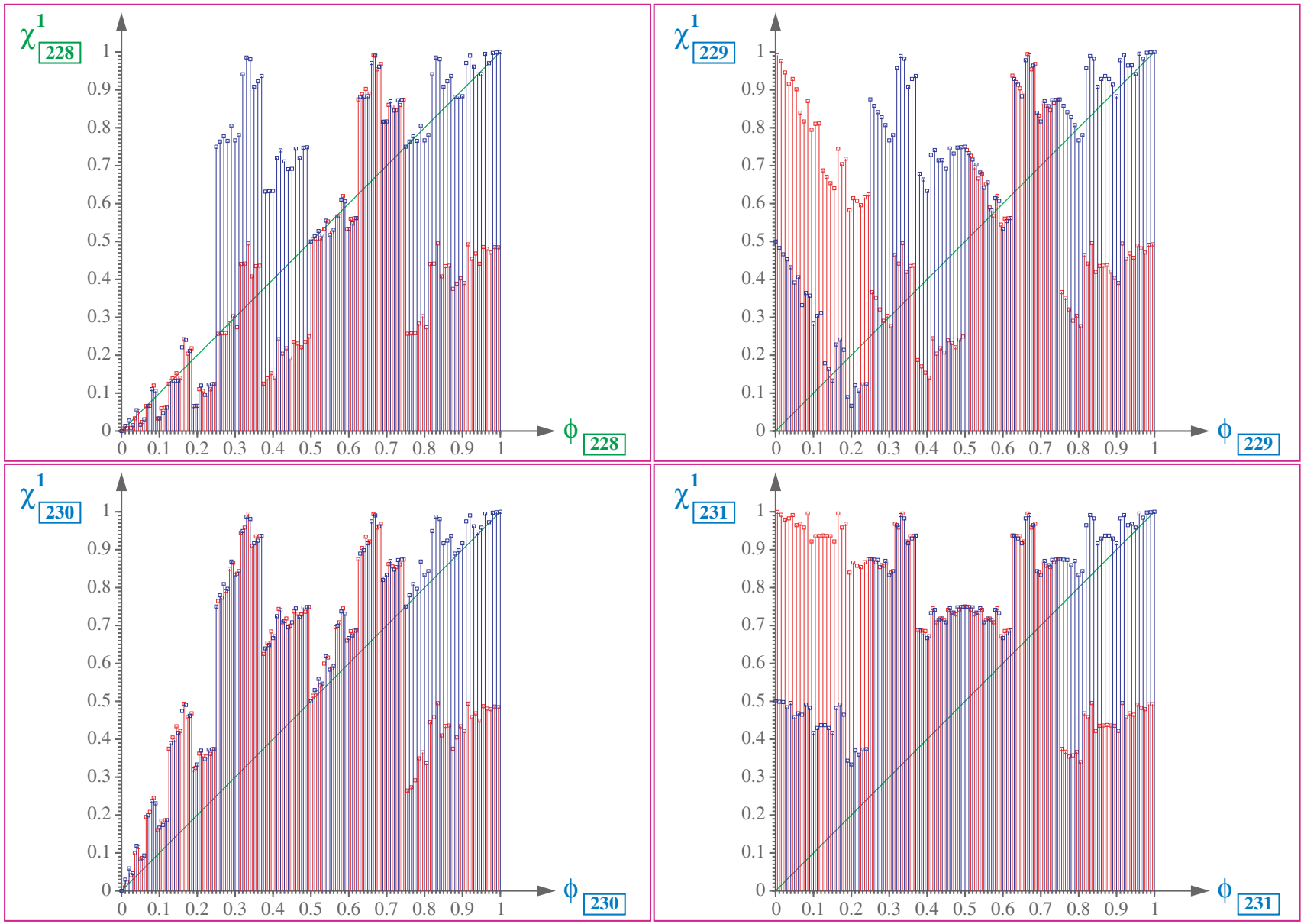


Table 2. (*Continued*)

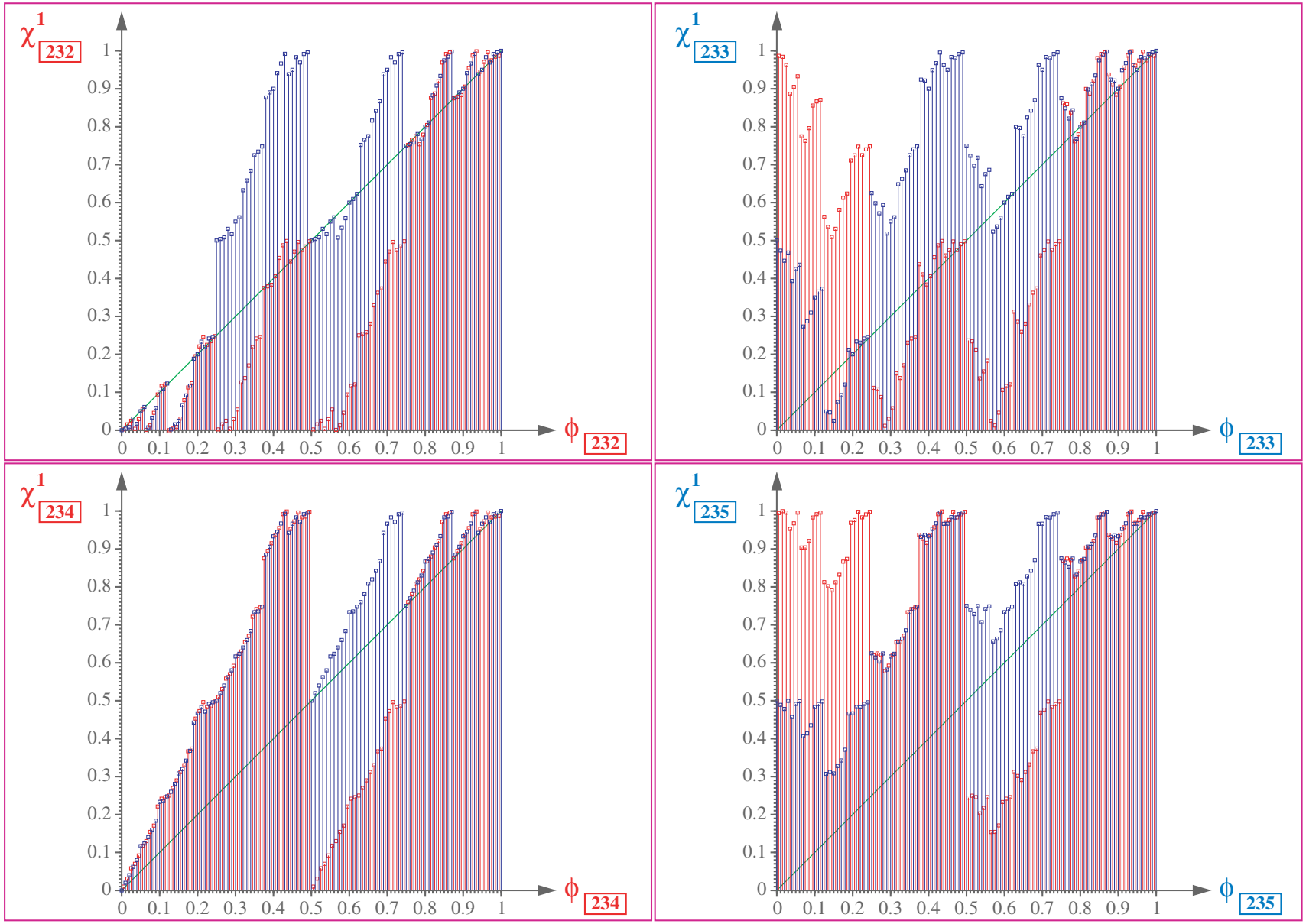


Table 2. (*Continued*)

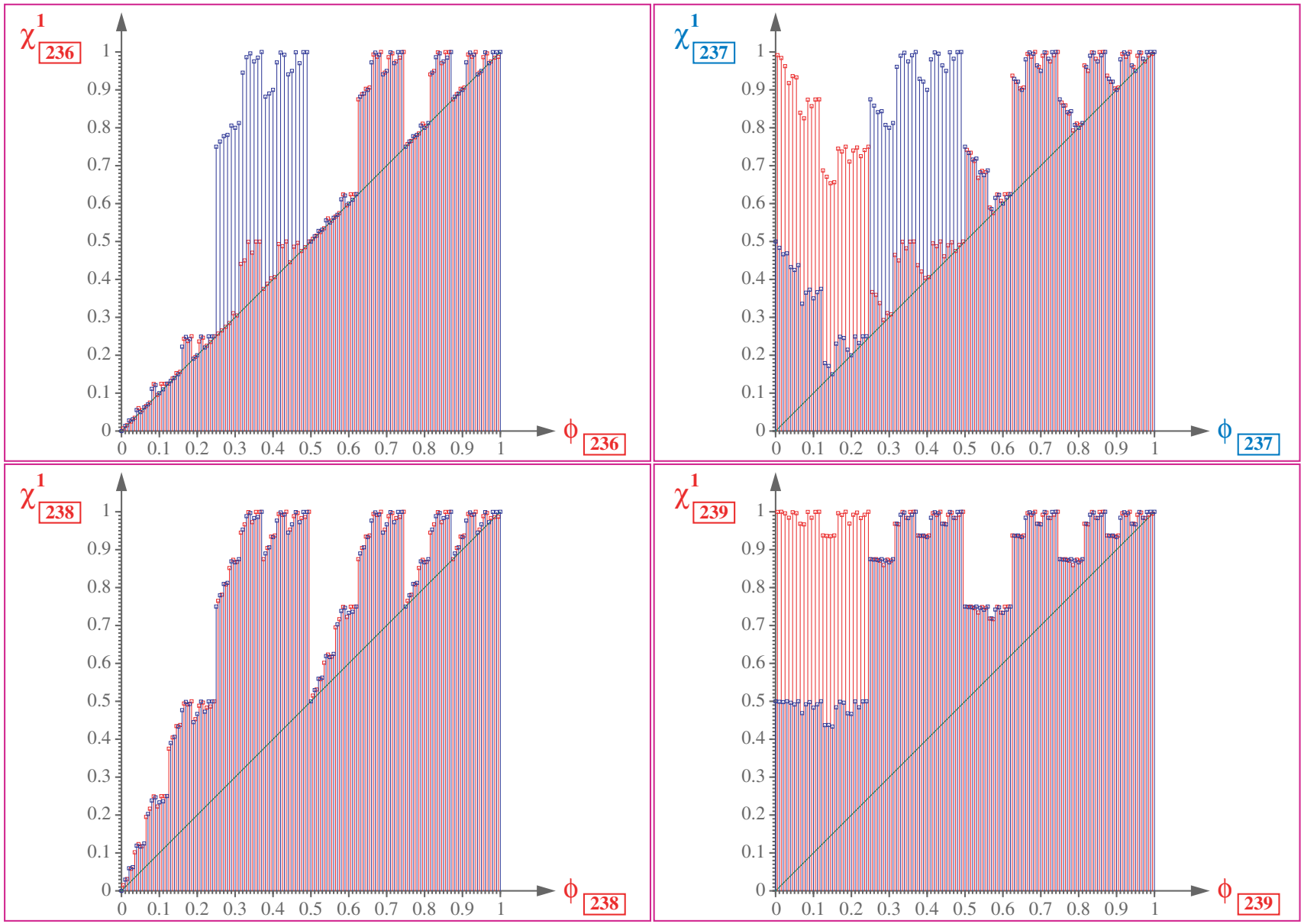


Table 2. (*Continued*)

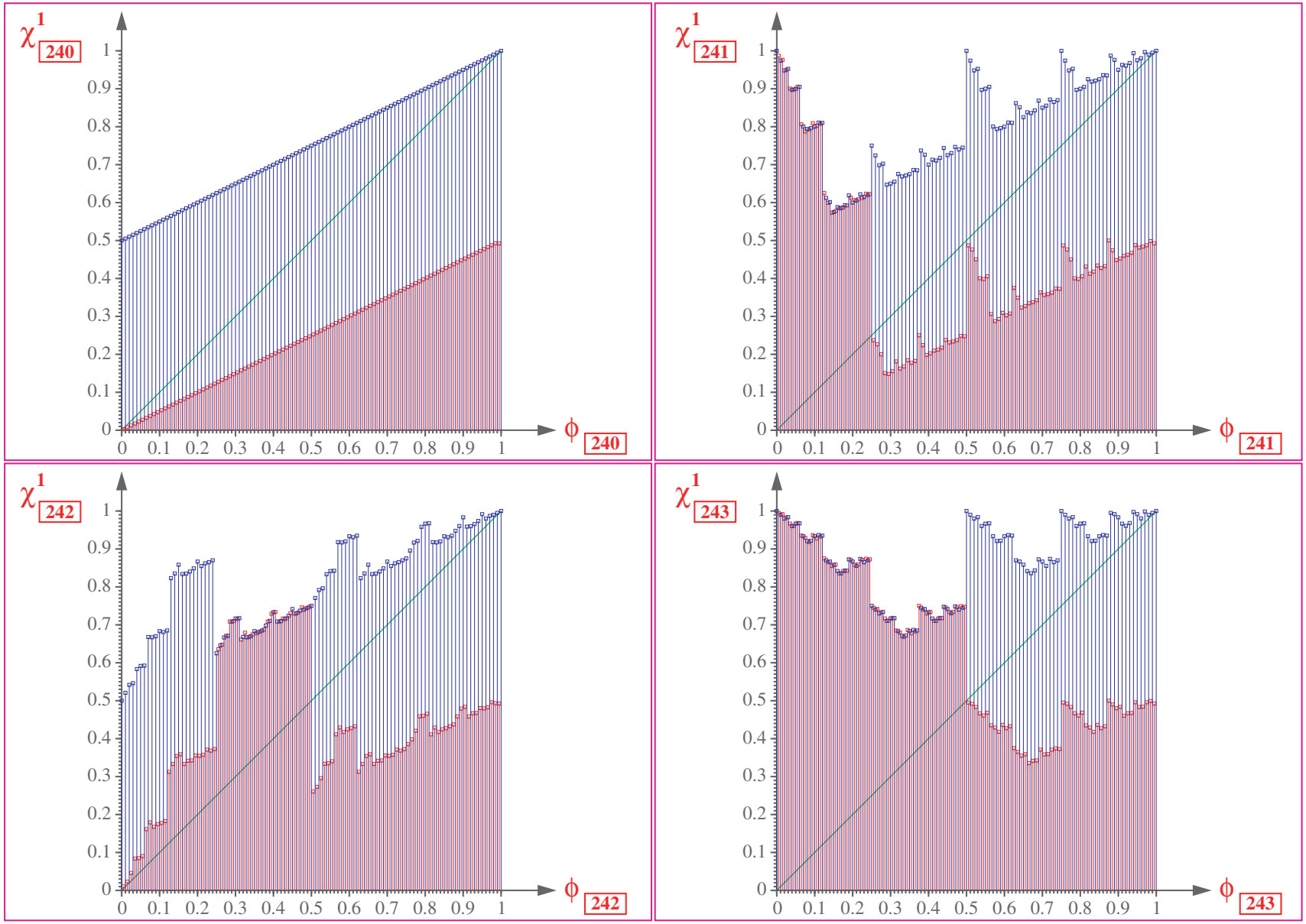


Table 2. (*Continued*)

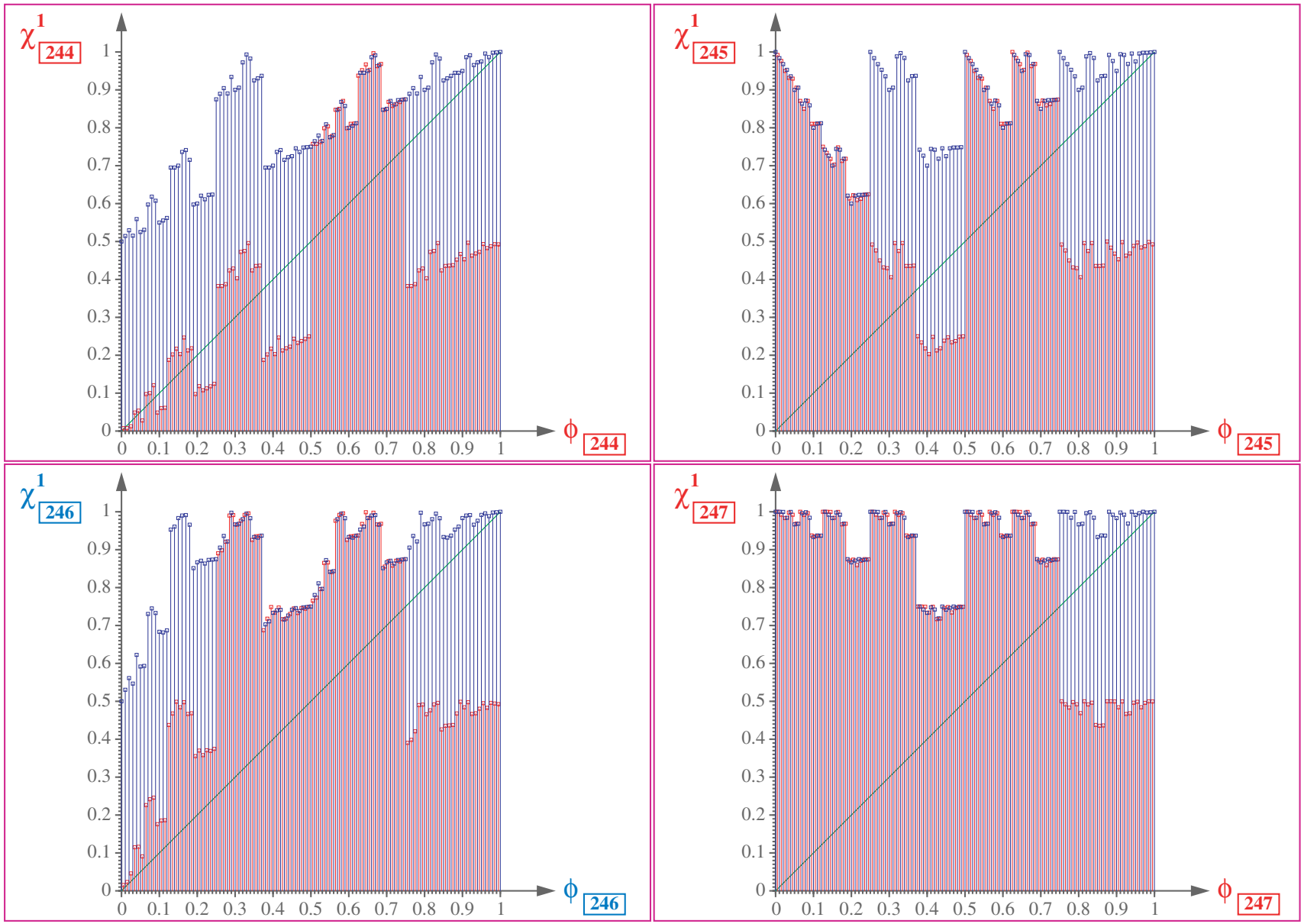


Table 2. (*Continued*)

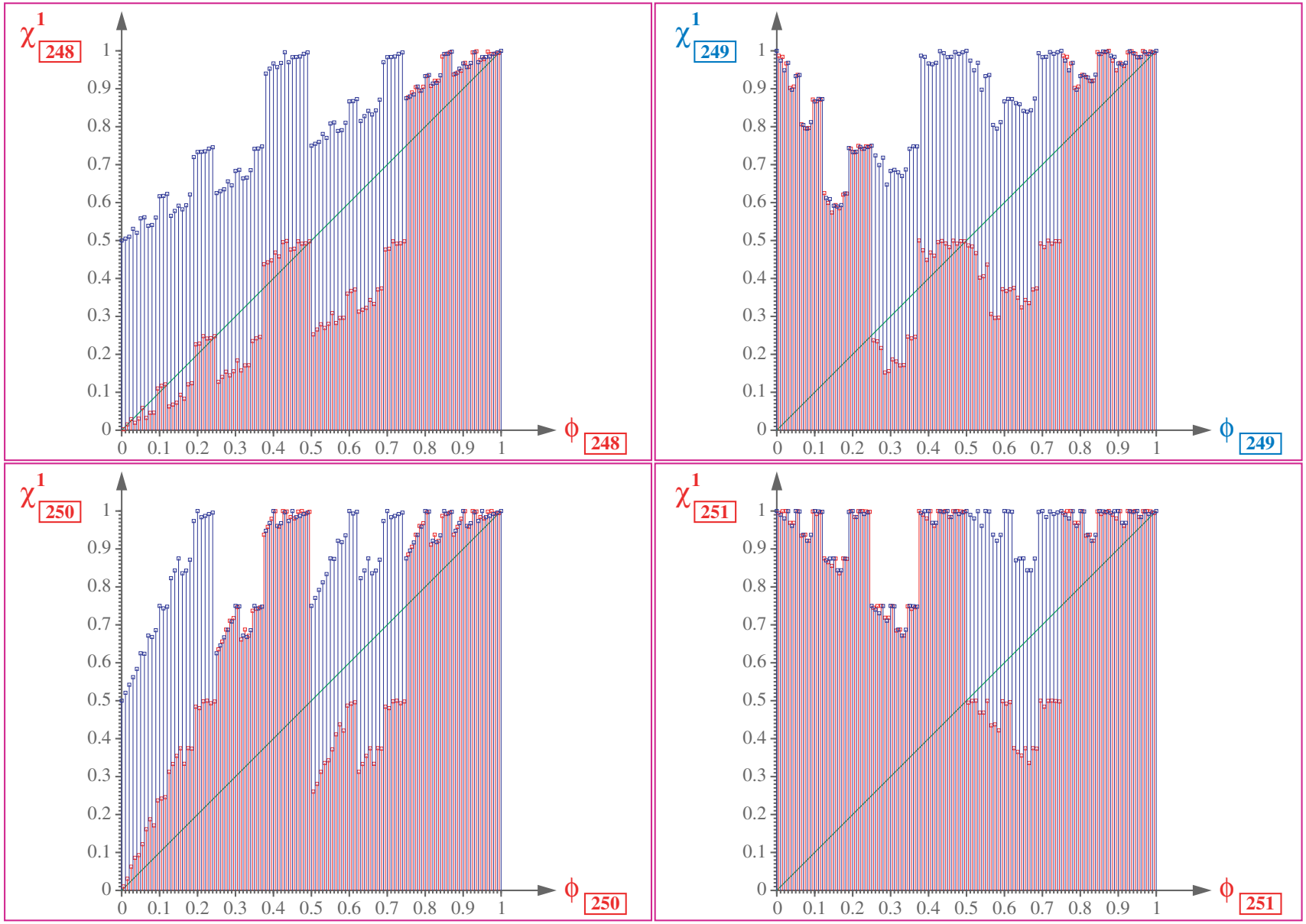
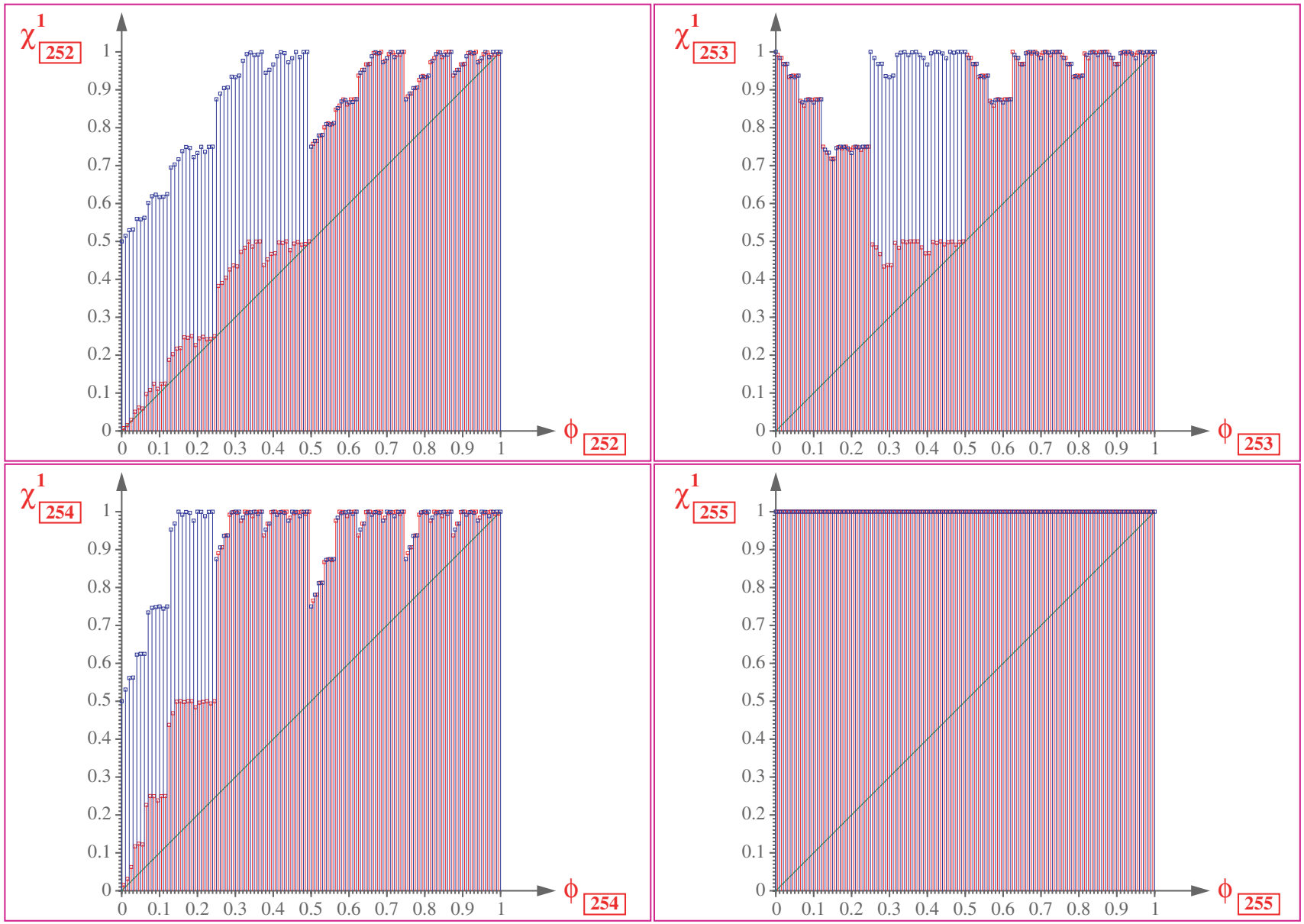


Table 2. (*Continued*)



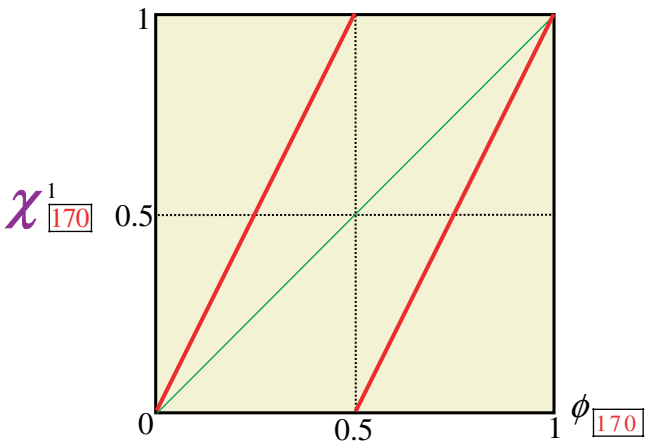


Fig. 3. The characteristic function of the "*right-copycat*" rule 170 converges to the *Bernoulli map*.

Since $x_I \in \{0,1\}$ is the *rightmost* bit of the binary string $\{x_0, x_1, x_2, \ldots, x_I\}$, it follows that the *graph* of the characteristic function $\chi^1_{240}(\phi)$ consists of two parallel branches, parameterized by the last binary bit x_I, as shown in Fig. 4.

Since the output of each pixel "i" of rule 240 in Table 1 is given simply by $y_i = x_{i-1}$, the local rule 240 consists of simply *copying* the "state" of the pixel "$i-1$" of the *left-neighboring* pixel. We will henceforth call rule 240 the *left-copycat rule*.

An examination of the graph of the characteristic functions χ^1_{170} in Fig. 3 and χ^1_{240} in Fig. 4 shows that they are symmetrical with respect to the main diagonal. In other words, the two graphs are *inverse* of each other. Observe that although the graph of χ^1_{240} in Fig. 4 appears to be a *double*-valued function, it is actually a well-defined single-valued

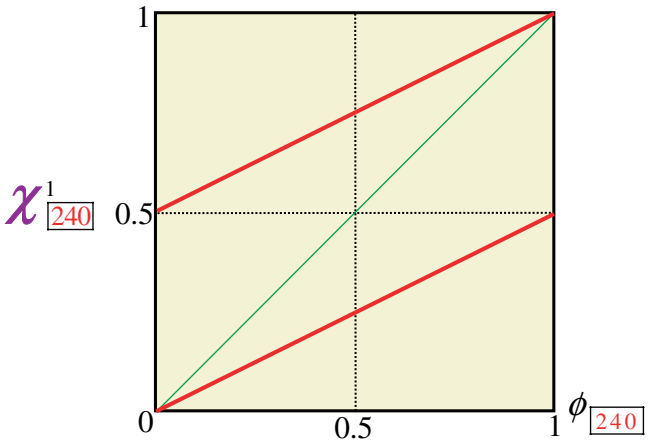


Fig. 4. The characteristic function of the "*left-copycat*" rule 240 converges to the *inverse Bernoulli map*.

function for all *finite* I, for x_I uniquely specifies whether the upper branch (if $x_I = 1$), or the lower branch (if $x_I = 0$) should be selected.

1.5. *Deriving affine (mod 1) characteristic functions*

We have shown in Secs. 1.3 and 1.4 that the characteristic functions χ^1_{170} and χ^1_{240} are *affine* (mod 1) functions for finite I. An examination of Table 2 reveals that there are only eight *affine* (mod 1) characteristic functions, namely, χ^1_{0}, χ^1_{15}, χ^1_{51}, χ^1_{85}, χ^1_{170}, χ^1_{204}, χ^1_{240} and χ^1_{255}. The explicit formula for each of these characteristic functions can be easily derived from Table 1 as in Secs. 1.3 and 1.4. Table 3 lists the explicit formulas defining these eight *affine* (*mod 1*) *local* rules and their *corresponding global* characteristic function. The graph of each characteristic function χ^1_N is shown in Table 4.

Remark 1.1. Since there exist infinitely many distinct sets of parameters $\{z_2, c_2, z_1, c_1, z_0, b_1, b_2, b_3\}$ [Chua *et al.*, 2003] from which the explicit formula Eq. (9) represents *the same* characteristic function χ^1_N, $N = 0, 1, 2, \ldots, 255$, the equations listed in Table 1 represent only *one* of many equivalent explicit formulas. In fact, we need to list explicit formulas for only 128 local rules since the simple transformation in the following proposition allows us to generate corresponding explicit formulas for the remaining 128 rules.

Proposition 1.1. *Given an explicit formula*

$$\chi^1_N = \sum_{i=0}^{I} 2^{-(i+1)} \delta\{f(x_{i-1}, x_i, x_{i+1})\} \tag{9a}$$

for local rule N, *the following corresponding equation gives an explicit formula for local rule* $N' \triangleq 255 - N$:

$$\chi^1_{255-N} = \sum_{i=0}^{I} 2^{-(i+1)} \delta\{-f(x_{i-1}, x_i, x_{i+1})\} \tag{9b}$$

Proof. Equation (9b) follows directly from Eq. (9a) and the identity

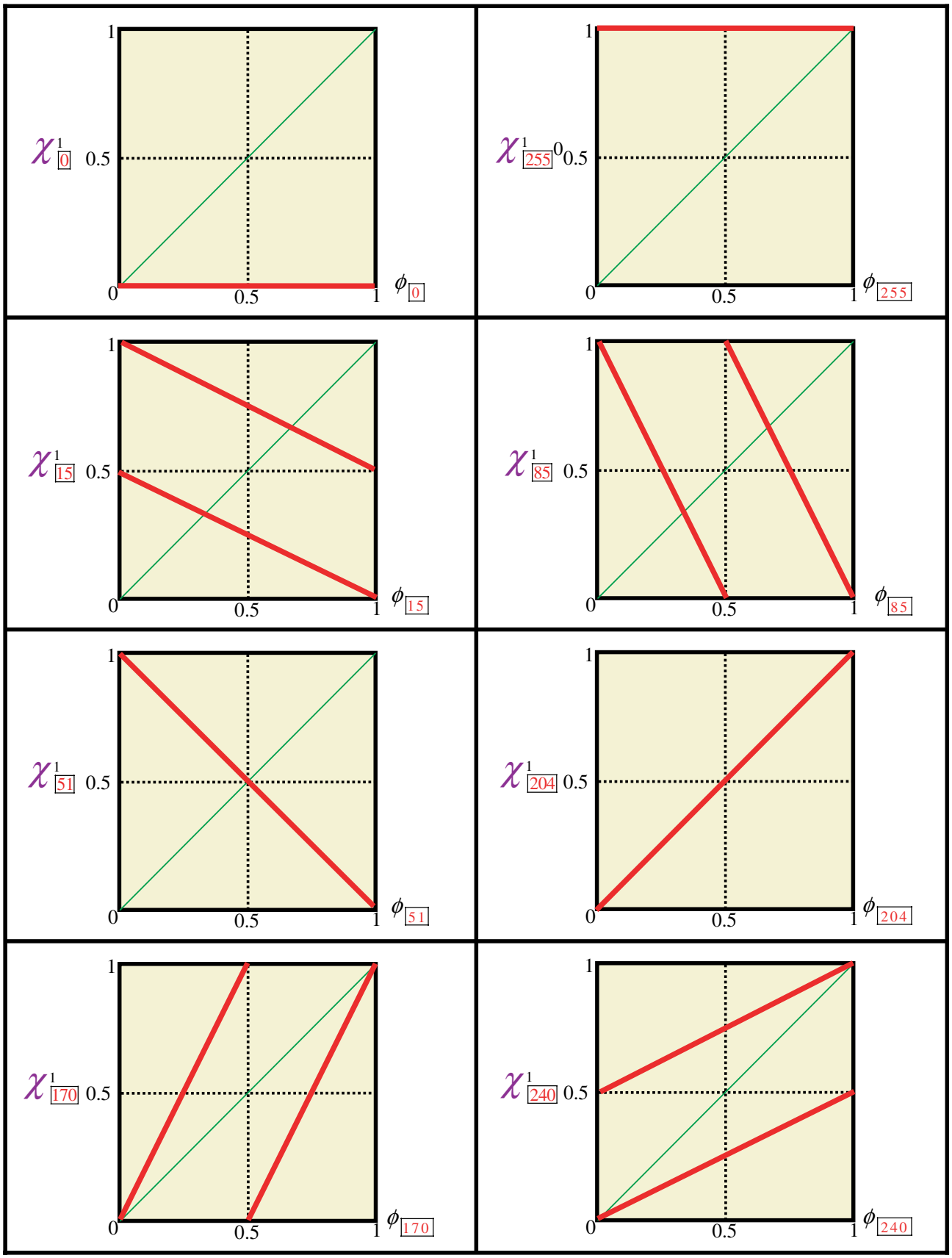
$$\boxed{\delta\{-f\} = 1 - \delta\{f\},} \tag{9c}$$

as can be verified by direct substitution. ■

Table 3. Explicit formulas defining the eight affine (mod 1) local rules and their associated characteristic functions. The *bar* above a binary bit means taking its complement, i.e. $\overline{0} = 1$ and $\overline{1} = 0$.

Affine (mod 1) Rule Number N	Local Rule Formula	Explicit formula for $\chi^1_{[N]}$
0	$x_i^{n+1} = 0$	$\chi^1_{[0]}(\phi) = 0$
15	$x_i^{n+1} = \overline{x_{i-1}^n}$	$\chi^1_{[15]}(\phi) = \begin{cases} -\frac{1}{2}\phi + 1 & , \text{ if } x_I = 0 \\ -\frac{1}{2}\phi + \frac{1}{2} & , \text{ if } x_I = 1 \end{cases}$
51	$x_i^{n+1} = \overline{x_i^n}$	$\chi^1_{[51]}(\phi) = -\phi + 1$
85	$x_i^{n+1} = \overline{x_{i+1}^n}$	$\chi^1_{[85]}(\phi) = \begin{cases} -2\phi + 1 & , \text{ if } x_1 = 0 \\ -2\phi + 2 & , \text{ if } x_1 = 1 \end{cases}$
170	$x_i^{n+1} = x_{i+1}^n$	$\chi^1_{[170]}(\phi) = 2\phi \bmod 1$
204	$x_i^{n+1} = x_i^n$	$\chi^1_{[204]}(\phi) = \phi$
240	$x_i^{n+1} = x_{i-1}^n$	$\chi^1_{[240]}(\phi) = \begin{cases} \frac{1}{2}\phi & , \text{ if } x_I = 0 \\ \frac{1}{2}\phi + \frac{1}{2} & , \text{ if } x_I = 1 \end{cases}$
255	$x_i^{n+1} = 1$	$\chi^1_{[255]}(\phi) = 1$

Table 4. Characteristic functions $\chi^1_{[N]}$ of Affine (mod 1) Rules.



Example 1.1. Given the following explicit formula

$$\boldsymbol{\chi}^1_{\boxed{110}} = \sum_{i=0}^{I} 2^{-(i+1)} \text{ɗ} \left\{ -1 + \left| \left(+1x_{i-1} + 2x_i - 3x_{i+1} - \frac{1}{2} \right) \right| \right\} \tag{9d}$$

for $\boxed{N} = \boxed{110}$, we apply Eq. (9b) to obtain the following explicit formula

$$\boldsymbol{\chi}^1_{\boxed{145}} = \sum_{i=0}^{I} 2^{-(i+1)} \text{ɗ} \left\{ +1 - \left| \left(+1x_{i-1} + 2x_i - 3x_{i+1} - \frac{1}{2} \right) \right| \right\} \tag{9e}$$

for $\boxed{N'} = \boxed{255-110} = \boxed{145}$.

Note that the above formula is *different* from the one listed in Table 1, since the formulas in Table 1 are constructed independently of Proposition 1.1.

Proposition 1.2. *The* graphs *of the characteristic functions for* $\boldsymbol{\chi}^1_{\boxed{N}}$ *and* $\boldsymbol{\chi}^1_{\boxed{255-N}}$ *are* symmetric *with respect to the* horizontal axis $\boldsymbol{\chi}^1_{\boxed{N}} = 0.5$. *In particular*,

$$\boldsymbol{\chi}^1_{\boxed{N}}(\phi) = 1 - \boldsymbol{\chi}^1_{\boxed{255-N}}(\phi) \tag{9f}$$

Proof. Equation (9f) follows directly from Proposition 1.1 and the identity (9c). ■

Remark 1.2. It would be instructive for the reader to verify the graphs of $\boldsymbol{\chi}^1_{\boxed{N}}$ in Table 2 for $N = 128, 129, \ldots, 255$ can be obtained by flipping the graphs of $\boldsymbol{\chi}^1_{\boxed{N}}$ for $N = 127, 126, 125, \ldots, 0$, respectively, about the $\phi_{\boxed{N}}$-axis, and then translating them upward by $\Delta\boldsymbol{\chi}^1_{\boxed{N}} = 1$.

Remark 1.3. It follows from [Chua *et al.*, 2004] that only 89 characteristic functions, out of 256, in Table 1, give *qualitatively distinct global dynamics*. All other characteristic functions can be generated trivially by applying the three global transformations $\mathbf{T}^\dagger$, $\overline{\mathbf{T}}$ and $\mathbf{T}^*$ from Klein's Vierergruppe.

Example 1.2. Applying $\mathbf{T}^\dagger$, $\overline{\mathbf{T}}$ and $\mathbf{T}^*$ to Eq. (9d), we obtain:

$$\boldsymbol{\chi}^1_{\boxed{124}} = \mathbf{T}^\dagger[\boldsymbol{\chi}^1_{\boxed{110}}] = \sum_{i=0}^{I} 2^{-(i+1)} \text{ɗ} \left\{ -1 + \left| \left(-3x_{i-1} + 2x_i + 1x_{i+1} - \frac{1}{2} \right) \right| \right\} \tag{9g}$$

$$\boldsymbol{\chi}^1_{\boxed{137}} = \overline{\mathbf{T}}[\boldsymbol{\chi}^1_{\boxed{110}}] = \sum_{i=0}^{I} 2^{-(i+1)} \text{ɗ} \left\{ +1 - \left| \left(-1x_{i-1} - 2x_i + 3x_{i+1} - \frac{1}{2} \right) \right| \right\} \tag{9h}$$

$$\boldsymbol{\chi}^1_{\boxed{193}} = \mathbf{T}^*[\boldsymbol{\chi}^1_{\boxed{110}}] = \sum_{i=0}^{I} 2^{-(i+1)} \text{ɗ} \left\{ +1 - \left| \left(+3x_{i-1} - 2x_i - 1x_{i+1} - \frac{1}{2} \right) \right| \right\} \tag{9i}$$

Remark 1.4. By choosing the characteristic function of only *one* local rule from each of the 15 local equivalence classes listed in the left column of Table 20 of [Chua *et al.*, 2004], we can apply the appropriate *rotation transformation* listed in Table 1 of [Chua *et al.*, 2004], and use *Proposition 1.1* to derive an explicit characteristic function formula for each of the remaining 241 local rules.

2. Lameray Diagram on $\boldsymbol{\chi}^1_{\boxed{N}}$ Gives Attractor Time-1 Maps

We have demonstrated in [Chua *et al.*, 2005] that the dynamics on each *attractor* of a local rule $\boxed{N}$ is uniquely characterized by the forward *time-1 return map*

$$\rho_1[N] : \phi_{n-1} \mapsto \phi_n \tag{14}$$

starting from any point on the attractor. For the 69 *period-1 rules* listed in Tables 3 and 4 of [Chua *et al.*, 2005], such time-1 maps consist of only *one* point on the main diagonal of the characteristic function $\boldsymbol{\chi}^1_{\boxed{N}}$, and is therefore trivial. For the 25 *period-2 rules* listed in Tables 7 and 8, such time-1 maps consist of *two* points on the main diagonal of $\boldsymbol{\chi}^1_{\boxed{N}}$, and is also trivial. Similarly, the time-1 map of the four *period-3 rules* listed in Table 9 consist of *three* points, as illustrated in Fig. 11 of [Chua *et al.*, 2005].

The most interesting and nontrivial time-1 maps considered so far are the 112 generalized Bernoulli σ_τ-shift rules listed in Tables 10–12 of [Chua *et al.*, 2005]. The time-1 maps of these rules, as well as those corresponding to the remaining 50 rules listed in Tables 17 and 18 of [Chua *et al.*, 2005] consist in general of an *uncountable* [Devaney, 1992] number of points $\phi \in [0, 1]$, assuming $I \to \infty$.

An instructive way to analyze the dynamics of such *time-1 maps* is to plot the *Lameray* (*cobweb*) diagram starting from any generic initial point, and observe how its "cobweb" loci evolves from this

initial point on the *characteristic function* $\boldsymbol{\chi}^1_{\boxed{N}}$. Let us study some of these rules.

2.1. *Lameray diagram of* $\boxed{170}$

The dynamic pattern of the first 65 iterations of rule $\boxed{170}$ (with complexity index $\kappa = 1$) starting from $\phi_0 = 0.0253584$ is shown in Fig. 5(a). The first 12 iterations of the Lameray diagram constructed from the characteristic function $\boldsymbol{\chi}^1_{\boxed{170}}$ are shown in Fig. 5(b) for ease of visualization. The continued iterations of the Lameray diagram for $\boxed{170}$ up to $n = 63$ are shown in Fig. 5(c). The color code on top of Fig. 5(a) denotes the iteration number $n = 0, 1, 2, \ldots, 63$.

A comparison of the *loci* (corner points not on the diagonal) in Fig. 5(c) with the forward time-1 map of $\boxed{170}$ in Table 2 (p. 1106) of [Chua *et al.*, 2005] clearly shows that they all fall on the graph of time-1 map. Indeed, as $n \to \infty$, this loci is seen (not shown) to converge on the complete graph of the forward time-1 map of $\boxed{170}$. Indeed, in this example, *all* points on the Lameray diagram, including *any* initial point, are seen to fall on the associated attractor. Note also that all points on the loci of the Lameray diagram of any rule $\boxed{N}$ must be a subset of the associated characteristic function $\boldsymbol{\chi}^1_{\boxed{N}}$, by construction.

2.2. *Lameray diagram of* $\boxed{240}$

The dynamic pattern of the first 65 iterations of rule $\boxed{240}$ (with complexity index $\kappa = 1$) starting from $\phi_0 = 0.0253584$, is shown in Fig. 6(a). The first 12 iterations of the Lameray diagram constructed from the characteristic function $\boldsymbol{\chi}^1_{\boxed{240}}$ are shown in Fig. 6(b) for ease of visualization. The continued iterations of the Lameray diagram for $\boxed{240}$ up to $n = 63$ are shown in Fig. 6(c).

A comparison of the *loci* in Fig. 6(c) with the forward time-1 map of $\boxed{240}$ in Table 2 (p. 1124) of [Chua *et al.*, 2005] clearly shows that they all fall on the graph of the time-1 map. Indeed, as $n \to \infty$, this loci is seen (not shown) to converge on the complete graph of the forward time-1 map of $\boxed{240}$. Indeed, in this example, *all* points on the Lameray diagram, including *any* initial point, are seen to fall on the associated attractor.

2.3. *Lameray diagram of* $\boxed{2}$

The dynamic pattern of the first 65 iterations of rule $\boxed{2}$ (with complexity index $\kappa = 1$) starting from $\phi_0 = 0.64368$ is shown in Fig. 7(a). The first six iterations of the Lameray diagram constructed from the characteristic function $\boldsymbol{\chi}^1_{\boxed{2}}$ are shown in Fig. 7(b) and the continued iterations up to $n = 63$ are shown in Fig. 7(c).

A comparison of the *loci* in Fig. 7(c) with the forward time-1 map of $\boxed{2}$ in Table 2 (p. 1064) of [Chua *et al.*, 2005] shows that except for the initial point (which *did not* fall on the attractor but belongs to the *basin of attraction* of the associated attractor), all other points of the loci fall on the time-1 map of $\boxed{2}$.

To demonstrate this result holds for any other initial point belonging to the same basin of attraction, Fig. 8 shows the Lameray diagram of $\boxed{2}$ (starting from a *different* initial point $\phi_0 = 0.343184$) over $n = 25$, 30, 35, 50, 75, 100, 150, 200 and 250 iterations, respectively. Again except for the initial point, the loci of the Lameray diagram is seen to converge on the forward time-1 map of $\boxed{2}$ in Table 2 of [Chua *et al.*, 2005].

2.4. *Lameray diagram of* $\boxed{3}$

The dynamic pattern of the first 65 iterations of rule $\boxed{3}$ (with complexity index $\kappa = 1$) starting from $\phi_0 = 0.64368$ is shown in Fig. 9(a). The first ten iterations of the Lameray diagram constructed from the characteristic function $\boldsymbol{\chi}^1_{\boxed{3}}$ are shown in Fig. 9(b) and the continued iterations up to $n = 63$ are shown in Fig. 9(c).

A comparison of the *loci* in Fig. 9(c) with the forward time-1 map of $\boxed{3}$ in Table 2 (p. 1064) of [Chua *et al.*, 2005] shows that except for the initial point (which *did not* fall on the attractor but belongs to its basin of attraction), all other points of the loci fall on the time-1 map of $\boxed{3}$.

To demonstrate this result holds for any other initial point belonging to the same basin of attraction, Fig. 10 shows the Lameray diagram of $\boxed{3}$ (starting from a *different* initial point $\phi_0 = 0.556412$) over $n = 5$, 10, 15, 20, 35, 50, 100, 150 and 250 iterations, respectively. Again, except for the initial point, the loci of the Lameray diagram is seen to converge on the forward time-1 map of $\boxed{3}$ in Table 2 of [Chua *et al.*, 2005].

2.5. *Lameray diagram of* $\boxed{46}$

The dynamic pattern of the first 65 iterations of rule $\boxed{46}$ (with complexity index $\kappa = 3$) starting from $\phi_0 = 0.895314$ is shown in Fig. 11(a). The first

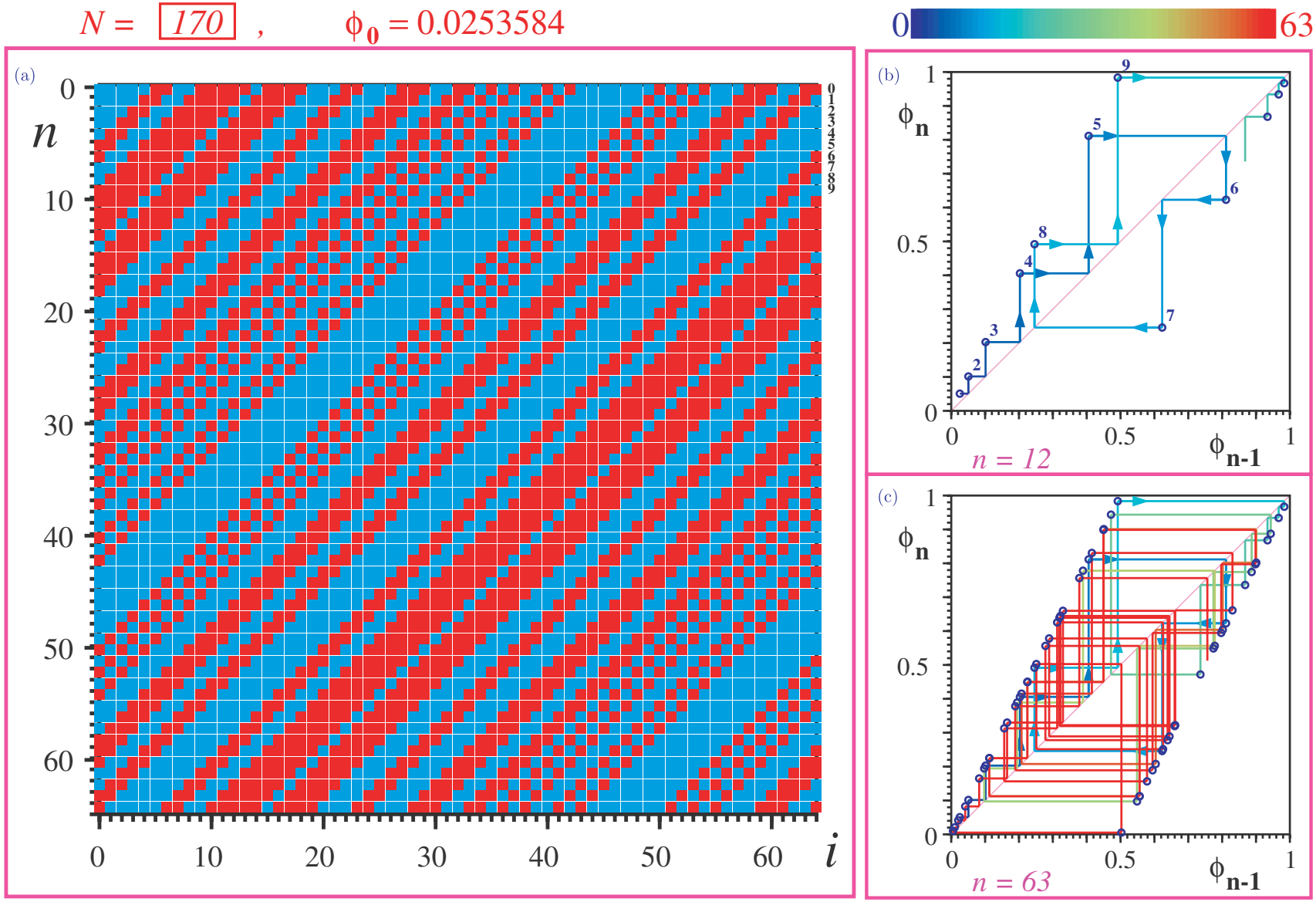


Fig. 5. (a) Dynamic pattern of 170 from $\phi_0 = 0.0253584$. (b) Lameray diagram for first 12 iterations. (c) Lameray diagram over 63 iterations.

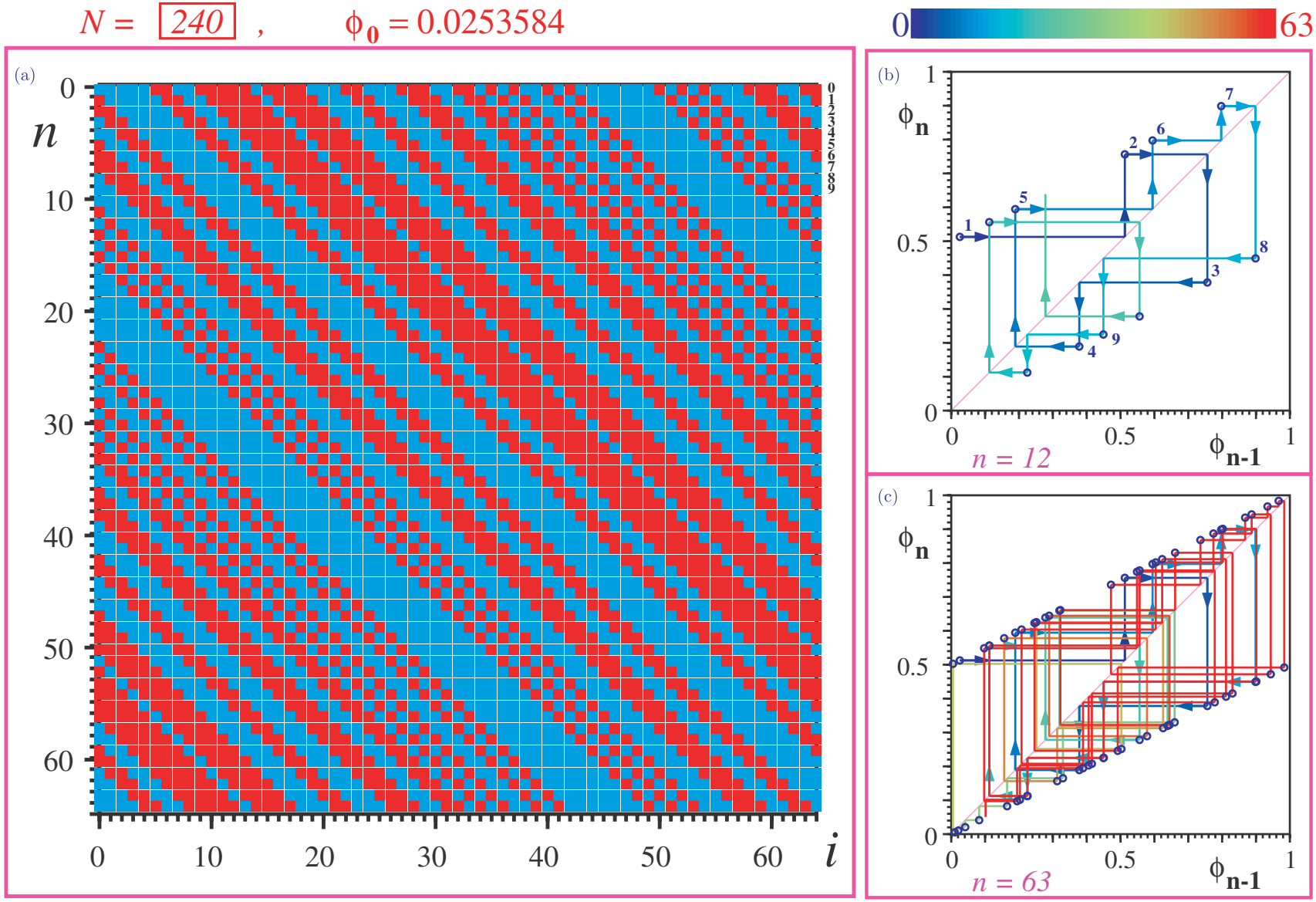


Fig. 6. (a) Dynamic pattern of 240 from $\phi_0 = 0.0253584$. (b) Lameray diagram for first 12 iterations. (c) Lameray diagram over 63 iterations.

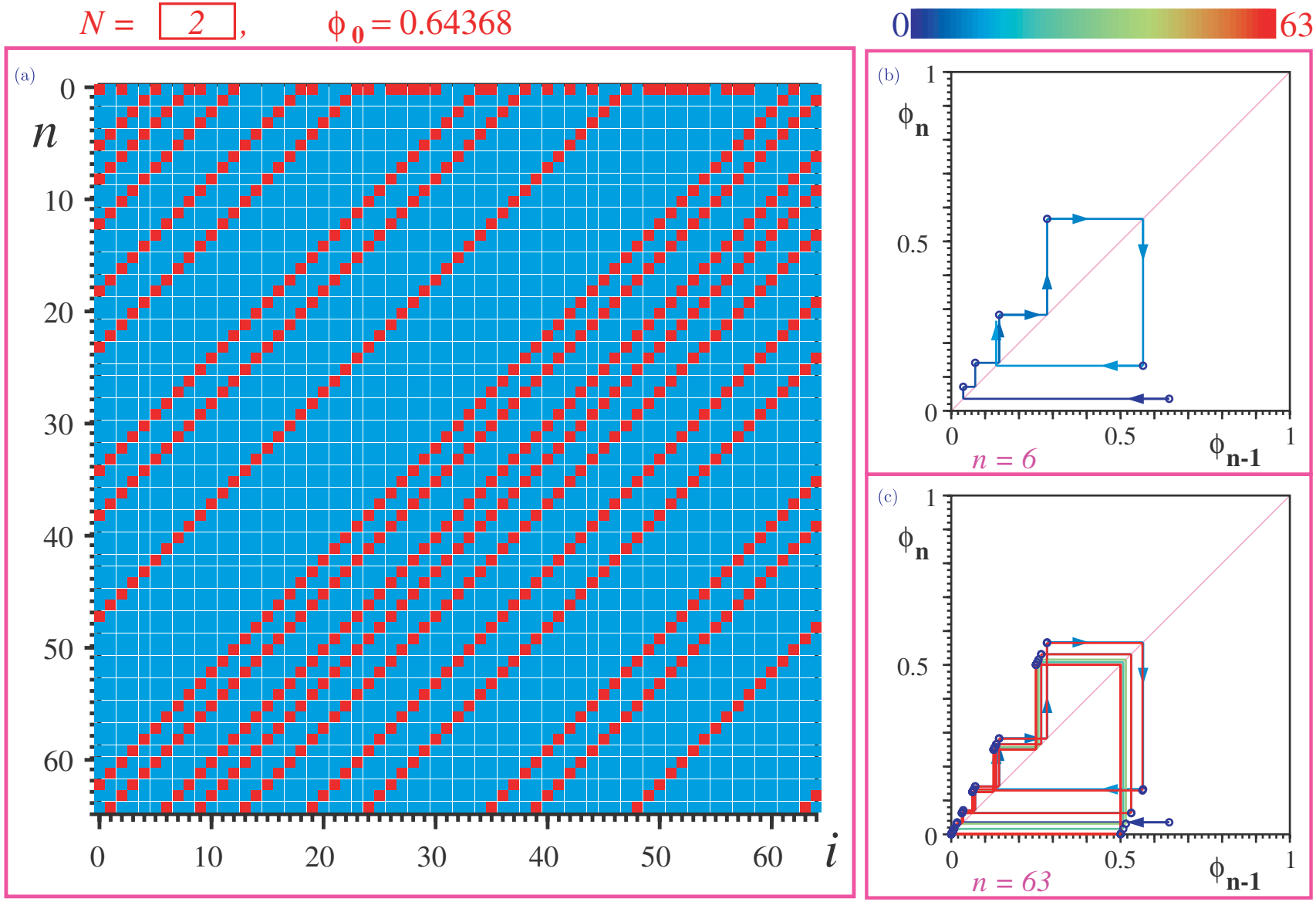


Fig. 7. (a) Dynamic pattern of 2 from $\phi_0 = 0.64368$. (b) Lameray diagram for first six iterations. (c) Lameray diagram over 63 iterations.

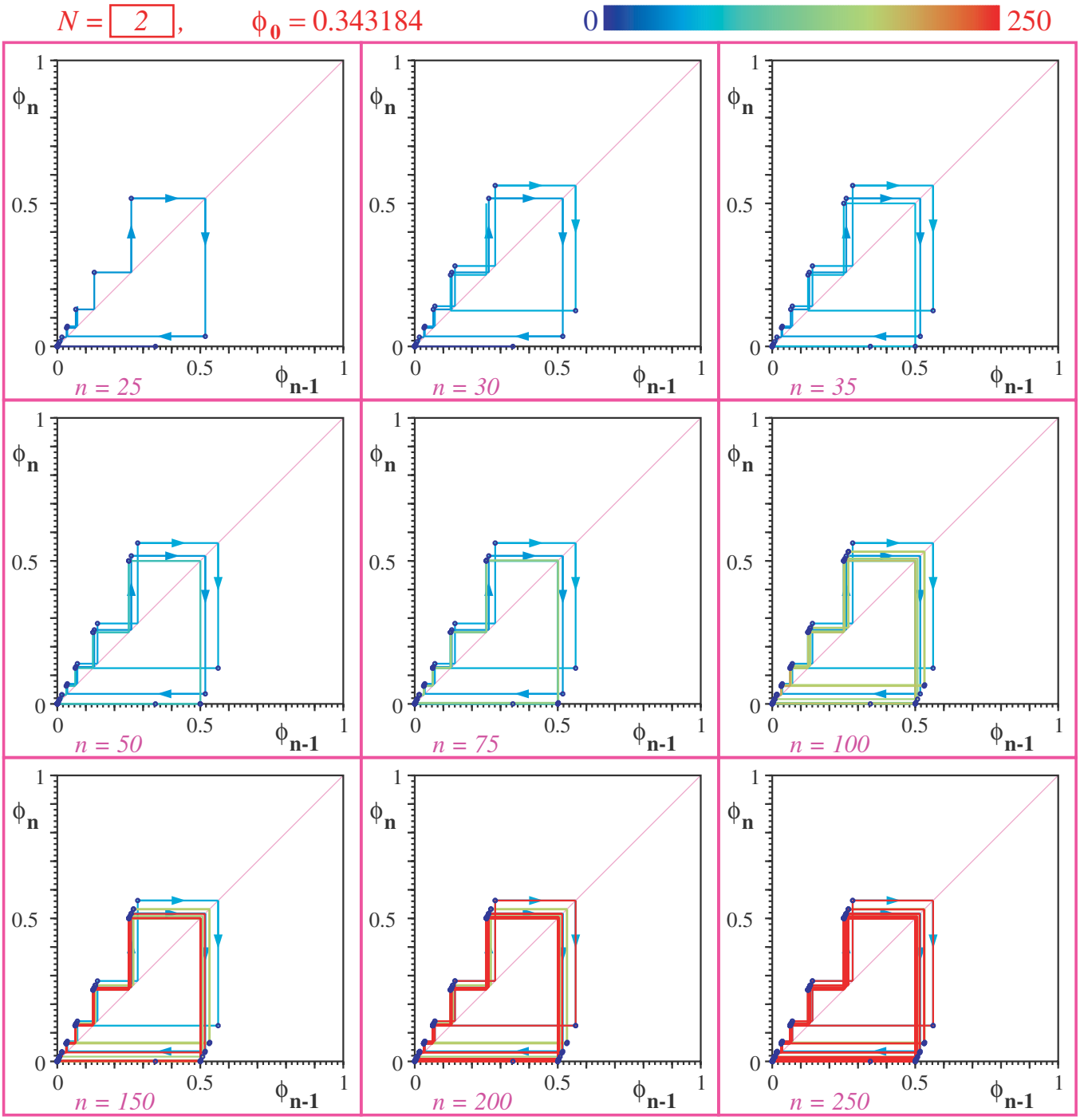


Fig. 8. Nine snapshots of the Lameray diagram of 2 starting from $\phi_0 = 0.343184$.

ten iterations of the Lameray diagram constructed from the characteristic function χ^1_{46} are shown in Fig. 11(b) and the continued iterations up to $n = 63$ are shown in Fig. 11(c).

A comparison of the *loci* in Fig. 11(c) with the forward time-1 map of 46 in Table 2 (p. 1075) of [Chua *et al.*, 2005] shows that except for the initial point (which *did not* fall on the attractor but belongs to its basin of attraction), all other points of the loci fall on the time-1 map of 46.

To demonstrate this result holds for any other initial point belonging to the same basin of attraction, Fig. 12 shows the Lameray diagram of 46 (starting from a *different* initial point $\phi_0 = 0.888034$) over $n = 7$, 15, 25, 50, 75, 100, 150, 200 and 250 iterations, respectively. Again, except for

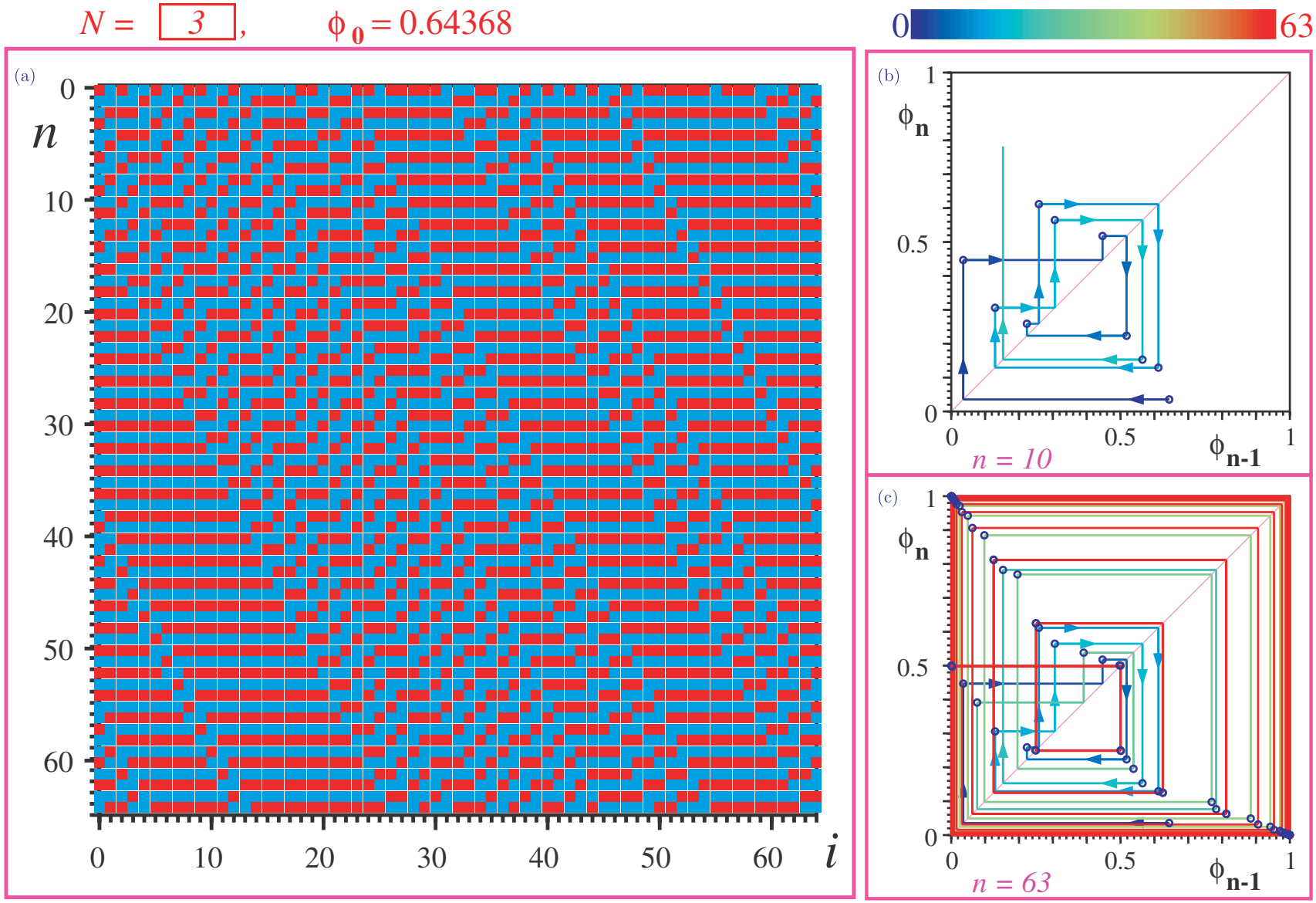


Fig. 9. (a) Dynamic pattern of 3 from $\phi_0 = 0.64368$. (b) Lameray diagram for first ten iterations. (c) Lameray diagram over 63 iterations.

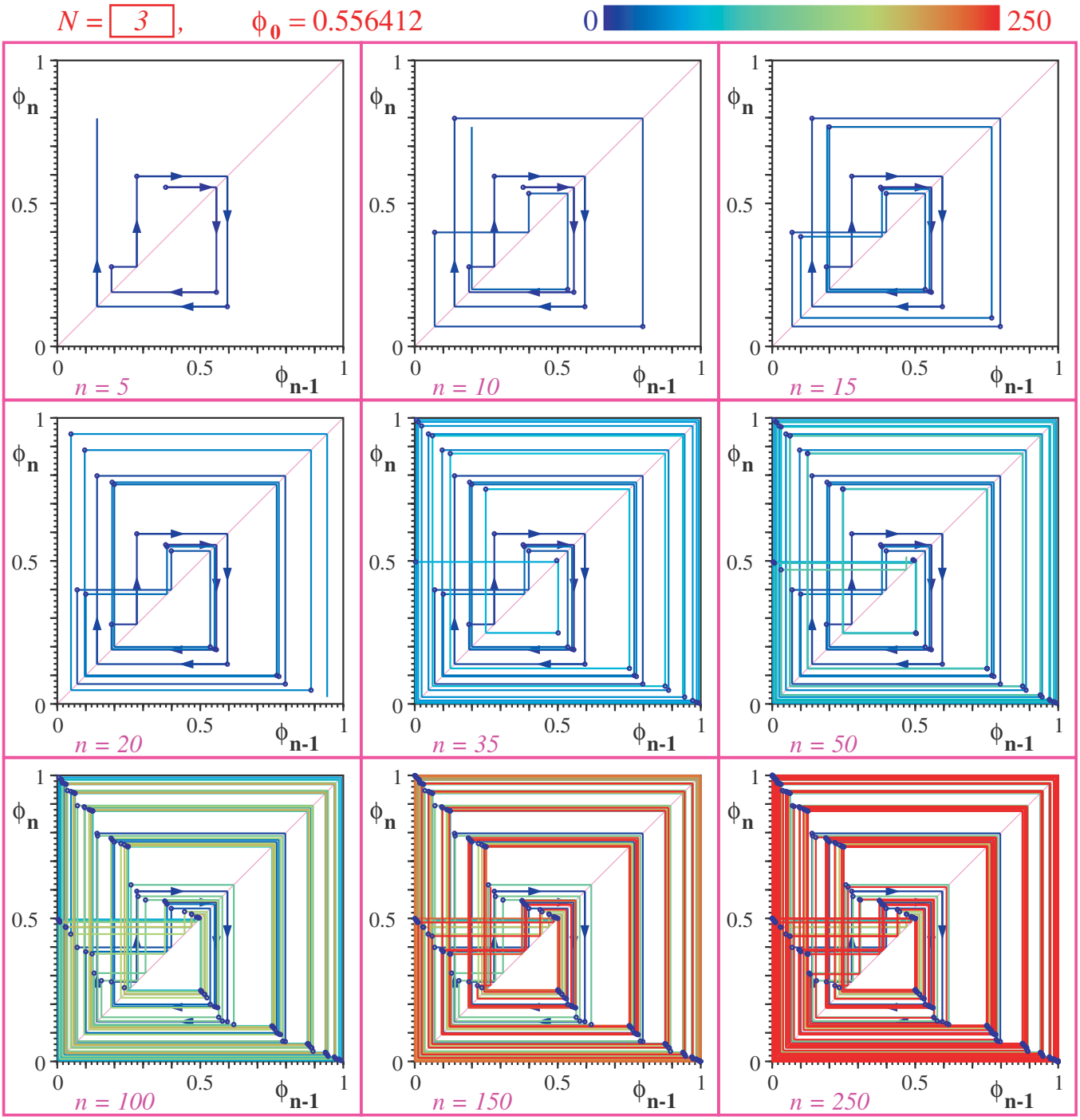


Fig. 10. Nine snapshots of the Lameray diagram of 3 starting from $\phi_0 = 0.556412$.

the initial point, the loci of the Lameray diagram is seen to converge on the forward time-1 map of 46 in Table 2 of [Chua *et al.*, 2005].

2.6. *Lameray diagram of* 110

The dynamic pattern of the first 65 iterations of rule 110 (with complexity index $\kappa = 2$) starting from $\phi_0 = 0.40653$ is shown in Fig. 13(a). The first five iterations of the Lameray diagram constructed from the characteristic function χ^1_{110} are shown in Fig. 13(b) and the continued iterations up to $n = 63$ are shown in Fig. 13(c).

A comparison of the *loci* in Fig. 13(c) with the forward time-1 map of 110 in Table 2 (p. 1091) of [Chua *et al.*, 2005] shows that except for some initial

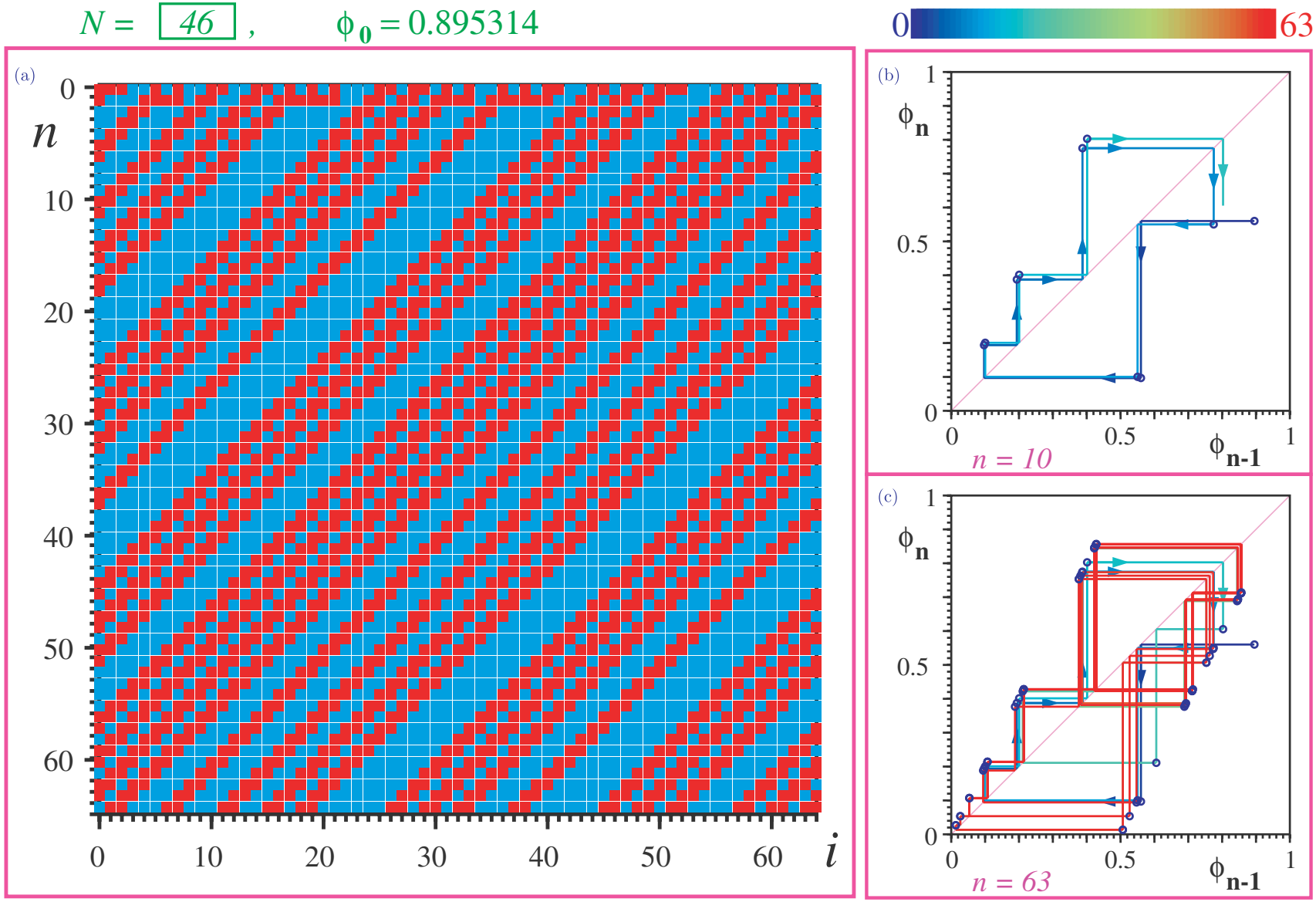


Fig. 11. (a) Dynamic pattern of 46 from $\phi_0 = 0.895314$. (b) Lameray diagram for first ten iterations. (c) Lameray diagram over 63 iterations.

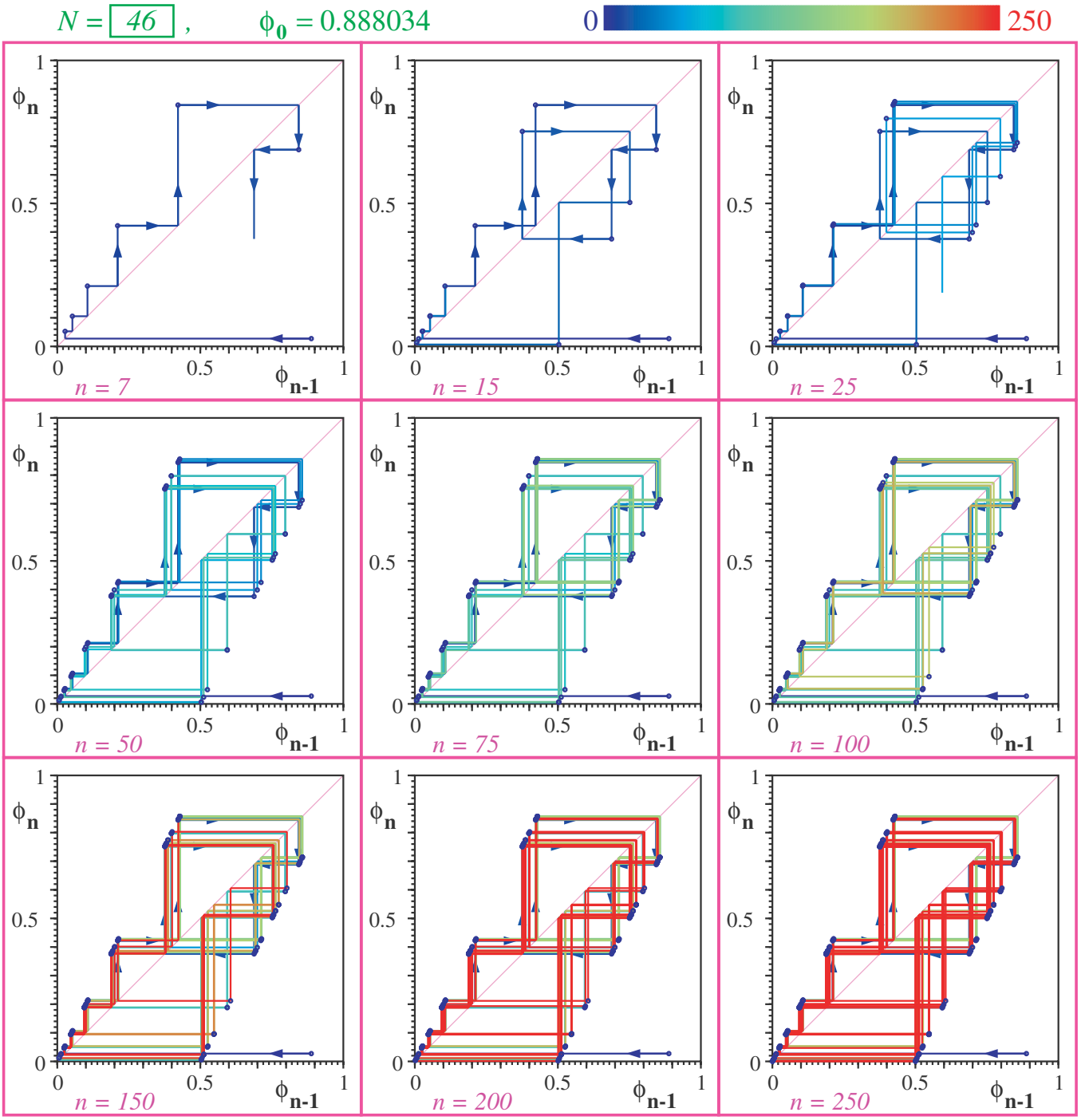


Fig. 12. Nine snapshots of the Lameray diagram of 46 starting from $\phi_0 = 0.888034$.

set of points (which may not fall on the attractor associated with the loci but belongs to its basin of attraction), all other points of the loci fall on the time-1 map of 110 associated with the corresponding attractor.

To demonstrate this result holds for any other initial point belonging to the same basin of attraction, Fig. 14 shows the Lameray diagram of 110 (starting from a *different* initial point $\phi_0 = 0.149766$) over $n = 5$, 10, 15, 25, 50, 75, 200, 350 and 500 iterations, respectively. Again, except for some initial set of points not belonging to the corresponding attractor of 110, the loci of the Lameray diagram is seen to converge to the forward time-1 map of 110 in Table 2 of [Chua *et al.*, 2005].

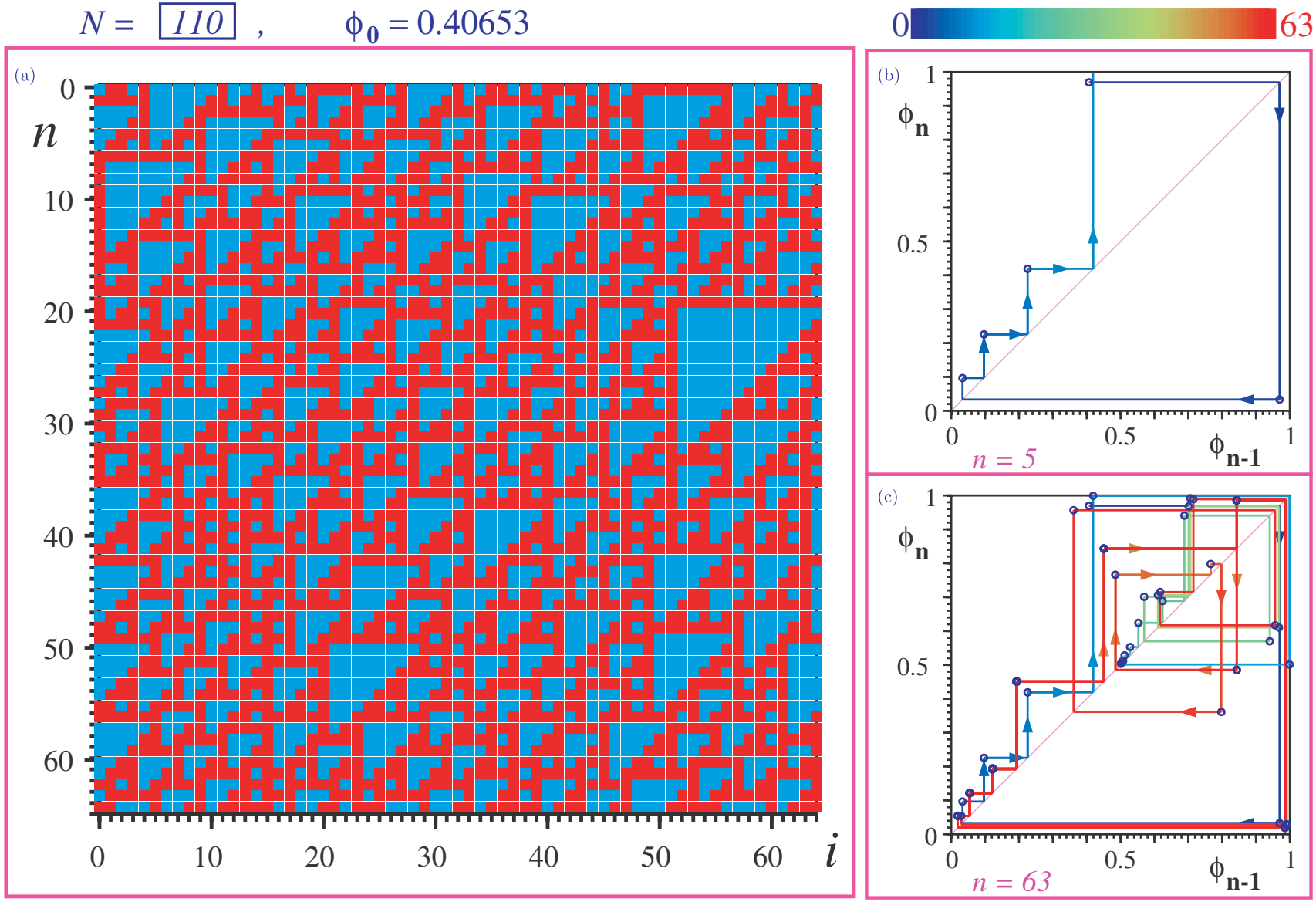


Fig. 13. (a) Dynamic pattern of 110 from $\phi_0 = 0.40653$. (b) Lameray diagram for first five iterations. (c) Lameray diagram over 63 iterations.

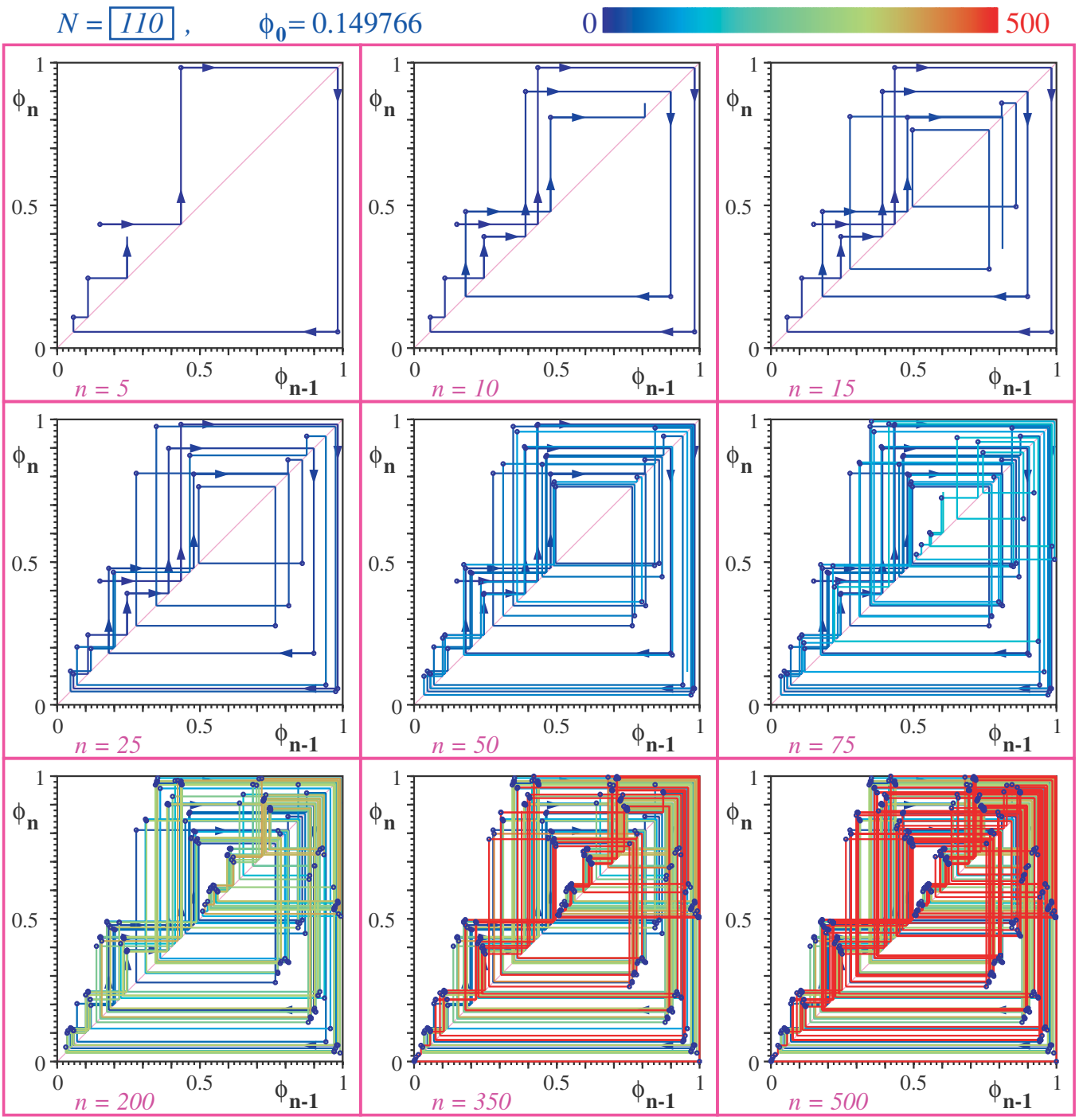


Fig. 14. Nine snapshots of the Lameray diagram of 110 starting from $\phi_0 = 0.149766$.

2.7. *Lameray diagram of* 30

The dynamic pattern of the first 65 iterations of rule 30 (with complexity index $\kappa = 2$) starting from $\phi_0 = 0.895314$ is shown in Fig. 15(a). The first ten iterations of the Lameray diagram constructed from the characteristic function χ^1_{30} are shown in Fig. 15(b), and the continued iterations up to $n = 63$ are shown in Fig. 15(c).

A comparison of the *loci* in Fig. 15(c) with the forward time-1 map of 30 in Table 2 (p. 1071) of [Chua *et al.*, 2005] shows that except for some initial set of points (which do not fall on the attractor associated with the loci but belong to its basin of

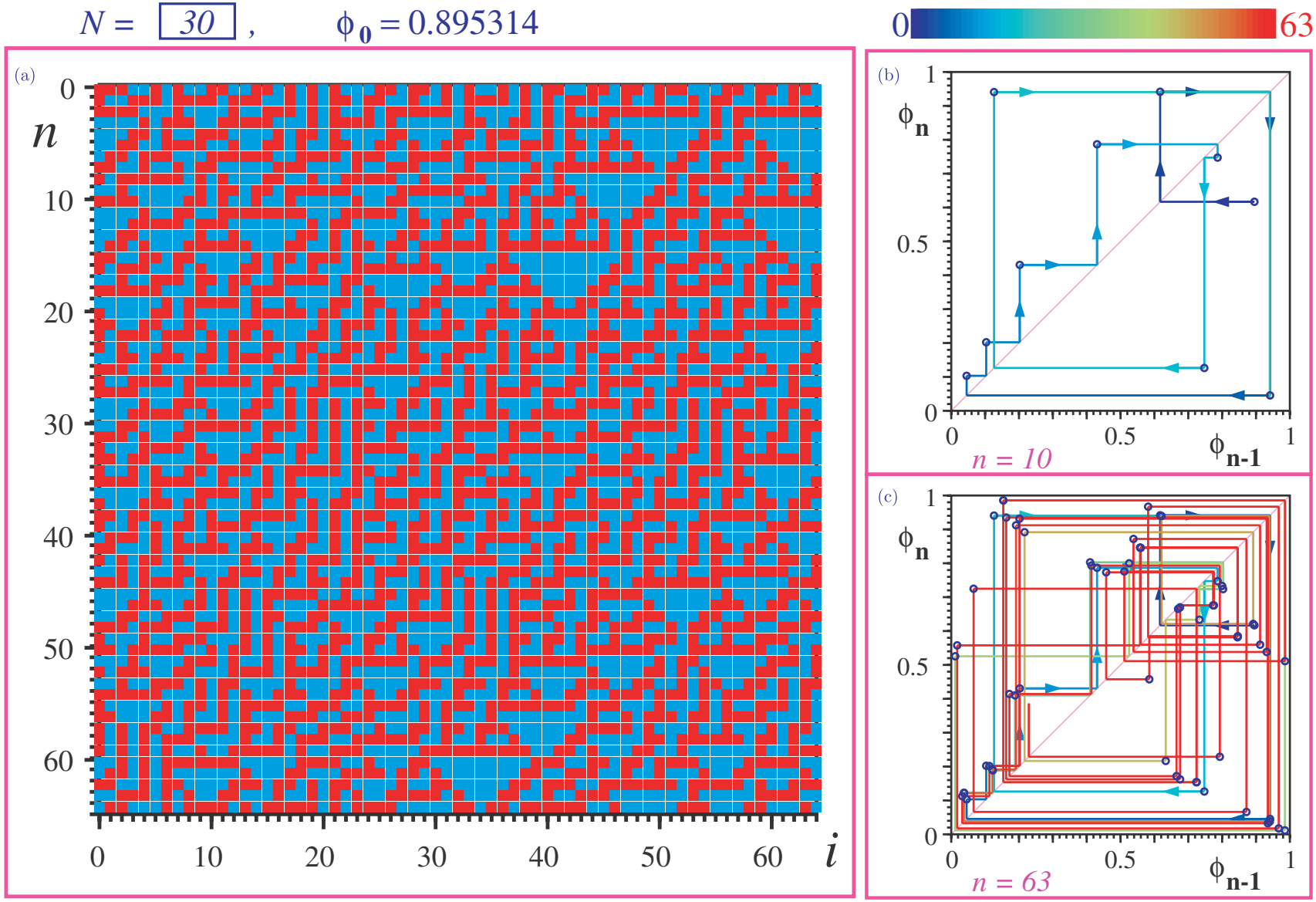


Fig. 15. (a) Dynamic pattern of 30 from $\phi_0 = 0.895314$. (b) Lameray diagram for first ten iterations. (c) Lameray diagram over 63 iterations.

attraction), all other points of the loci fall on the time-1 map of [30] associated with the corresponding attractor.

To demonstrate this result holds for any other initial point belonging to the same basin of attraction, Fig. 16 shows the Lameray diagram of [30] (starting from a *different* initial point $\phi_0 = 0.149766$) over $n = 7$, 14, 21, 50, 75, 100, 200, 300 and 500 iterations, respectively. Again except for some initial set of points not belonging to the corresponding attractor of [30], the loci of the Lameray diagram is seen to converge to the forward time-1 map of [30] in Table 2 of [Chua *et al.*, 2005].

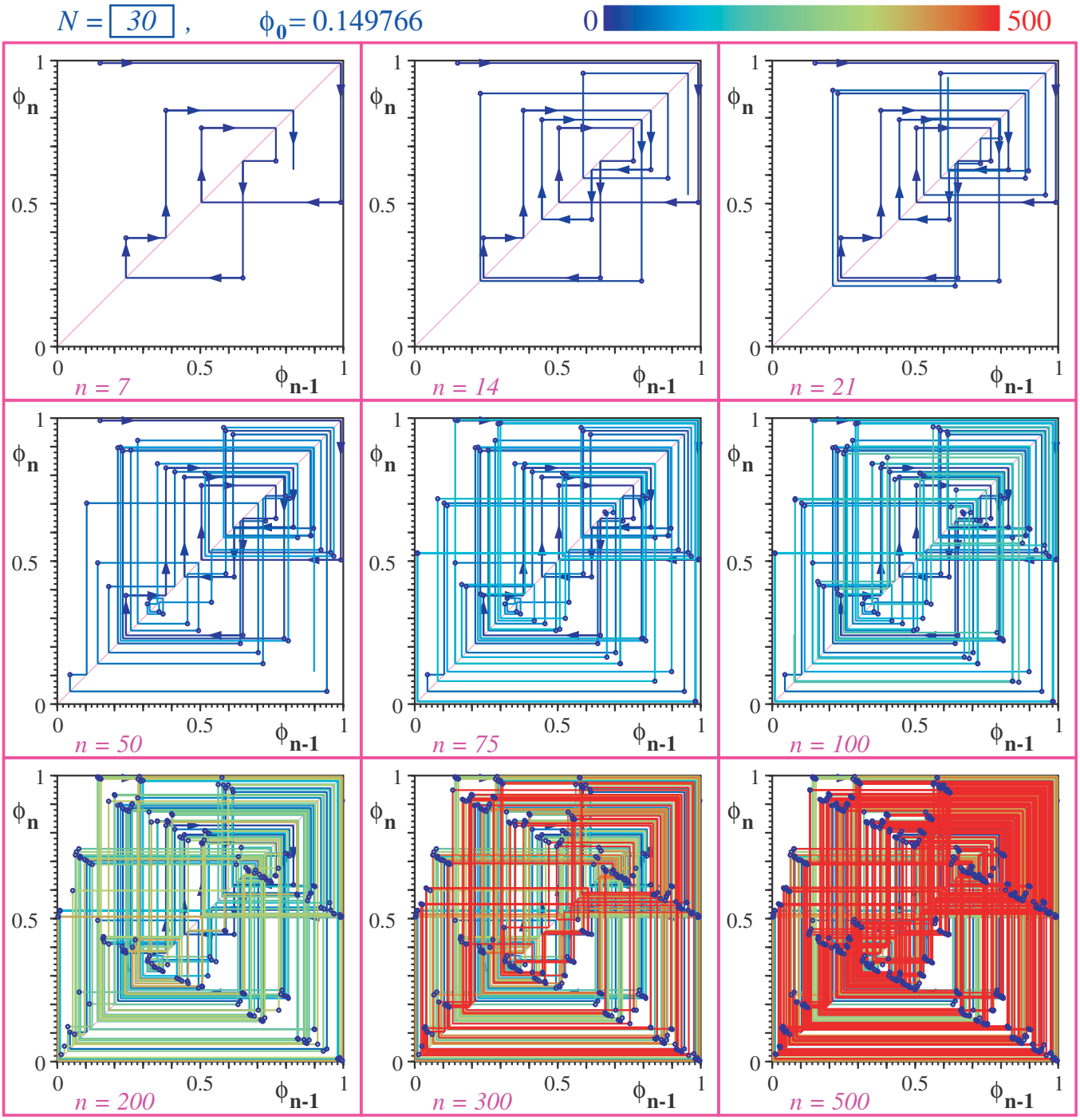


Fig. 16. Nine snapshots of the Lameray diagram of [30] starting from $\phi_0 = 0.149766$.

3. Characteristic Functions are Fractals

A careful examination of the characteristic functions $\boldsymbol{\chi}^1_{\boxed{N}}$ in Table 2 would reveal that each graph of $\boldsymbol{\chi}^1_{\boxed{N}}$ is composed of many subpatterns which are *self-similar* in the sense that each can be rescaled by appropriate horizontal and vertical scaling factors so that it coincides with a part of the composite pattern. Let us illustrate this *fractal* geometry [Barnsley, 1988] with some examples.

Example 3.1 [Characteristic function $\boldsymbol{\chi}^1_{\boxed{2}}$]. Let us repeat the characteristic function $\boldsymbol{\chi}^1_{\boxed{2}}$ from Table 2 in Fig. 17(a) by passing a curve through the small red and blue squares while deleting the red and blue vertical bars to avoid clutter. We will henceforth refer to this curve as the *graph* of $\boldsymbol{\chi}^1_{\boxed{N}}$. Let us examine two subpatterns of this graph. Subpattern 1 covers the "cyan" rectangular area bounded by $\phi_{\boxed{2}} \in [0.5, 1.0]$ and $\boldsymbol{\chi}^1_{\boxed{2}} \in [0, 0.2]$. To show that this subpattern can be used as a *template*, which upon rescaling by appropriate horizontal and vertical scaling factors, can reproduce exactly corresponding portions of the graph at arbitrarily small scales, we have enlarged it as subpattern ① in Fig. 17(a), by a factor of 2 in both horizontal and vertical directions.

Let us observe next that the smaller "cyan" rectangle "2" bounded by $\phi_{\boxed{2}} \in [0.25, 0.5]$ and $\boldsymbol{\chi}^1_{\boxed{2}} \in [0.5, 0.6]$ can be enlarged by a horizontal scale $= 2^2$ and a vertical scale $= 2^2$ to obtain the subpattern ② which is identical to the "template" ① directly above it.

Let us examine next the smaller cyan rectangle "3" in subpattern ② bounded by $\phi_{\boxed{2}} \in [0.28125, 0.3125]$ and $\boldsymbol{\chi}^1_{\boxed{2}} \in [0.5625, 0.575]$, and observe that it too coincides with the template ① upon enlarging it horizontally by 2^5 and vertically by 2^5.

The above process can be repeated any number of times with appropriate choice of scaling factors, commensurate with the computer word length.

Repeating the above scaling process to the three small cyan rectangles labeled "4", "5", and "6" in Fig. 17(b), we obtain the three subpatterns shown in ④, ⑤, and ⑥ of Fig. 17(b), each one is again found to be identical to the original *template* ① in Fig. 17(a).

We conclude therefore that the graph of $\boldsymbol{\chi}^1_{\boxed{2}}$ near the origin consists of infinitely many scaled infinitesimal subpatterns of template ①. In other words, the graph of $\boldsymbol{\chi}^1_{\boxed{2}}$ exhibits a *fractal* geometry in the sense that it is composed of infinitely many *self-similar* subpatterns.

Example 3.2 [Characteristic function $\boldsymbol{\chi}^1_{\boxed{3}}$]. The graph of characteristic function $\boldsymbol{\chi}^1_{\boxed{3}}$ replotted from Table 2 is shown in Fig. 18. By rescaling the three cyan rectangles labeled "1", "2", and "3" by appropriate scaling factors, we obtain the corresponding subpatterns ①, ② and ③ in Fig. 18. Observe that these three subpatterns are all identical. Continuing this process, we found the graph of $\boldsymbol{\chi}^1_{\boxed{3}}$ is composed of infinitely many scaled copies of template ①.

Example 3.3 [Characteristic function $\boldsymbol{\chi}^1_{\boxed{10}}$]. The graph of characteristic function $\boldsymbol{\chi}^1_{\boxed{10}}$ replotted from Table 2 is shown in Fig. 19. Observe the three cyan areas labeled "1", "2", and "3" are identical after appropriate rescaling, as shown in subpatterns ①, ② and ③ in Fig. 19.

Example 3.4 [Characteristic function $\boldsymbol{\chi}^1_{\boxed{11}}$]. The graph of characteristic function $\boldsymbol{\chi}^1_{\boxed{11}}$ is replotted from Table 2 in Fig. 20. Observe the cyan area labeled "1" and rescaled as template ① contains infinitely many scaled copies of itself, as illustrated in subpattern ② in Fig. 20.

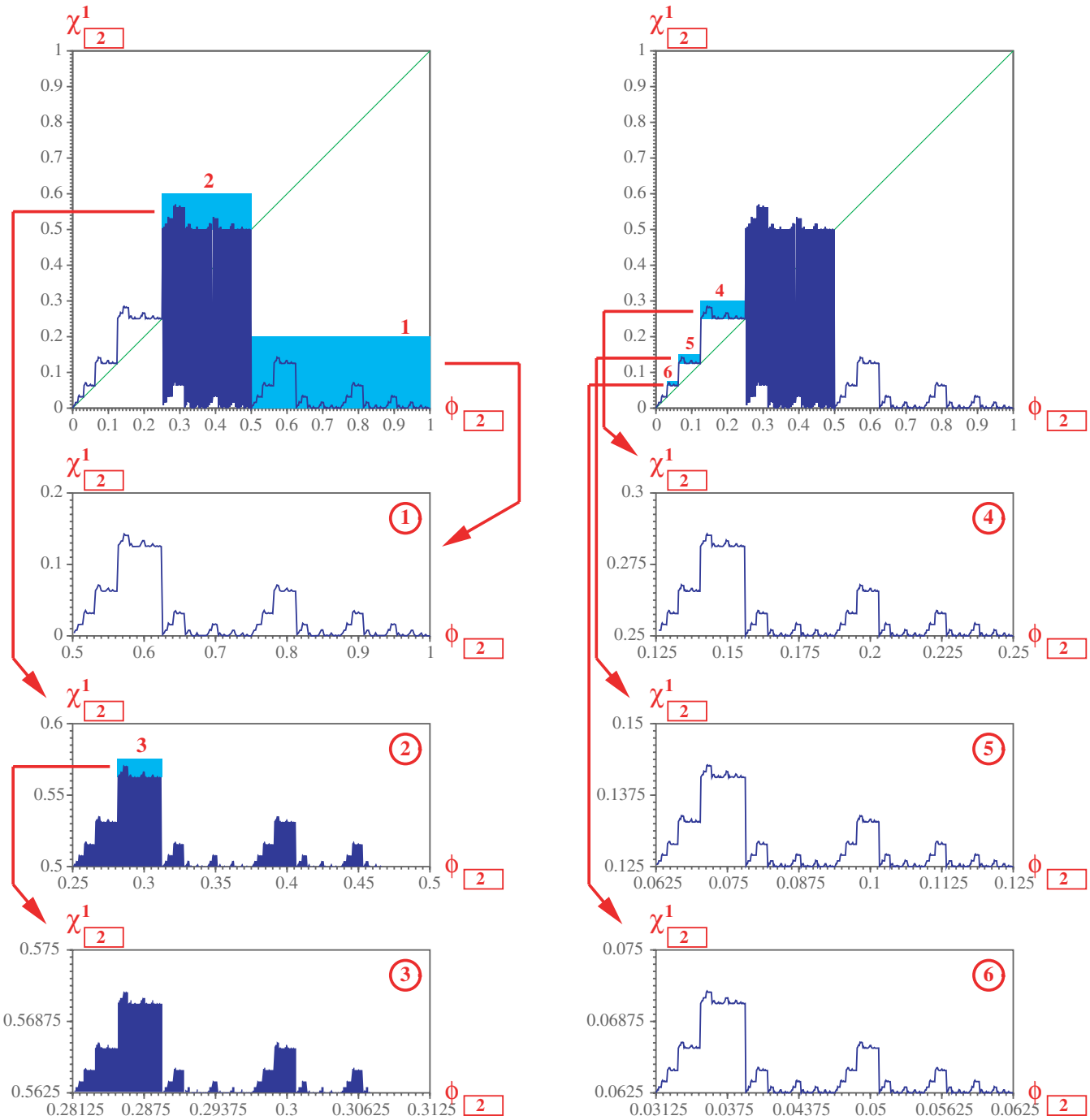
Example 3.5 [Characteristic function $\boldsymbol{\chi}^1_{\boxed{17}}$]. The graph of characteristic function $\boldsymbol{\chi}^1_{\boxed{17}}$ replotted from Table 2 is shown in Fig. 21. The fractal geometry of $\boldsymbol{\chi}^1_{\boxed{17}}$ is obvious from the rescaled patterns ① and ②.

Example 3.6 [Characteristic function $\boldsymbol{\chi}^1_{\boxed{110}}$]. The graph of characteristic function $\boldsymbol{\chi}^1_{\boxed{110}}$ replotted from Table 2 is shown in Fig. 22. The two subpatterns ① and ② reveal the fractal geometry of $\boldsymbol{\chi}^1_{\boxed{110}}$.

Example 3.7 [Characteristic function $\boldsymbol{\chi}^1_{\boxed{124}}$]. The graph of characteristic function $\boldsymbol{\chi}^1_{\boxed{124}}$ replotted from Table 2 is shown in Fig. 23. The two subpatterns ① and ② illustrate the fractal geometry of $\boldsymbol{\chi}^1_{\boxed{124}}$.

Example 3.8 [Characteristic function $\boldsymbol{\chi}^1_{\boxed{137}}$]. The graph of characteristic function $\boldsymbol{\chi}^1_{\boxed{137}}$ replotted from Table 2 is shown in Fig. 24. The two subpatterns ① and ② reveal the fractal geometry of $\boldsymbol{\chi}^1_{\boxed{137}}$.

Example 3.9 [Characteristic function $\boldsymbol{\chi}^1_{\boxed{193}}$]. The graph of characteristic function $\boldsymbol{\chi}^1_{\boxed{193}}$ replotted from Table 2 is shown in Fig. 25. The two subpatterns ① and ② reveal the fractal geometry of $\boldsymbol{\chi}^1_{\boxed{193}}$.



(a) subpattern ①: horizontal scaling = 2^1, vertical scaling = 2^1
subpattern ②: horizontal scaling = 2^2, vertical scaling = 2^2
subpattern ③: horizontal scaling = 2^5, vertical scaling = 2^5

(b) subpattern ④: horizontal scaling = 2^3, vertical scaling = 2^3
subpattern ⑤: horizontal scaling = 2^4, vertical scaling = 2^4
subpattern ⑥: horizontal scaling = 2^5, vertical scaling = 2^5

Fig. 17. Fractal compositions of $\chi^1_{[2]}$.

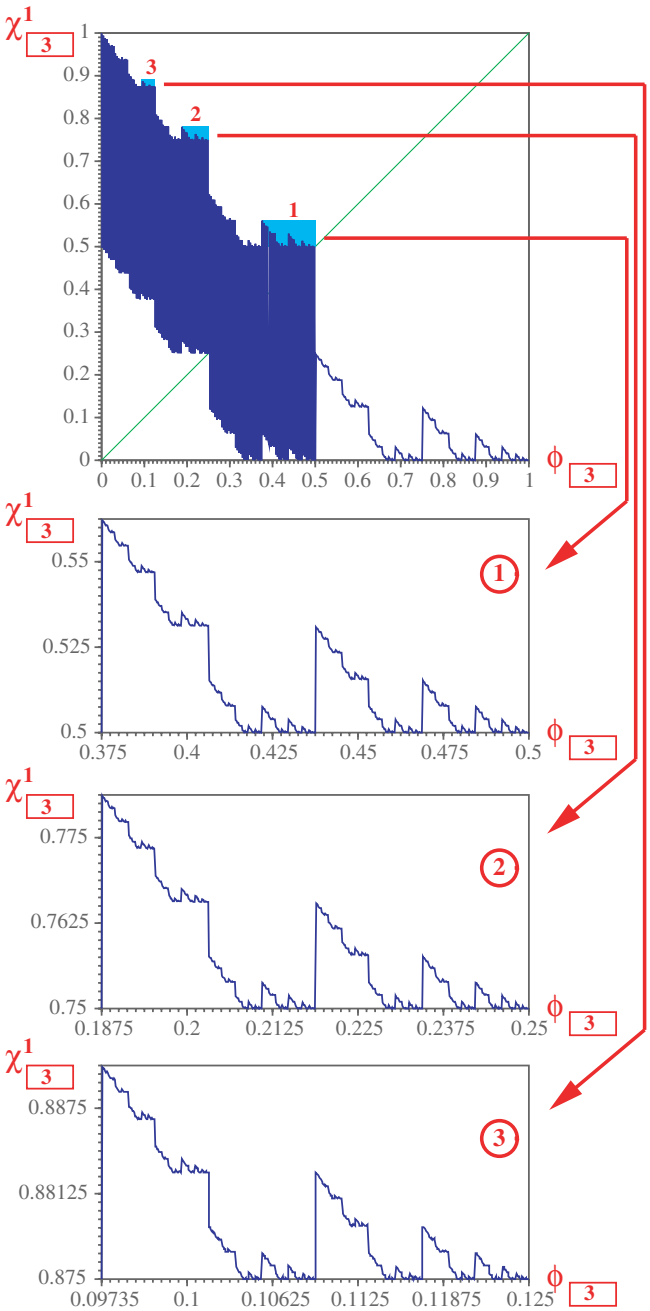


Fig. 18. Fractal compositions of $\chi^1_{\boxed{3}}$.

subpattern ①: horizontal scaling $= 2^3$, vertical scaling $= 2^3$
subpattern ②: horizontal scaling $= 2^4$, vertical scaling $= 2^4$
subpattern ③: horizontal scaling $= 2^5$, vertical scaling $= 2^5$

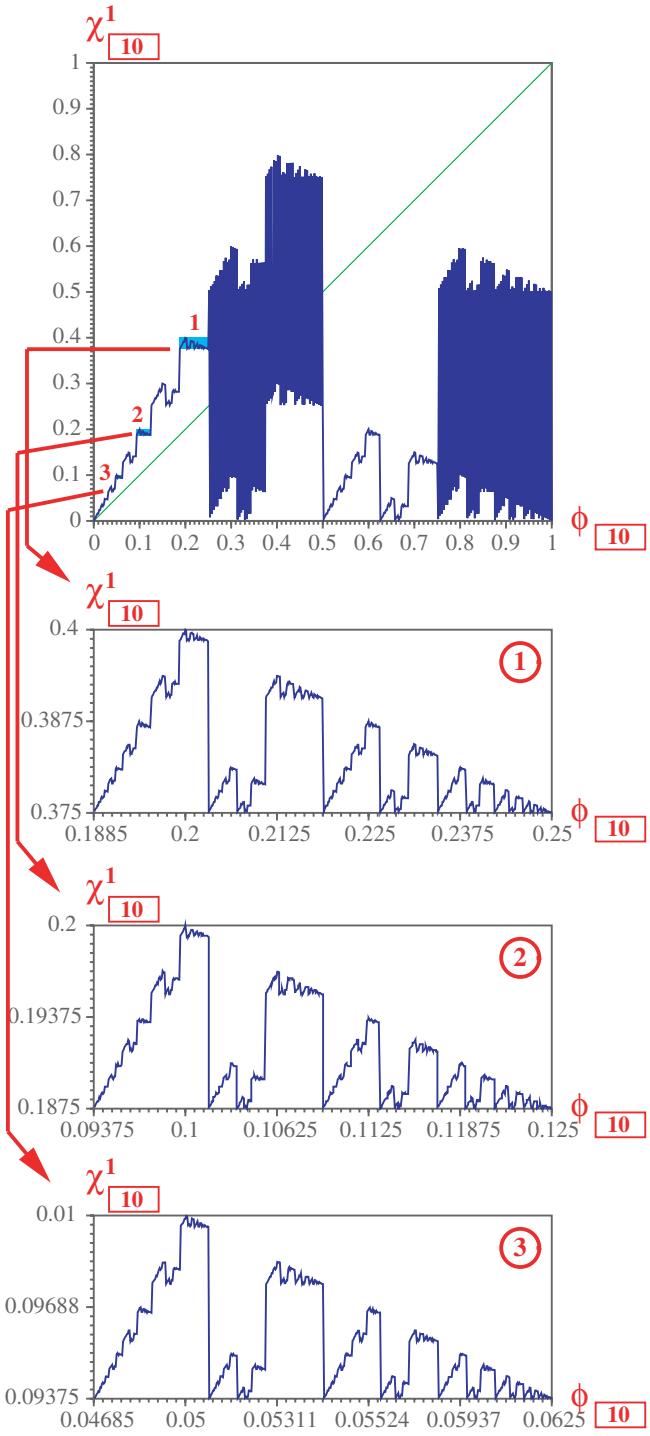


Fig. 19. Fractal compositions of $\chi^1_{\boxed{10}}$.

subpattern ①: horizontal scaling $= 2^4$, vertical scaling $= 2^4$
subpattern ②: horizontal scaling $= 2^5$, vertical scaling $= 2^5$
subpattern ③: horizontal scaling $= 2^6$, vertical scaling $= 2^6$

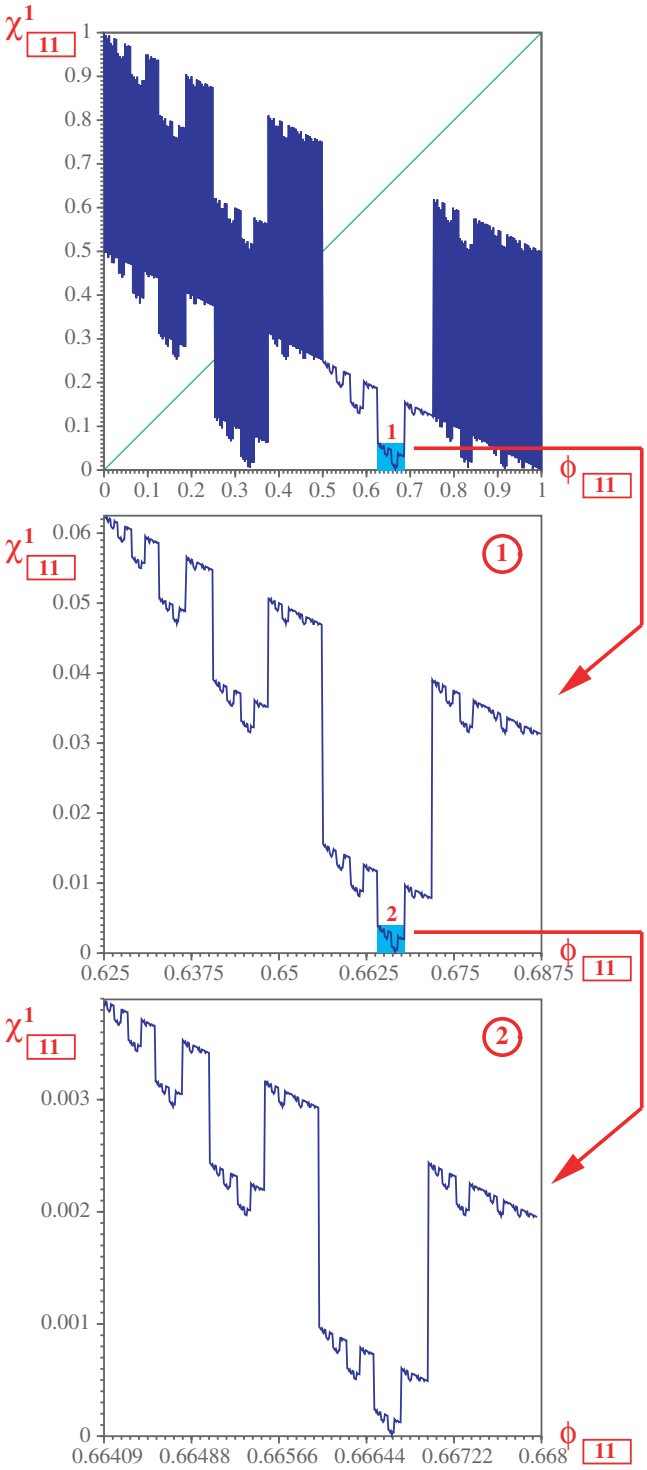


Fig. 20. Fractal compositions of $\chi^1_{\boxed{11}}$.

subpattern ①: horizontal scaling $= 2^4$,
vertical scaling $= 2^4$
subpattern ②: horizontal scaling $= 2^8$,
vertical scaling $= 2^8$

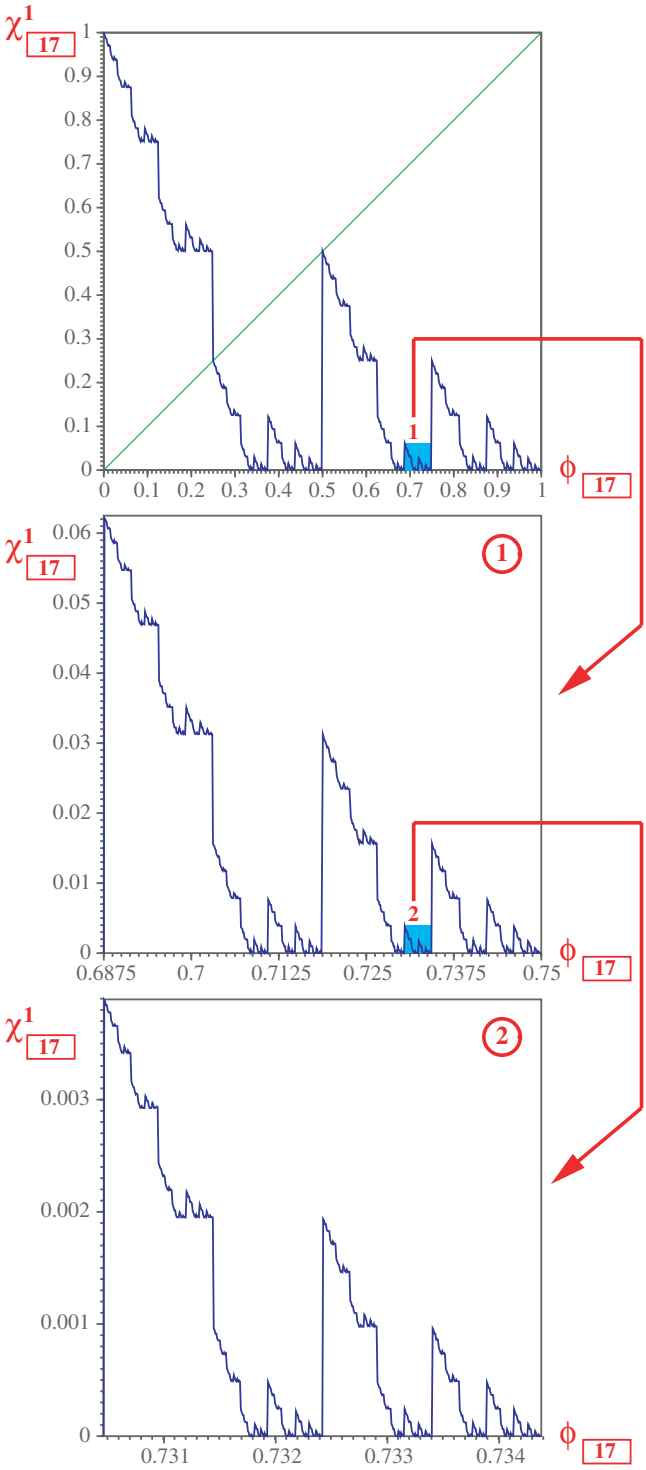


Fig. 21. Fractal compositions of $\chi^1_{\boxed{17}}$.

subpattern ①: horizontal scaling $= 2^4$,
vertical scaling $= 2^4$
subpattern ②: horizontal scaling $= 2^8$,
vertical scaling $= 2^8$

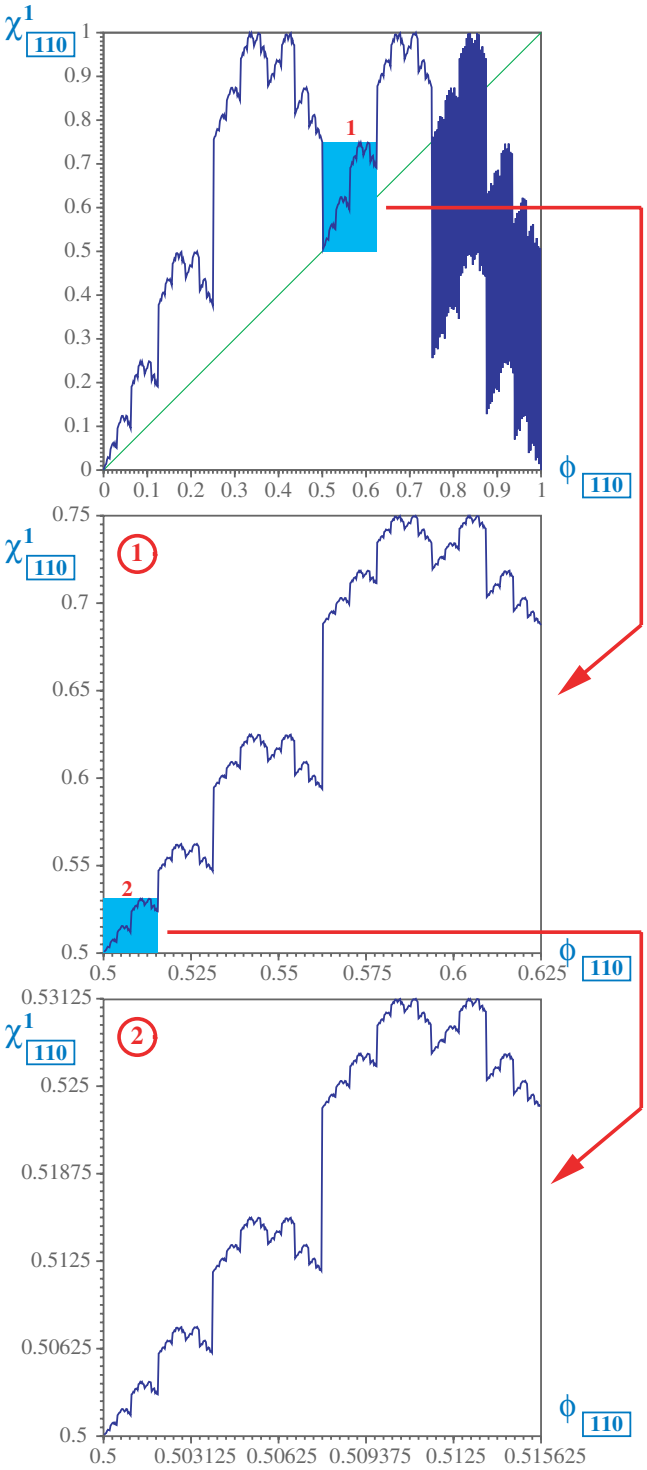


Fig. 22. Fractal compositions of $\chi^1_{\boxed{110}}$.

subpattern ①: horizontal scaling $= 2^3$, vertical scaling $= 2^2$
subpattern ②: horizontal scaling $= 2^6$, vertical scaling $= 2^5$

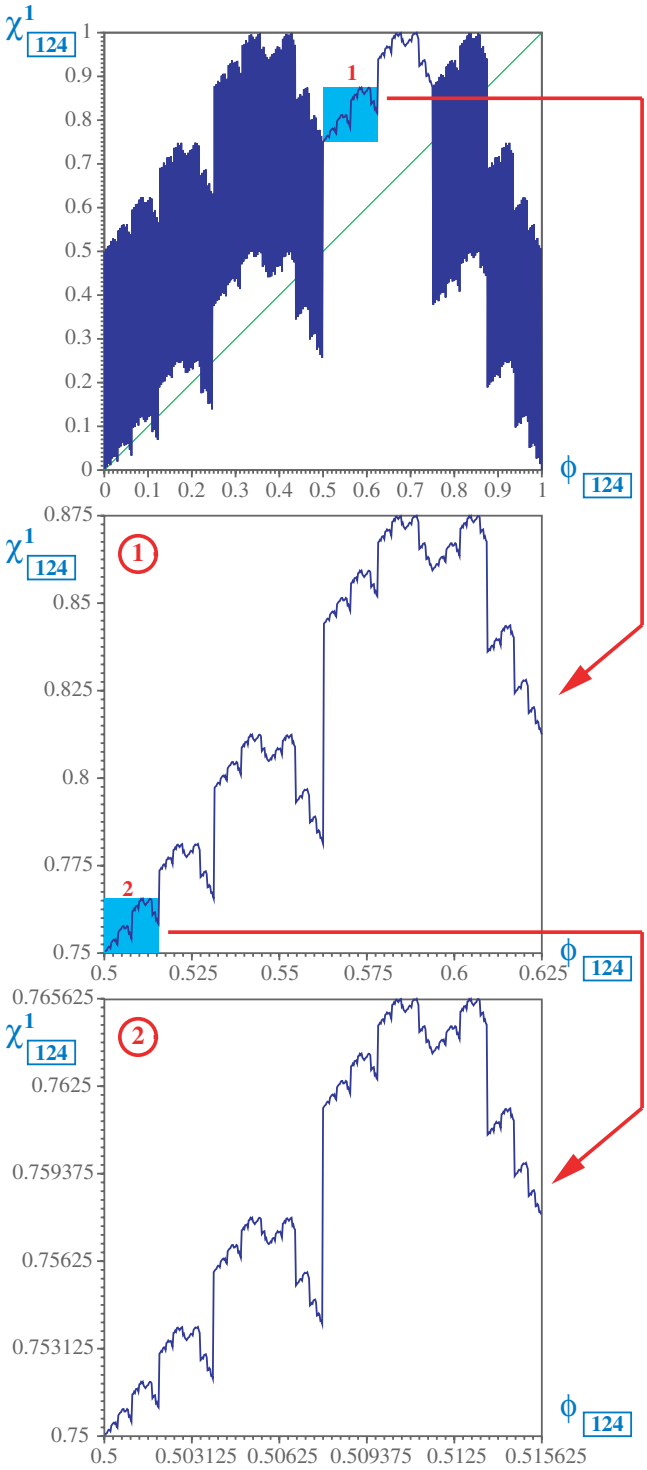


Fig. 23. Fractal compositions of $\chi^1_{\boxed{124}}$.

subpattern ①: horizontal scaling $= 2^3$, vertical scaling $= 2^3$
subpattern ②: horizontal scaling $= 2^6$, vertical scaling $= 2^6$

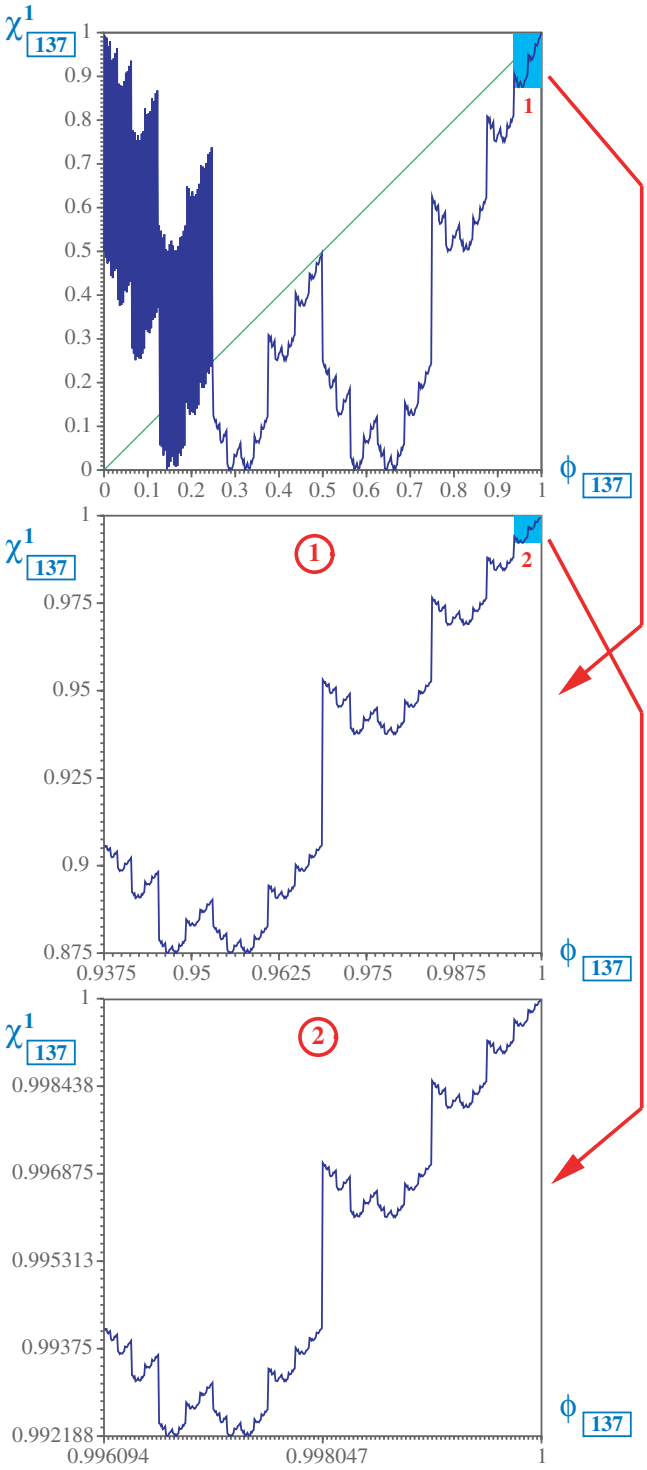


Fig. 24. Fractal compositions of $\chi^1_{\boxed{137}}$.

subpattern ①: horizontal scaling $= 2^4$, vertical scaling $= 2^3$
subpattern ②: horizontal scaling $= 2^8$, vertical scaling $= 2^7$

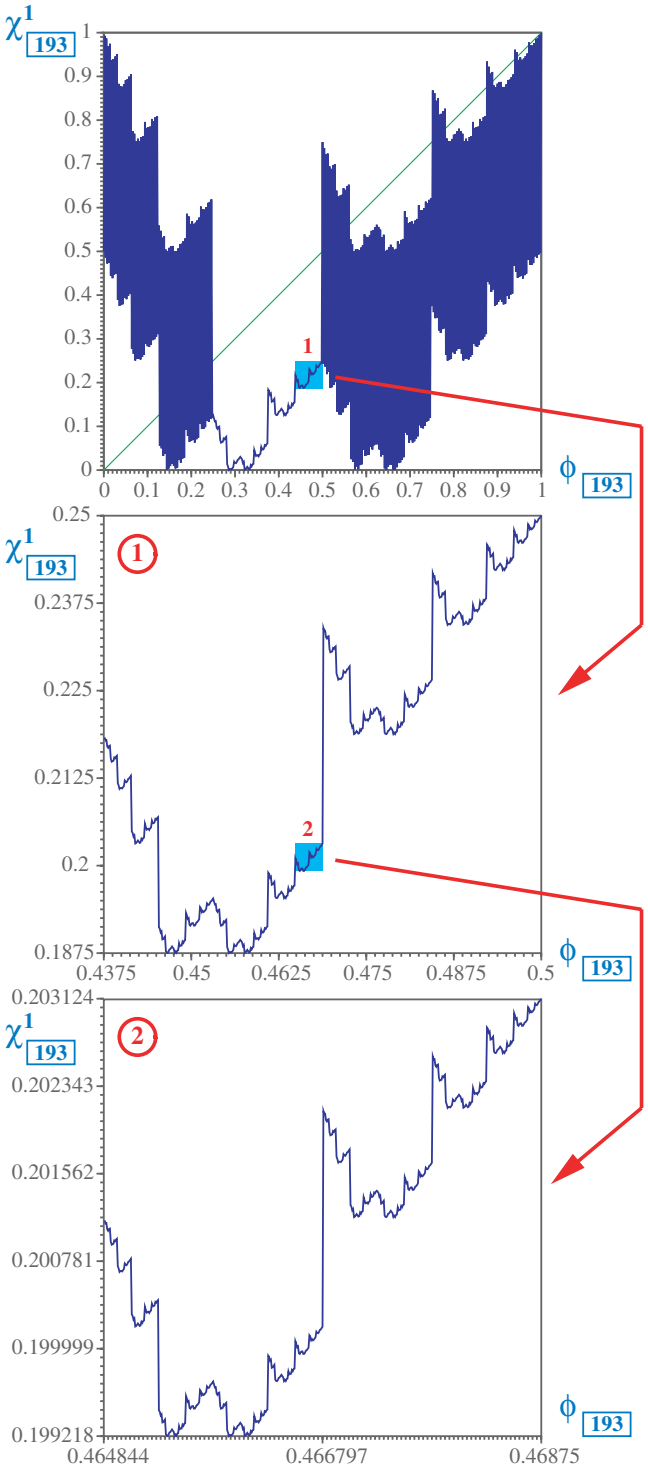


Fig. 25. Fractal compositions of $\chi^1_{\boxed{193}}$.

subpattern ①: horizontal scaling $= 2^4$, vertical scaling $= 2^4$
subpattern ②: horizontal scaling $= 2^8$, vertical scaling $= 2^8$

Example 3.10 [Characteristic function $\chi^1_{[30]}$]. The graph of characteristic function $\chi^1_{[30]}$ replotted from Table 2 is shown in Fig. 26. The two subpatterns ① and ② reveal the fractal geometry of $\chi^1_{[30]}$.

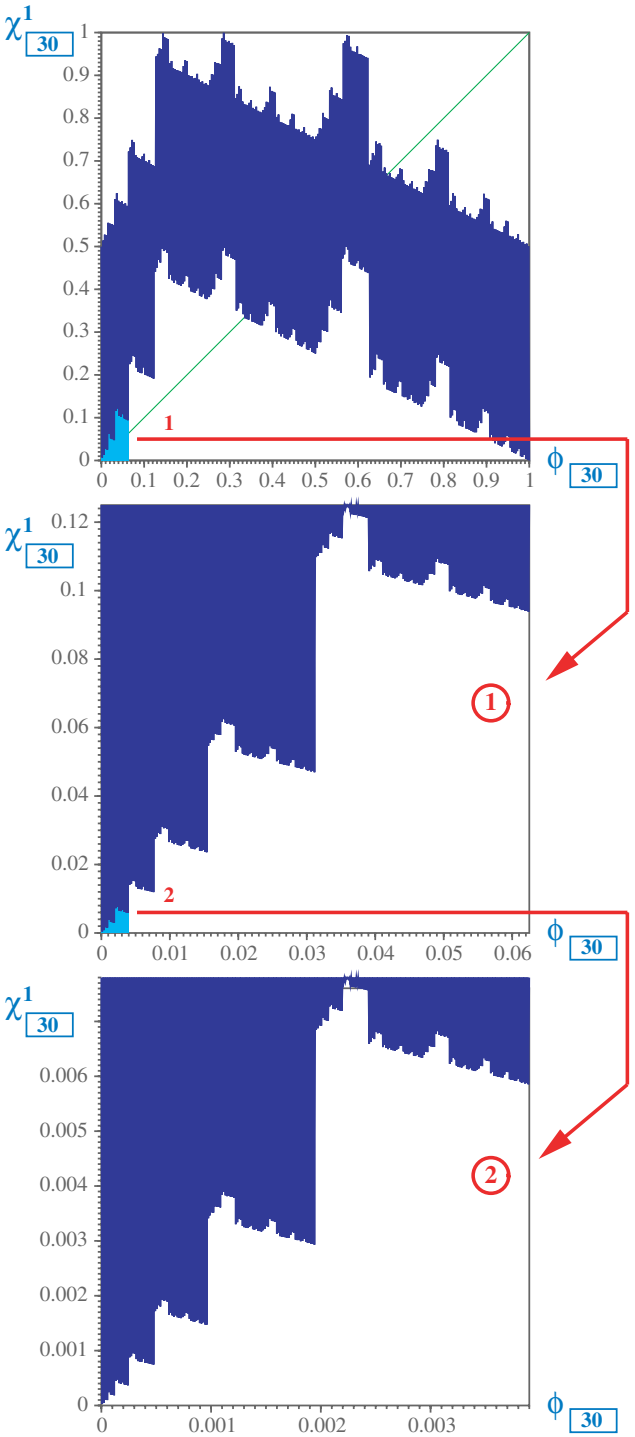


Fig. 26. Fractal compositions of $\chi^1_{[30]}$.
subpattern ①: horizontal scaling $= 2^4$, vertical scaling $= 2^3$
subpattern ②: horizontal scaling $= 2^8$, vertical scaling $= 2^7$

Example 3.11 [Characteristic function $\chi^1_{[135]}$]. The graph of characteristic function $\chi^1_{[135]}$ replotted from Table 2 is shown in Fig. 27. The two subpatterns ① and ② reveal the fractal geometry of $\chi^1_{[135]}$.

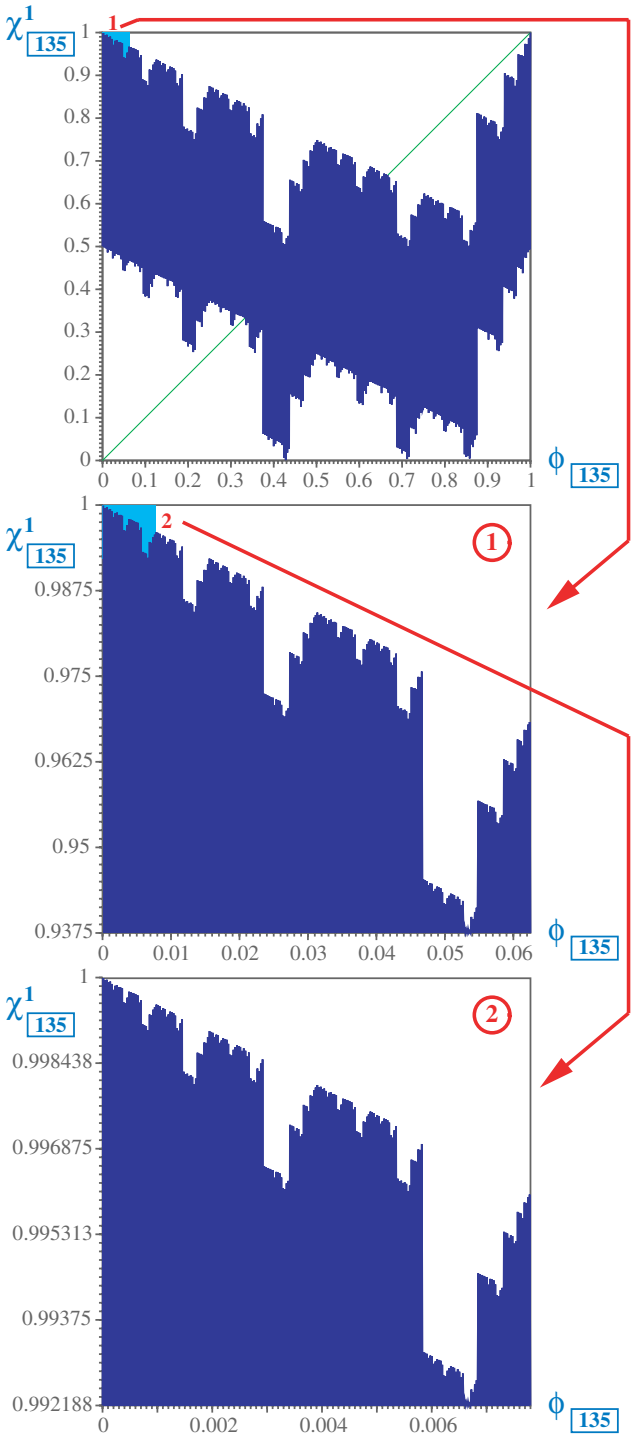


Fig. 27. Fractal compositions of $\chi^1_{[135]}$.
subpattern ①: horizontal scaling $= 2^4$, vertical scaling $= 2^4$
subpattern ②: horizontal scaling $= 2^7$, vertical scaling $= 2^7$

Example 3.12 [Characteristic function $\chi^1_{[90]}$]. The graph of characteristic function $\chi^1_{[90]}$ replotted from Table 2 is shown in Fig. 28. The two subpatterns ① and ② reveal the fractal geometry of $\chi^1_{[90]}$.

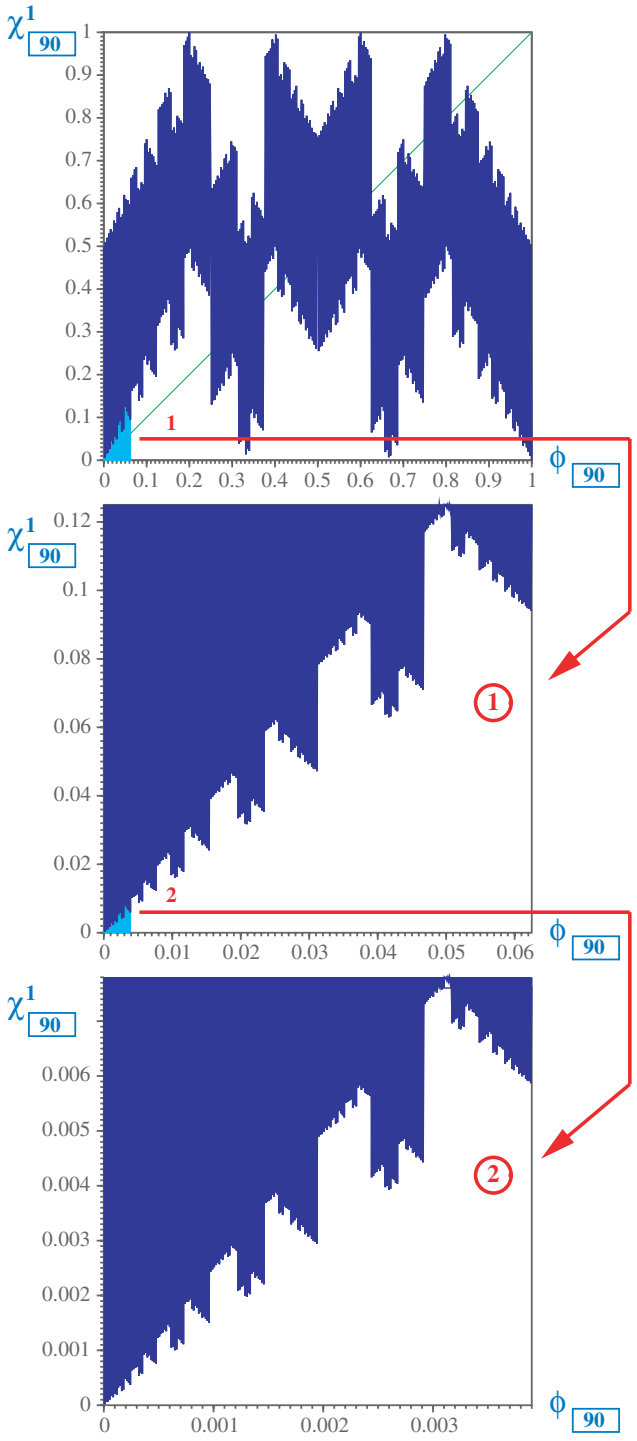


Fig. 28. Fractal compositions of $\chi^1_{[90]}$.

subpattern ①: horizontal scaling $= 2^4$,
vertical scaling $= 2^3$
subpattern ②: horizontal scaling $= 2^8$,
vertical scaling $= 2^7$

Example 3.13 [Characteristic function $\chi^1_{[150]}$]. The graph of characteristic function $\chi^1_{[150]}$ replotted from Table 2 is shown in Fig. 29. The two subpatterns ① and ② reveal the fractal geometry of $\chi^1_{[150]}$.

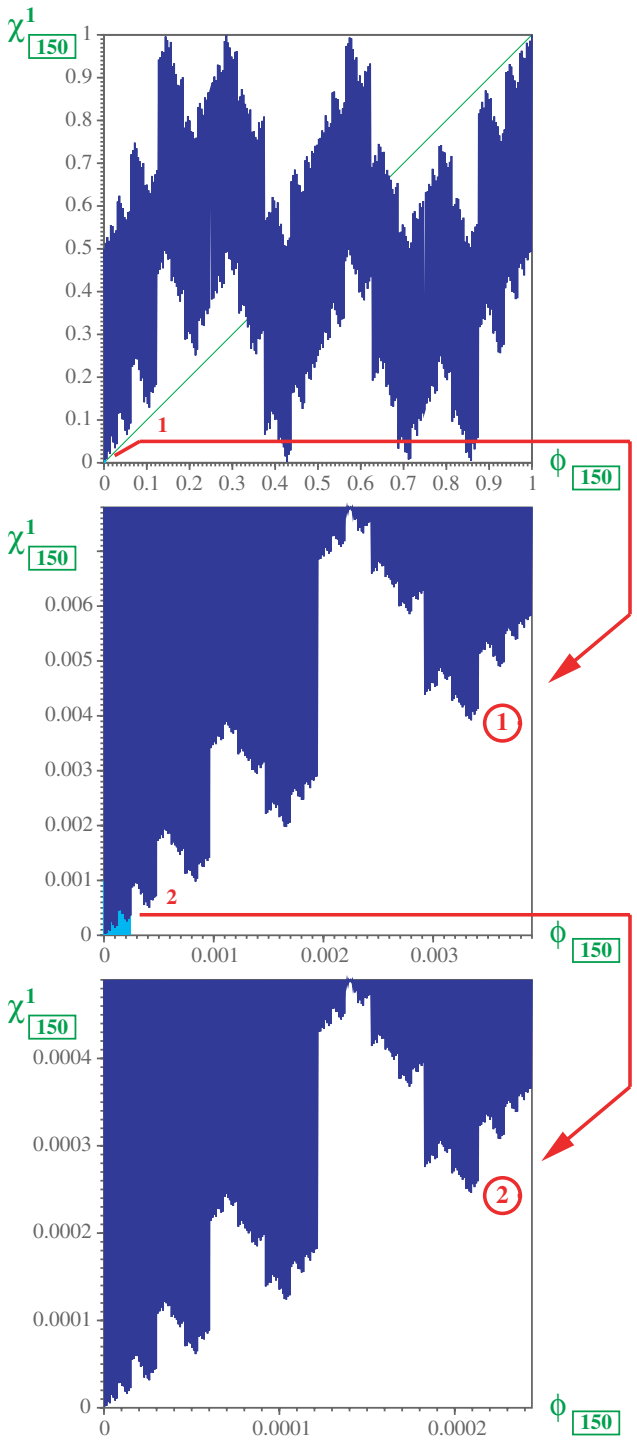


Fig. 29. Fractal compositions of $\chi^1_{[150]}$.

subpattern ①: horizontal scaling $= 2^8$,
vertical scaling $= 2^7$
subpattern ②: horizontal scaling $= 2^{12}$,
vertical scaling $= 2^{11}$

4. Predicting the Fractal Structures

The *fractal* structure of each characteristic function $\boldsymbol{\chi}^1_{\boxed{N}}$ in Table 2 can be analyzed and predicted using the properties of characteristic functions to be presented below, and from the coefficient b_1 in the explicit formulas from Table 1.

4.1. *Two-level fractal stratifications*

Let us partition the unit interval [0,1] into four subintervals $\Phi_1 \triangleq [0, 0.25)$, $\Phi_2 \triangleq [0.25, 0.5)$, $\Phi_3 \triangleq [0.5, 0.75)$, and $\Phi_4 \triangleq [0.75, 1.0]$. It follows from the binary-to-decimal conversion formula

$$\{x_0, x_1, x_2, \ldots, x_I\} \mapsto \phi = \sum_{i=0}^{I} 2^{-(i+1)} x_i \tag{15}$$

that each binary string belonging to these four subintervals must have the following form:

$$\left.\begin{array}{l} \{0,\, 0,\, x_2,\, x_3,\, x_4,\, \ldots,\, x_I\} \in \Phi_1 \\ \{0,\, 1,\, x_2,\, x_3,\, x_4,\, \ldots,\, x_I\} \in \Phi_2 \\ \{1,\, 0,\, x_2,\, x_3,\, x_4,\, \ldots,\, x_I\} \in \Phi_3 \\ \{1,\, 1,\, x_2,\, x_3,\, x_4,\, \ldots,\, x_I\} \in \Phi_4 \end{array}\right\} \tag{16}$$

Let $\{y_0, y_1, y_2, \ldots, y_I\}$ denote the image of $\{x_0, x_1, x_2, \ldots, x_I\}$ under local rule $\boxed{N}$:

$$\{x_0, x_1, x_2, \ldots, x_I\} \overset{T_{\boxed{N}}}{\longmapsto} \{y_0, y_1, y_2, \ldots, y_I\} \tag{17}$$

where

$$\{y_0, y_1, y_2, \ldots, y_I\} \mapsto \boldsymbol{\chi}^1_{\boxed{N}}(\phi) \tag{18}$$

and ϕ is the decimal representation in Eq. (15), namely,

$$\boxed{\boldsymbol{\chi}^1_{\boxed{N}}(\phi) = \sum_{i=0}^{I} 2^{-(i+1)} y_i} \tag{19}$$

Observe that if we let the binary string $\{x_0, x_1, x_2, \ldots, x_I\}$ assume all binary combinations from $\{0, 0, 0, \ldots, 0\}$ to $\{1, 1, 1, \ldots, 1\}$ in Eq. (17), and calculate the corresponding decimal value from Eq. (19), we would obtain the coordinates $(\phi_{\boxed{N}}, \boldsymbol{\chi}^1_{\boxed{N}})$ for plotting the characteristic functions in Table 2.

Observe also that the first binary bit "y_0" of Eq. (17) is given by the first step function ($i = 0$) in Table 1, as defined by Eq. (7). The value of y_0 is therefore determined by the three binary bits

$$(x_{-1}, x_0, x_1) = (x_I, x_0, x_1) \tag{20}$$

in view of the *periodic* boundary condition $x_{-1} = x_I$ in Fig. 1(a). In other words, we have:

Property 4.1. *The* first *binary bit* y_0 *of* $\boldsymbol{\chi}^1_{\boxed{N}}$ *of Eq. (18) depends in general on the* last *binary bit* x_I *of the input binary string of Eq. (15).*

Since the first binary bit y_0 of Eq. (18) contributes the largest component $2^{-1} = 0.5$ (if $y_0 = 1$), and since the last binary bit x_I alternates between "0" and "1" as we increase $\phi_{\boxed{N}}$ from $\phi_{\boxed{N}} = 0$ to $\phi_{\boxed{N}} = 1$ in Table 2, it follows that, *depending* on the formula in Table 1 for local rule $\boxed{N}$, the characteristic function $\boldsymbol{\chi}^1_{\boxed{N}}$ *may* exhibit a *discontinuous* jump in $\boldsymbol{\chi}^1_{\boxed{N}}$ equal to $\Delta\boldsymbol{\chi}^1_{\boxed{N}} = 0.5$. This implies that certain subintervals of $\boldsymbol{\chi}^1_{\boxed{N}}$ may exhibit vertical jumps equal to 0.5 between *adjacent* red and blue bars in Table 2, resulting in a *two-level stratification* of $\boldsymbol{\chi}^1_{\boxed{N}}$.

In view of Property 4.1, the characteristic function $\boldsymbol{\chi}^1_{\boxed{N}}$ in Table 2 may exhibit a *discontinuous* jump by an amount equal to $\Delta\boldsymbol{\chi}^1_{\boxed{N}} = 0.5$ over different subintervals Φ_1, Φ_2, Φ_3 and Φ_4, respectively. An examination of the graph of each characteristic function $\boldsymbol{\chi}^1_{\boxed{N}}$ in Table 2 shows that within each subinterval Φ_i, one of the following groupings of small *red squares* (resp. *blue squares*) on top of each thin red bar (resp. blue bar) apply to *all* small squares located within *the same* subinterval Φ_i, $i = 1, 2, 3, 4$ (this information is coded in color *red*, *blue* or *violet*, in Table 5):

Group 1. All small red squares have $\boldsymbol{\chi}^1_{\boxed{N}} \geq 0.5$ and all small blue squares (in the case where there are two-level stratifications) have $\boldsymbol{\chi}^1_{\boxed{N}} < 0.5$. In this case, we will paint the upper rectangle of $\boxed{N}$ in column Φ_i of Table 5 in *red*, and the rectangle below it will be painted *blue*.

Group 2. The small red and blue squares are located opposite to those of *Group 1*. In this case, the *upper* rectangle of Table 5 will be painted *blue*, and the *lower* rectangle will be painted *red*.

Group 3. There is no stratification and all small adjacent red and blue squares have $\boldsymbol{\chi}^1_{\boxed{N}} \geq 0.5$. In this case, only the *upper* rectangle is painted in *violet* color,[2] while the lower rectangle is left blank.

[2]We have chosen the violet color as the nearest approximation of the color combination between the red and blue colors.

Table 5. Stratification of characteristic functions over subintervals $\Phi_1 \in [0, 0.25)$, $\Phi_2 \in [0.25, 0.5)$, $\Phi_3 \in [0.5, 0.75)$, and $\Phi_4 \in [0.75, 1]$.

N	Φ_1	Φ_2	Φ_3	Φ_4
0				
1				
2				
3				
4				
5				
6				
7				
8				
9				
10				
11				
12				
13				
14				
15				
16				
17				
18				
19				
20				
21				
22				
23				
24				
25				
26				
27				
28				
29				
30				
31				

N	Φ_1	Φ_2	Φ_3	Φ_4
32				
33				
34				
35				
36				
37				
38				
39				
40				
41				
42				
43				
44				
45				
46				
47				
48				
49				
50				
51				
52				
53				
54				
55				
56				
57				
58				
59				
60				
61				
62				
63				

Table 5. (*Continued*)

N	Φ_1	Φ_2	Φ_3	Φ_4
64				
65				
66				
67				
68				
69				
70				
71				
72				
73				
74				
75				
76				
77				
78				
79				
80				
81				
82				
83				
84				
85				
86				
87				
88				
89				
90				
91				
92				
93				
94				
95				

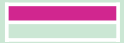
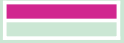
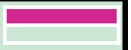
N	Φ_1	Φ_2	Φ_3	Φ_4
96				
97				
98				
99				
100				
101				
102				
103				
104				
105				
106				
107				
108				
109				
110				
111				
112				
113				
114				
115				
116				
117				
118				
119				
120				
121				
122				
123				
124				
125				
126				
127				

Table 5. (*Continued*)

N	Φ_1	Φ_2	Φ_3	Φ_4
128				
129				
130				
131				
132				
133				
134				
135				
136				
137				
138				
139				
140				
141				
142				
143				
144				
145				
146				
147				
148				
149				
150				
151				
152				
153				
154				
155				
156				
157				
158				
159				

N	Φ_1	Φ_2	Φ_3	Φ_4
160				
161				
162				
163				
164				
165				
166				
167				
168				
169				
170				
171				
172				
173				
174				
175				
176				
177				
178				
179				
180				
181				
182				
183				
184				
185				
186				
187				
188				
189				
190				
191				

Table 5. (*Continued*)

N	Φ_1	Φ_2	Φ_3	Φ_4
192				
193				
194				
195				
196				
197				
198				
199				
200				
201				
202				
203				
204				
205				
206				
207				
208				
209				
210				
211				
212				
213				
214				
215				
216				
217				
218				
219				
220				
221				
222				
223				

N	Φ_1	Φ_2	Φ_3	Φ_4
224				
225				
226				
227				
228				
229				
230				
231				
232				
233				
234				
235				
236				
237				
238				
239				
240				
241				
242				
243				
244				
245				
246				
247				
248				
249				
250				
251				
252				
253				
254				
255				

Group 4. The small red and blue squares are located opposite to those of *Group 3*. In this case, only the *lower* rectangle is painted in *violet* color, while the upper rectangle is left blank.

4.1.1. *Stratification prediction procedure*

The color painted in each of the two rectangles located in each subinterval Φ_i of the characteristic function $\boldsymbol{\chi}^1_{\boxed{N}}$ of Table 5 is obtained by inspection of the graph of $\boldsymbol{\chi}^1_{\boxed{N}}$ in Table 2. We will now show how these colors can be *predicted* directly from the "*firing patterns*" [Chua *et al.*, 2003] of each rule $\boxed{N}$; namely, from the "three-bit pattern" associated with each *red* vertex of the *Boolean cube* representing $\boxed{N}$ in Fig. 1(e).

Our goal is to determine the color of the first output bit y_0 from these firing patterns. In particular, y_0 depends on the three binary bits $\{x_{-1}, x_0 \text{ and}, x_1\}$, as shown in Fig. 30, where $x_{-1} = x_I$ in view of the periodic boundary condition in Fig. 1(a). The "color" of $\boxed{x_0}$ and $\boxed{x_1}$ in Fig. 30 is chosen from the subinterval Φ_i as defined by the first two columns of Eq. (16); namely,

Φ_i	x_0	x_1
Φ_1	0	0
Φ_2	0	1
Φ_3	1	0
Φ_4	1	1

The color of x_{-1} in Fig. 30 is chosen as follows:

1. $\boxed{x_{-1} = 0, \quad \text{if} \quad x_I = 0}$

Using the bar-coloring scheme described in p. 1049 of [Chua *et al.*, 2005], this corresponds to the case where the *right-most* bar of $\boldsymbol{\chi}^1_{\boxed{N}}$ in Table 2 is a *red* bar.

2. $\boxed{x_{-1} = 1, \quad \text{if} \quad x_I = 1}$

This corresponds to the case where the *right-most* bar of $\boldsymbol{\chi}^1_{\boxed{N}}$ in Table 2 is a *blue* bar.

Since both $\boxed{x_{-1}}$ and $\boxed{y_0}$ can assume a "0" or a "1", there are four possible outcomes:

Outcome 1: $\boxed{x_{-1}} = \boxed{0}, \boxed{y_0} = \boxed{0}$

In this case, all bars belonging to subinterval Φ_i are colored *red* and lie *below* $\boldsymbol{\chi}^1_{\boxed{N}} = 0.5$.

Outcome 2: $\boxed{x_{-1}} = \boxed{0}, \boxed{y_0} = \boxed{1}$

In this case, all bars belonging to subinterval Φ_i are colored *red* and lie *above* $\boldsymbol{\chi}^1_{\boxed{N}} = 0.5$.

Outcome 3: $\boxed{x_{-1}} = \boxed{1}, \boxed{y_0} = \boxed{0}$

In this case, all bars belonging to subinterval Φ_i are colored *blue* and lie *below* $\boldsymbol{\chi}^1_{\boxed{N}} = 0.5$.

Outcome 4: $\boxed{x_{-1}} = \boxed{1}, \boxed{y_0} = \boxed{1}$

In this case, all bars belonging to subinterval Φ_i are colored *blue* and lie *above* $\boldsymbol{\chi}^1_{\boxed{N}} = 0.5$.

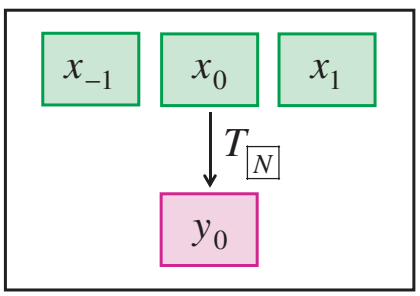


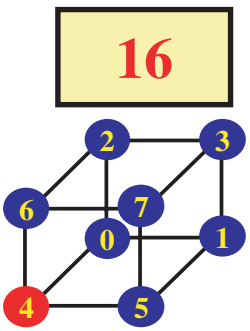
Fig. 30. The left-most output bit y_0 of $\boldsymbol{\chi}^1_{\boxed{N}}$ is "1" if $\{x_{-1}, x_0, x_1\} = \{x_I, x_0, x_1\}$ is a firing pattern of $\boxed{N}$. Otherwise, $y_0 = 0$.

4.1.2. *Examples illustrating stratification prediction procedure*

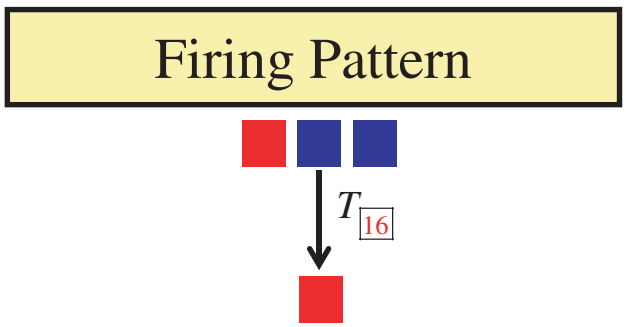
Let us illustrate the above "*stratification prediction*" procedure with some examples.

Example 4.1 [Predicting Stratification for $\boldsymbol{\chi}^1_{\boxed{16}}$]. The Boolean cube for rule $\boxed{16}$ is reproduced from Table 1 of [Chua *et al.*, 2003] in Fig. 31(a). Since only vertex ④ is painted red in this Boolean cube, there is only one firing pattern ■■■ → $\boxed{1}$ $\boxed{0}$ $\boxed{0}$, as shown in Fig. 31(b).

For each subinterval Φ_i, $i = 1, 2, 3, 4$, we insert the corresponding $\boxed{x_0}$ and $\boxed{x_1}$ as specified in the preceding table. We then assign $x_{-1} = 0$ (for *red* bars) on the left column and $x_{-1} = 1$ (for *blue* bars) on the right column for each Φ_i. The color of y_0 in each case is then determined from the firing patterns in Fig. 31(b). In this case, $y_0 = 1$ only in (row 1, column 2). Since $y_0 = 0$ in the left column of Φ_1 and $y_0 = 1$ in the right column of Φ_1, it follows that $\boldsymbol{\chi}^1_{\boxed{16}}$ has two stratifications over the subinterval Φ_1, where the *red bars* are *below* $\boldsymbol{\chi}^1_{\boxed{16}} = 0.5$ and the *blue bars* are *above* $\boldsymbol{\chi}^1_{\boxed{16}} = 0.5$.



(a)



(b)

Φ_1	$x_{-1}=0$, $x_0=0$, $x_1=0$, T_{16}, $y_0=0$	$x_{-1}=1$, $x_0=0$, $x_1=0$, T_{16}, $y_0=1$
Φ_2	$x_{-1}=0$, $x_0=0$, $x_1=1$, T_{16}, $y_0=0$	$x_{-1}=1$, $x_0=0$, $x_1=1$, T_{16}, $y_0=0$
Φ_3	$x_{-1}=0$, $x_0=1$, $x_1=0$, T_{16}, $y_0=0$	$x_{-1}=1$, $x_0=1$, $x_1=0$, T_{16}, $y_0=0$
Φ_4	$x_{-1}=0$, $x_0=1$, $x_1=1$, T_{16}, $y_0=0$	$x_{-1}=1$, $x_0=1$, $x_1=1$, T_{16}, $y_0=0$

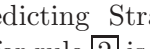
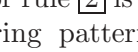
(c)

Fig. 31. Predicting stratification for rule 16. (a) Boolean cube for 16. (b) Firing patterns for 16. (c) Stratification determination data.

Since $y_0 = 0$ for all other cases in Fig. 31(c), it follows that there are no stratifications in subinterval Φ_2, Φ_3 and Φ_4, and all red and blue bars in these three subintervals are located below $\chi^1_{\boxed{16}} = 0.5$, as is indeed the case in Table 2.

Example 4.2 [Predicting Stratification for $\chi^1_{\boxed{2}}$]. The Boolean cube for rule $\boxed{2}$ is shown in Fig. 32(a). It has only one firing pattern  $\rightarrow$ $\boxed{0}$ $\boxed{0}$ $\boxed{1}$, as shown in Fig. 32(b). The corresponding stratification determination data is shown in Fig. 32(c). From these data, we conclude that only subinterval Φ_2 has a stratification in $\chi^1_{\boxed{2}}$ where all *red* bars lie *above*, and all *blue* bars lie *below* $\chi^1_{\boxed{2}} = 0.5$. Since $y_0 = 0$ in the other three subintervals Φ_1, Φ_3 and Φ_4, all red and blue bars must lie below $\chi^1_{\boxed{2}} = 0.5$. Observe that this prediction is consistent with Table 2, as expected.

Example 4.3 [Predicting Stratification for $\chi^1_{\boxed{4}}$]. The Boolean cube for rule $\boxed{4}$ is shown in Fig. 33(a). It has only one firing pattern  $\rightarrow$ $\boxed{0}$ $\boxed{1}$ $\boxed{0}$, as shown in Fig. 33(b). In this case, only subinterval Φ_3 in Fig. 33(c) has a stratification in $\chi^1_{\boxed{4}}$ where all *red* bars must lie above $\chi^1_{\boxed{4}} = 0.5$, and all *blue* bars must lie below $\chi^1_{\boxed{4}} = 0.5$. All red and blue bars in the other three subintervals Φ_1, Φ_2 and Φ_4 must lie below $\chi^1_{\boxed{4}} = 0.5$, because $y_0 = 0$. Again, this prediction is consistent with Table 2.

Example 4.4 [Predicting Stratification for $\chi^1_{\boxed{110}}$]. The Boolean cube for rule $\boxed{110}$ is shown in Fig. 34(a). It has five firing patterns,  $\rightarrow$ $\boxed{0}$ $\boxed{0}$ $\boxed{1}$,  $\rightarrow$ $\boxed{0}$ $\boxed{1}$ $\boxed{0}$,  $\rightarrow$ $\boxed{0}$ $\boxed{1}$ $\boxed{1}$,  $\rightarrow$ $\boxed{1}$ $\boxed{0}$ $\boxed{1}$, $\rightarrow$ $\boxed{1}$ $\boxed{1}$ $\boxed{0}$, as shown in Fig. 34(b). The stratification determination data in Fig. 34(c) shows only subinterval Φ_4 has a stratification where all *red* bars must lie above $\chi^1_{\boxed{110}} = 0.5$, and all *blue* bars must lie below it.

Since $y_0 = 0$ in both columns of Φ_1, it follows that all *red* and *blue* bars must lie below $\chi^1_{\boxed{110}} = 0.5$.

On the other hand, since $y_0 = 1$ in both columns of Φ_2 and Φ_3, it follows that all red and blue bars in subintervals Φ_2 and Φ_3 must lie above $\chi^1_{\boxed{110}} = 0.5$. All of these predictions are consistent with Table 2, as expected.

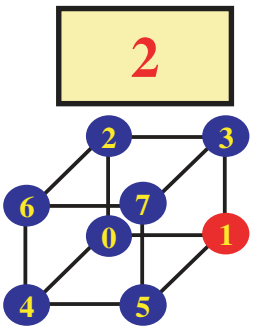
4.1.3. $\{\Phi_1, \Phi_2, \Phi_3, \Phi_4\}$ — *stratified families*

If we examine the color of the rectangles of the four subintervals Φ_1, Φ_2, Φ_3 and Φ_4 in Table 5 and code each *violet* rectangle by a "0" binary bit, and all other rectangles by a "1" binary bit, we will discover the first 16 rules follow the four-bit binary number system as shown below, henceforth called the stratified family "0".

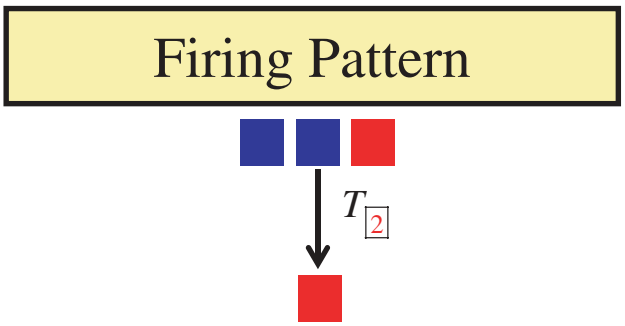
Stratified Family "0"

N	ψ	Φ_1	Φ_2	Φ_3	Φ_4	Equivalent Decimal Number
0	ψ_0	0	0	0	0	0
1	ψ_1	1	0	0	0	1
2	ψ_2	0	1	0	0	2
3	ψ_3	1	1	0	0	3
4	ψ_4	0	0	1	0	4
5	ψ_5	1	0	1	0	5
6	ψ_6	0	1	1	0	6
7	ψ_7	1	1	1	0	7
8	ψ_8	0	0	0	1	8
9	ψ_9	1	0	0	1	9
10	ψ_{10}	0	1	0	1	10
11	ψ_{11}	1	1	0	1	11
12	ψ_{12}	0	0	1	1	12
13	ψ_{13}	1	0	1	1	13
14	ψ_{14}	0	1	1	1	14
15	ψ_{15}	1	1	1	1	15

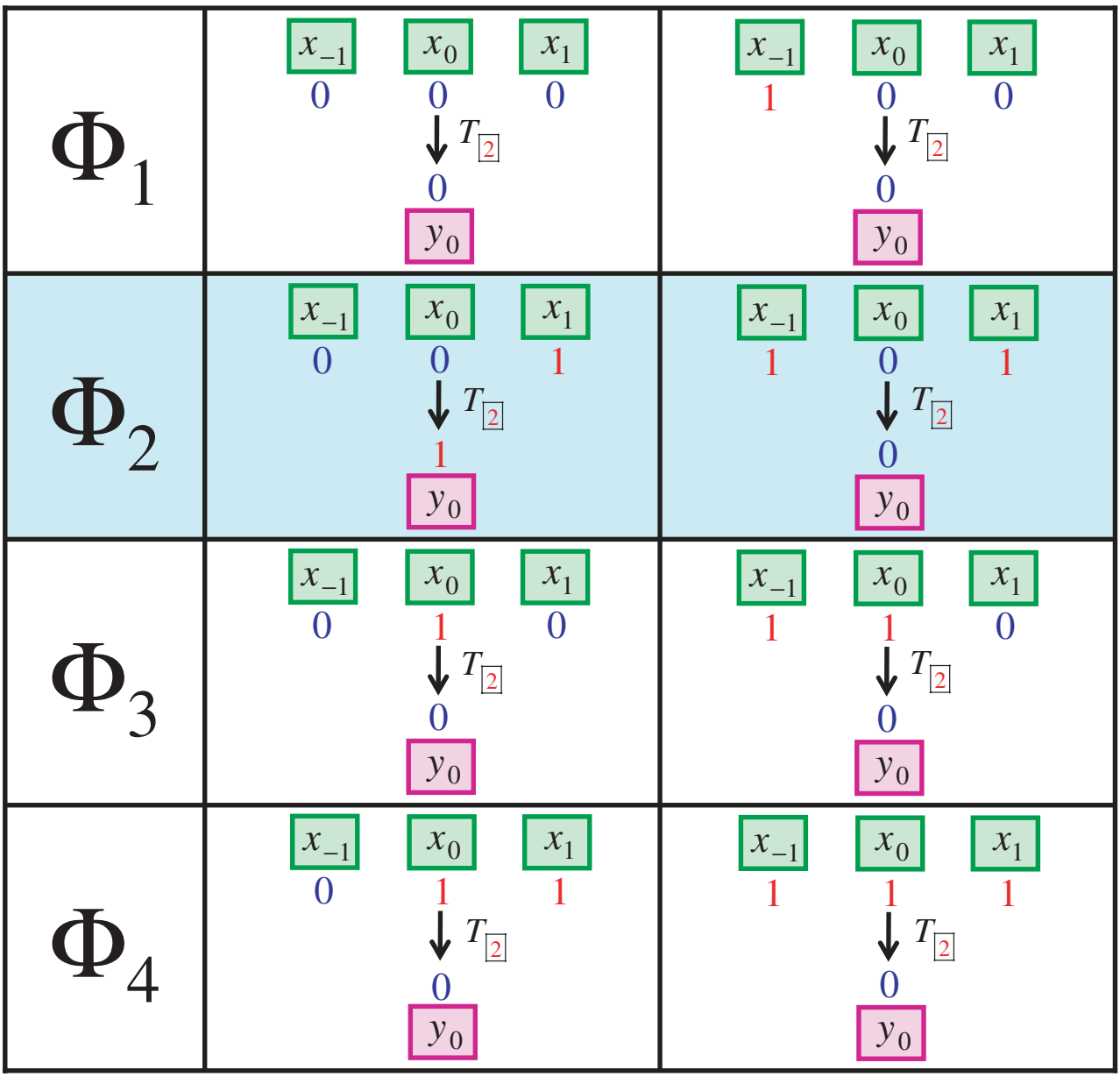
Observe that the color background of Table 1 is determined from this coding scheme, where "0" is coded "light blue", while "1" is coded "light pink" in Table 1.



(a)

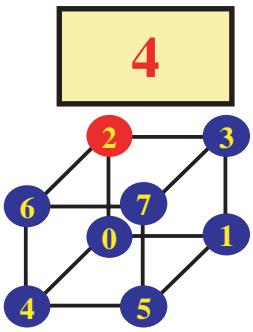


(b)

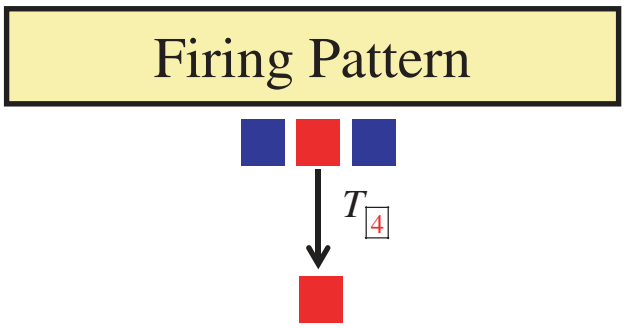


(c)

Fig. 32. Predicting stratification for rule [2]. (a) Boolean cube for [2]. (b) Firing patterns for [2]. (c) Stratification determination data .



(a)

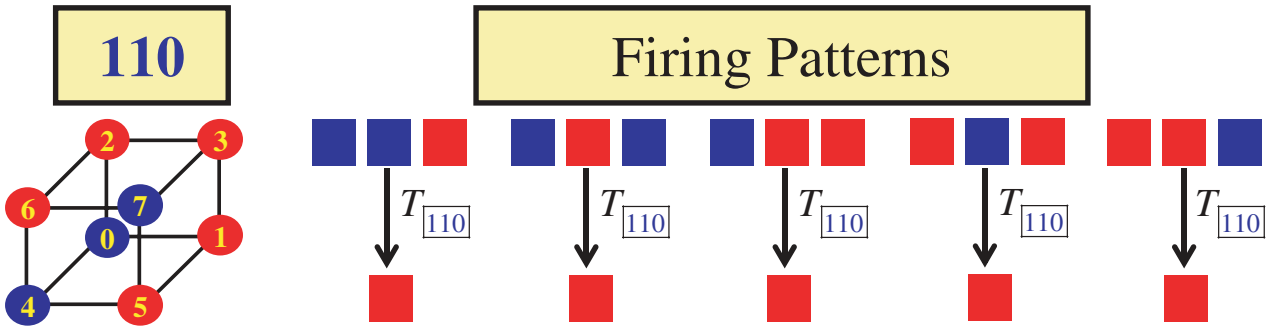


(b)

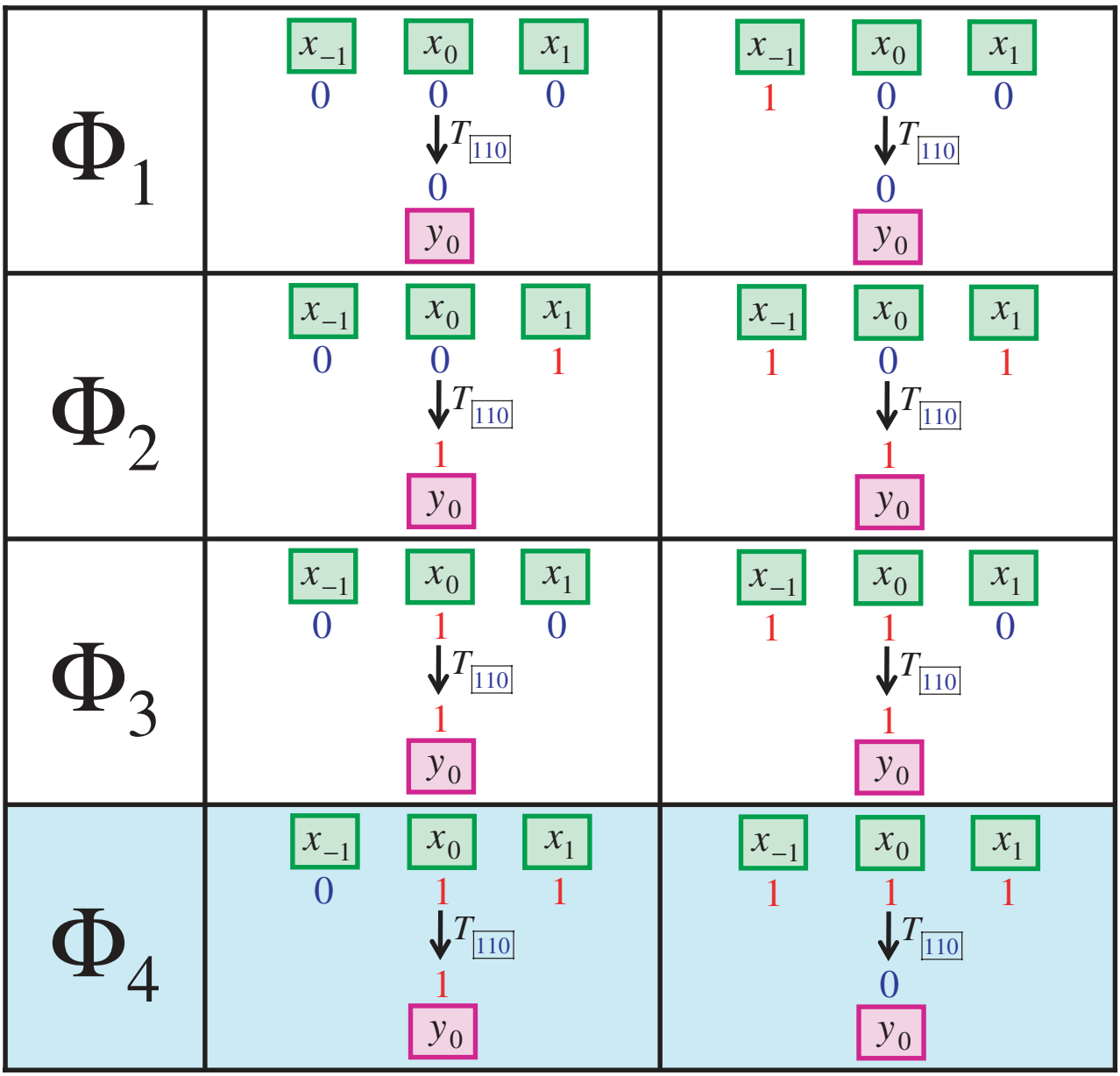
Φ_1	$x_{-1}\,0$ $x_0\,0$ $x_1\,0$ $\downarrow T_{[4]}$ 0 y_0	$x_{-1}\,1$ $x_0\,0$ $x_1\,0$ $\downarrow T_{[4]}$ 0 y_0
Φ_2	$x_{-1}\,0$ $x_0\,0$ $x_1\,1$ $\downarrow T_{[4]}$ 0 y_0	$x_{-1}\,1$ $x_0\,0$ $x_1\,1$ $\downarrow T_{[4]}$ 0 y_0
Φ_3	$x_{-1}\,0$ $x_0\,1$ $x_1\,0$ $\downarrow T_{[4]}$ 1 y_0	$x_{-1}\,1$ $x_0\,1$ $x_1\,0$ $\downarrow T_{[4]}$ 0 y_0
Φ_4	$x_{-1}\,0$ $x_0\,1$ $x_1\,1$ $\downarrow T_{[4]}$ 0 y_0	$x_{-1}\,1$ $x_0\,1$ $x_1\,1$ $\downarrow T_{[4]}$ 0 y_0

(c)

Fig. 33. Predicting stratification for rule [4]. (a) Boolean cube for [4]. (b) Firing patterns for [4]. (c) Stratification determination data.



(a) (b)



(c)

Fig. 34. Predicting stratification for rule 110. (a) Boolean cube for 110. (b) Firing patterns for 110. (c) Stratification determination data.

Observe that no two members of the stratified family "0" have identical four-bit binary patterns. Since there are only 16 distinct combinations of four binary bits, the stratified family "0" had already consumed all of them and it is clear that the remaining rules in Table 5 must consist of repetitions of these patterns. A careful analysis of the next 16 rules reveals, however, that the four-bit binary patterns of the next 16 rules $\{16, 17, \ldots, 31\}$ are mere *permutations* of the stratified family "0", as illustrated below (henceforth called stratified family "1"):

Stratified Family "1"

N	ψ	Φ_1	Φ_2	Φ_3	Φ_4	Equivalent Decimal Number
16	ψ_0	1	0	0	0	1
17	ψ_1	0	0	0	0	0
18	ψ_2	1	1	0	0	3
19	ψ_3	0	1	0	0	2
20	ψ_4	1	0	1	0	5
21	ψ_5	0	0	1	0	4
22	ψ_6	1	1	1	0	7
23	ψ_7	0	1	1	0	6
24	ψ_8	1	0	0	1	9
25	ψ_9	0	0	0	1	8
26	ψ_{10}	1	1	0	1	11
27	ψ_{11}	0	1	0	1	10
28	ψ_{12}	1	0	1	1	13
29	ψ_{13}	0	0	1	1	12
30	ψ_{14}	1	1	1	1	15
31	ψ_{15}	0	1	1	1	14

Observe that the 4-bit code $\psi = \{\Phi_1, \Phi_2, \Phi_3, \Phi_4\}$ of stratified family "1" and stratified family "0" are related by a 16×16 permutation matrix; namely,

$$\begin{bmatrix} \psi_0(1) \\ \psi_1(1) \\ \psi_2(1) \\ \psi_3(1) \\ \psi_4(1) \\ \psi_5(1) \\ \psi_6(1) \\ \psi_7(1) \\ \psi_8(1) \\ \psi_9(1) \\ \psi_{10}(1) \\ \psi_{11}(1) \\ \psi_{12}(1) \\ \psi_{13}(1) \\ \psi_{14}(1) \\ \psi_{15}(1) \end{bmatrix} = \underbrace{\begin{bmatrix} 0 & 1 & 0 & 0 & 0 & 0 & 0 & 0 & 0 & 0 & 0 & 0 & 0 & 0 & 0 & 0 \\ 1 & 0 & 0 & 0 & 0 & 0 & 0 & 0 & 0 & 0 & 0 & 0 & 0 & 0 & 0 & 0 \\ 0 & 0 & 0 & 1 & 0 & 0 & 0 & 0 & 0 & 0 & 0 & 0 & 0 & 0 & 0 & 0 \\ 0 & 0 & 1 & 0 & 0 & 0 & 0 & 0 & 0 & 0 & 0 & 0 & 0 & 0 & 0 & 0 \\ 0 & 0 & 0 & 0 & 0 & 1 & 0 & 0 & 0 & 0 & 0 & 0 & 0 & 0 & 0 & 0 \\ 0 & 0 & 0 & 0 & 1 & 0 & 0 & 0 & 0 & 0 & 0 & 0 & 0 & 0 & 0 & 0 \\ 0 & 0 & 0 & 0 & 0 & 0 & 0 & 1 & 0 & 0 & 0 & 0 & 0 & 0 & 0 & 0 \\ 0 & 0 & 0 & 0 & 0 & 0 & 1 & 0 & 0 & 0 & 0 & 0 & 0 & 0 & 0 & 0 \\ 0 & 0 & 0 & 0 & 0 & 0 & 0 & 0 & 0 & 1 & 0 & 0 & 0 & 0 & 0 & 0 \\ 0 & 0 & 0 & 0 & 0 & 0 & 0 & 0 & 1 & 0 & 0 & 0 & 0 & 0 & 0 & 0 \\ 0 & 0 & 0 & 0 & 0 & 0 & 0 & 0 & 0 & 0 & 0 & 1 & 0 & 0 & 0 & 0 \\ 0 & 0 & 0 & 0 & 0 & 0 & 0 & 0 & 0 & 0 & 1 & 0 & 0 & 0 & 0 & 0 \\ 0 & 0 & 0 & 0 & 0 & 0 & 0 & 0 & 0 & 0 & 0 & 0 & 0 & 1 & 0 & 0 \\ 0 & 0 & 0 & 0 & 0 & 0 & 0 & 0 & 0 & 0 & 0 & 0 & 1 & 0 & 0 & 0 \\ 0 & 0 & 0 & 0 & 0 & 0 & 0 & 0 & 0 & 0 & 0 & 0 & 0 & 0 & 0 & 1 \\ 0 & 0 & 0 & 0 & 0 & 0 & 0 & 0 & 0 & 0 & 0 & 0 & 0 & 0 & 1 & 0 \end{bmatrix}}_{\mathbf{M}_{1,0}} \begin{bmatrix} \psi_0(0) \\ \psi_1(0) \\ \psi_2(0) \\ \psi_3(0) \\ \psi_4(0) \\ \psi_5(0) \\ \psi_6(0) \\ \psi_7(0) \\ \psi_8(0) \\ \psi_9(0) \\ \psi_{10}(0) \\ \psi_{11}(0) \\ \psi_{12}(0) \\ \psi_{13}(0) \\ \psi_{14}(0) \\ \psi_{15}(0) \end{bmatrix}$$

It turns out that the remaining rules can be partitioned in a similar way into a stratified family "2", "3", . . . , "15". Together, these 16 families correspond exactly to the 16 rules listed in the 16 pages of Table 1, respectively. Let us summarize this remarkable organization as follows:

Property 4.2. *The 16 rules listed in each of the 16 pages of Table 1 form a stratified family whose four-bit binary patterns* $\psi(k)$, $k = 0, 1, 2, \ldots, 15$, *are related to each other by a* 16×16 *permutation matrix*

$$\boldsymbol{\psi}(k) = \mathbf{M}_{k,l}\,\boldsymbol{\psi}(l)$$

Table 6 lists 16 matrices which transform $\boldsymbol{\psi}(0)$ from stratified family "0" into $\boldsymbol{\psi}(k)$ of stratified family "k", $k = 0, 1, 2, \ldots, 15$.

The four-bit binary patterns of the last eight rules of each stratified family "k" can be obtained by copying the four-bit binary patterns of the first eight rules and then complementing the fourth bit corresponding to Φ_4. Observe that, in Table 5, the four color codes of all Φ_i's of each local rule $\boxed{N}$ is equivalent to the vertically-switched color codes of all Φ_i's of the corresponding local rule $\boxed{255 - N}$ as illustrated below:



For example, the color code of each Φ_i of $\boxed{0}$, $\boxed{24}$, $\boxed{120}$ and $\boxed{220}$ in Table 5 can be obtained by switching vertically the color code of the corresponding Φ_i of $\boxed{255}$, $\boxed{231}$, $\boxed{135}$ and $\boxed{35}$, respectively.

4.2. *Rules having no fractal stratifications*

Since the occurrence of two-level stratifications comes from the term $b_1 x_{-1}$ [$i = 0$ in Eq. (7)] in Table 1, it follows that no such stratification can occur in $\boldsymbol{\chi}^1_{\boxed{N}}$ if $b_1 = 0$ for rule $\boxed{N}$. An examination of Table 2 shows that there are only 16 rules with $b_1 = 0$. These 16 x_I-insensitive rules are listed in Table 7. Observe that these 16 rules can be generated from the following formula:

$$\boxed{N} = \boxed{17\,\beta}, \quad \beta = 0, 1, 2, \ldots, 15$$

This relationship can be derived from Table 6. In particular, since the right-most bit x_I-insensitive rules corresponds to $\psi_i = \{\Phi_1, \Phi_2, \Phi_3, \Phi_4\} = \{0, 0, 0, 0\}$, it follows from Tables 1 and 6 that $\psi_i = \{0, 0, 0, 0\}$ is repeated after integer multiplies of 17, and hence all x_I-insensitive rules $\boxed{N}$ must satisfy $N = 17k$, $k = 0, 1, 2, \ldots, 15$.

These 16 rules are composed of the corresponding $(k+1)$th members in the stratified family "k", $k = 0, 1, 2, \ldots, 15$. For example, $\boxed{0}$ is the first member of the stratified family "0", $\boxed{17}$ is the second member of the stratified family "1", . . . , and $\boxed{225}$ is the sixteenth member of the stratified family "15".

Property 4.3. *The following 16 characteristic functions have no stratifications*:

Single-Level Fractals

$$\boldsymbol{\chi}^1_{\boxed{0}},\ \boldsymbol{\chi}^1_{\boxed{17}},\ \boldsymbol{\chi}^1_{\boxed{34}},\ \boldsymbol{\chi}^1_{\boxed{51}},\ \boldsymbol{\chi}^1_{\boxed{68}},\ \boldsymbol{\chi}^1_{\boxed{85}},\ \boldsymbol{\chi}^1_{\boxed{102}},\ \boldsymbol{\chi}^1_{\boxed{119}},$$
$$\boldsymbol{\chi}^1_{\boxed{136}},\ \boldsymbol{\chi}^1_{\boxed{153}},\ \boldsymbol{\chi}^1_{\boxed{170}},\ \boldsymbol{\chi}^1_{\boxed{187}},\ \boldsymbol{\chi}^1_{\boxed{204}},\ \boldsymbol{\chi}^1_{\boxed{221}},\ \boldsymbol{\chi}^1_{\boxed{238}},\ \text{and}\ \boldsymbol{\chi}^1_{\boxed{255}}$$

4.3. *Origin of the fractal structures*

We will now uncover a basic mechanism responsible for the presence of fractals in the characteristic functions shown in Table 2. Let us examine an infinitesimally small neighborhood of the origin of $\boldsymbol{\chi}^1_{\boxed{N}}$ by considering the input string

$$\left\{\underbrace{0, 0, \ldots, 0}_{\text{first } k \text{ entries}}, x_k, x_{k+1}, \ldots, x_I\right\} \mapsto \phi$$
$$= \sum_{i=0}^{I} 2^{-(i+1)} x_i \qquad (21)$$

If we multiply ϕ by 2^k in Eq. (21), we would obtain

$$\phi \bullet 2^k = \sum_{i=k}^{I} 2^{-(i+1)+k} x_i = \sum_{j=0}^{I-k} 2^{-(j+1)} x_j \qquad (22)$$

where $j \triangleq (i-k)$. Observe that, as $I \to \infty$, Eq. (22) converges to the binary string in Eq. (15). It follows that no matter how close the binary string in Eq. (21) is to the origin, we can always rescale it to recover the original string in Eq. (15). Moreover, except possibly for the $(k+1)$th term $x_k = 1$, all other terms $x_{k+1}, x_{k+2}, \ldots, x_I$ in Eq. (21) will

Table 6. List of 16 permutation matrices $\mathbf{M}_{k,l}$ which transform $\boldsymbol{\psi}(0)$ from stratified family "0" into $\boldsymbol{\psi}(k)$ of stratified family "k", $k = 0, 1, 2, \ldots, 15$.

$$M_{0,0} = \begin{bmatrix}
1&0&0&0&0&0&0&0&0&0&0&0&0&0&0&0\\
0&1&0&0&0&0&0&0&0&0&0&0&0&0&0&0\\
0&0&1&0&0&0&0&0&0&0&0&0&0&0&0&0\\
0&0&0&1&0&0&0&0&0&0&0&0&0&0&0&0\\
0&0&0&0&1&0&0&0&0&0&0&0&0&0&0&0\\
0&0&0&0&0&1&0&0&0&0&0&0&0&0&0&0\\
0&0&0&0&0&0&1&0&0&0&0&0&0&0&0&0\\
0&0&0&0&0&0&0&1&0&0&0&0&0&0&0&0\\
0&0&0&0&0&0&0&0&1&0&0&0&0&0&0&0\\
0&0&0&0&0&0&0&0&0&1&0&0&0&0&0&0\\
0&0&0&0&0&0&0&0&0&0&1&0&0&0&0&0\\
0&0&0&0&0&0&0&0&0&0&0&1&0&0&0&0\\
0&0&0&0&0&0&0&0&0&0&0&0&1&0&0&0\\
0&0&0&0&0&0&0&0&0&0&0&0&0&1&0&0\\
0&0&0&0&0&0&0&0&0&0&0&0&0&0&1&0\\
0&0&0&0&0&0&0&0&0&0&0&0&0&0&0&1
\end{bmatrix}$$

$$M_{1,0} = \begin{bmatrix}
0&1&0&0&0&0&0&0&0&0&0&0&0&0&0&0\\
1&0&0&0&0&0&0&0&0&0&0&0&0&0&0&0\\
0&0&0&1&0&0&0&0&0&0&0&0&0&0&0&0\\
0&0&1&0&0&0&0&0&0&0&0&0&0&0&0&0\\
0&0&0&0&0&1&0&0&0&0&0&0&0&0&0&0\\
0&0&0&0&1&0&0&0&0&0&0&0&0&0&0&0\\
0&0&0&0&0&0&0&1&0&0&0&0&0&0&0&0\\
0&0&0&0&0&0&1&0&0&0&0&0&0&0&0&0\\
0&0&0&0&0&0&0&0&0&1&0&0&0&0&0&0\\
0&0&0&0&0&0&0&0&1&0&0&0&0&0&0&0\\
0&0&0&0&0&0&0&0&0&0&0&1&0&0&0&0\\
0&0&0&0&0&0&0&0&0&0&1&0&0&0&0&0\\
0&0&0&0&0&0&0&0&0&0&0&0&1&0&0&0\\
0&0&0&0&0&0&0&0&0&0&0&0&0&1&0&0\\
0&0&0&0&0&0&0&0&0&0&0&0&0&0&0&1\\
0&0&0&0&0&0&0&0&0&0&0&0&0&0&1&0
\end{bmatrix}$$

$$M_{2,0} = \begin{bmatrix}
0&0&1&0&0&0&0&0&0&0&0&0&0&0&0&0\\
0&0&0&1&0&0&0&0&0&0&0&0&0&0&0&0\\
1&0&0&0&0&0&0&0&0&0&0&0&0&0&0&0\\
0&1&0&0&0&0&0&0&0&0&0&0&0&0&0&0\\
0&0&0&0&0&0&1&0&0&0&0&0&0&0&0&0\\
0&0&0&0&0&0&0&1&0&0&0&0&0&0&0&0\\
0&0&0&0&1&0&0&0&0&0&0&0&0&0&0&0\\
0&0&0&0&0&1&0&0&0&0&0&0&0&0&0&0\\
0&0&0&0&0&0&0&0&0&0&1&0&0&0&0&0\\
0&0&0&0&0&0&0&0&0&0&0&1&0&0&0&0\\
0&0&0&0&0&0&0&0&1&0&0&0&0&0&0&0\\
0&0&0&0&0&0&0&0&0&1&0&0&0&0&0&0\\
0&0&0&0&0&0&0&0&0&0&0&0&0&0&1&0\\
0&0&0&0&0&0&0&0&0&0&0&0&0&0&0&1\\
0&0&0&0&0&0&0&0&0&0&0&0&1&0&0&0\\
0&0&0&0&0&0&0&0&0&0&0&0&0&1&0&0
\end{bmatrix}$$

$$M_{3,0} = \begin{bmatrix}
0&0&0&1&0&0&0&0&0&0&0&0&0&0&0&0\\
0&0&1&0&0&0&0&0&0&0&0&0&0&0&0&0\\
0&1&0&0&0&0&0&0&0&0&0&0&0&0&0&0\\
1&0&0&0&0&0&0&0&0&0&0&0&0&0&0&0\\
0&0&0&0&0&0&0&1&0&0&0&0&0&0&0&0\\
0&0&0&0&0&0&1&0&0&0&0&0&0&0&0&0\\
0&0&0&0&0&1&0&0&0&0&0&0&0&0&0&0\\
0&0&0&0&1&0&0&0&0&0&0&0&0&0&0&0\\
0&0&0&0&0&0&0&0&0&0&0&1&0&0&0&0\\
0&0&0&0&0&0&0&0&0&0&1&0&0&0&0&0\\
0&0&0&0&0&0&0&0&0&1&0&0&0&0&0&0\\
0&0&0&0&0&0&0&0&1&0&0&0&0&0&0&0\\
0&0&0&0&0&0&0&0&0&0&0&0&0&0&0&1\\
0&0&0&0&0&0&0&0&0&0&0&0&0&0&1&0\\
0&0&0&0&0&0&0&0&0&0&0&0&0&1&0&0\\
0&0&0&0&0&0&0&0&0&0&0&0&1&0&0&0
\end{bmatrix}$$

$$M_{4,0} = \begin{bmatrix}
0&0&0&0&1&0&0&0&0&0&0&0&0&0&0&0\\
0&0&0&0&0&1&0&0&0&0&0&0&0&0&0&0\\
0&0&0&0&0&0&1&0&0&0&0&0&0&0&0&0\\
0&0&0&0&0&0&0&1&0&0&0&0&0&0&0&0\\
1&0&0&0&0&0&0&0&0&0&0&0&0&0&0&0\\
0&1&0&0&0&0&0&0&0&0&0&0&0&0&0&0\\
0&0&1&0&0&0&0&0&0&0&0&0&0&0&0&0\\
0&0&0&1&0&0&0&0&0&0&0&0&0&0&0&0\\
0&0&0&0&0&0&0&0&0&0&0&0&1&0&0&0\\
0&0&0&0&0&0&0&0&0&0&0&0&0&1&0&0\\
0&0&0&0&0&0&0&0&0&0&0&0&0&0&1&0\\
0&0&0&0&0&0&0&0&0&0&0&0&0&0&0&1\\
0&0&0&0&0&0&0&0&1&0&0&0&0&0&0&0\\
0&0&0&0&0&0&0&0&0&1&0&0&0&0&0&0\\
0&0&0&0&0&0&0&0&0&0&1&0&0&0&0&0\\
0&0&0&0&0&0&0&0&0&0&0&1&0&0&0&0
\end{bmatrix}$$

$$M_{5,0} = \begin{bmatrix}
0&0&0&0&0&1&0&0&0&0&0&0&0&0&0&0\\
0&0&0&0&1&0&0&0&0&0&0&0&0&0&0&0\\
0&0&0&0&0&0&0&1&0&0&0&0&0&0&0&0\\
0&0&0&0&0&0&1&0&0&0&0&0&0&0&0&0\\
0&1&0&0&0&0&0&0&0&0&0&0&0&0&0&0\\
1&0&0&0&0&0&0&0&0&0&0&0&0&0&0&0\\
0&0&0&1&0&0&0&0&0&0&0&0&0&0&0&0\\
0&0&1&0&0&0&0&0&0&0&0&0&0&0&0&0\\
0&0&0&0&0&0&0&0&0&0&0&0&1&0&0&0\\
0&0&0&0&0&0&0&0&0&0&0&0&0&1&0&0\\
0&0&0&0&0&0&0&0&0&0&0&0&0&0&0&1\\
0&0&0&0&0&0&0&0&0&0&0&0&0&0&1&0\\
0&0&0&0&0&0&0&0&0&0&1&0&0&0&0&0\\
0&0&0&0&0&0&0&0&0&0&0&1&0&0&0&0\\
0&0&0&0&0&0&0&0&0&0&0&0&1&0&0&0\\
0&0&0&0&0&0&0&0&0&0&0&0&0&1&0&0
\end{bmatrix}$$

$$M_{6,0} = \begin{bmatrix}
0&0&0&0&0&0&1&0&0&0&0&0&0&0&0&0\\
0&0&0&0&0&0&0&1&0&0&0&0&0&0&0&0\\
0&0&0&0&0&1&0&0&0&0&0&0&0&0&0&0\\
0&0&0&0&0&0&1&0&0&0&0&0&0&0&0&0\\
0&0&1&0&0&0&0&0&0&0&0&0&0&0&0&0\\
0&0&0&1&0&0&0&0&0&0&0&0&0&0&0&0\\
1&0&0&0&0&0&0&0&0&0&0&0&0&0&0&0\\
0&1&0&0&0&0&0&0&0&0&0&0&0&0&0&0\\
0&0&0&0&0&0&0&0&0&0&0&0&0&0&1&0\\
0&0&0&0&0&0&0&0&0&0&0&0&0&0&0&1\\
0&0&0&0&0&0&0&0&0&0&0&0&1&0&0&0\\
0&0&0&0&0&0&0&0&0&0&0&0&0&1&0&0\\
0&0&0&0&0&0&0&0&0&0&1&0&0&0&0&0\\
0&0&0&0&0&0&0&0&0&0&0&1&0&0&0&0\\
0&0&0&0&0&0&0&0&1&0&0&0&0&0&0&0\\
0&0&0&0&0&0&0&0&0&1&0&0&0&0&0&0
\end{bmatrix}$$

$$M_{7,0} = \begin{bmatrix}
0&0&0&0&0&0&0&1&0&0&0&0&0&0&0&0\\
0&0&0&0&0&0&1&0&0&0&0&0&0&0&0&0\\
0&0&0&0&0&0&0&1&0&0&0&0&0&0&0&0\\
0&0&0&0&0&1&0&0&0&0&0&0&0&0&0&0\\
0&0&0&0&1&0&0&0&0&0&0&0&0&0&0&0\\
0&0&1&0&0&0&0&0&0&0&0&0&0&0&0&0\\
0&1&0&0&0&0&0&0&0&0&0&0&0&0&0&0\\
1&0&0&0&0&0&0&0&0&0&0&0&0&0&0&0\\
0&0&0&0&0&0&0&0&0&0&0&0&0&0&0&1\\
0&0&0&0&0&0&0&0&0&0&0&0&0&0&1&0\\
0&0&0&0&0&0&0&0&0&0&0&0&0&1&0&0\\
0&0&0&0&0&0&0&0&0&0&0&0&1&0&0&0\\
0&0&0&0&0&0&0&0&0&0&0&1&0&0&0&0\\
0&0&0&0&0&0&0&0&0&0&1&0&0&0&0&0\\
0&0&0&0&0&0&0&0&0&1&0&0&0&0&0&0\\
0&0&0&0&0&0&0&0&1&0&0&0&0&0&0&0
\end{bmatrix}$$

Table 6. (*Continued*)

$$M_{8,0} = \begin{bmatrix}
0&0&0&0&0&0&0&0&1&0&0&0&0&0&0&0\\
0&0&0&0&0&0&0&0&0&1&0&0&0&0&0&0\\
0&0&0&0&0&0&0&0&0&0&1&0&0&0&0&0\\
0&0&0&0&0&0&0&0&0&0&0&1&0&0&0&0\\
0&0&0&0&0&0&0&0&0&0&0&0&1&0&0&0\\
0&0&0&0&0&0&0&0&0&0&0&0&0&1&0&0\\
0&0&0&0&0&0&0&0&0&0&0&0&0&0&1&0\\
0&0&0&0&0&0&0&0&0&0&0&0&0&0&0&1\\
1&0&0&0&0&0&0&0&0&0&0&0&0&0&0&0\\
0&1&0&0&0&0&0&0&0&0&0&0&0&0&0&0\\
0&0&1&0&0&0&0&0&0&0&0&0&0&0&0&0\\
0&0&0&1&0&0&0&0&0&0&0&0&0&0&0&0\\
0&0&0&0&1&0&0&0&0&0&0&0&0&0&0&0\\
0&0&0&0&0&1&0&0&0&0&0&0&0&0&0&0\\
0&0&0&0&0&0&1&0&0&0&0&0&0&0&0&0\\
0&0&0&0&0&0&0&1&0&0&0&0&0&0&0&0
\end{bmatrix}$$

$$M_{9,0} = \begin{bmatrix}
0&0&0&0&0&0&0&0&0&1&0&0&0&0&0&0\\
0&0&0&0&0&0&0&0&1&0&0&0&0&0&0&0\\
0&0&0&0&0&0&0&0&0&0&0&1&0&0&0&0\\
0&0&0&0&0&0&0&0&0&0&0&1&0&0&0&0\\
0&0&0&0&0&0&0&0&0&0&0&0&0&1&0&0\\
0&0&0&0&0&0&0&0&0&0&0&0&1&0&0&0\\
0&0&0&0&0&0&0&0&0&0&0&0&0&0&0&1\\
0&0&0&0&0&0&0&0&0&0&0&0&0&0&1&0\\
0&1&0&0&0&0&0&0&0&0&0&0&0&0&0&0\\
1&0&0&0&0&0&0&0&0&0&0&0&0&0&0&0\\
0&0&0&1&0&0&0&0&0&0&0&0&0&0&0&0\\
0&0&1&0&0&0&0&0&0&0&0&0&0&0&0&0\\
0&0&0&0&0&1&0&0&0&0&0&0&0&0&0&0\\
0&0&0&0&1&0&0&0&0&0&0&0&0&0&0&0\\
0&0&0&0&0&0&1&0&0&0&0&0&0&0&0&0\\
0&0&0&0&0&0&0&1&0&0&0&0&0&0&0&0
\end{bmatrix}$$

$$M_{10,0} = \begin{bmatrix}
0&0&0&0&0&0&0&0&0&0&1&0&0&0&0&0\\
0&0&0&0&0&0&0&0&0&0&0&1&0&0&0&0\\
0&0&0&0&0&0&0&0&0&1&0&0&0&0&0&0\\
0&0&0&0&0&0&0&0&0&0&1&0&0&0&0&0\\
0&0&0&0&0&0&0&0&0&0&0&0&0&0&1&0\\
0&0&0&0&0&0&0&0&0&0&0&0&0&0&0&1\\
0&0&0&0&0&0&0&0&0&0&0&0&1&0&0&0\\
0&0&0&0&0&0&0&0&0&0&0&0&0&1&0&0\\
0&0&1&0&0&0&0&0&0&0&0&0&0&0&0&0\\
0&0&0&1&0&0&0&0&0&0&0&0&0&0&0&0\\
1&0&0&0&0&0&0&0&0&0&0&0&0&0&0&0\\
0&1&0&0&0&0&0&0&0&0&0&0&0&0&0&0\\
0&0&0&0&0&0&1&0&0&0&0&0&0&0&0&0\\
0&0&0&0&0&0&0&1&0&0&0&0&0&0&0&0\\
0&0&0&0&1&0&0&0&0&0&0&0&0&0&0&0\\
0&0&0&0&0&1&0&0&0&0&0&0&0&0&0&0
\end{bmatrix}$$

$$M_{11,0} = \begin{bmatrix}
0&0&0&0&0&0&0&0&0&0&0&1&0&0&0&0\\
0&0&0&0&0&0&0&0&0&0&0&1&0&0&0&0\\
0&0&0&0&0&0&0&0&0&0&1&0&0&0&0&0\\
0&0&0&0&0&0&0&0&0&1&0&0&0&0&0&0\\
0&0&0&0&0&0&0&0&0&0&0&0&0&0&0&1\\
0&0&0&0&0&0&0&0&0&0&0&0&0&0&1&0\\
0&0&0&0&0&0&0&0&0&0&0&0&0&1&0&0\\
0&0&0&0&0&0&0&0&0&0&0&0&1&0&0&0\\
0&0&0&1&0&0&0&0&0&0&0&0&0&0&0&0\\
0&0&1&0&0&0&0&0&0&0&0&0&0&0&0&0\\
0&1&0&0&0&0&0&0&0&0&0&0&0&0&0&0\\
1&0&0&0&0&0&0&0&0&0&0&0&0&0&0&0\\
0&0&0&0&0&0&0&1&0&0&0&0&0&0&0&0\\
0&0&0&0&0&0&1&0&0&0&0&0&0&0&0&0\\
0&0&0&0&0&1&0&0&0&0&0&0&0&0&0&0\\
0&0&0&0&1&0&0&0&0&0&0&0&0&0&0&0
\end{bmatrix}$$

$$M_{12,0} = \begin{bmatrix}
0&0&0&0&0&0&0&0&0&0&0&0&1&0&0&0\\
0&0&0&0&0&0&0&0&0&0&0&0&0&1&0&0\\
0&0&0&0&0&0&0&0&0&0&0&0&0&0&1&0\\
0&0&0&0&0&0&0&0&0&0&0&0&0&0&0&1\\
0&0&0&0&0&0&0&0&1&0&0&0&0&0&0&0\\
0&0&0&0&0&0&0&0&0&1&0&0&0&0&0&0\\
0&0&0&0&0&0&0&0&0&0&1&0&0&0&0&0\\
0&0&0&0&0&0&0&0&0&0&0&1&0&0&0&0\\
0&0&0&0&1&0&0&0&0&0&0&0&0&0&0&0\\
0&0&0&0&0&1&0&0&0&0&0&0&0&0&0&0\\
0&0&0&0&0&0&1&0&0&0&0&0&0&0&0&0\\
0&0&0&0&0&0&0&1&0&0&0&0&0&0&0&0\\
1&0&0&0&0&0&0&0&0&0&0&0&0&0&0&0\\
0&1&0&0&0&0&0&0&0&0&0&0&0&0&0&0\\
0&0&1&0&0&0&0&0&0&0&0&0&0&0&0&0\\
0&0&0&1&0&0&0&0&0&0&0&0&0&0&0&0
\end{bmatrix}$$

$$M_{13,0} = \begin{bmatrix}
0&0&0&0&0&0&0&0&0&0&0&0&0&1&0&0\\
0&0&0&0&0&0&0&0&0&0&0&0&0&0&1&0\\
0&0&0&0&0&0&0&0&0&0&0&0&0&0&0&1\\
0&0&0&0&0&0&0&0&0&0&0&0&0&0&1&0\\
0&0&0&0&0&0&0&0&0&0&0&1&0&0&0&0\\
0&0&0&0&0&0&0&0&0&0&0&0&1&0&0&0\\
0&0&0&0&0&0&0&0&0&0&0&0&0&1&0&0\\
0&0&0&0&0&0&0&0&0&0&0&0&1&0&0&0\\
0&0&0&0&0&0&1&0&0&0&0&0&0&0&0&0\\
0&0&0&0&0&1&0&0&0&0&0&0&0&0&0&0\\
0&0&0&0&0&0&0&1&0&0&0&0&0&0&0&0\\
0&0&0&0&0&0&0&0&1&0&0&0&0&0&0&0\\
0&1&0&0&0&0&0&0&0&0&0&0&0&0&0&0\\
1&0&0&0&0&0&0&0&0&0&0&0&0&0&0&0\\
0&0&0&1&0&0&0&0&0&0&0&0&0&0&0&0\\
0&0&1&0&0&0&0&0&0&0&0&0&0&0&0&0
\end{bmatrix}$$

$$M_{14,0} = \begin{bmatrix}
0&0&0&0&0&0&0&0&0&0&0&0&0&0&1&0\\
0&0&0&0&0&0&0&0&0&0&0&0&0&0&0&1\\
0&0&0&0&0&0&0&0&0&0&0&0&0&1&0&0\\
0&0&0&0&0&0&0&0&0&0&0&0&0&0&1&0\\
0&0&0&0&0&0&0&0&0&0&0&1&0&0&0&0\\
0&0&0&0&0&0&0&0&0&0&0&0&1&0&0&0\\
0&0&0&0&0&0&0&0&0&1&0&0&0&0&0&0\\
0&0&0&0&0&0&0&0&0&0&1&0&0&0&0&0\\
0&0&0&0&0&0&1&0&0&0&0&0&0&0&0&0\\
0&0&0&0&0&0&0&1&0&0&0&0&0&0&0&0\\
0&0&0&0&1&0&0&0&0&0&0&0&0&0&0&0\\
0&0&0&0&0&1&0&0&0&0&0&0&0&0&0&0\\
0&0&1&0&0&0&0&0&0&0&0&0&0&0&0&0\\
0&0&0&1&0&0&0&0&0&0&0&0&0&0&0&0\\
1&0&0&0&0&0&0&0&0&0&0&0&0&0&0&0\\
0&1&0&0&0&0&0&0&0&0&0&0&0&0&0&0
\end{bmatrix}$$

$$M_{15,0} = \begin{bmatrix}
0&0&0&0&0&0&0&0&0&0&0&0&0&0&0&1\\
0&0&0&0&0&0&0&0&0&0&0&0&0&0&1&0\\
0&0&0&0&0&0&0&0&0&0&0&0&0&1&0&0\\
0&0&0&0&0&0&0&0&0&0&0&0&1&0&0&0\\
0&0&0&0&0&0&0&0&0&0&0&1&0&0&0&0\\
0&0&0&0&0&0&0&0&0&0&1&0&0&0&0&0\\
0&0&0&0&0&0&0&0&0&1&0&0&0&0&0&0\\
0&0&0&0&0&0&0&0&1&0&0&0&0&0&0&0\\
0&0&0&0&0&0&0&1&0&0&0&0&0&0&0&0\\
0&0&0&0&0&0&1&0&0&0&0&0&0&0&0&0\\
0&0&0&0&0&1&0&0&0&0&0&0&0&0&0&0\\
0&0&0&0&1&0&0&0&0&0&0&0&0&0&0&0\\
0&0&0&1&0&0&0&0&0&0&0&0&0&0&0&0\\
0&0&1&0&0&0&0&0&0&0&0&0&0&0&0&0\\
0&1&0&0&0&0&0&0&0&0&0&0&0&0&0&0\\
1&0&0&0&0&0&0&0&0&0&0&0&0&0&0&0
\end{bmatrix}$$

Table 7. List of 16 right-most bit x_I-insensitive local rules.

0	17	34	51
68	85	102	119
136	153	170	187
204	221	238	255

generate the same corresponding output binary bit y_i, $i = k+1, k+2, \ldots, I$, because the same local rule $\boxed{N}$ is used. Hence, by rescaling $\chi^1_{\boxed{N}}$ accordingly, we can recover the corresponding original graph. To determine the appropriate scaling factor, it is necessary to examine the output binary bit y_i, $i = 0, 1, 2, \ldots, k-1$ because it may *not* be zero for two reasons:

(i) $y_{k-1} = 1$ if

$$(x_{k-2}, x_{k-1}, x_k) = (0,0,1) \overset{T_{\boxed{N}}}{\longmapsto} 1 \tag{23}$$

In other words, if is a *firing pattern* [Chua *et al.*, 2003] of Rule $\boxed{N}$, or equivalently, if vertex ① in the Boolean cube in Fig. 1(e) is painted in *red* color.

(ii) $y_i = 1$ if

$$(x_{i-1}, x_i, x_{i+1}) = (0,0,0) \overset{T_{\boxed{N}}}{\longmapsto} 1 \tag{24}$$

for $i = 0, 1, 2, \ldots, k-2$. In other words, if is a *firing pattern* of Rule $\boxed{N}$, or equivalently, if vertex ⓪ in the Boolean cube in Fig. 1(e) is painted in *red* color. Let us examine now the consequences of the occurrence of one or both of these two cases. There are four possible scenarios:

Scenario 1. $(0,0,0)$ *is not a firing pattern*[3] *but* $(0,0,1)$ *is a firing pattern of* $\boxed{N}$, *and* $x_I = 0$.

An example satisfying scenario 1 is Rule $\boxed{2}$, where vertex ⓪ is *blue* but vertex ① is *red*. In this case, $y_{k-1} = 1$ and the output binary pattern has the form

$$\left\{\underbrace{0,0,\ldots,0,y_{k-1}}_{\text{first } k \text{ terms}}, y_k, y_{k+1}, \ldots, y_I\right\} \mapsto \chi^1_{\boxed{N}}$$
$$= \sum_{i=k-1}^{I} 2^{-(i+1)} y_i \tag{25}$$

Multiplying the right side of Eq. (25) by $2^{(k-1)}$ we obtain

$$\chi^1_{\boxed{N}}(2^{k-1}) = \sum_{i=k-1}^{I} 2^{-(i+1)+(k-1)} y_i$$
$$= \sum_{j=0}^{I-k+1} 2^{-(j+1)} y_j$$
$$= \sum_{i=0}^{I} 2^{-(i+1)} y_i, \quad \text{as } I \to \infty \tag{26}$$

Hence, by multiplying the output string in Eq. (25) by the factor $2^{(k-1)}$, we obtain Eq. (26), which is identical to Eq. (18) as $I \to \infty$. In other words, in *Scenario 1*, the characteristic function $\chi^1_{\boxed{N}}$ arbitrarily near the origin can be rescaled to obtain the corresponding original graph by multiplying $\phi_{\boxed{N}}$ by 2^k and $\chi^1_{\boxed{N}}$ by $2^{(k-1)}$.

Scenario 2. $(0,0,0)$ *is not a firing pattern but* $(1,0,0)$ *is a firing pattern of* $\boxed{N}$, *and* $x_I = 1$ *with* $b_1 \neq 0$.

In this case, $y_0 = 1$ in view of Eq. (19), and the output binary string assumes the form:

$$\{1,0,0,\ldots,0,y_{k-1},y_k,y_{k+1},\ldots,y_I\}$$
$$\mapsto \frac{1}{2} + \sum_{i=k-1}^{I} 2^{-(i+1)} y_i \tag{27}$$

It follows from Eq. (27) that

$$\tilde{\chi}^1_{\boxed{N}} \triangleq \chi^1_{\boxed{N}} - \frac{1}{2} = \sum_{i=k-1}^{I} 2^{-(i+1)} y_i$$
$$= \sum_{i=0}^{I} 2^{-(i+1)} y_i, \quad \text{as } I \to \infty \tag{28}$$

as in Eq. (26). Hence, apart from a translation by $\Delta\chi^1_{\boxed{N}} = 1/2$, the infinitesimal pattern near the origin can be rescaled to coincide with the corresponding original pattern.

[3] An examination of the Boolean cubes in Table 1 of [Chua *et al.*, 2003] shows $(0,0,0)$ is *not* a firing pattern for rules with an even number: i.e. $N = 2n$, $n = 0, 1, 2, \ldots, 128$.

Scenario 3. $(0,0,0)$ *is a firing pattern of* $\boxed{N}$, *and* $x_I = 0$.

In this case, y_i, $i = 0, 1, 2, \ldots, k-2$; namely,

$$\left\{ \underbrace{1, 1, \ldots, 1,}_{\text{first } k-1 \text{ terms}} \; y_{k-1}, y_k, y_{k+1}, \ldots, y_I \right\} \mapsto \boldsymbol{\chi}^1_{\boxed{N}} \quad (29)$$

where

$$\begin{aligned} \boldsymbol{\chi}^1_{\boxed{N}} &= \sum_{i=0}^{k-2} 2^{-(i+1)} + \sum_{i=k-1}^{I} 2^{-(i+1)} y_i \\ &= 1 - 2^{-(k-1)} + \sum_{i=k-1}^{I} 2^{-(i+1)} y_i \end{aligned} \quad (30)$$

It follows from Eq. (30) that

$$\tilde{\boldsymbol{\chi}}^1_{\boxed{N}} \triangleq 1 - \boldsymbol{\chi}^1_{\boxed{N}} = 2^{-(k-1)} - \sum_{i=k-1}^{I} 2^{-(i+1)} y_i \quad (31)$$

Multiplying both sides of Eq. (31) by the scaling factor $2^{(k-1)}$, we obtain

$$\begin{aligned} \tilde{\boldsymbol{\chi}}^1_{\boxed{N}} \bullet 2^{(k-1)} &= 1 - \sum_{i=k-1}^{I} 2^{-(i+1)+(k-1)} y_i \\ &= 1 - \sum_{i=0}^{I} 2^{-(i+1)} y_i, \quad \text{as } I \to \infty \end{aligned} \quad (32)$$

as in Eq. (26).

Since Eq. (32) is an affine transformation of Eq. (26), it follows that the fractal pattern arbitrarily near the origin is preserved upon scaling, apart from an *affine* transformation.

Scenario 4. $(0,0,0)$ *is a firing pattern of* $\boxed{N}$, *but* $(1,0,0)$ *is not a firing pattern of* $\boxed{N}$, *and* $x_I = 1$ *with* $b_1 \neq 0$.

In this case, $y_0 = 0$, in view of Eq. (18); namely,

$$\left\{ \underbrace{0, 1, 1, \ldots, 1, y_{k-1}}_{\text{first } k \text{ terms}}, y_k, y_{k+1}, \ldots, y_I \right\} \mapsto \boldsymbol{\chi}^1_{\boxed{N}} \quad (33)$$

where

$$\begin{aligned} \boldsymbol{\chi}^1_{\boxed{N}} &= \sum_{i=1}^{I} 2^{-(i+1)} y_i \\ &= \sum_{i=1}^{k-2} 2^{-(i+1)} + \sum_{i=k-1}^{I} 2^{-(i+1)} y_i \\ &= \frac{1}{2} - 2^{-(k-1)} + \sum_{i=k-1}^{I} 2^{-(i+1)} y_i \end{aligned} \quad (34)$$

It follows from Eq. (34) that

$$\begin{aligned} \tilde{\boldsymbol{\chi}}^1_{\boxed{N}} &\triangleq \left(1 - \boldsymbol{\chi}^1_{\boxed{N}}\right) - \frac{1}{2} \\ &= 2^{-(k-1)} - \sum_{i=k-1}^{I} 2^{-(i+1)} y_i \\ &= 2^{-(k-1)} - \sum_{i=0}^{I} 2^{-(i+1)} y_i, \quad \text{as } I \to \infty \end{aligned} \quad (35)$$

as in Eq. (26).

Since Eq. (34) is an affine transformation of Eq. (26), it follows that the fractal pattern arbitrarily near the origin is preserved upon scaling, apart from an *affine* transformation.

5. Gardens of Eden

A cursory inspection of the graphs of the characteristic functions $\boldsymbol{\chi}^1_{\boxed{N}}$ displayed in Table 2 reveals that most of these graphs exhibit a *discontinuous* jump over a finite range $\Delta\boldsymbol{\chi}^1_{\boxed{N}} = \boldsymbol{\chi}^1_{\boxed{N}}(\phi^+_{\text{jump}}) - \boldsymbol{\chi}^1_{\boxed{N}}(\phi^-_{\text{jump}})$ at various discrete points $\phi_{\text{jump}} \in [0,1]$ where all points within the interval $(\boldsymbol{\chi}^1_{\boxed{N}}(\phi^+_{\text{jump}}), \boldsymbol{\chi}^1_{\boxed{N}}(\phi^-_{\text{jump}}))$ have *no preimage* under $\boldsymbol{\chi}^1_{\boxed{N}}$. Such a characteristic function is therefore not a *surjective* (onto) function. Points within such intervals are special cases of the following interesting class of initial bit-string configurations.

Definition 5.1. *Garden of Eden of* $\boxed{N}$. An $(I+1)$-bit binary string $\{x_0, x_1, x_2, \ldots, x_I\}$ is said to be a *garden of Eden* of a local rule $\boxed{N}$ *iff* it does *not* have a *predecessor* under the local rule transformation $T_{\boxed{N}}$.

It follows from Definition 5.1 that a *garden of Eden* $\phi_0 \triangleq \sum_{i=0}^{I} 2^{-(i+1)} x_i$ of $\boxed{N}$ can never occur as a point on an orbit of $\boxed{N}$ arising from some *initial* bit-string configuration whose decimal equivalent is different from ϕ_0. Hence, *a garden of Eden has no past, but only present and future.*[4]

[4]The name *garden of Eden* was first introduced by Moore in the context of von Neumann's *self-reproducing automata* [Moore, 1962].

Table 8. A compendium of all gardens of Eden (colored in *green*) over the range $[0, 1]$ of $\boldsymbol{\chi}^{1}_{\boxed{N}}$.

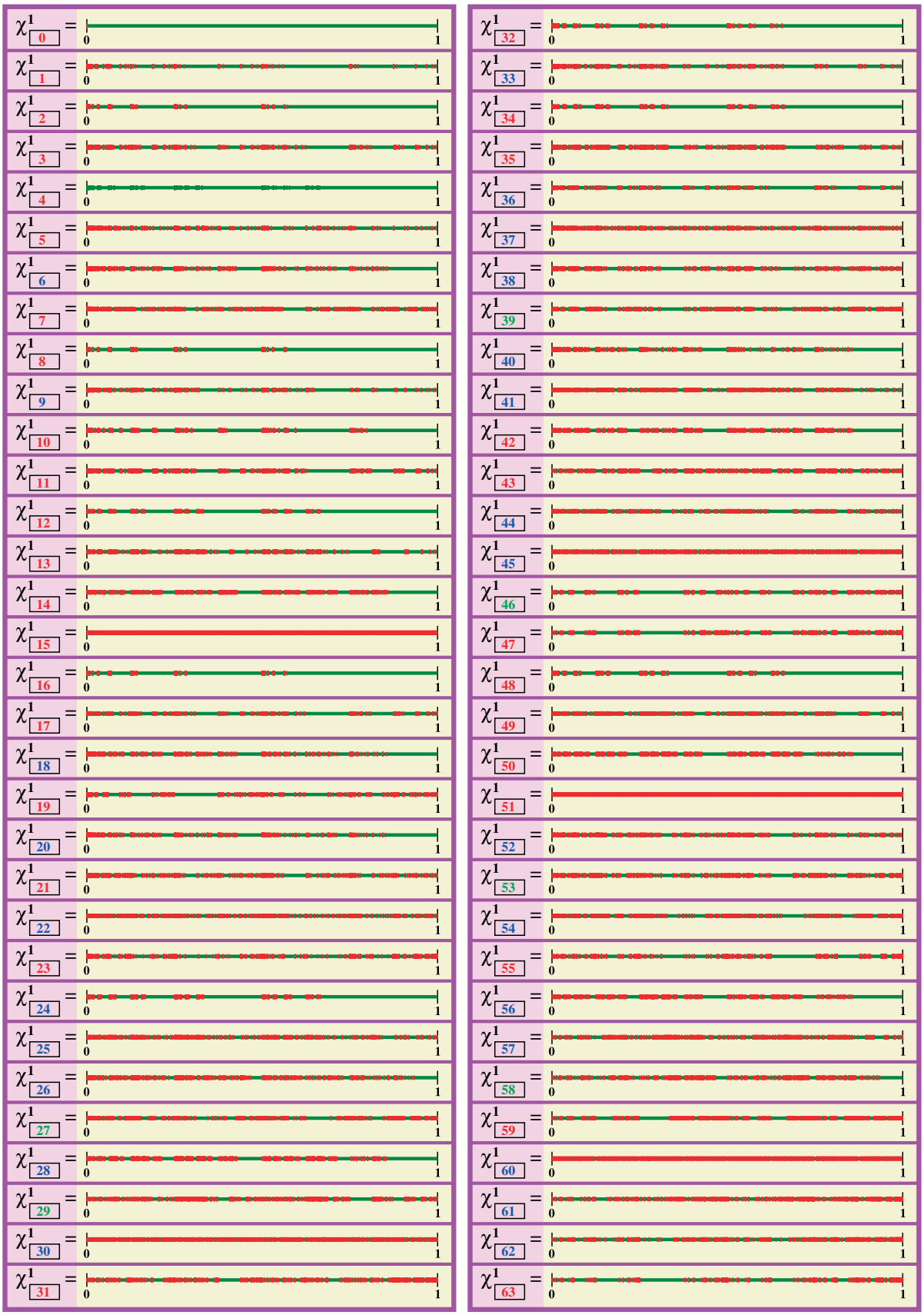


Table 8. (*Continued*)

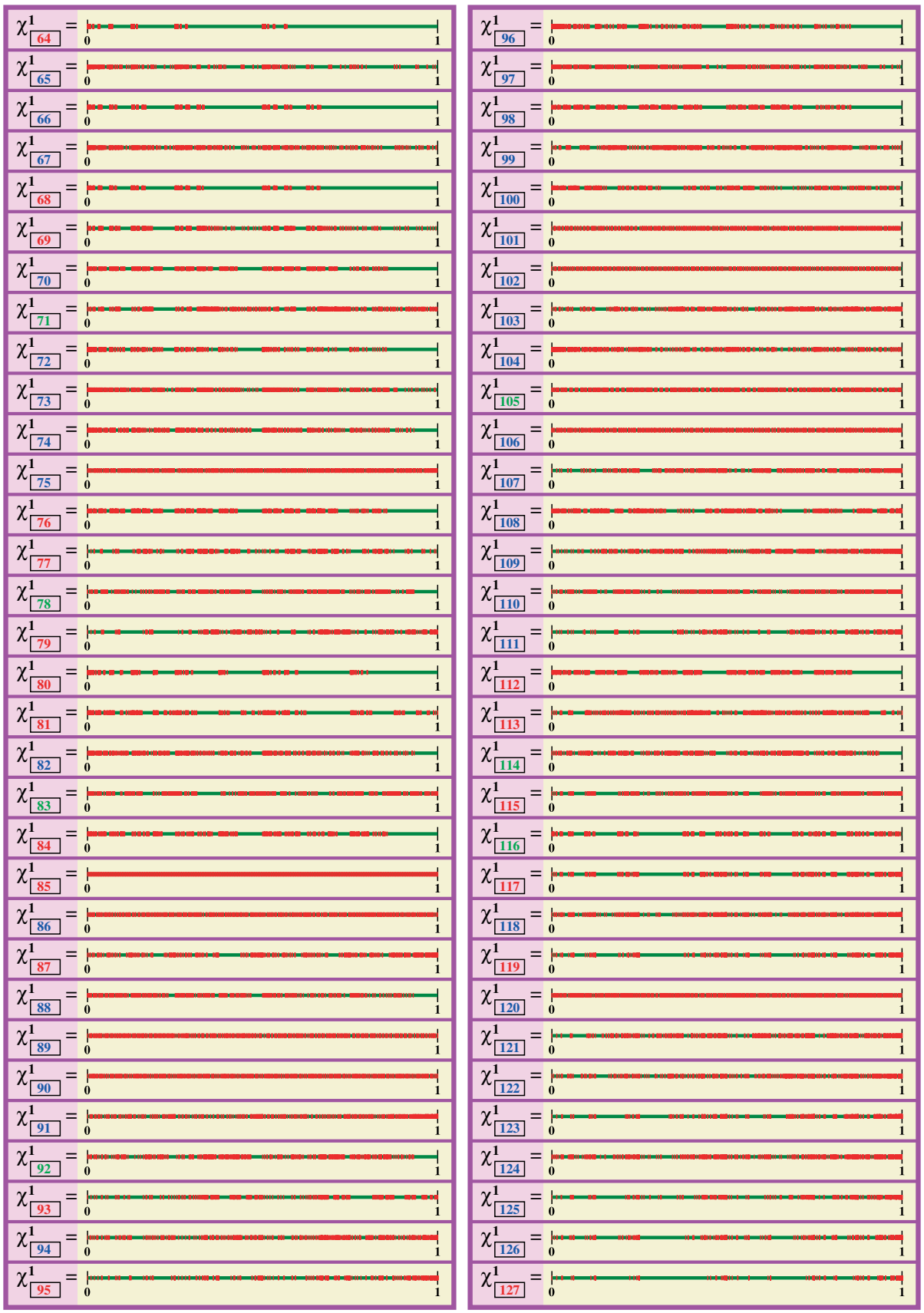


Table 8. (*Continued*)

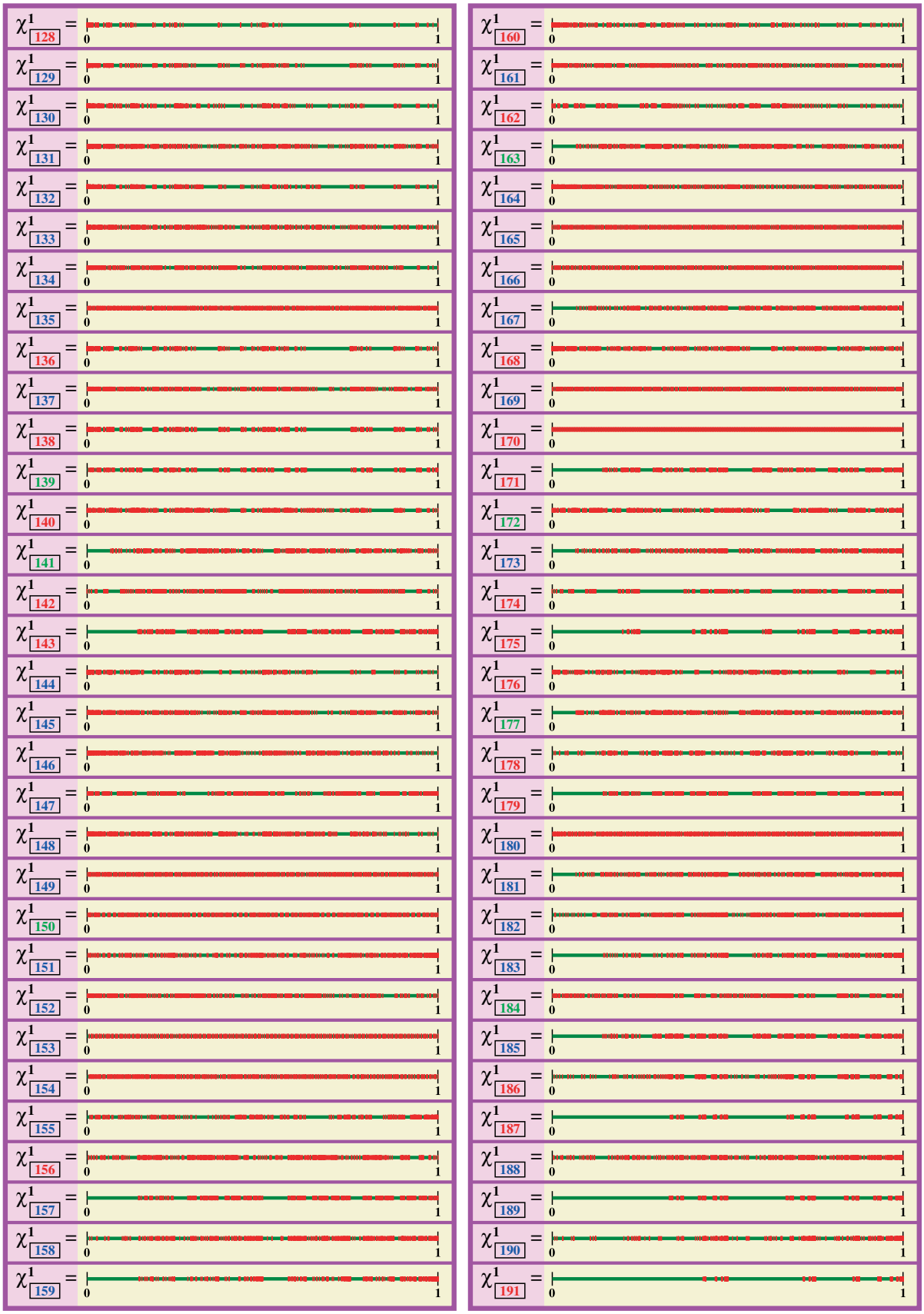


Table 8. (*Continued*)

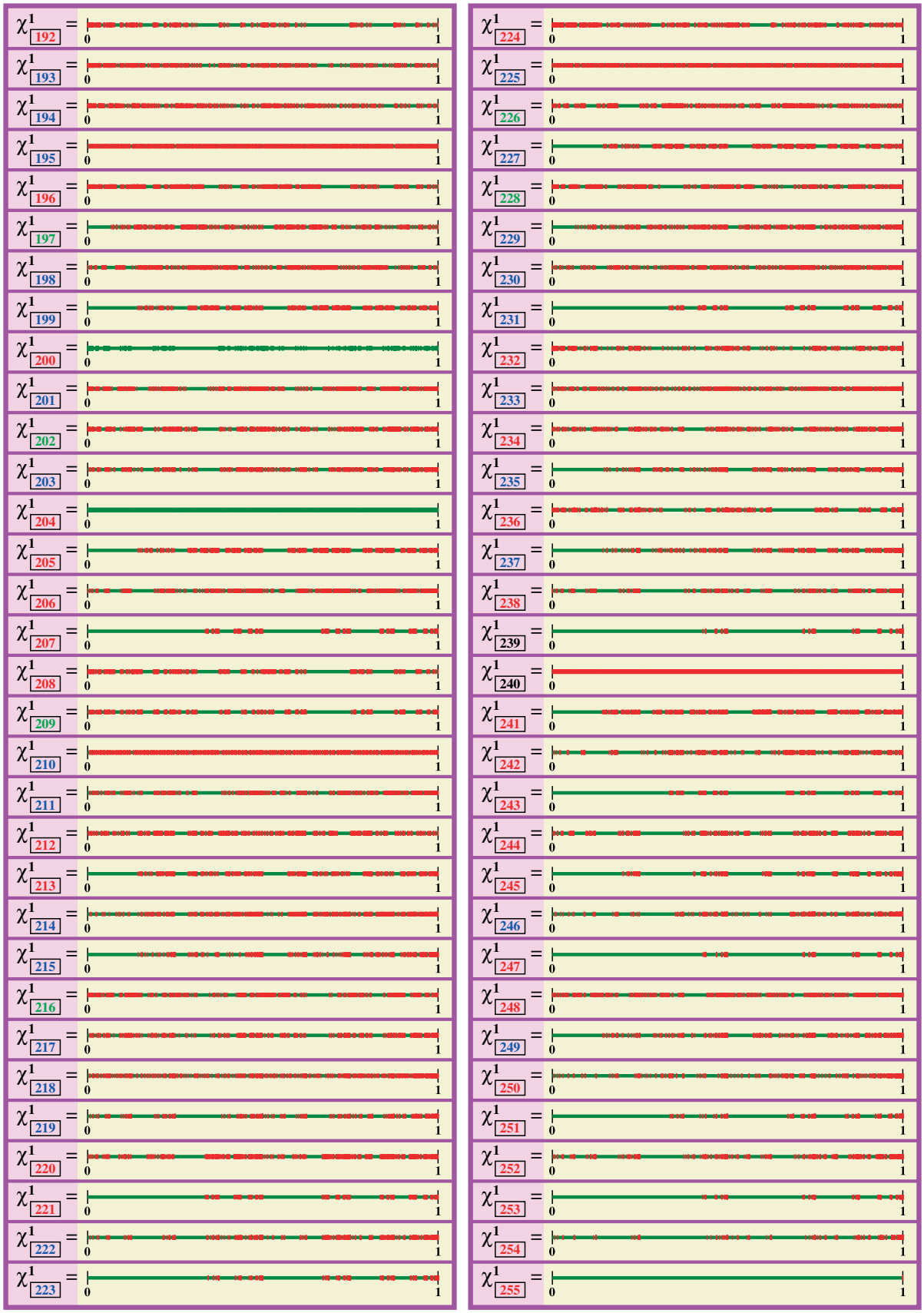
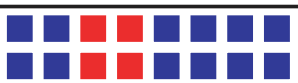
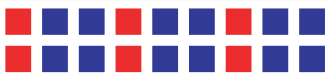
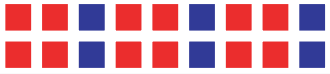


Table 9. A compendium of *period-n* isles of Eden of $\boxed{N}$.

Table 9-1(a). Period-1 isles of Eden.

n	*Period-1* Isle of Eden	Rules Endowed with Isle of Eden
1		134 140 142 148 150 156 158 162 166 170 172 174 176 180 182 184 186 188 190 196 198 204 206 212 214 220 222 226 228 230 234 236 238 240 242 244 246 248 250 252 254
2		128 130 132 134 136 138 140 142 144 146 148 150 152 154 156 158 160 162 168 170 176 184 186 192 194 196 198 200 202 204 206 208 210 212 214 216 220 224 226 240 242
3		4 6 7 12 14 15 20 21 22 23 30 31 68 84 85 86 87 132 134 135 140 142 143 148 149 150 151 158 159 196 204 206 207 212 213 214 215 220 221 222 223
4		72 73 76 104 105 108 109 200 201 204 205 233 236 237
5		72 76 200 204 236
6		200 204 205 236 237
7*		45 101 173 204 205 229
8*		74 75 88 89 204

* Here *I* +1 must be divisible by 3.

Table 9-1(b). Additional period-1 isles of Eden.

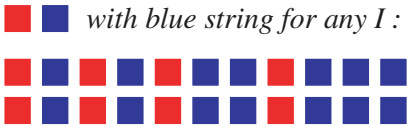
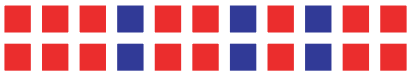
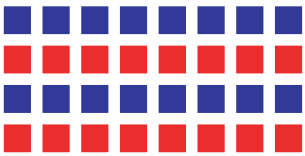
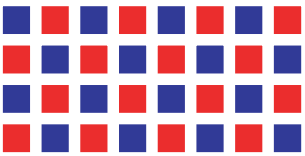
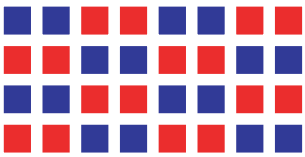
n	*Period-1* Isle of Eden	Rules Endowed with Isle of Eden
9		4 204
10		4 204
11	*any combination of*  *with blue string for any I :*	4 204
12		204 223
13		204 223
14	*any combination of*  *with red string for any I :*	204 223
15		200 204
16		200 204
17	*any combination of*  *with blue string for any I :*	200 204
18		204 236
19		204 236
20	*any combination of*  *with red string for any I :*	204 236
21	*any pattern and any I*	204

Table 9-2. Period-2 isles of Eden.

n	*Period-2* Isle of Eden	Rules Endowed with Isle of Eden
1		13 15 27 29 35 41 43 49 51 57 59 69 71 77 79 85 93 97 99 105 107 113 115 121
2		32 33 34 35 40 41 42 43 48 49 51 59 96 97 104 105 106 107 112 113 115 120 121 123 168 169 170 171 187 224 225 232 233 234 235 240 241 243 248 249 251
3		18 19 22 23 50 51 54 55 146 147 150 151 178 179 182 182
4	*any pattern and any I*	51

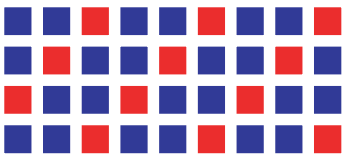
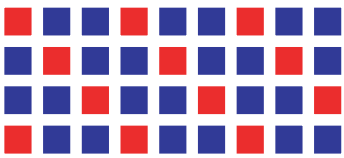
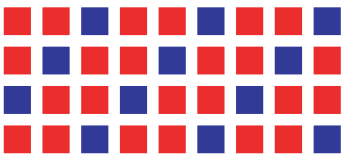
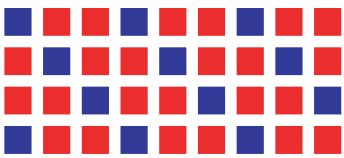
Remarks :

For n = 1, ***Period-2*** Isles of Eden can exist for any I.

For n = 2, ***Period-2*** Isles of Eden can exist for any I + 1 that is divisible by 2.

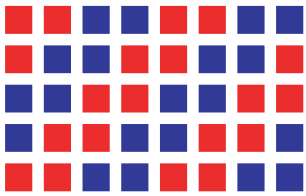
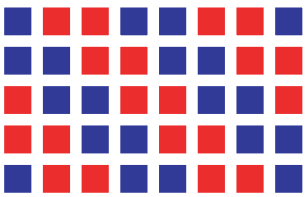
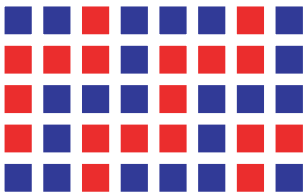
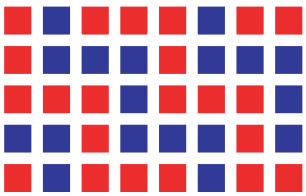
For n = 3, ***Period-2*** Isles of Eden can exist for any I + 1 that is divisible by 4.

Table 9-3. Period-3 isles of Eden.

n	*Period-3* Isle of Eden	Rules Endowed with Isle of Eden
1		2, 3, 42, 43, 75, 99, 106, 107, 130, 131, 170, 171, 202, 203, 226, 227, 234, 235
2		16, 17, 57, 89, 112, 113, 120, 121, 144, 145, 184, 185, 216, 217, 240, 241, 248, 249
3		40, 41, 42, 43, 44, 45, 56, 57, 62, 63, 168, 169, 170, 171, 172, 184, 190, 191
4		96, 97, 98, 99, 100, 101, 112, 113, 118, 119, 224, 225, 226, 228, 240, 241, 246, 247

Period-3 Isles of Eden can exist for any I + 1 that is divisible by 3.

Table 9-4. Period-4 isles of Eden.

n	*Period-4* Isle of Eden	Rules Endowed with Isle of Eden
1		10 15 170 175
2		80 85 240 245
3		15
4		85

Period-4 Isles of Eden can exist for any *l* + 1 that is divisible by 4.

Table 9-5(a). Period-5 isles of Eden.

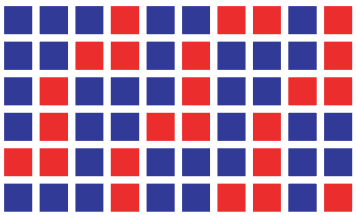
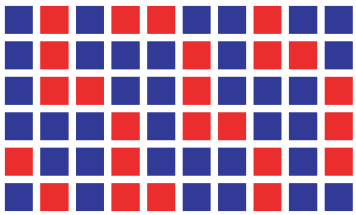
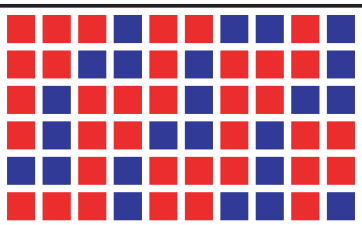
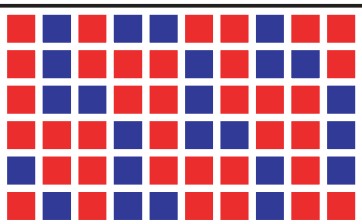
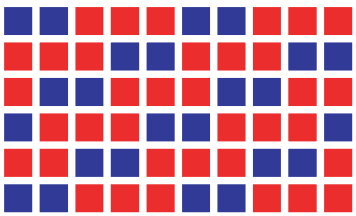
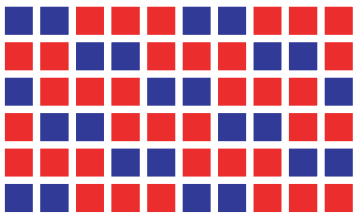
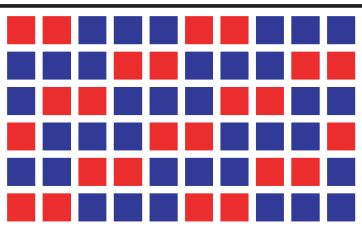
n	*Period-5* Isle of Eden	Rules Endowed with Isle of Eden
1		6
2		20
3		159
4		215
5		26 27 31 58 58 63
6		82 83 87 114 115 119
7		3 7 35 39 163 167

Table 9-5(b). Additional period-5 isles of Eden.

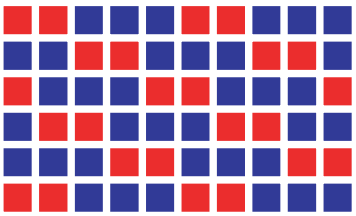
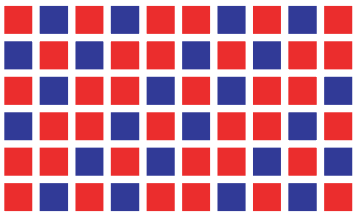
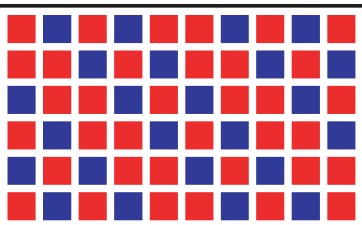
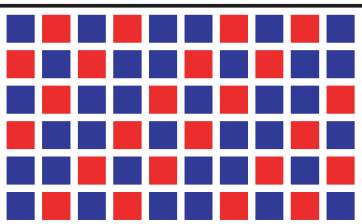
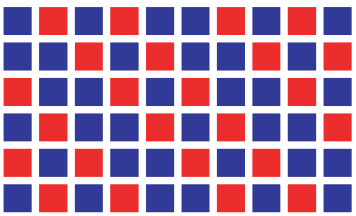
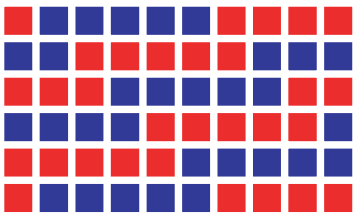
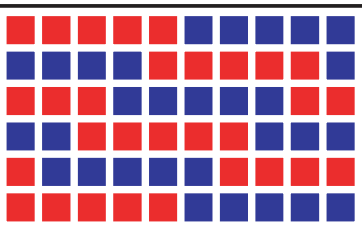
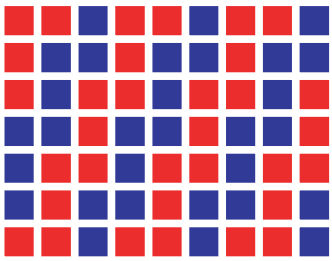
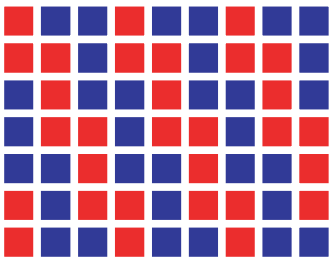
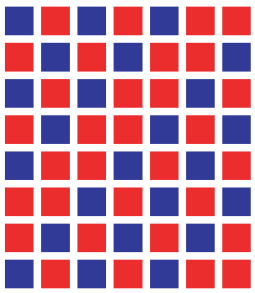
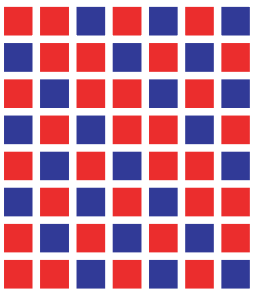
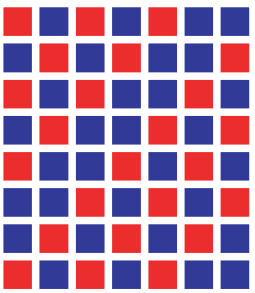
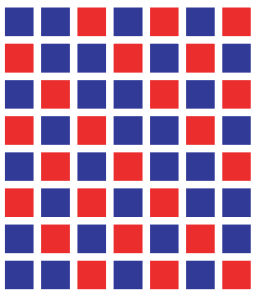
n	*Period-5* Isle of Eden	Rules Endowed with Isle of Eden
8		17 21 49 53 117 181
9		40 41 42 43 56 170
10		96 97 98 112 113 240
11		43 107 170 171 227 235
12		113 121 185 240 241 249
13		15 43
14		85 113

Table 9-6. Period-6 isles of Eden.

n	***Period-6* Isle of Eden**	**Rules Endowed with Isle of Eden**
1		14 15 142 143
2		84 85 212 213
3	*any pattern at I = 5*	170 240

Period-6 Isles of Eden can exist for any *I* + 1 that is divisible by 3.

Table 9-7. Period-7 isles of Eden.

n	*Period-7* Isle of Eden	Rules Endowed with Isle of Eden
1		40 41 42 43 169 170
2		96 97 112 113 225 240
3		43 106 107 170 171 235
4		113 120 121 240 241 249

Period-7 Isles of Eden can exist for any $l + 1$ that is divisible by 7.

Table 9-8(a). Period-8 isles of Eden.

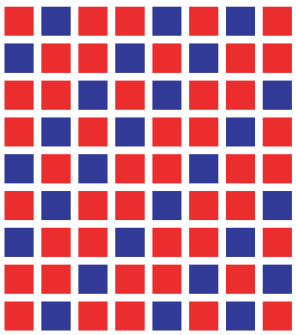
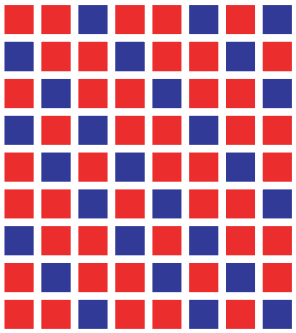
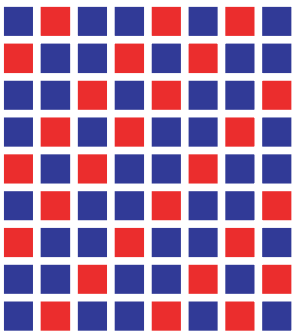
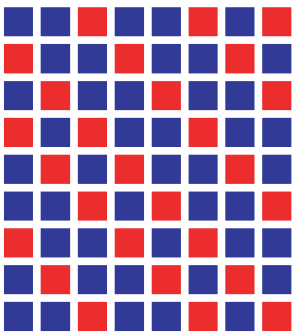
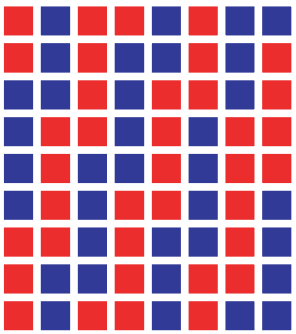
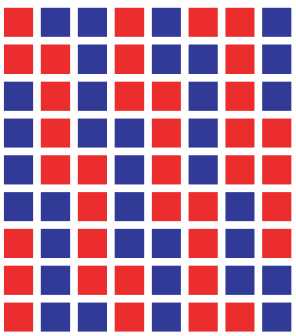
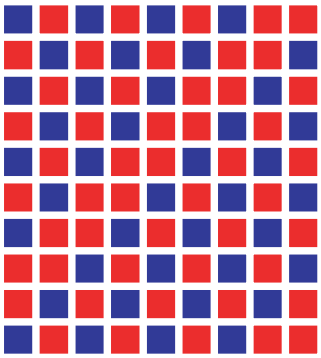
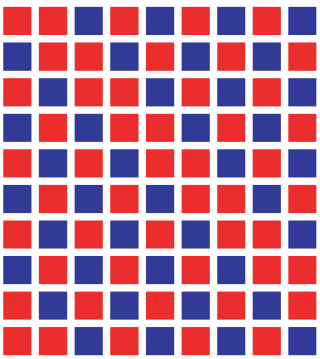
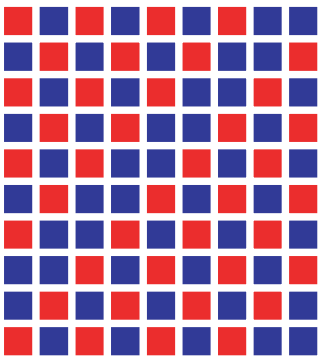
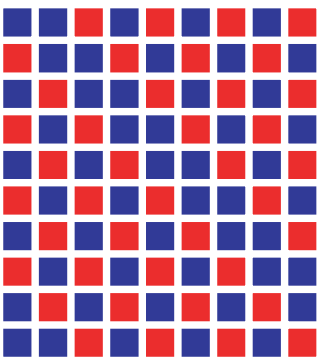
n	*Period-8* Isle of Eden	Rules Endowed with Isle of Eden
1		40 41 42 43 56 169 170
2		96 97 98 112 113 225 240
3		43 106 107 170 171 227 235
4		113 120 121 185 240 241 249

Table 9-8(b). Additional period-8 isles of Eden.

n	*Period-8* Isle of Eden	Rules Endowed with Isle of Eden
5		14 15 142 143
6		84 85 212 213

Period-8 Isles of Eden can exist for any $I + 1$ that is divisible by 4.

Table 9-9. Period-9 isles of Eden.

n	*Period-9* Isle of Eden	Rules Endowed with Isle of Eden
1		40 41 42 43 169 170
2		96 97 112 113 225 240
3		43 106 107 170 171 235
4		113 120 121 240 241 249

Period-9 Isles of Eden can exist for any $I + 1$ that is divisible by 9.

Table 9-10(a). Period-10 isles of Eden.

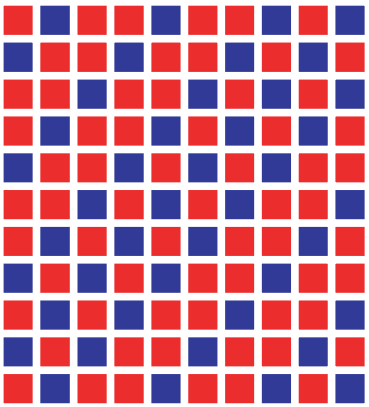
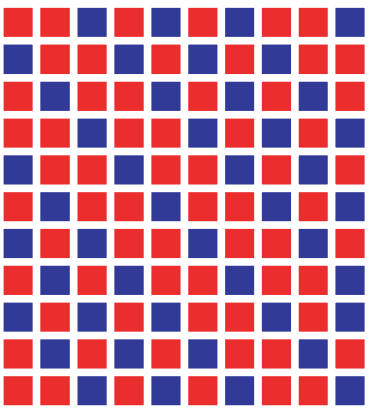
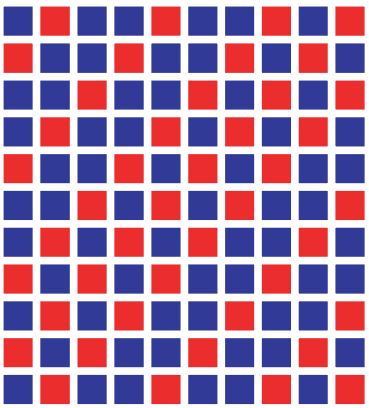
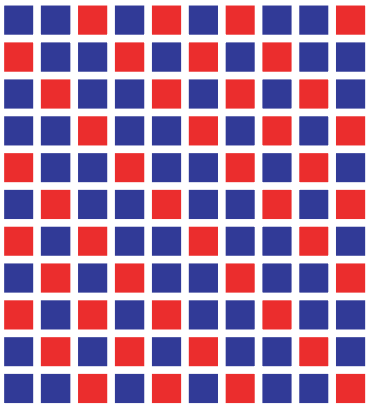
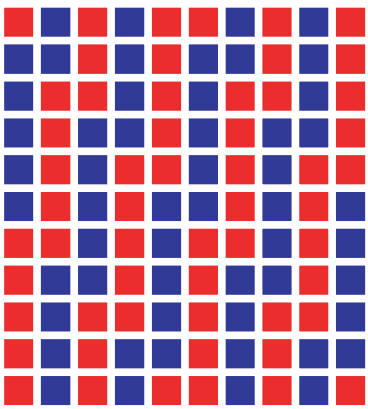
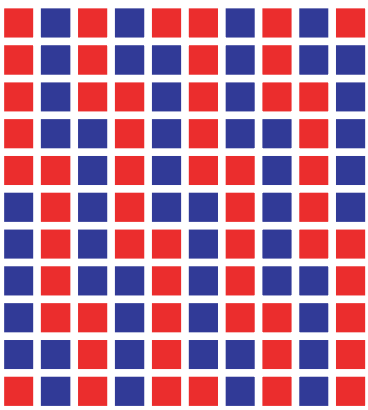
n	*Period-10* Isle of Eden	Rules Endowed with Isle of Eden
1		40 41 42 43 169 170
2		96 97 112 113 225 240
3		43 106 107 170 171 235

Table 9-10(b). Additional period-10 isles of Eden.

n	*Period-10* Isle of Eden	Rules Endowed with Isle of Eden
4		113 120 121 240 241 249
5		14 15 142 143
6		84 85 212 213

Period-10 Isles of Eden can exist for any $I + 1$ that is divisible by 5.

Table 9-11(a). Period-11 isles of Eden.

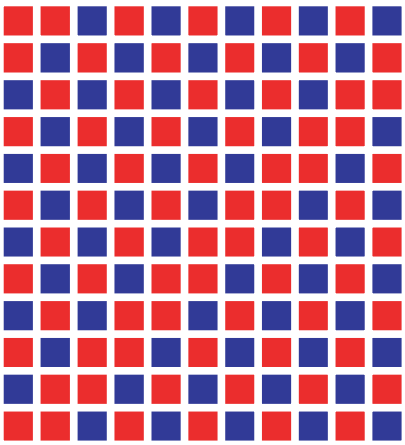
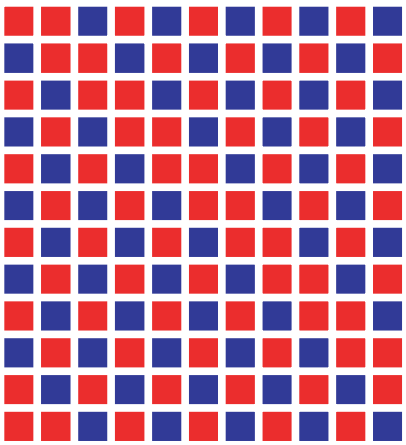
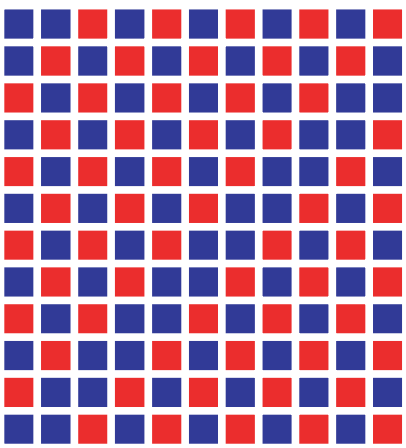
n	*Period-11* Isle of Eden	Rules Endowed with Isle of Eden
1		40 41 42 43 169 170
2		96 97 112 113 225 240
3		43 106 107 170 171 235

Table 9-11(b). Additional period-11 isles of Eden.

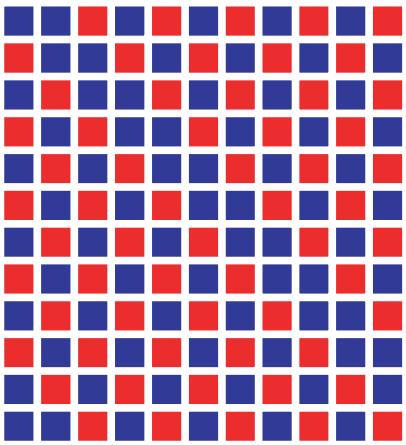
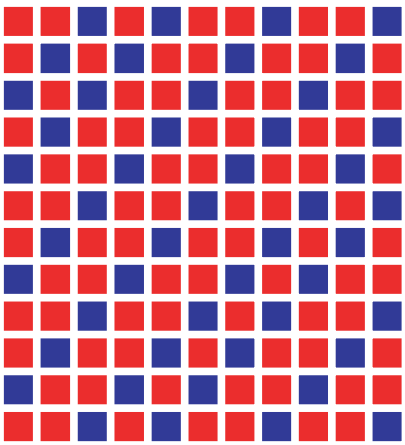
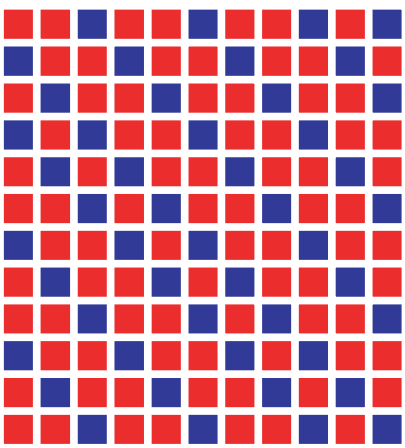
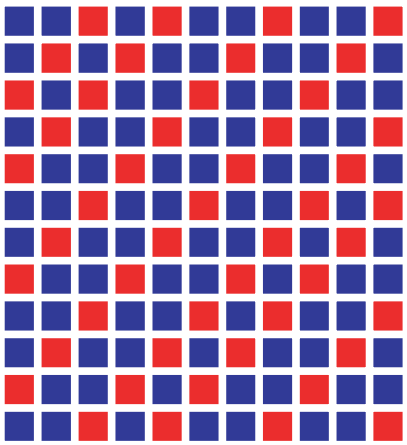
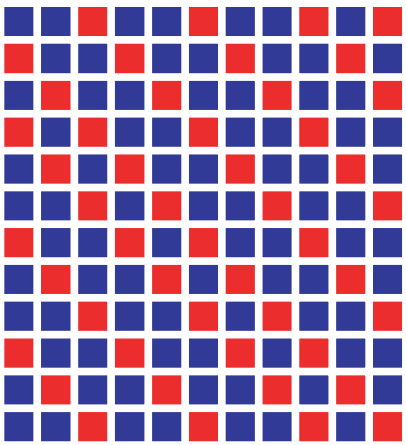
n	*Period-11* Isle of Eden	Rules Endowed with Isle of Eden
4		113 120 121 240 241 249
5		40 41 42 43 169 170
6		96 97 112 113 225 240

Table 9-11(c). Additional period-11 isles of Eden.

n	*Period-11* Isle of Eden	Rules Endowed with Isle of Eden
7		43 106 107 170 171 235
8		113 120 121 240 241 249

Period-11 Isles of Eden can exist for any *I* + 1 that is divisible by 11.

Observe that any binary string

$$\{x_0, x_1, x_2, \ldots, x_I\} \mapsto \phi_0 = \sum_{i=0}^{I} 2^{-(i+1)} x_i \qquad (36)$$

which has no *preimage* under $\chi^1_{\boxed{N}}$ (i.e. ϕ_0 does not belong to the *range* of $\chi^1_{\boxed{N}}$) is a *garden of Eden* of $\boxed{N}$. In other words, $\phi_0 \in [0,1]$ is a garden of Eden of $\boxed{N}$ if there does *not* exist a $\phi_{-1} \in [0,1]$ such that $\phi_0 = \chi^1_{\boxed{N}}(\phi_{-1})$, where $\phi_{-1} \neq \phi_0$. Note that this property is *only* a sufficient condition for ϕ_0 to be a garden of Eden. In the next section, we will see that there exist some rather special points which violate this property, but is nevertheless a garden of Eden because it satisfies Definition 5.1.

A compendium of all gardens of Eden belonging to each local rule $\boxed{N}$ is listed in Table 8. Each point $\phi_0 \in [0,1]$ printed in green along the $\chi^1_{\boxed{N}}$ axis does *not* have a preimage under $\chi^1_{\boxed{N}}$ and is therefore a garden of Eden.

6. Isle of Eden

For most rules $\boxed{N}$, there exist some special *period-1* points which have no predecessors in the sense that no orbits from other initial bit-string

Table 10. Rules without period-k isles of Eden, $k < 12$.

0	1	5	8	9	11	24	25
28	36	37	38	46	47	52	60
61	64	65	66	67	70	78	81
90	91	92	94	95	102	103	110
111	116	117	122	124	125	126	127
129	133	137	139	141	153	155	157
161	164	165	189	193	195	197	199
209	211	218	219	231	239	253	255

configurations can converge to such points, and hence they are also *gardens of Eden* in view of Definition 5.1. Moreover, since each of these points is a *period-1* point, they have a preimage under $\boldsymbol{\chi}^1_{\boxed{N}}$; namely, itself. Such special points (obtained by exhaustive computer search) are henceforth called isles of Eden of $\boxed{N}$. Observe that an isle of Eden has no past, and no future (in the *poetic* sense that time stood still)!

A compendium of all period-1 isles of Eden of $\boxed{N}$ for binary strings of various length $I+1$ is listed in Tables 9-1(a) and 9-1(b).

Let us now generalize the concept of period-1 isle of Eden for "*time-n*" *characteristic functions* $\boldsymbol{\chi}^n_{\boxed{N}}$. Since such special *period-n points* also have no predecessors under the "nth iterated" map $\boldsymbol{\chi}^n_{\boxed{N}}$, they are henceforth called *period-n isles of Eden*. Table 9-k lists all *period-k* isles of Eden, $k = 1, 2, 3, \ldots, 11$, obtained by an exhaustive computer search over all binary bit-strings of length $I + 1 = 8, 9, 10, 11$, respectively. In most cases, the same bit-string configurations can be extended to arbitrarily large I, provided $I + 1$ is divisible by some integer specified in the table.

Finally, we remark that based on exhaustive computer search, there are 64 local rules that do *not* have *period-k isles of Eden*, at least for $k < 12$. They are listed in Table 10.

7. Concluding Remarks

We have demonstrated that except for the eight *affine* (*mod 1*) rules listed in Table 3, the graph of all characteristic functions $\boldsymbol{\chi}^1_{\boxed{N}}$ in Table 2 are endowed with a *fractal* structure. Indeed, even the graph of the eight affine (mod 1) rules can be considered to exhibit a *degenerate* form of fractal structure since arbitrarily short segments of the graph can be made to coincide with corresponding portions of the original graphs by appropriate affine transformations. We have traced the origin of these fractals to the *decimal* representation of binary bit-strings in Eq. (2), as well as to the *local rule*, which must apply to any bit string, regardless of the number of "zeros" in front of it.

The explicit formulas in Table 1 for converting any bit string $\{x_0, x_1, x_2, \ldots, x_I\}$ into a *real* number $\boldsymbol{\chi}^1_{\boxed{N}} \in [0, 1]$ is remarkable for its scope of potential applications. Indeed, these formulas can be interpreted as a *digital-to-analog* converter in closed form. Such formulas could not have been derived without the explicit "universal" formula derived in [Chua *et al.*, 2003] for all local rules.

The widespread presence of *period-k* "*isles of Eden*" came as a surprise since they certainly have no counter part in hyperbolic differential equations. To dramatize this phenomenon, we end Part V with our following *poetic* interpretation of the above new phenomenon: *Hidden within the* "*garden of Eden*", *which has no past, one finds immortality in an* "*isle of Eden*", *which has neither past nor future.*

Acknowledgments

This paper is supported in part by the MURI contract no. N00014-03-1-0698, the DURINT contract no. N00014-01-0741, the MARCO Microelectronics Advances Research Corporation FENA Award no. 442521/WK57015, the NSF grant CHE-0103447, the UNIVERSITE du SUD, TOULON-VAR, France, the Foundations Francqui Fonds, Belgium, and the ministry of university research and education, Italy, under the field project number RBNE012NFW.

References

Barnsley, M. F. [1988] *Fractals Everywhere* (Academic Press).

Billingsley, P. [1978] *Ergodic Theory and Information* (Robert Keirger Publishing Company, Huntington).

Chua, L. O., Yoon, S. & Dogaru, R. [2002] "A nonlinear dynamics perspective of Wolfram's new kind of science. Part I: Threshold of complexity," *Int. J. Bifurcation and Chaos* **12**, 2655–2766.

Chua, L. O., Sbitnev, V. I. & Yoon, S. [2003] "A nonlinear dynamics perspective of Wolfram's new kind of science. Part II: Universal neuron," *Int. J. Bifurcation and Chaos* **13**, 2377–2491.

Chua, L. O., Sbitnev, V. I. & Yoon, S. [2004] "A nonlinear dynamics perspective of Wolfram's new kind of

science. Part III: Predicting the unpredictable," *Int. J. Bifurcation and Chaos* **14**, 3689–3820.

Chua, L. O., Sbitnev, V. I. & Yoon, S. [2005] "A nonlinear dynamics perspective of Wolfram's new kind of science. Part IV: From Bernoulli shift to 1/f spectrum," *Int. J. Bifurcation and Chaos* **15**, 1045–1183.

Devaney, R. L. [1992] *A First Course in Chaotic Dynamic Systems*: *Theory and Experiment* (Addison-Wesley, Reading, MA).

Moore, E. F. [1962] "Machine models of self-reproduction," *Proc. Fourteenth Symp. Applied Mathematics*, pp. 17–33.